

General Disclaimer

One or more of the Following Statements may affect this Document

- This document has been reproduced from the best copy furnished by the organizational source. It is being released in the interest of making available as much information as possible.
- This document may contain data, which exceeds the sheet parameters. It was furnished in this condition by the organizational source and is the best copy available.
- This document may contain tone-on-tone or color graphs, charts and/or pictures, which have been reproduced in black and white.
- This document is paginated as submitted by the original source.
- Portions of this document are not fully legible due to the historical nature of some of the material. However, it is the best reproduction available from the original submission.

TOPICS CONCERNING STATE VARIABLE FEEDBACK IN AUTOMATIC CONTROL SYSTEMS

PART I - Specification

PART II - Sensitivity

PART III - Intentional Nonlinearities

PART IV - Unavailable States

Prepared under Grant NGR-03-002-115
National Aeronautics and Space Administration

N 69-15412	
(ACCESSION NUMBER)	(THRU)
349	
(PAGES)	(CODE)
CR 99038	10
(NASA CR OR TMX OR AD NUMBER)	(CATEGORY)



ENGINEERING EXPERIMENT STATION
COLLEGE OF ENGINEERING
THE UNIVERSITY OF ARIZONA
TUCSON, ARIZONA

TOPICS CONCERNING STATE VARIABLE FEEDBACK
in AUTOMATIC CONTROL SYSTEMS

PART I - Specification

PART II - Sensitivity

PART III - Intentional Nonlinearities

PART IV - Unavailable States

Prepared Under Grant NGR-03-002-115
National Aeronautics and Space Administration

by

Donald G. Schultz
Robert C. White
Joseph H. Dial
Hasmukhrai B. Parekh
Milo E. Muterspaugh

Electrical Engineering Department
The University of Arizona
Tucson, Arizona
1968

Engineering Experiment Station
The University of Arizona
College of Engineering
Tucson, Arizona

TABLE OF CONTENTS

Introduction and Discussion of Contents

**PART I - The Specification and Synthesis of
High-Order Control Systems**

**PART II - Sensitivity and State Variable Feed-
back**

**PART III - Intentional Nonlinearity in a State
Variable Feedback System**

**PART IV - State Variable Feedback and Unavailable
States**

INTRODUCTION AND DISCUSSION OF CONTENTS

This is a summary type report that actually contains four separate reports on matters relating to state variable feedback methods in automatic control systems. This introductory material is included to give the necessary background and to link the four reports with each other and with what has been done in the past.

The idea of state variable feedback in linear control systems is one of the important practical results that have resulted from the so called modern control theory. Means by which state variable feedback can be used to realize any desired closed loop transfer function have previously been reported under this contract, NASA Document #CR-77901 (1). A more recent discussion of the same topic is included in the author's graduate text (2), and state variable feedback forms the basic foundation for a senior level book soon to be published by McGraw-Hill (3). The point being made here is that state variable feedback methods are becoming well known, and the reader is assumed to have a basic understanding of such techniques.

The material described in this report is not well known. An alternate title for this report might well be "How to Make State Variable Feedback Work". The implication is that state variable feedback doesn't work, and,

"REPRODUCIBILITY OF THE ORIGINAL PAGE IS POOR."

in many practical situations, this is true. The difficulty is not with the theory, but with the intentional or unintentional violations of basic assumptions.

A basic claim of state variable is that any desired closed loop transfer function may be realized, providing, of course, that the pole-zero excess of the resulting system is at least as great as that of the plant being controlled. A prime problem then is having a desired closed loop transfer function to meet time or frequency domain specification of accuracy, stability, speed of response, and sensitivity. This is the topic of Part I of the report, "The Specification and Synthesis of High-Order Control Systems". The three reports that follow this one all assume that the selection of the desired closed loop transfer function has been accomplished according to the procedure outlined in Part I.

The ability of a closed loop control system to respond according to any desired closed loop transfer function is not a new idea. This was the approach of the Guillemin-Truxal method of series equalization described so aptly in Truxal's classic book(4). Essentially the series equalizer cancelled $(n-1)$ poles of the plant, and substituted for these $(n-1)$ new poles to ensure the desired result when the output was feedback to form the closed loop system. From an input-output point of view, a Guillemin-Truxal type system and a state variable feed-

back system might tend to be identical. In fact, they are identical, as long as all system parameters are exactly those assumed in modeling the given plant. Of course, this is never the case in practice, and the question of which closed loop system can be expected to function as desired in the face of uncertainties in plant parameters reduces to one of sensitivity. Part II of the report discusses this question under the heading of "Sensitivity and State Variable Feedback".

Part III, titles "Intentional Nonlinearity in a State Variable Feedback System" is concerned with a closed loop system configuration that is specifically designed to be insensitive to changes in a particular forward gain $K(5)$. Actually, the utility of the gain insensitive design described here goes far beyond that class of systems for which the gain may actually be changing due to inherent physical factors. The practical utilization of the intentional nonlinearity is to insure that the plant being controlled does not saturate. By not saturating is meant that none of the state variables of the plant is ever allowed to exceed a value imposed by physical limitations. For example, temperature may be a state variable, and it may not exceed a value beyond which a component destroys itself or melts.

The need for some type of limiting action goes back to the basic ability of state variable feedback to realize

any closed loop transfer function, regardless of the plant. For a plant with a natural time constant of 1 second, a response of a microsecond time constant might be specified. That such a rapid response could be realized for such a slow given plant violates our intuition. Also, violated in practice are physical state variable constraints and the assumption of linearity. The gain insensitive design is one means of solving this problem.

Along with state variable constraints, another basic fact of life is the unavailability of one or more of the state variables. Any one state variable may simply be too difficult, too expensive, or too noisy to measure. In the face of such a situation, how does one proceed to use the state variable feedback methods. Part IV, "State Variable Feedback and Unavailable States", discusses this problem from the point of view of generating unavailable states from those that are available. The basis for the method discussed here is the so-called "observer" system of Luenberger. The result is a modified observer type system that overcomes many of the practical difficulties in building an observer type system.

Each of the four parts of this report was written as a Masters Thesis in Electrical Engineering at the University of Arizona in Support of the NASA Grant NGR-03-002-115. Thus, each of the separate parts of this summary report is complete in itself, with its own abstract, table

or contents, list of figures and pagination. Although two of these reports, Parts I and II, have previously been submitted under the contract cited above, it is felt that the purposes of NASA are best served by gathering these four reports under one title. The common factor that unites these reports is the desire to realize a desired closed loop transfer function exactly. Approximate realizations, particularly those involving plant conditioning, are the subject of future reports.

BIBLIOGRAPHY

1. Schultz, D.G., "A New Method of Design of Linear Systems", NASA Contractors Report, CR-77901, August, 1966.
2. Schultz, D.G. and J.L. Melsa, "State Functions and Linear Control Systems", McGraw-Hill Inc., New York, 1967.
3. Melsa, J.L. and D.G. Schultz, Linear Control Theory, in press, McGraw-Hill Inc., New York, 1969.
4. Truxal, J.G., Automatic Feedback Control System Synthesis, McGraw-Hill Book Company, New York, 1955.
5. Herring, J.E., "Design of Linear and Nonlinear Control Systems via State Variable Feedback", Doctoral Dissertation, University of Arizona, Tucson, Arizona, 1967.
6. D.G. Luenberger, "Observing the State of a Linear System", IEEE Transactions on Military Electronics, April, 1964.

PART I

**THE SPECIFICATION AND SYNTHESIS OF HIGH-ORDER
CONTROL SYSTEMS**

**Prepared Under Grant NGR-03-002-115
National Aeronautics and Space Administration**

by

**Joseph H. Dial
and
Donald G. Schultz**

**Electrical Engineering Department
The University of Arizona
Tucson, Arizona**

ABSTRACT

The synthesis of linear control systems is a threefold problem: (1) selecting values for the performance specifications, (2) the use of those specifications to derive a model response and (3) the extension of that model to a $C(s)/R(s)$ function which is realizable using state variable feedback.

In this thesis, general rules are given for the selection of the performance measures M_p , ω_p , BW, DR, T_s , T_d , T_r , P_0 and FVE. Design charts are presented so that a low-order model can be constructed from the design specifications. The last synthesis problem is solved by defining an equation, similar to the Kalman Equation, which extends the low-order model to a $C(s)/R(s)$ function compatible with the complexity of the plant.

TABLE OF CONTENTS

	Page
LIST OF ILLUSTRATIONS	vi
ABSTRACT	viii
CHAPTER	
I. INTRODUCTION	1
II. PERFORMANCE SPECIFICATION	6
Selection of Measures	6
Accuracy	11
Stability	12
Speed	12
Sensitivity	13
Summary	14
III. THE SPECIFICATION AND SOLUTION OF LOW-ORDER MODELS	15
Background	15
The Second-Order Model Without Zeros	18
The Second-Order Model With One Zero	22
The Third-Order Model	25
Summary	31
IV. THE SENSITIVITY-OPTIMALITY CONDITION	32
Classical Sensitivity	32
Optimality	41
Summary	43
V. THE SPECIFICATION OF HIGH-ORDER MODELS	44
Extension of Low-Order Characteristic Equations	44
Extension of the General "Ideal" Model	49
Summary	53
VI. THE SOLUTION OF HIGH-ORDER SYSTEMS	54
Calculation of $H_{eq}(s)$	54

TABLE OF CONTENTS--Continued

	Page
Saturation	64
Summary	65
VII. CONCLUSIONS	67
REFERENCES	69

LIST OF ILLUSTRATIONS

Figure	Page
1. The Closed Loop System	3
2. Specification of $C(s)/R(s)$ for a System with Load Disturbances	8
3. Specification of $c(t)$	10
4. Low Order Approximation of High Order Response	17
5. Performance Measures of Second-Order Systems .	21
6. Performance Measures of Second-Order System with One Zero	24
7. Performance Measures for Third-Order System with One Zero and Damping Ratio of 0.5 . .	27
8. Performance Measures for Third-Order System with One Zero and Damping Ratio of 0.707 .	28
9. Single-Input, Single-Output System	33
10. System With Open-Loop Pole at α	34
11. Second-Order System with State Variable Feedback	37
12. A Typical Plot of $DR^{-1}(jW)$ for $n = 3$	41
13. Root Locus of Optimal Models for Third-Order Example	48
14. Root Locus of Optimal Models for Fifth-Order Example	52
15. Block Diagram of Third-Order Example	56
16. Frequency Response of Third-Order System and "Ideal" Model	57

LIST OF ILLUSTRATIONS--Continued

	Page
17. Time Response of Third-Order System and "Ideal" Model	58
18. Block Diagram of Fifth-Order Example	59
19. Zeros in the First Block of a Block Diagram .	60
20. Frequency Response of Fifth-Order System and "Ideal" Model	63
21. Optimum Controller for First-Order System . .	64
22. Optimum Controller With Two Modes	66

CHAPTER I

INTRODUCTION

This study outlines methods for specifying a desired closed-loop transfer function on the basis of typical time and frequency domain performance requirements. This study is motivated by the ability to realize any desired closed-loop transfer function in a single-input, single-output, linear control system in which all of the state variables are fed back.

While there are numerous treatments of first and second-order control systems to be found in the literature, systems of higher order are usually handled by the use of dominate roots or approximations based on the system's behavior in the vicinity of the open-loop, gain-crossover frequency. By applying state-variable feedback techniques, coupled with a necessary condition for optimality as defined by the Kalman Equation, the poles and zeros of the higher, closed-loop system can be intelligently placed and the necessary feedback coefficients calculated.

The investigation is limited to constant coefficient, linear systems as described by the following set of matrix equations:

$$\dot{\underline{x}} = \underline{A}\underline{x} + \underline{b}\underline{u} \quad (1.1)$$

$$\underline{u} = \underline{r} - \underline{k}^T \underline{x} \quad (1.2)$$

$$\underline{c} = \underline{f}^T \underline{x} \quad (1.3)$$

Where $\underline{x} \triangleq$ column matrix or vector of the n state variables in time domain

$\dot{\underline{x}}$ \triangleq time derivative of \underline{x}

$\underline{A} \triangleq$ n^{th} order square matrix or system matrix of constant coefficients

$\underline{b} \triangleq$ n^{th} order column matrix, the control matrix

$\underline{u} \triangleq$ control function in time domain

$\underline{r} \triangleq$ reference or input function

$\underline{k} \triangleq$ n^{th} order column matrix, the feedback matrix of constant feedback coefficients

$\underline{f} \triangleq$ n^{th} order column matrix, the output matrix

$\underline{c} \triangleq$ output function

On the basis of these matrix equations, transfer functions may be defined and block diagrams drawn which are related to conventional control-system representation. By Laplace transforming Equation (1.1), a forward transfer function $G(s)$ may be defined as

$$\frac{C(s)}{U(s)} = G(s) = \underline{f}^T \underline{\Phi}(s) \underline{b} \quad (1.4)$$

where

$$\underline{\Phi}(s) = [s\underline{I} - \underline{A}]^{-1}$$

and is called the resolvent matrix, the Laplace transform of the state transition matrix.

In a similar fashion, an equivalent feedback transfer function, $H_{eq}(s)$, may be defined as

$$H_{eq}(s) = \frac{\underline{k}^T \underline{x}}{\underline{f}^T \underline{x}} = \frac{\underline{k}^T \underline{\Phi}(s) \underline{b}}{\underline{f}^T \underline{\Phi}(s) \underline{b}} \quad (1.5)$$

The resulting closed-loop system is represented in block diagram form in Figure 1. Note here that $G(s)$ includes any series compensation $G_c(s)$, along with the unalterable plant transfer function $G_p(s)$. This representation assumes that the state variables have been chosen so that $H_{eq}(s)$ includes all the zeroes of $G(s)$.

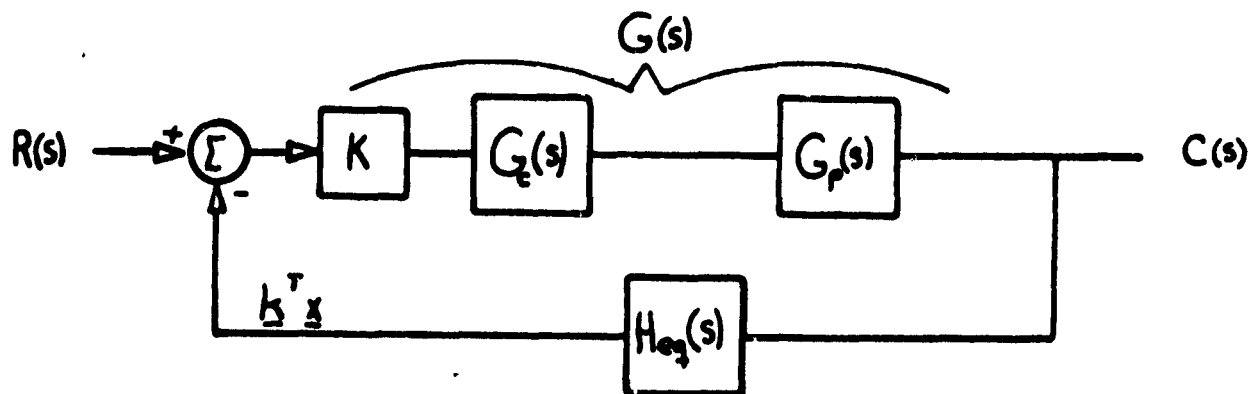


Fig. 1. The Closed Loop System

Further assumptions made throughout this study are that the gain K of the forward transfer function is

specified and that the desired input-output dynamics of the system exhibit an underdamped response with zero steady-state position error.

The investigation begins in Chapter II with a brief discussion of performance measurements and their specification. Here the choice of specification is based solely upon a desired performance, and is in no way influenced by the given, unalterable plant. Of the multitude of performance measures, only Bandwidth (BW), M-Peak (M_p), Final Value of Error (FVE), Delay Time (T_d), Rise Time (T_r), Settling Time (T_s), Percent Overshoot (PO) and Output Impedance (Z_o) are selected for use in specifying the step and sinusoidal responses of the system. Chapter III supplies the graphical aids and procedures for synthesizing low-order, closed-loop models (two or three poles with or without a zero), to meet closed-loop design specifications.

This low-order model of $C(s)/R(s)$ has satisfactory dynamics, but its sensitivity to load changes, i.e., Z_o , is partly determined by open loop functions $G(s)$ and $H_{eq}(s)$. The discussion of Z_o and sensitivity in general is given in Chapter IV. The often disregarded Deviation Ratio, DR, is shown to be intimately related to system sensitivity (including Z_o) and system optimality. Methods for determining DR (its frequency spectrum) are given, as are the implications of DR on the low-order model. The optimality equations of Chapter IV are used in Chapter V to define an

optimime-root-locus, which permits the extension of the low-order model to one of correct order as required by the compensated plant $G(s)$.

The synthesis problem is concluded in Chapter VI with a discussion of the mechanics of the high-order extension and the calculation of k . The problem of saturation is described and a method of circumventing this type of nonlinearity is suggested as an extension of the modeling process proposed by this thesis.

CHAPTER II

PERFORMANCE SPECIFICATION

The problem of system performance specification forms the basis of the system synthesis. This chapter begins with a statement of the criteria used by Gibson, Leedham et al. (1960) to select a sufficient set of performance measures. The definitions of the performance measures and then the assignment of values to these measures, making them performance specifications, conclude this section.

Selection of Measures

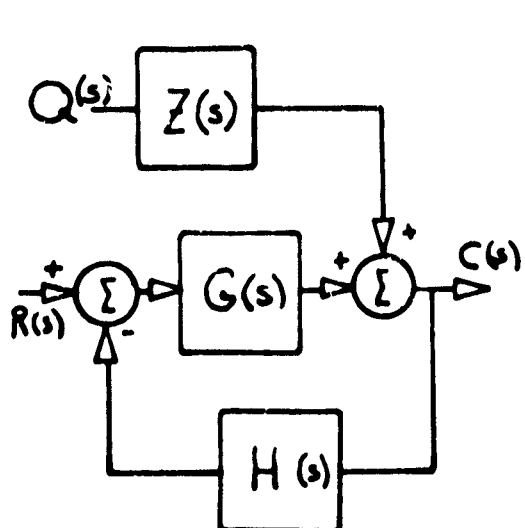
Performance measures are grouped into four general performance areas, each describing an important quality of the system's response. These are: (1) accuracy, (2) speed, (3) relative stability, (4) sensitivity. There are a multitude of performance measures to be found in the literature which could be used to describe each area. To reduce the number of eligible measures, only those measures are selected which: (1) convey an easily interpretable quality of the system's response, (2) are applicable to and valid for systems of any order or configuration, (3) express an input-output relationship or quality in terms

of closed-loop parameters, (4) provide a sensitive and discriminative measure.

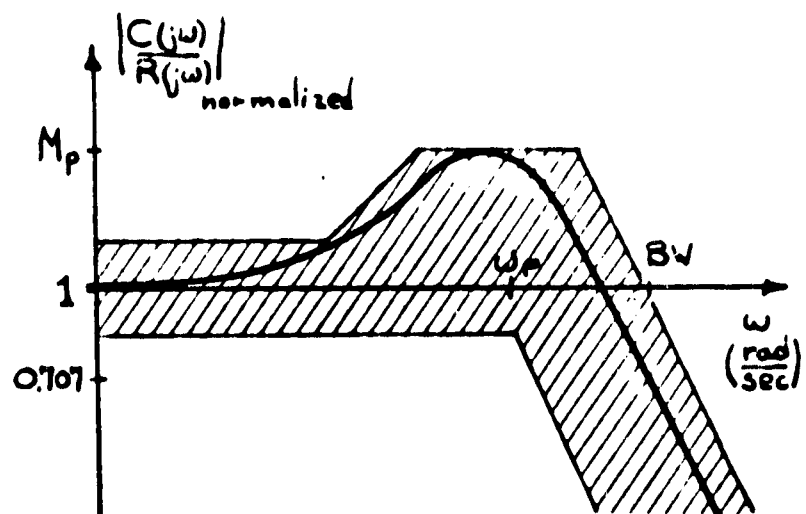
Two sets of performance measures which meet these restrictions may be chosen, one set in the frequency domain and the other in the time domain.

The frequency domain performance measures and their definitions are:

1. M-Peak, M_p , is the maximum value of the magnitude of the normalized, closed-loop transfer function. The normalized function is obtained by dividing $|C(s)/R(s)|$ by its value at a low enough frequency such that it is essentially independent of frequency, i.e., the "flat part" of the frequency response.
2. W-peak, ω_p , is the frequency in rad/sec at which M_p occurs.
3. Bandwidth, BW, is the range of frequencies in rad/sec between zero and the frequency at which the normalized closed-loop transfer function has a magnitude of 0.707.
4. Output Impedance, $Z_o(s)$, is the function which relates the sinusoidal output due to a load disturbance, to that load disturbance. In Figure 2a, $Z_o(s)$ is defined as:



(a)



(b)

Fig. 2. Specification of $C(s)/R(s)$ for a System with Load Disturbances

$$Z_o(s) = \frac{C(s)}{Q(s)} = \frac{Z(s)}{1 + G(s)H_{eq}(s)}$$

5. Deviation Ratio, $DR(s)$, is defined as

$$DR(s) = \left| \frac{1}{1 + G(s)H_{eq}(s)} \right|$$

The frequency domain measures BW, M_p , and ω_p outline a region of permitted locations of the magnitude closed-loop frequency response, as shown in Figure 2b. The speed and stability of the system's response to sinusoids is therefore specified by these parameters. Output Impedance and $DR(s)$ indicate the system's sensitivity, for which there is no time domain measure.

The proposed time domain performance measures also "box-in" the unit step response of the system as in

Figure 3. If the output does not have a final value of unity, the performance measures are applied to the normalized output which does have a forced response of one. The two performance measures describing the leading edge of the transient for a high-order system are assumed to apply to the smoothest fit of that transient. Definitions of these specifications are:

1. Delay Time, T_d , is the time elapsed in seconds, after the application of a step input until the average normalized output reaches 0.5.
2. Rise Time, T_r , is the time required by the system to rise from 10% to 90% of its final value.
3. Settling Time, T_s , is the time required for the response to fall to and remain within a band of $\pm x\%$ of its final value. Typical values for x are two and five.
4. Percent overshoot, PO , is defined as the maximum value of response minus the final value of response divided by the final value of response. The resulting value is then multiplied by one hundred.
5. Final Value of Error, FVE , is the percentage by which the final value of the normalized output fails to reach unity.

The speed and stability of the step response are measured by T_d , T_r , T_s and PO , while its accuracy is

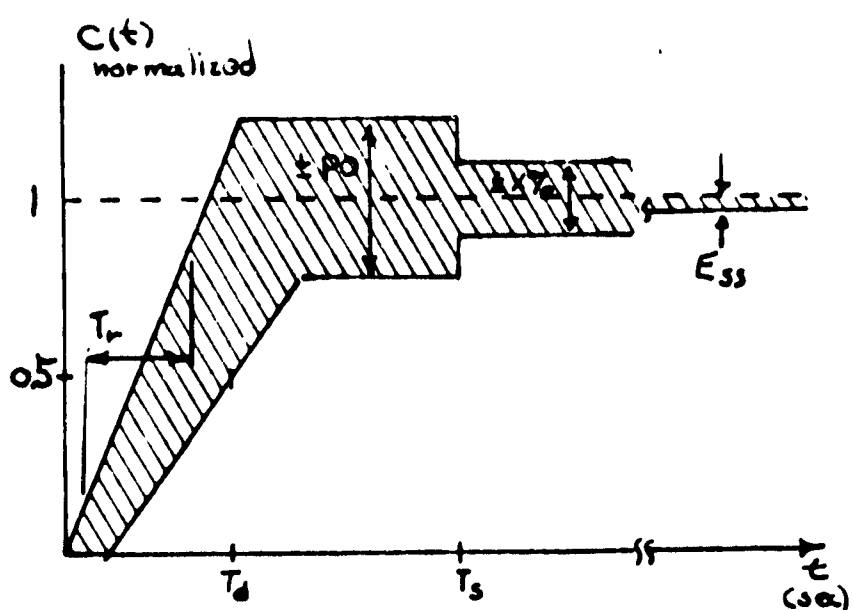


Fig. 3. Specification of $c(t)$

measured by FVE. The Final Value of Error is determined experimentally in the time domain, but is also easily computed in the frequency domain. This measure, therefore, seems to be basic.

Specification of the input-output dynamics involves the assignment of values or ranges of values to these time or frequency domain measures. These measures can be grouped according to the system characteristic each describes: accuracy, stability, speed or sensitivity.

Accuracy

For any input represented by the polynomial $r(t) = \sum_{n=0}^N a_n t^n$, the final value of error may be calculated from the Laplace transform of the error transfer function:

$$\frac{U(s)}{R(s)} = \frac{1}{1 + G(s)H_{eq}(s)}$$

where the disturbance $Q(s)$ of Figure 2a is neglected.

Maclaurin Taylor series expansion of the right hand side defines the error constants which relate the system's error to the input, as

$$\frac{U(s)}{R(s)} = \frac{1}{1 + K_p} + \frac{1}{K_v} s + \frac{1}{K_a} s^2 + \dots \quad (2.2)$$

These error constants, K_p , K_v , K_a , for steady-state position, velocity, and acceleration error, are the most convenient form for expressing the error of the system's response. They may be computed (Truxal 1955) in terms of closed-loop pole-zero locations, and gain, with tractable formulas. This feature, plus the hybrid quality of the measurement, make the error constants a desirable performance measure.

In this study, it is assumed that the system being designed has zero steady-state position-error, i.e., $K_p = \infty$. The specification of accuracy for the remaining classes of inputs is restricted to the steady-state velocity error. This error is equal to the input-ramp

slope a_1 , divided by K_v , the velocity error coefficient. In general, K_v is made as large as possible for satisfactory system accuracy in tracking a ramp input.

Stability

The relative stability of the system can be specified either in the time domain by P_0 or in the frequency domain by M_p . The specification of stability is unique in the sense that it is the only measure which may be specified by other than a "large" or "small" qualitative criteria. It has been shown (D'Azzo and Houpis 1960) that P_0 should be between ten and forty per cent or that M_p should have a value from 1.1 to 1.5 for "good" system response (Truxal 1955).

The measure M_p indicates the least stable response of the system to sinusoidal inputs. If systems are to be cascaded, it may be important that the M_p of the individual systems do not coincide. Thus, ω_p should be specified when systems are cascaded. The stability specification stressed in this thesis is P_0 because it is the best and most commonly used of all closed-loop stability measurements.

Speed

Bandwidth in the frequency domain and T_d , T_r and T_s in the time domain are performance measures which are used to specify system speed. The speed of the system should be fast enough to respond to the expected range of

input signals and slow enough so that the system does not respond to noise. All of these measures are popular for use as specifications. In this thesis, BW is stressed for convenience, but solutions for T_r and T_d are given for the simplest (second order) and the most complex (third order with zero) models discussed.

Sensitivity

The fourth performance area, sensitivity, is the most difficult to specify because it is a function of frequency. In almost all system applications, the sensitivity to unwanted disturbances should be made as small as possible. The sensitivity measure Z_o is made even more difficult to handle since the transfer function $Z(s)$ may not be completely known or linear.

The specification of Z_o or DR may be simplified, with some loss of information, by specifying its "worst-case" (maximum) value. This is tantamount to specifying the entire dynamic response, $C(s)/R(s)$, by just one "worst-case" value M_p . The Deviation Ratio, or its reciprocal, $|1 + G(s) H_{eq}(s)|$ is stressed in this study, not only because $Z(s)$ adds unnecessary complication, but because

$$|1 + G(s) H_{eq}(s)| \geq 1 \quad (2.3)$$

defines a condition for optimality (Schultz and Melsa 1967).

Summary

The time and frequency domain performance measures indicating speed (T_d , T_r , T_s and BW), stability (PO and M_p), accuracy (K_v) and sensitivity (DR) have been defined and are used in the next chapter to specify a desired model transfer function, $C(s)/R(s)$. Deviation ratio, its effect on several classical sensitivity measures, and its relationship to optimal control systems are extensively discussed in Chapter IV.

CHAPTER III

THE SPECIFICATION AND SOLUTION OF LOW-ORDER MODELS

In this chapter, graphical and, where possible, analytical techniques for determining a desired low-order transfer function, $C(s)/R(s)$, are presented. This model's existence and the means of locating its poles and zeros from performance specifications of Chapter II, are discussed. Three models and their design charts are given in the order of increasing complexity:

1. The second-order model without zeros.
2. The second-order model with one zero.
3. The third-order model with one zero.

In an example problem which concludes the chapter, a low-order plant is series-compensated and feedback coefficients are determined for the realization of the desired model closed loop transfer function, $C(s)/R(s)$.

Background

A low-order model can usually be found to meet a combination of performance specifications measuring speed, stability and accuracy, if the specifications are not self-contradictory. The performance of a high-order system meeting very stringent specifications, can be closely duplicated by a low-order model.

The existence of the low-order approximation is verified by the arguments of dominate root approximation (D'Azzo and Houpis 1960) and a similar method of duplicating open-loop transfer functions in a narrow region near the crossover frequency (Chen 1957).

The system's time response is dominated by transient components contributed by dominate roots (those relatively near the origin) if:

1. The other poles are far enough to the left of the dominate poles so that the transients due to these poles quickly decay.
2. The other poles are far enough away from the dominate poles or near enough to a zero that the initial magnitude of the transients are small.

When either of these conditions are met, the dominate pole response closely resembles the actual response. Neglecting the other poles results in a slightly faster response.

Analogous arguments in the frequency domain support the validity of low-order model approximations. The open-loop transfer function $G(j\omega)H_{eq}(j\omega)$ can be sufficiently described by its behavior in a narrow region, i.e., $\pm 15\text{db}$, near the gain-crossover frequency. Roots located to the left are approximated by a constant gain while those to the right are neglected, as shown in Figure 4. The desired $C(s)/R(s)$ model constructed from the approximation of $G(s)H_{eq}(s)$ derived in this manner is similar to the

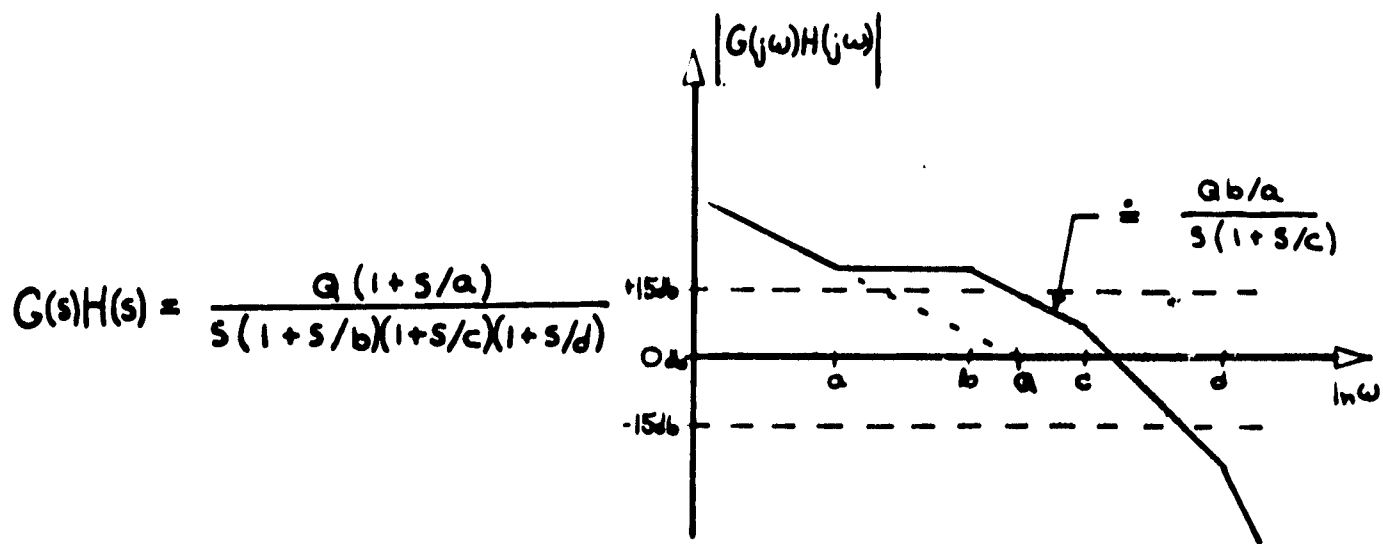


Fig. 4. Low Order Approximation of High Order Response

dominate pole approximation just mentioned. In conclusion, low-order models of one, two or three poles and up to one zero can be found which cover the spectrum of possible step or sinusoidal responses.

Having established the existence of low-order models meeting compatible performance specifications, the formalization of the construction of that model is now presented. The model is made to meet the stability, speed and accuracy specifications of the previous chapter. In general, the order of the model is determined by the number and severity of those specifications. The assumption of underdamped response rules out a first-order model. Specification of zero steady-state velocity error requires the use of a zero in the second- or third-order models. If more than two specifications (other than K_v) are to be realized, the third-order model must be used.

The requirement of a pair of complex poles for an underdamped response permits normalization of the s -domain by the natural undamped frequency, ω_n , of those poles for the three models to be discussed. This makes it possible to decrease the number of independent parameters by one, so that the dimensionality of the design charts is similarly decreased. All design charts apply to the normalized model having complex-conjugate poles on the unit circle in the $s_n = s/\omega_n$ plane. The time domain is correspondingly normalized, $t_n = t \cdot \omega_n$.

The Second-Order Model Without Zeros

The simplest and therefore most well known underdamped system is the second-order system without zeros. This second-order model is written as:

$$C(s)/R(s) = \frac{\omega_n^2}{s^2 + 2\zeta\omega_n s + \omega_n^2} \quad (3.1)$$

with a damping ratio ζ . This model has a zero steady-state position error but a finite velocity error.

Equation (3.2), the normalized model equation, is obtained by dividing the Laplacian operator, s , in Equation (3.1), by ω_n .

$$C(s_n)/R(s_n) = \frac{1}{s_n^2 + 2\zeta s_n + 1} \quad (3.2)$$

The frequency response of this system is plotted in many basic control-system texts (Thaler and Brown 1960). The designer may use these curves to determine ζ for any M_p , ω_p/ω_n or BW/ω_n , or he may solve for these performance measures using analytical expressions:

$$BW/\omega_n = \left[1 - 2\zeta^2 + \sqrt{2 - 4\zeta^2 + 4\zeta^4} \right]^{1/2} \quad (\text{Truxal 1955})$$

$$M_p = 1/2 \zeta \sqrt{1 - \zeta^2} \quad (\text{Sawant 1958})$$

$$\omega_p/\omega_n = \sqrt{1 - \zeta^2} \quad (\text{D'Azzo and Houpis 1960})$$

The time response to a unit step for this model is easily found to be

$$c(t) = 1 - e^{-\zeta \omega_n t} \left[\cos \omega_n \sqrt{1-\zeta^2} + \sqrt{\frac{\zeta^2}{1-\zeta^2}} \sin \omega_n \sqrt{1-\zeta^2} \right]$$

where $\zeta < 1$. Analytical solutions for T_r , T_p , T_s and PO , given ζ , may be obtained from this expression, so that

$$T_r \cdot \omega_n = \frac{7.04^2 + 0.2}{2\zeta} \quad \text{for } 0.1 \leq \zeta \leq 1.0$$

(Graham, McRuer et al. 1962)

$$T_d \cdot \omega_n = 1 + 0.7\zeta \quad (\text{Graham, McRuer et al. 1962})$$

$$PO = 1 + e^{-\zeta \pi / \sqrt{1-\zeta^2}} \quad (\text{Truxal 1955})$$

$$T_s \cdot \omega_n \approx 3/\zeta$$

for $\zeta < 0.9$ and $x = 5$

(Grabbe, Ramo and Wooldridge 1958)

and

$$\frac{1}{K_v} = \sum \frac{2\zeta}{\omega_n} + \sum \frac{1}{\text{poles of } C/R} - \sum \frac{1}{\text{zeros of } C/R}$$

(Truxal 1955)

The most straight forward solution of the second-order model is the graphical one obtained from plots of performance measures versus the damping ratio, as shown in Figure 5. These curves, developed by Hauserbauer (1957), Truxal (1955) and others, give frequency domain measures normalized by ω_n and time domain measures normalized by $1/\omega_n$ for the model of Equation (3.2).

The second-order model provides two adjustable parameters, ζ and ω_n , with which any one of the stability specifications (M_p , P_0) and any one of the speed specifications may be exactly realized if finite. The damping ratio is determined by the stability measure. The remaining parameter ω_n , can then be chosen, and the model scaled to meet one of the speed measurements (BW , T_r , T_d , T_s). If one or both of these specifications lead to a permissible range of parameter choices, the added flexibility can be used to increase K_v .

If a second-order model can be found to meet all requirements except accuracy, then dipole compensation should be added to increase K_v to the desired value or

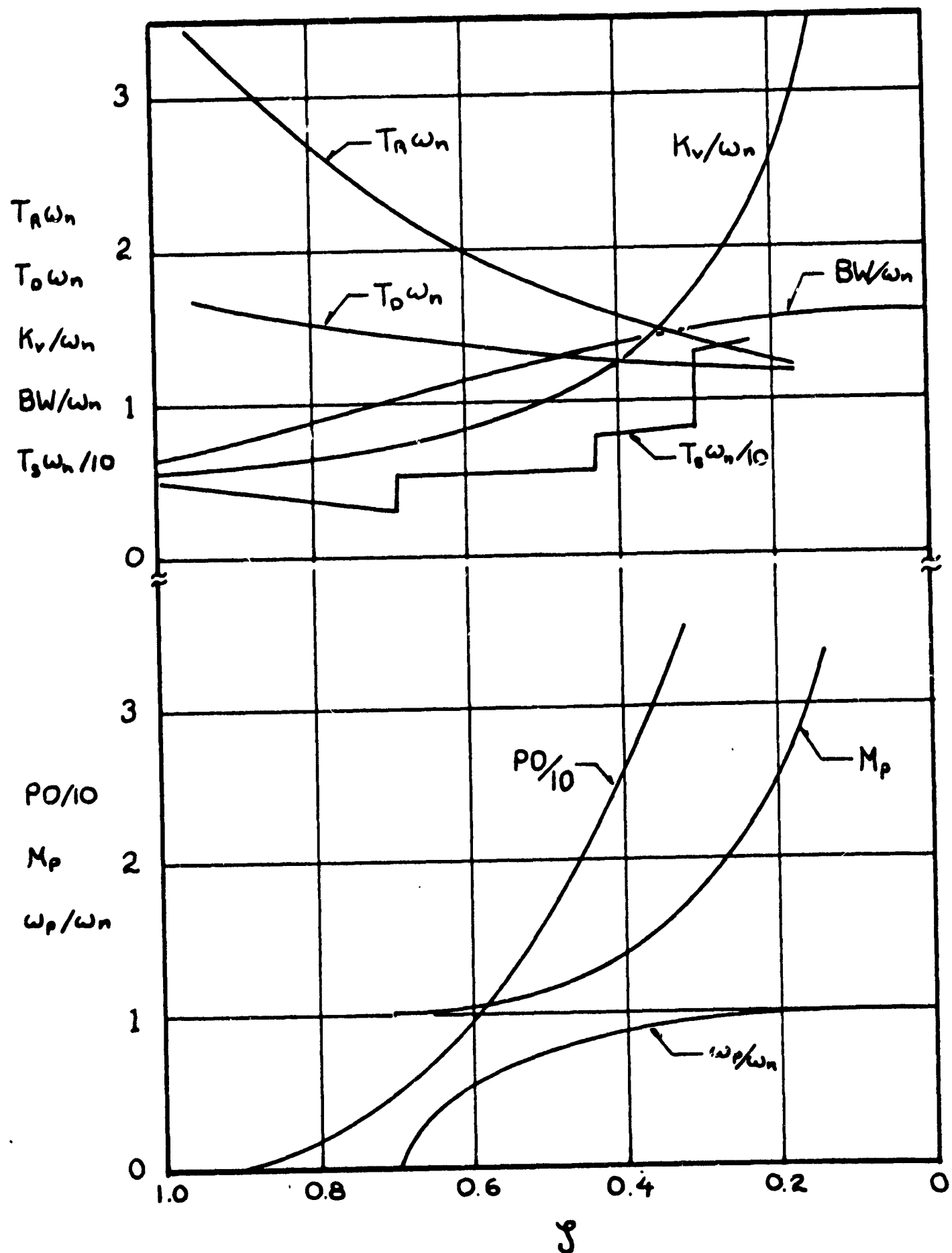


Fig. 5. Performance Measures of Second-Order Systems

infinity. The dipole addition places a pole and zero very close to the origin so that the transient response is altered only by the addition of small but slowly decaying transient in such a fashion that K_v is correctly increased according to Equation (2.2).

A simple example illustrates the procedure outlined above:

Specifications: $P_0 = 25\%$, $T_s = 5$ seconds

Synthesis: From the stability specifications plot in Figure 5, read the required damping ratio $\zeta = 0.45$. From the same figure, read the value of normalized setting time $T_s \cdot \omega_n / 10 = 5.5$. Solving for ω_n : $\omega_n = 11$ rad/sec.

$$C(s)/R(s) = \frac{121}{s^2 + 10s + 121}$$

The Second-Order Model With One Zero

The second-order model with one zero can be chosen such that any speed (BW), stability (P_0) or accuracy (K_v) specification is met, including an infinite velocity error coefficient. All three system parameters, ω_n , ζ and z (the negative real-axis zero) of the model, Equation (3.3), affect both time and frequency domain performance measures. The addition of a zero to a model having only a pair of

complex poles increases the system's speed and accuracy, while decreasing its stability.

$$C(s)/R(s) = \frac{\omega_n^2}{z} \frac{s + z}{s^2 + 2\zeta\omega_n s + \omega_n^2} \quad (3.3)$$

The performance measures for the normalized form of Equation (3.3), given in Equation (3.4), are plotted in Figure 6. The damping ratio ζ and velocity error coefficient are plotted as a family of curves in the z/ω_n - P_0 plane. Bandwidth is given at selected points in this plane, adding a third dimension of freedom and difficulty.

$$C(s_n)/R(s_n) = \frac{\omega_n}{z} \frac{(s_n + z/\omega_n)}{s_n^2 + 2\zeta s_n + 1} \quad (3.4)$$

The choice of ω_n can be delayed to last if the chart's normalized performance measures, K_v/ω_n and BW/ω_n , are taken as a ratio. The desired ratio, obtained from the specification of K_v and BW , can then be located on the chart for any P_0 , thereby determining ζ and z/ω_n . The synthesis of $C(s)/R(s)$ from performance specifications is completed by using the bandwidth specification to determine ω_n . The procedure is best illustrated by an example.

Specifications: $P_0 = 25\%$, $K_v \geq 400$ and $150 \text{ rad/sec} \leq BW \leq 200 \text{ rad/sec}$.

Synthesis: By observing Figure 6, it can be seen

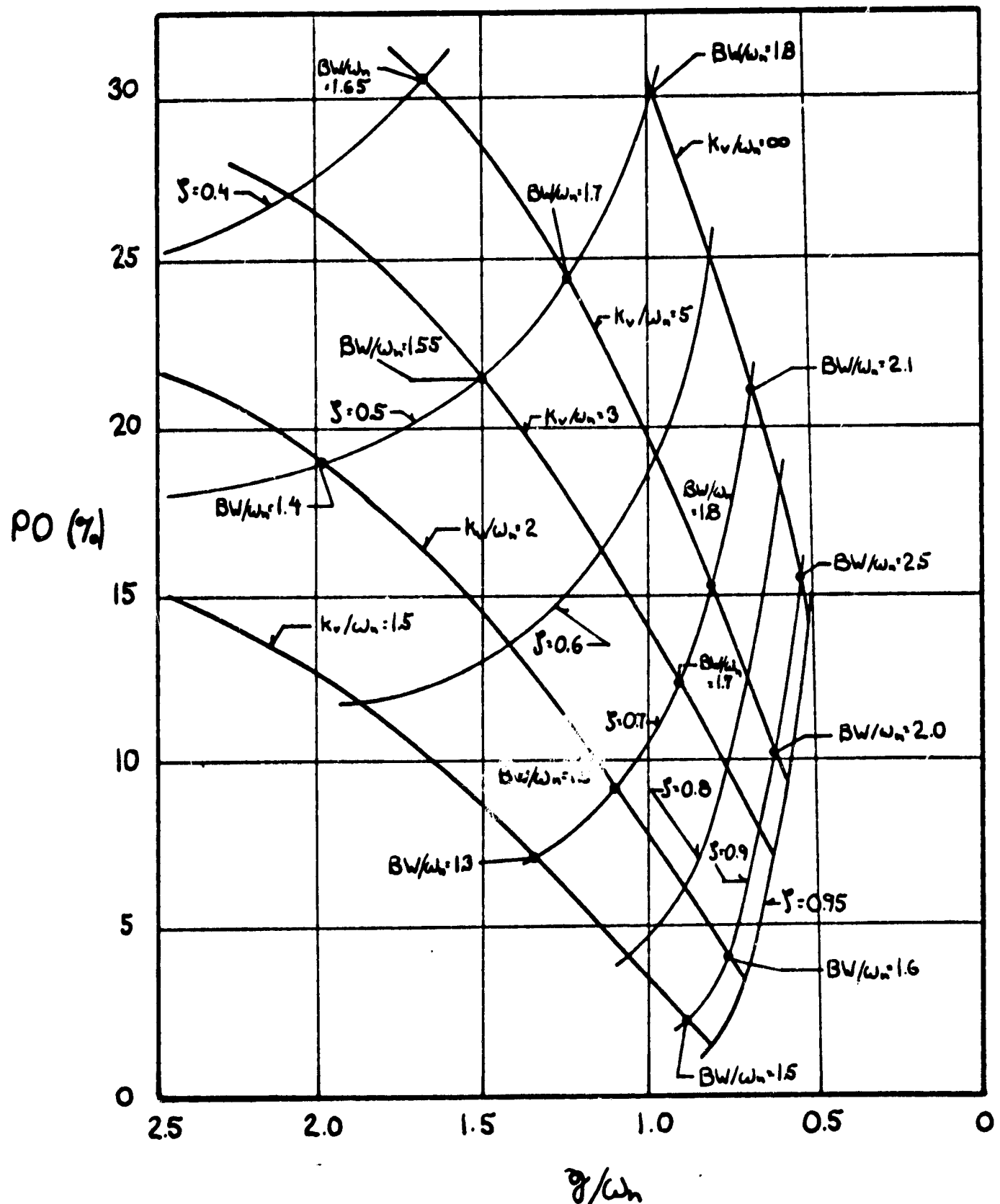


Fig. 6. Performance Measures of Second-Order System with One Zero

that any K_v may be obtained from the model and the stability specification met if $\zeta \geq 0.6$ and $z/\omega_n \geq 0.6$. A damping ratio of 0.7 is selected and ratios of $(K_v/\omega_n)/(BW/\omega_n)$ along this curve are calculated. A comparison of the minimum desired ratio,

$$K_v/BW = 400/200 = 2$$

with the calculated ratios indicates that the zero location must be less than $0.85 \omega_n$. A value of $z/\omega_n = 0.8$ is chosen and ω_n may be calculated from $BW/\omega_n = 1.8$

For a median value of bandwidth, $BW = 180$ rad/sec, the result is $\omega_n = 100$ rad/sec. The velocity error coefficient for the parameters chosen is $K_v = 5 \cdot \omega_n = 500$. The model equation is therefore,

$$C(s)/R(s) = 1.25 \cdot 10^3 \frac{s + 80}{s^2 + 140s + 10^4}$$

The Third-Order Model

The closed-loop transfer function with three poles has the same number of adjustable design parameters as the second-order model with one zero, but the performance of this function is much more sluggish and less accurate. The limited usefulness of a model having only three poles

suggests that it be cast aside in favor of third-order models with zeros.

The third order model with one zero is expressed in Equation (3.5). This equation also applies to the second-order model with a dipole mentioned earlier in this chapter. This section concentrates on selection of the four parameters, ζ , ω_n , z and ρ (the negative real-axis pole location), in such a way that not only is K_v determined by z and ρ as in the dipole addition, but speed and stability characteristics are also adjusted. It will be seen in Chapter IV that when $\rho \gg \omega_n$ the system insensitivity is greatly improved.

$$C(s)/R(s) = \frac{\omega_n^2 \rho}{z} \frac{(s + z)}{(s^2 + 2\zeta \omega_n s + \omega_n^2)(s + \rho)} \quad (3.5)$$

For the normalized model of Equation (3.6), the graphical determination of the system's parameters would require a three dimensional plot for each normalized performance measure. The design charts of Figure 7 and Figure 8 restrict the choice of ζ to two values: 0.5 and 0.7 respectively. The normalized parameter, ρ/ω_n , is used to determine speed and stability measures. Accuracy, K_v , is held fixed by the correct placement of z/ω_n . These design charts, obtained from Hausenbauer (1957), lead to three general conclusions concerning the normalized parameter, ρ/ω_n .

Fig. 7. Performance Measures for Third-Order System
with One Zero and Damping Ratio of 0.5

$$\zeta = .5$$
$$K_v/\omega_n = \begin{cases} 1.5 & \text{---} \\ 2 & \cdots\cdots \\ 5 & \text{----} \end{cases}$$

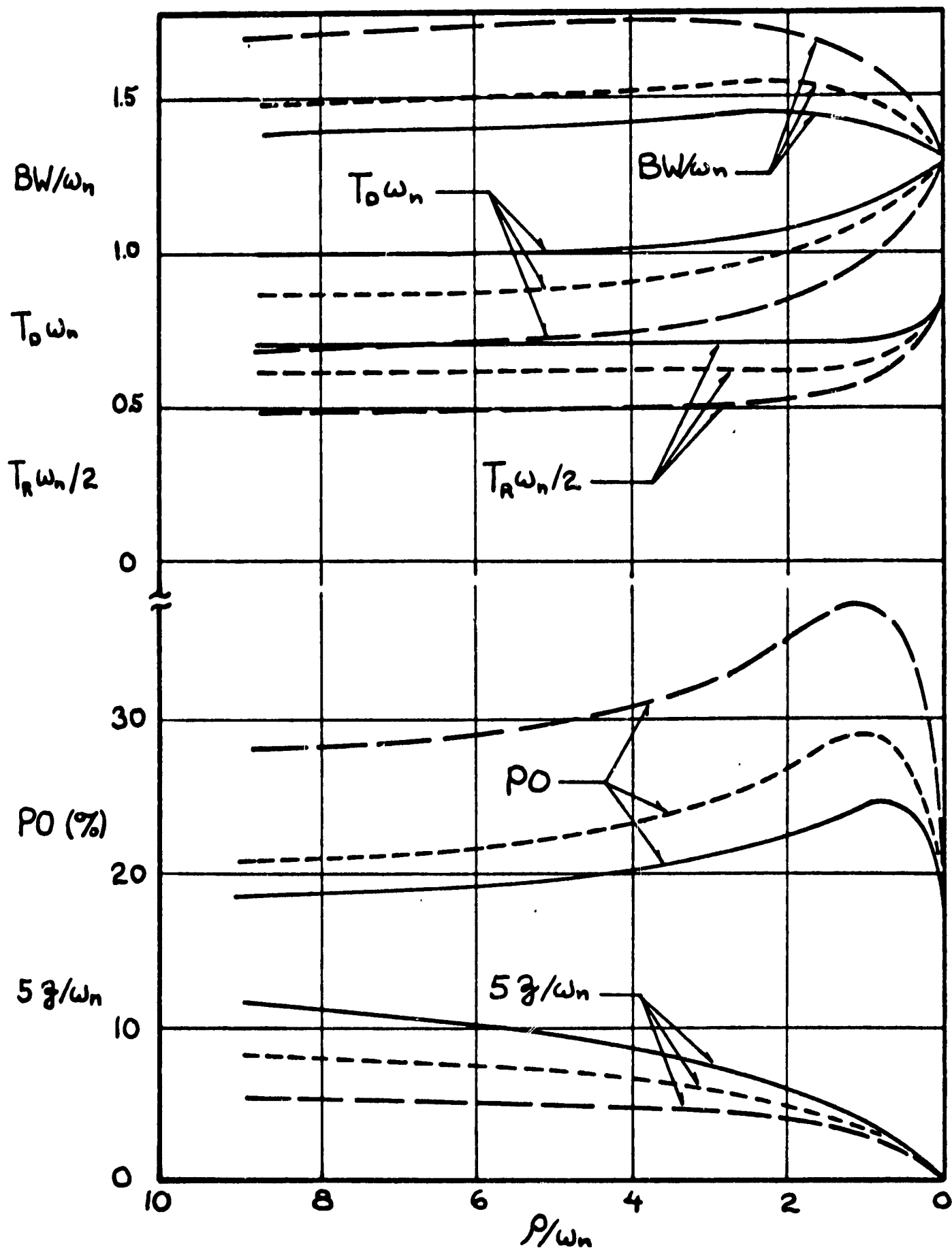


Fig. 7. Performance Measures for Third-Order System with One Zero and Damping Ratio of 0.5

**Fig. 8. Performance Measures for Third-Order System
with One Zero and Damping Ratio of 0.707**

$$\zeta = .707$$
$$K_v/\omega_n = \left\{ \begin{array}{ll} 1.5 & \text{---} \\ 2 & \text{-----} \\ 5 & \text{---} \\ \infty & \text{---} \end{array} \right.$$

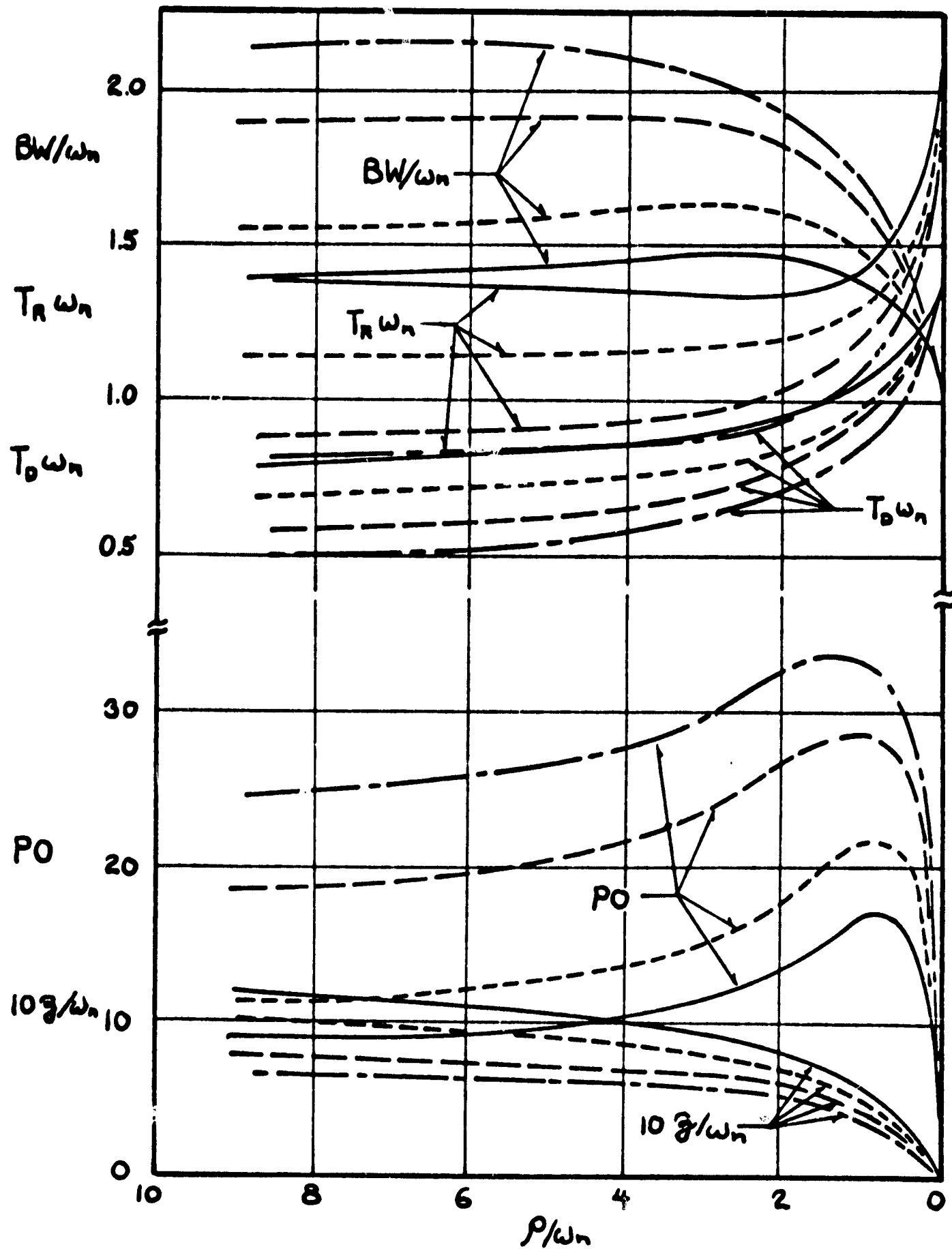


Fig. 8. Performance Measures for Third-Order System with One Zero and Damping Ratio of 0.707

1. For a given K_v the bandwidth remains approximately constant and equal to the value of a second-order single-zero model having a similar damping ratio. This correspondence holds for $\rho/\omega_n > 1$.
2. For $\rho/\omega_n = 1$, the model has an additional 10% overshoot compared to a second-order, single-zero model with similar K_v and ζ .
3. For $\rho/\omega_n < 1$ the model quickly approaches the performance of a dipole compensated second-order model.

The particular method of synthesis using the design charts is determined by the specifications given. The following example illustrates one of those procedures.

Specifications: $100 \text{ rad/sec} \leq \text{BW} \leq 150 \text{ rad/sec}$, $K_v \geq 200$, $PO = (20 \pm 1)\%$.

Synthesis: Note that for $\zeta = 0.7$ (selected arbitrarily) and $\rho/\omega_n > 1$, BW/ω_n is from 1.5 to 2.0. Using "worst-case" values of the specified BW, ω_n is restricted to the range $66 \text{ rad/sec} \leq \omega_n \leq 75 \text{ rad/sec}$. Then for a satisfactory K_v , the plots of $K_v/\omega_n = 3$ (or greater) must be used.

Select $K_v/\omega_n = 4$, giving $K_v = 280$. Performance measure plots for this value must be interpolated from the $K_v/\omega_n = 2$ and $K_v/\omega_n = 5$ plots.

The stability specification requires that for $\zeta = 0.7$ and $K_v/\omega_n = 4$,

$$3 < \rho/\omega_n < 4.3$$

Also, for these values, BW/ω_n is approximately 1.8.

The range of permitted pole positions can be chosen on the basis of T_d or T_r . Delay time is usually desired as small as possible, so the value

$\rho/\omega_n = 4.3$ or $\rho = 4.3 \omega_n = 300$ rad/sec is chosen minimizing T_d . The model having $K_v = 280$, $BW = 126$ rad/sec, $PO = 19\%$, and $T_d = 10^{-2}$ sec., $T_r = 14 \cdot 10^{-3}$ sec. is then

$$C(s)/R(s) = 3 \cdot 10^4 \frac{(s + 49)}{(s^2 + 100s + 4900)(s + 300)}$$

It should be noted that if the plant were second-order and of the form

$$G_p(s) = \frac{3 \cdot 10^4}{s(s + \beta)}$$

where β is positive, a series compensator of the form

$$G_c(s) = \frac{s + 49}{s + \alpha}$$

where $0 \leq \alpha \leq 300$ rad/sec, could be added and feedback coefficients k_2 and k_3 ($k_1 = 1$, for $K_p = \infty$) determined by equating coefficients in Equation (3.6).

$$C(s)/R(s) = \frac{G(s)}{1 + G(s)H_{eq}(s)} \quad (3.6)$$

Summary

Methods for synthesizing low-order, closed-loop transfer functions have been developed from performance measures of Chapter II. If the forward transfer function can be compensated to have zeros identical to those of the model and the same number of poles as the model, then the synthesis is completed by solving for the feedback coefficients.

When the plant is complicated by having zeros not found in $C(s)/R(s)$ or more than three poles, two alternatives are possible. The most difficult of these alternatives is to specify a high-order model from the specifications. The other method, to be explained in Chapter V, is to specify a low-order, "ideal" model and extend it to the desired high-order form as required by the forward transfer function.

In the next chapter, the equation forming the foundation for the model extension is developed. It is shown that this equation also relates the compensated plant to the model being specified through the sensitivity measure, $DR(s)$.

CHAPTER IV

THE SENSITIVITY-OPTIMALITY CONDITION

The performance area, sensitivity, is intimately related to optimal control systems by the Sensitivity-Optimality Condition. Equation (2.3) is repeated here for convenience.

$$\left| 1 + G(s)H_{eq}(s) \right| \geq 1$$

In this chapter, examples of classical sensitivity functions are shown to be related to Equation (2.3). Graphical and, for low-order cases, analytical techniques are developed for determining $DR^{-1}(s)$. The implications of the Sensitivity-Optimality Condition in terms of the open-loop and closed-loop transfer functions are then stated.

It is shown that if this condition is met, the resulting closed-loop transfer function minimizes a quadratic cost function of $\underline{x}(t)$ and $u(t)$.

Classical Sensitivity

The system's sensitivity to disturbances at the output is defined in Chapter II. The appearance of $(1 + G(s)H_{eq}(s))$ in the equation defining $Z_o(s)$ in terms of open-loop functions is the first illustration of its

importance. In this section $DR^{-1}(s)$ is shown to be of similar importance to the system's sensitivity to variations in open-loop gain, K_1 , and to open-loop pole movements.

The sensitivity of $C(s)/R(s)$ to gain K_1 is defined as:

$$\frac{C/R}{K_1}(s) \triangleq \frac{K_1}{C(s)/R(s)} \frac{\partial}{\partial K_1} [C(s)/R(s)]$$

For the single-input, single-output system shown in Figure 9, the sensitivity function is easily calculated illustrating the importance of making $1 + G(s)H_{eq}(s)$ as large as possible.

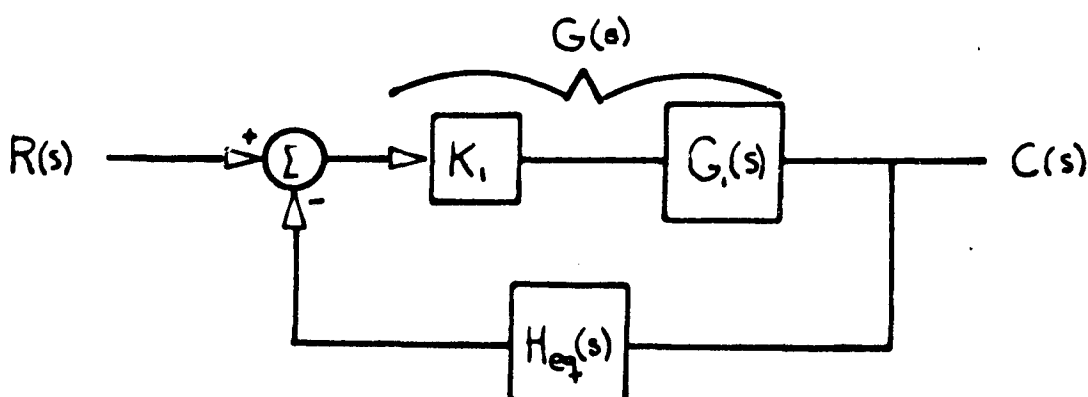


Fig. 9. Single-Input, Single-Output System

For Figure 9 $C(s)/R(s)$ is

$$C(s)/R(s) = \frac{K_1 G_1(s)}{1 + K_1 G_1(s) H_{eq}(s)}$$

and

$$\frac{C/R}{K_1}(s) = K_1 \left[\frac{1 + K_1 G_1(s) H_{eq}(s)}{K_1 G_1(s)} \right] \left[\frac{G_1(s)}{(1 + K_1 G_1(s) H_{eq}(s))^2} \right]$$

$$= [1 + G(s) H_{eq}(s)]^{-1}$$

The sensitivity of $C(s)/R(s)$ to the movement of an open-loop pole at $-\alpha$, shown as an interior block of the system in Figure 10, is similarly defined and calculated.

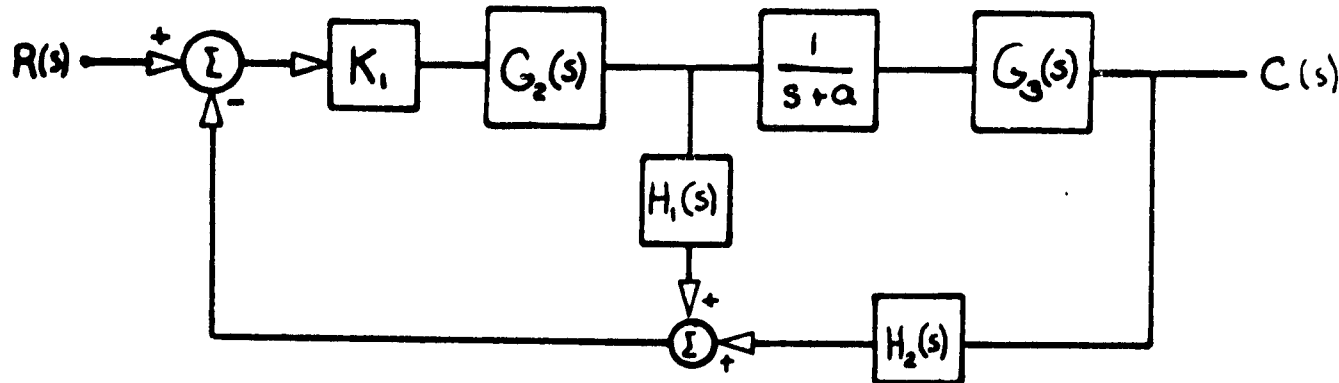


Fig. 10. System With Open-Loop Pole at α

If sensitivity is defined as

$$\frac{C/R}{\alpha}(s) \triangleq \frac{\alpha}{C(s)/R(s)} \frac{\partial}{\partial \alpha} [C(s)/R(s)]$$

and another function $F(s)$ as:

$$F(s) \triangleq 1 + K_1 G_2(s) H_1(s)$$

and

$$G(s) = K_1 \frac{G_2(s) G_3(s)}{(s + \alpha)}$$

$$H_{eq}(s) = H_2(s) + \frac{s + \alpha}{G_2(s)} H_1(s)$$

Then

$$\begin{aligned} \frac{C}{R}(s) &= \alpha \left[\frac{1 + G(s) H_{eq}(s)}{G(s)} \right] \frac{\partial}{\partial \alpha} \left[\frac{K_1 G_2(s) G_3(s)}{s F(s) + K_1 G_2(s) G_3(s) H_2(s) + \alpha F(s)} \right] \\ &= -\alpha \frac{F(s)/(s+\alpha)}{1+G(s)H_{eq}(s)} \end{aligned}$$

The importance of making $|1 + G(s) H_{eq}(s)|$ as large as possible for all 's' has again been demonstrated.

In its present form, a plot of $DR^{-1}(s)$ along the $j\omega$ -axis would require calculation of the K 's to form $H_{eq}(s)$. This would make the use of $DR^{-1}(s)$ in specifying $C(s)/R(s)$ a difficult and time consuming process. By writing $DR^{-1}(s)$ in terms of the projected model $C(s)/R(s)$ and the open-loop plant $G(s)$, the design procedure can quickly determine $DR^{-1}(s)$ for any model chosen. The model chosen must have the same order and gain as the plant, and is now further related to $G(s)$ by the sensitivity measure.

Assume the forward and open-loop transfer functions are written as

$$G(s) = K_1 \frac{N(s)}{D(s)}, \quad C(s)/R(s) = K \frac{N(s)}{D_c(s)}$$

They must have identical zeros. The static loop-sensitivity K_1 must equal K since $H_{eq}(s)$ has $(n - 1)$ zeros, where n is the order of both $D(s)$ and $D_c(s)$. By expanding the closed-loop transfer function in terms of $G(s)$, it is seen that

$$1 + G(s)H_{eq}(s) = \frac{R(s)}{C(s)} G(s) = D_c(s)/D(s)$$

therefore,

$$DR^{-1}(s) \equiv |1 + G(s)H_{eq}(s)| = |D_c(s)/D(s)| \quad (4.1)$$

This function has one important feature; since the order of each polynomial is n , $DR^{-1}(s)$ must always approach unity (1/0°) as s becomes infinite.

It is instructive to form analytic expressions for the second and third-order cases. Once again, the normalized form of $C(s)/R(s)$ and $G(s)$, ($G(s/\omega_n)$) are used without loss of generality. The second-order, normalized model first introduced in Chapter III is

$$C(s_n)/R(s_n) = \frac{1}{s_n^2 + 2s_n + 1}$$

which corresponds to a forward transfer function

$$G(s_n) = \frac{1}{s_n(s_n + \alpha/\omega_n)}$$

where α is the unnormalized plant pole shown in Figure 11.

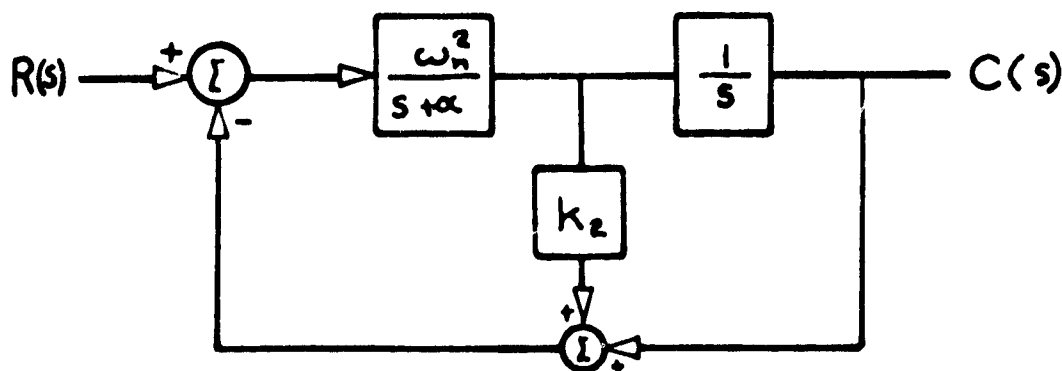


Fig. 11. Second-Order System with State Variable Feedback

Expanding Equation (4.1), in terms of $j\omega$, where

$$s_n = j\omega, \text{ and } A = \alpha/\omega_n$$

$$DR^{-1}(j\omega) = \left[\frac{-\omega^2 + j2\zeta\omega + 1}{-\omega^2 + j\omega A} \frac{-\omega^2 - j2\zeta\omega + 1}{-\omega^2 - j\omega A} \right]^{1/2}$$

A reasonable criteria for $DR^{-1}(j\omega)$ is that it be greater than unity, i.e., the Sensitivity Optimality Condition, Equation (2.3). This condition is met when

$$\zeta \geq \left[\frac{2 + A^2}{4} \right]^{1/2} \quad (4.2)$$

Equation (4.2) indicates that at best ($A = 0$), the damping for a second-order, closed-loop transfer

function should be greater than 0.707. Thus sensitivity is improved by increasing ζ corresponding to increased accuracy and stability.

The analytical solution for the parameters of a third-order system (ρ and z) that meet the Condition Equation is much more interesting. The normalized model and forward transfer functions are

$$C(s_n)/R(s_n) = \frac{\rho/\omega_n}{(s_n^2 + 2\zeta s_n + 1)(s_n + \rho/\omega_n)}$$

and

$$G(s_n) = \frac{\rho/\omega_n}{s_n(s_n + \alpha/\omega_n)(s_n + \beta/\omega_n)}$$

Substitution of the denominators into Equation (4.1) and setting $DR(jW)_{-1} > 1$ leads to the following equation

$$\left[4\zeta^2 + P^2 - A^2 - B^2 - 2\right]Y^4 + \left[4\zeta^2 P^2 - 2P^2 - B^2 A^2 + 1\right]Z^2 + P^2 \geq 0$$

where $P = \rho/\omega_n$ and $B = \beta/\omega_n$. The coefficient of Y^4 , Y , must be positive if the inequality is to hold as W becomes infinite. The restriction on the coefficient of Z^2 , Z , depends on the magnitude of Y and P and is unwieldy. But, the increased flexibility of the third-order case is evident in the expression obtained by requiring Y to be positive.

$$\zeta \geq \left[\frac{2 + A^2 + B^2 - P^2}{4} \right]^{1/2} \quad (4.3)$$

Thus if the closed-loop pole P is made large enough (greater than $A^2 + B^2 + 2$), ζ is limited only by stability considerations. Comparison of Equations (4.2) and (4.3) leads to the conclusion that a necessary condition for systems of any order, n , is

$$\zeta \geq \left[\frac{2 + \sum_n [\text{poles of } G(s_n)]^2 - \sum_n [\text{poles of } C(s_n)/R(s_n)]^2}{4} \right]^{1/2} \quad (4.4)$$

Graphical techniques for high-order systems provide more insight in placing the poles of $C(s_n)/R(s_n)$ for a given $G(s_n)$. A straight-line approximation of $|D_c(jW)/D(jW)|$ is quickly drawn using the property

$$\lim_{W \rightarrow \infty} \left| \frac{D_c(jW)}{D(jW)} \right| = 1$$

mentioned before. Starting at a large value of W , where $DR^{-1}(jW) = 1$, the function is plotted as W is decreased, making the usual slope changes at the breakpoints of $D_c(jW)$ and $D(jW)$.

The procedure is demonstrated by obtaining the straight line plot of $DR^{-1}(jW)$ for the example problem of Chapter III. The model and forward transfer functions of that example are:

$$C(s)/R(s) = 3 \cdot 10^4 \frac{s + 40}{(s^2 + 100s + 4000)(s + 300)}$$

and

$$G(s) = 3 \cdot 10^4 \frac{s + 40}{s(s + a)(s + b)}$$

By writing only the denominator of each and normalizing by $\omega_n = 70$ rad/sec the results are

$$D_c(s_n) = (s_n^2 + 1.4s_n + 1)(s_n + 4.3)$$

and

$$D(s_n) = s_n(s_n + A)(s_n + B)$$

Let the compensator pole \bar{b} be at 56 rad/sec, then $B = 0.8$.

The sensitivity measure, $DR^{-1}(j\omega)$ is plotted in Figure 12, for the various values of pole position A . The importance of placing the model pole further from the origin than all plant poles is indicated. The magnitude of $DR(j\omega)^{-1}$ is greatest at all frequencies for the plant pole A_3 .

In conclusion, the closed-loop transfer function is least sensitive to output disturbances, static-loop sensitivity variations and plant pole movements when the closed-loop poles are placed far from $s = 0$. Since the static-loop sensitivity for systems using state-variable feedback and having zero steady-state position error is equal to the product of closed-loop poles, divided by the

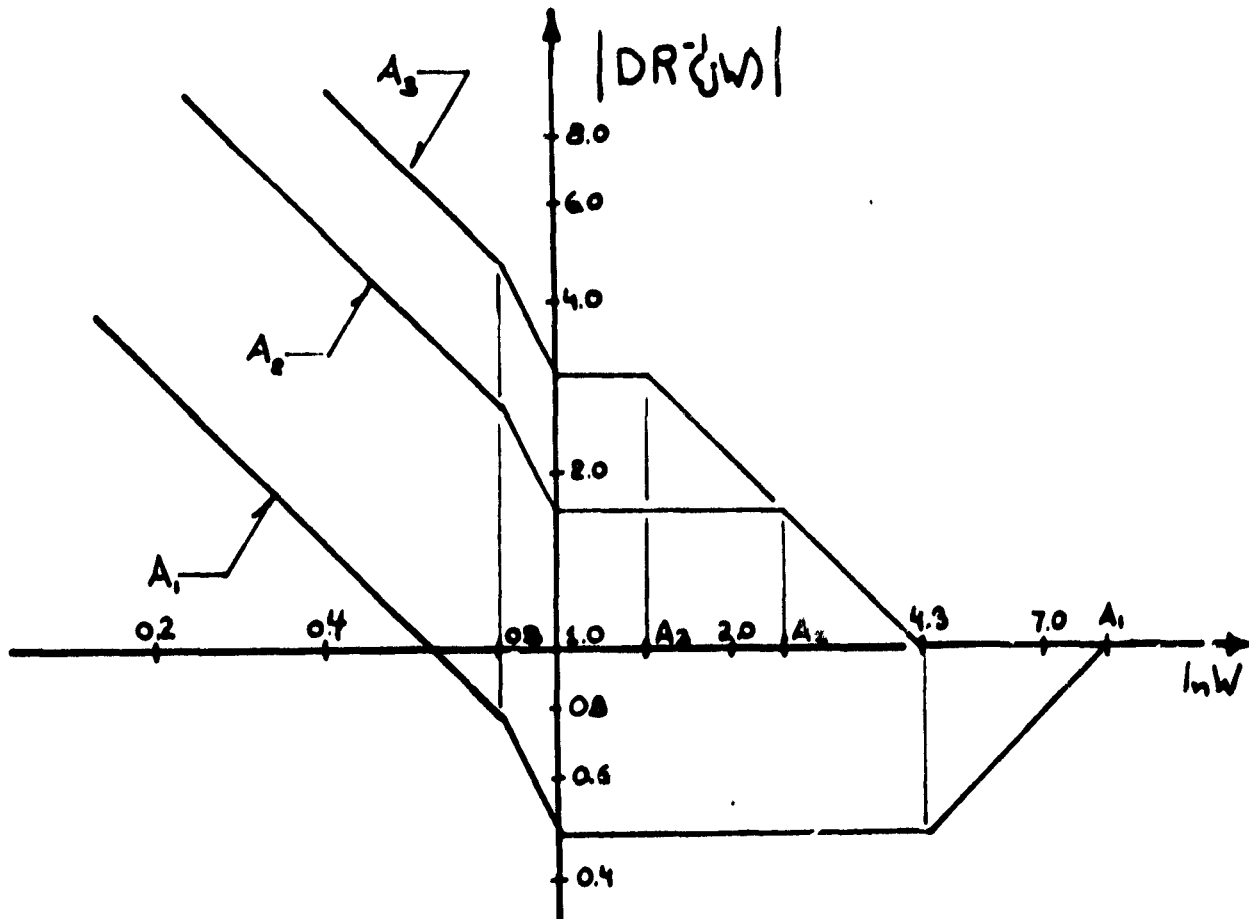


Fig. 12. A Typical Plot of $DR^{-1}(jw)$ for $n = 3$

product of closed-loop zeros, K must also be large. In the next section, it is shown that not only is sensitivity decreased by making $DR^{-1}(s)$ large, but also that the closed-loop model defined by $C(s)/R(s)$ is optimized.

Optimality

The performance measures of Chapter II are used to specify a model transfer function in Chapter III. These measures are often used to judge the "goodness" of the system's response; i.e., the system which minimizes T_s for a given plant is "best." Other criteria for optimum

systems are the indicial error measures (Graham, McRuer et al. 1962).

Indical error criteria typically measure the integrated function of the error response to a step input. One of the most useful of these indicial error criteria is the integrated error-squared (ISE) criteria given by

$$ISE = \int_0^{\infty} u^2(t) dt$$

A more general performance index using a quadradic cost function is

$$PI = \int_0^{\infty} \left[(\underline{\gamma}^T \underline{x}(t))^2 + pu^2(t) \right] dt \quad (4.4)$$

where $\underline{\gamma}$ is a weighting vector of the form

$$\underline{\gamma}^T = [\gamma_1, \gamma_2, \dots, \gamma_{n-1}, 0]$$

and p is a positive scalar, is minimized by a closed-loop system derived from Equation (4.5). This is called the Kalman Equation. For a system defined by Equations (1.1), (1.2), and (1.3) the Kalman Equation takes the form

$$\left| 1 + \underline{k}^T \underline{\Phi}(s) \underline{b} \right|^2 = 1 + \frac{1}{p} \left| \underline{\gamma}^T \underline{\Phi}(s) \underline{b} \right|^2 \quad (4.5)$$

(Schultz and Melsa 1967)

or

$$\left| 1 + G(s) H_{eq}(s) \right|^2 = 1 + \frac{1}{p} \left| \Gamma(s) \right|^2 \quad (4.6)$$

It has been shown (Schultz and Meisa 1967) that $\Gamma(s)$ is the product of $G(s)$ and the characteristic equation $D_m(s)$ of a model response determined by $\underline{\gamma}^T x(t)$. The pole-zero excess of $\Gamma(s)$ must be greater than zero.

The magnitude of the right hand side of Equation (4.6) can never be less than unity. Thus the optimum nature of the inequality given by the Sensitivity-Optimality Condition, Equation (2.3), is shown. If a system is chosen to meet this condition, there exists a weighting vector of positive coefficients, $\underline{\gamma}$, and a performance index which is minimized.

Summary

In this chapter the importance of the Sensitivity-Optimality Condition, which forces $DR^{-1}(s)$ to be greater than unity, is illustrated. An equation is given, (4.6), which defines $H_{eq}(s)$ and therefore $C(s)/R(s)$, such that $C(s)/R(s)$ optimally approximates a lower-order model having poles determined by $D^m(s)$. This equation is used in the next chapter to extend low-order models specified by the methods of Chapter III to high-order models compatible with the forward transfer functions.

CHAPTER V

THE SPECIFICATION OF HIGH-ORDER MODELS

Performance specifications are used in Chapter III to specify a low-order, "ideal," closed-loop model. The feedback coefficients k may be determined from this model if:

1. $C(s)/R(s)$ includes all the zeros of the forward transfer function $G(s)$.
2. The order of the denominators of both $C(s)/R(s)$ and $G(s)$ are equal.
3. The plant's static loop sensitivity equals the closed-loop gain, K .

In this chapter, the low-order model is optimally modified by the addition of poles and zeros such that all these restrictions are met for any $G(s)$.

Extension of Low-Order Characteristic Equations

Equation (4.5) may be rewritten using the relationship given by Equation (4.3), to form

$$\left| \frac{D_C(s)}{D(s)} \right|^2 = 1 + \frac{1}{p} \left| K \frac{D_m(s)N(s)}{D(s)} \right|^2 \quad (5.1)$$

where $D_m(s)$ is the characteristic equation of the "ideal" model. The expanded form of Equation (5.1) is

$$\frac{D_c(s)D_c(-s)}{D(s)D(-s)} = 1 + \frac{K^2}{p} \left(\frac{D_m(s)N(s)D_m(-s)N(-s)}{D(s)D(-s)} \right) \quad (5.2)$$

Both sides of this equation have poles and zeros in the left and right halves of the s -plane.

If the closed-loop model being specified is stable, it must contain poles only in the left half of the s -plane. Therefore, the poles of that model (the roots of $D_c(s)$) are the left half plane roots of the right-hand side of Equation (5.2), denoted here as,

$$D_c(s) = \left[D(s)D(-s) + \frac{K^2}{p} \left(D_m(s)N(s)D_m(-s)N(-s) \right) \right]_{\text{LHP}} \quad (5.3)$$

Since $D(s)$ is assumed to be a high-order polynomial ($n \geq 3$), the zeros of Equation (5.3) are difficult to obtain by direct factorization. A root locus, however, is easily plotted. The root locus contains $2n$ branches originating at the $2n$ zeros of $D(s)D(-s)$. The work is greatly simplified by the quadrantal symmetry of the singularities in Equation (5.3).

This symmetry may assist the designer in several ways: (1) the centroid of all asymptotes is the origin, (2) only the roots in one quadrant must be plotted, (3) the roots going to infinity may be approximately located for large values of K by placing them at a radius $r = K^{1/2}$ from the origin. The coefficient L is determined by

$$L = (n-m-n_m) \geq 1$$

where m is the order of $N(s)$ and n_m the order of $D_m(s)$. It should be noted that if L is even, a 0° locus is plotted instead of the usual 180° locus which is required when L is odd.

The equations defining the slopes, θ , of the asymptotes lead to two important conclusions. The equations are

$$\theta = (2g-1) \frac{\pi}{2L} \quad \text{for } L \text{ even}$$

$$\theta = g \frac{\pi}{L} \quad \text{for } L \text{ odd}$$

and $g = 1, \dots, 2L$. The first observation is that the jw -axis is never an asymptote. The second observation is that for very large static gains, the excess roots in the left-half plane approach the location of an L^{th} order Butterworth polynomial, $B(s)$.

If the gain K is infinite, Equation (5.3) reduces to

$$D_c(s) = KD_m(s)N(s)B(s)$$

The n poles of the extended model are placed such that (1) $D_c(s)$ has n_m roots where $D_m(s)$ has roots, (2) $D_c(s)$ has m roots where $N(s)$ has roots, canceling all the zeros from the plant and (3) $D_c(s)$ has L roots of a maximally flat function, $B(s)$, at infinity.

Small values of gain make $D_c(s)$ identical to the compensated plant's denominator, $D(s)$. For values of gain between the two extremes, the poles of the extended model are determined by the loci of optimum roots which minimize the performance index of Equation (4.4). The extended model is the "best" approximation of low-order "ideal" model for a given K .

An example illustrates the procedure.

Specifications: $P_0 = 25\%$, $T_s = 5$ seconds and a plant given by

$$G(s) = \frac{1700}{s(s+5)(s+10)}$$

Synthesis: A second-order model was determined in Chapter III meeting the performance specifications P_0 and T_s . The "ideal" model is therefore

$$C(s)/R(s) = \frac{121}{s^2 + 10s + 121} = \frac{121}{(s+5)^2 + 9.8^2}$$

The root locus is defined by substituting into Equation (5.3) and solving for the roots,

$$-s^2(s+5)(s+10)(s-5)(s-10) - \frac{(1700)^2}{p} (s^2 + 10s + 121) \\ (s^2 - 10s + 121) = 0$$

Later in this chapter it is shown that $p^{1/2}$ is equal to the "ideal" model gain which for this example is 121. The root locus is plotted in Figure 13 by observing

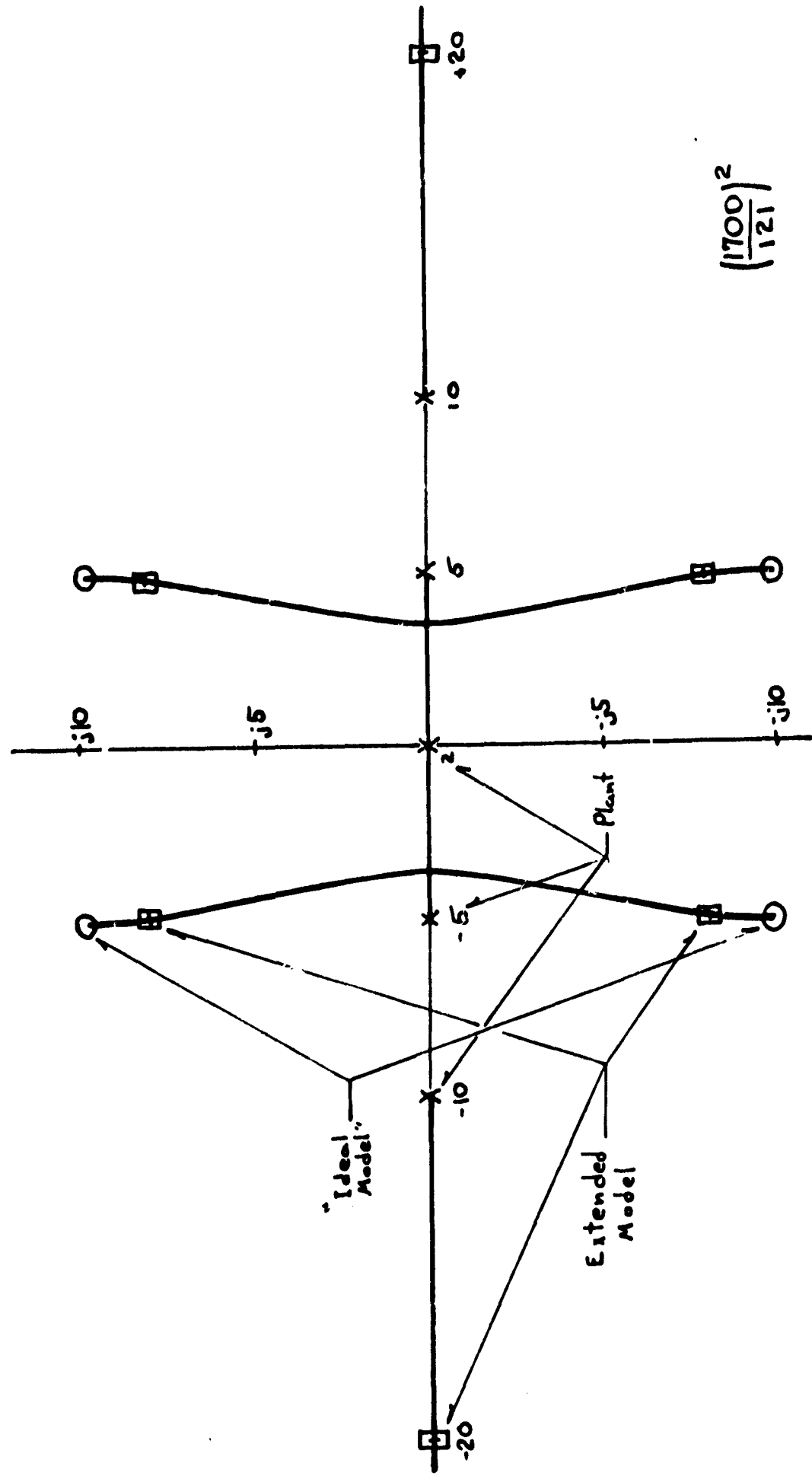


Fig. 13. Root Locus of Optimal Models for Third-Order Example

$$L = 3-2 = 1$$

$$\theta = 0^\circ, 180^\circ$$

The roots of $D_c(s)$, in the left-half plane for $\nu^{1/2} = 121$ are $-20, -4.7 \pm j8$ and the specified closed-loop function is

$$C(s)/R(s) = \frac{1700}{[(s + 4.7)^2 + 8^2](s + 20)}$$

The velocity error coefficient of the "ideal" model can be obtained from $\omega_n = 11$ rad/sec and Figure 5. The value of K_v is 143. The extended model does not improve K_v . If a larger K_v is desired, a zero and pole are added to the plant in the usual fashion. The zero could be placed according to Figure 6 for an infinite K_v in the "ideal" model. But when the model is extended as above, a pole of $C(s)/R(s)$ is placed by the root locus such that it tends to cancel the desired zero. If K is large, the increase in K_v for $C(s)/R(s)$ will be negligible. This difficulty is a consequence of Equation (5.1) which does not permit inclusion of the "ideal" model's zeros in $\Gamma(s)$.

Extension of the General "Ideal" Model

The author suggests that the Kalman Equation for single-input, single-output systems be modified to include the "ideal" model zeros, $N_m(s)$. The equation is rewritten as

$$\left| \frac{D_c(s)}{D(s)} \right|^2 = 1 + \frac{1}{p} \left| K \frac{D_m(s)}{N_m(s)} \frac{N(s)}{D(s)} \right|^2 \quad (5.4)$$

If the operator s is made very small, the left-hand side of Equation (5.4) approaches a large number $|d_{co}/s|^2$, where d_{co} is the coefficient of s^0 in $D_c(s)$. The other side of the equation approaches

$$\frac{1}{p} \left| K \frac{d_{mo}}{n'_{mo}} \frac{n_o}{s} \right|^2$$

where d_{mo} , n'_{mo} , and n_o are the coefficients of s^0 in $D_m(s)$, $N_m(s)$ and $N(s)$. Since $K_p = \infty$, $K = d_{co}/n_o$ and the coefficient p is given by

$$p^{1/2} = d_{mo}/n'_{mo}$$

This is also equal to the static gain of the "ideal" model if K_p for that model is infinite as assumed in Chapter III. Therefore, Equation (5.4) may be expressed in the final form

$$\left| \frac{D_c(s)}{D(s)} \right|^2 = 1 + \left| \frac{G(s)}{[C(s)/R(s)] \text{"ideal"}} \right|^2 \quad (5.5)$$

For an example, the third-order "ideal" model of Chapter III is extended using Equation (5.5). The performance specifications of that model are: (1) 100 rad/sec \leq BW \leq 150 rad/sec, (2) $K_v \geq 200$ and (3)

$P_0 = (20 \pm 1)\%$. The "ideal" model meeting these specifications is

$$[G(s)/R(s)]_{\text{"ideal"}} = \frac{3 \cdot 10^4 (s + 49)}{(s^2 + 100s + 4900)(s + 300)}$$

If the given plant is

$$G_p(s) = \frac{45 \cdot 10^6 (s + 200)}{s(s + 100)(s + 150)(s + 400)},$$

then a compensator must be added with the form

$$G_c(s) = \frac{s + 49}{s + \alpha}$$

The roots of Equation (5.5) are found by equating it to zero,

$$1 + 225 \cdot 10^6 \left| \frac{(s^2 + 100s + 4900)(s + 300)(s + 200)}{s(s + 100)(s + 400)(s + 150)(s + \alpha)} \right|^2 = 0$$

Notice that the desired zero will not affect the root locus, and that a new L' must be defined as

$$L' = L - (\text{Number of desired zeros}) \leq 1$$

The root-locus defined above is plotted in Figure 14. The value of α is chosen to be 300 in order to reduce the labor involved. This pole, the zero at 300 and the root loci originating at ± 400 are not shown in the figure so that the more critical root loci near the origin are emphasized. The model specified by the root-locus extension is

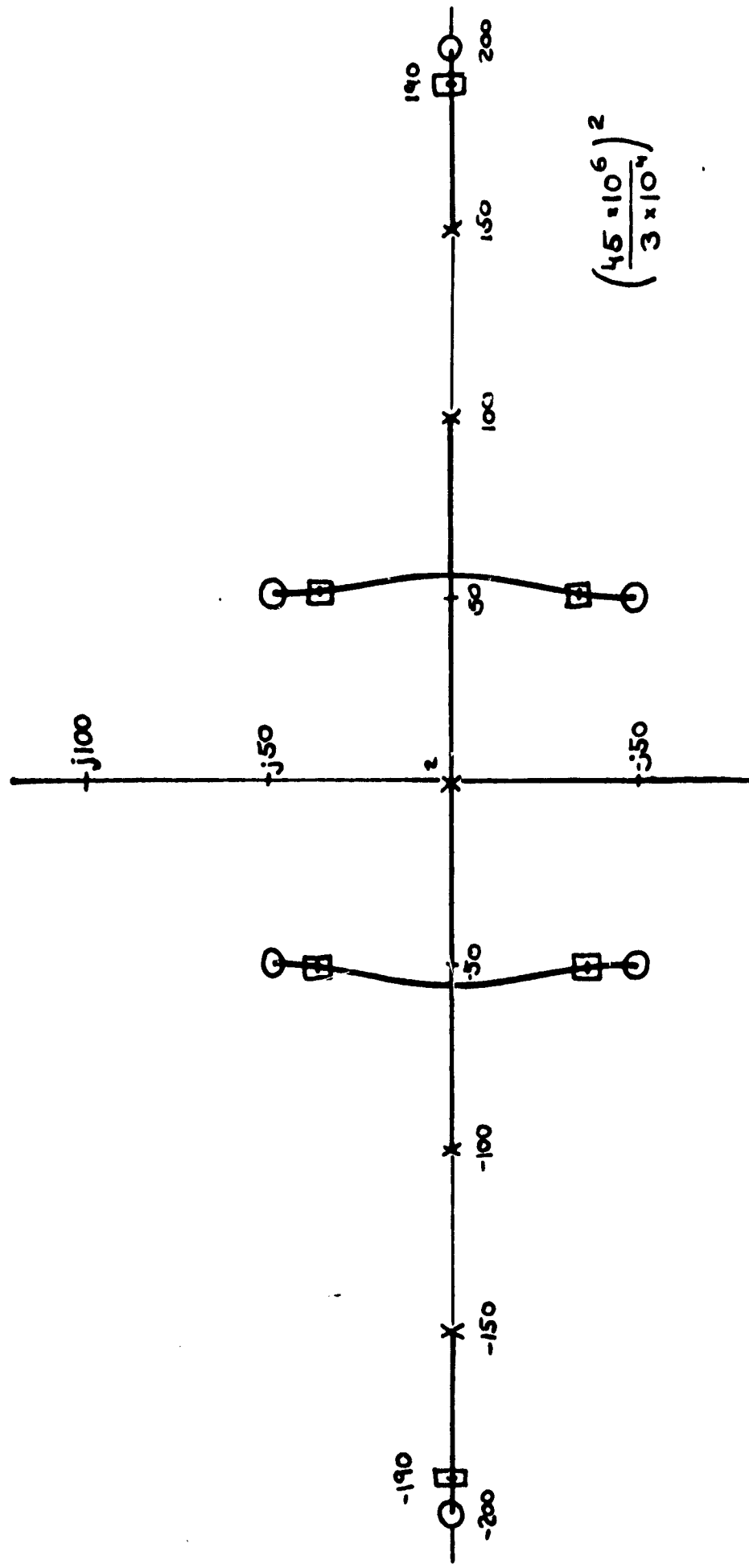


Fig. 14. Root Locus of Optimal Models for Fifth-Order Example

$$C(s)/R(s) = \frac{45 \cdot 10^6 (s+200)(s+49)}{(s^2 + 106s + 3850)(s+190)(s+300)(s+2000)}$$

This model is very close to the "ideal" model for the large gain constant as expected. The unwanted zero at 200 is approximately canceled by the pole at 190. The remaining excess pole is a first-order Butterworth polynomial with a bandwidth of 2000 rad/sec, more than ten times that of the "ideal" model.

Summary

Although the model extension equation, Equation (5.5), cannot be derived from the quadratic performance index of Chapter IV, the results are the same as those based on the Kalman Equation. For large values of gain K, the specified model approaches the "ideal" model with excess poles placed in Butterworth fashion.

In the next chapter, the synthesis is completed with the calculation of the feedback coefficients \underline{k} and a comparison made of the actual time and frequency responses of both the "ideal" and extended functions.

CHAPTER VI

THE SOLUTION OF HIGH-ORDER SYSTEMS

The calculation of feedback coefficients that realize a specified high-order model, completes the system synthesis. The example problems of Chapter III are completed here. These two examples also serve to illustrate typical difficulties in the realization of \underline{k} . The chapter concludes with a discussion of an important difficulty, saturation.

Calculation of $H_{eq}(s)$

The final step in the synthesis is the determination of feedback coefficients of the compensated, linear plant. These coefficients define an equivalent feedback function $H_{eq}(s)$. The restrictions on $H_{eq}(s)$ made throughout this study are summarized as:

1. $H_{eq}(s)$ has $(n-1)$ zeros determined by \underline{k} .
2. Since $K_p = \infty$, the output state variable x_1 must have unity gain feedback, $k_1 = 1$.
3. All zeros of the compensated plant $G(s)$ must be poles of $H_{eq}(s)$.

The restriction on k_1 is not critical. This coefficient adjusts the static gain to match the

coefficients of s^0 in both $D_c(s)$ and $D(s) [1 + G(s)H_{eq}(s)]$, but these coefficients have already been matched by the modeling process. Thus, the remaining $(n-1)$ k 's can be chosen so that any $C(s)/R(s)$ can be realized.

Completion of the synthesis of the specified second-order "ideal" model of Chapter IV illustrates the procedure. The specified $C(s)/R(s)$ function and given plant are

$$C(s)/R(s) = \frac{1700}{[(s + 4.7)^2 + 8^2](s + 20)}$$

$$G(s) = G_p(s) = \frac{1700}{s(s + 5)(s + 10)}$$

By expressing $C(s)/R(s)$ in terms of $G(s)$ and $H_{eq}(s)$ obtained from the system block diagram, Figure 15, we get

$$C(s)/R(s) = \frac{1700}{s(s+5)(s+10) + 1700[1 + (k_2 + 10k_3)s + k_3s^2]}$$

and equating to the specified $C(s)/R(s)$, the k 's are determined as

$$29.4 = 15 + 1700k_3$$

$$274 = 50 + 1700(k_2 + 10k_3)$$

The solution for \underline{k} is

$$\underline{k} = \begin{bmatrix} 1 \\ 8.5 \cdot 10^{-3} \\ 47 \cdot 10^{-3} \end{bmatrix}$$

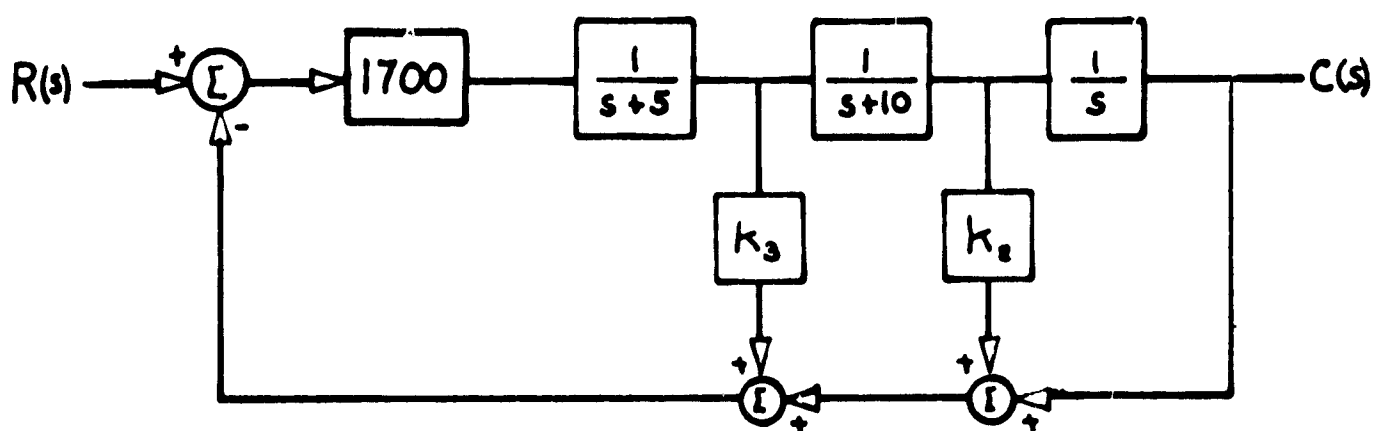


Fig. 15. Block Diagram of Third-Order Example

The frequency response, Figure 16, and time response, Figure 17, of both the system and the "ideal" model indicate the low gain used. A higher gain would improve the approximation.

The third restriction is a possible difficulty only when a zero exists in the first block of the system's block diagram. This zero, unlike all the others, does not become a pole of H_{eq} unless special care is taken in selecting the n^{th} state variable that is fed back. The other example of Chapter IV, having two zeros and five poles has a compensator zero in the first block. Completing the synthesis of this system illustrates the difficulty and its solution.

The specified model and the compensated plant equations are

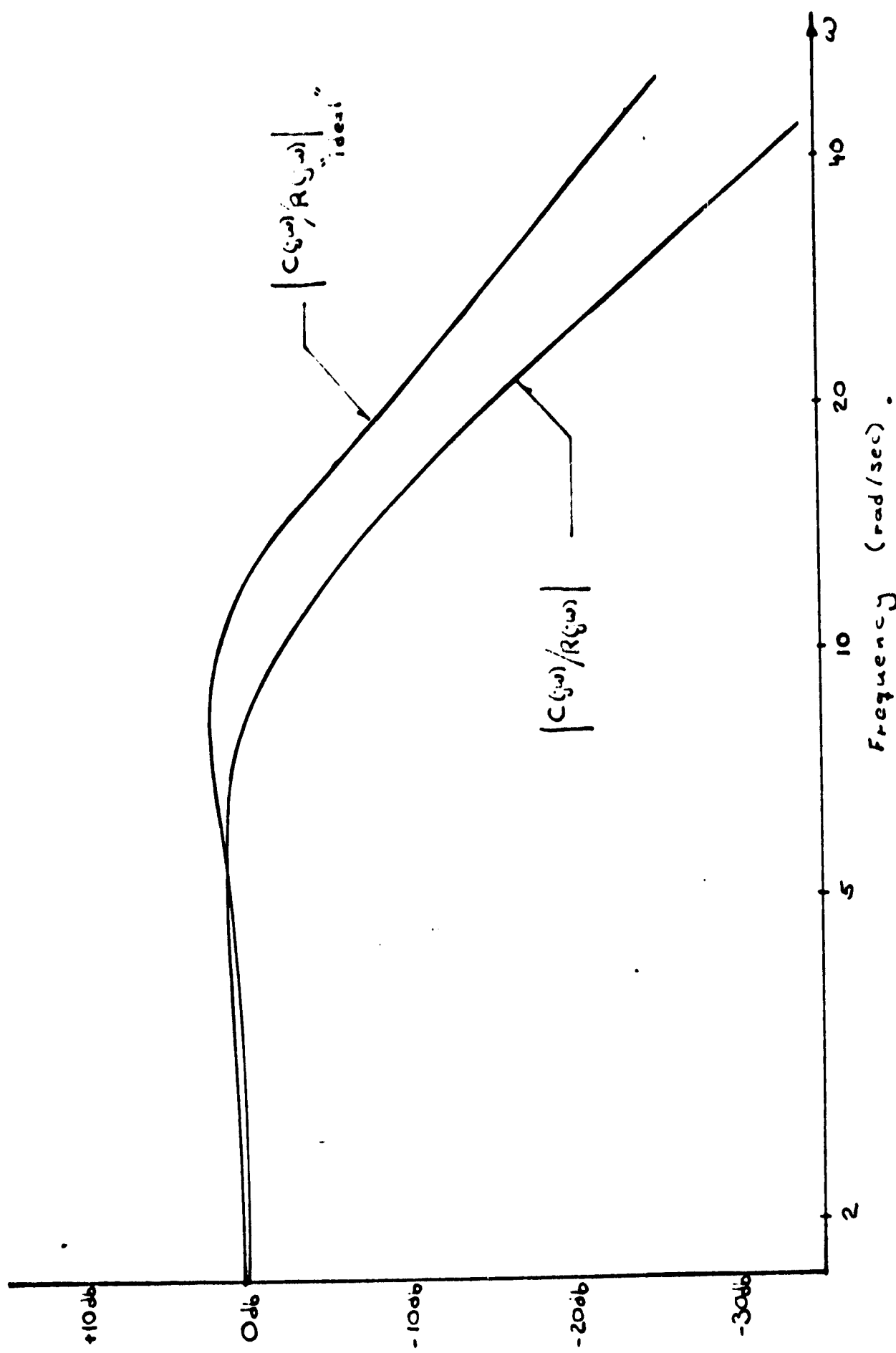


Fig. 16. Frequency Response of Third-Order System and "Ideal" Model

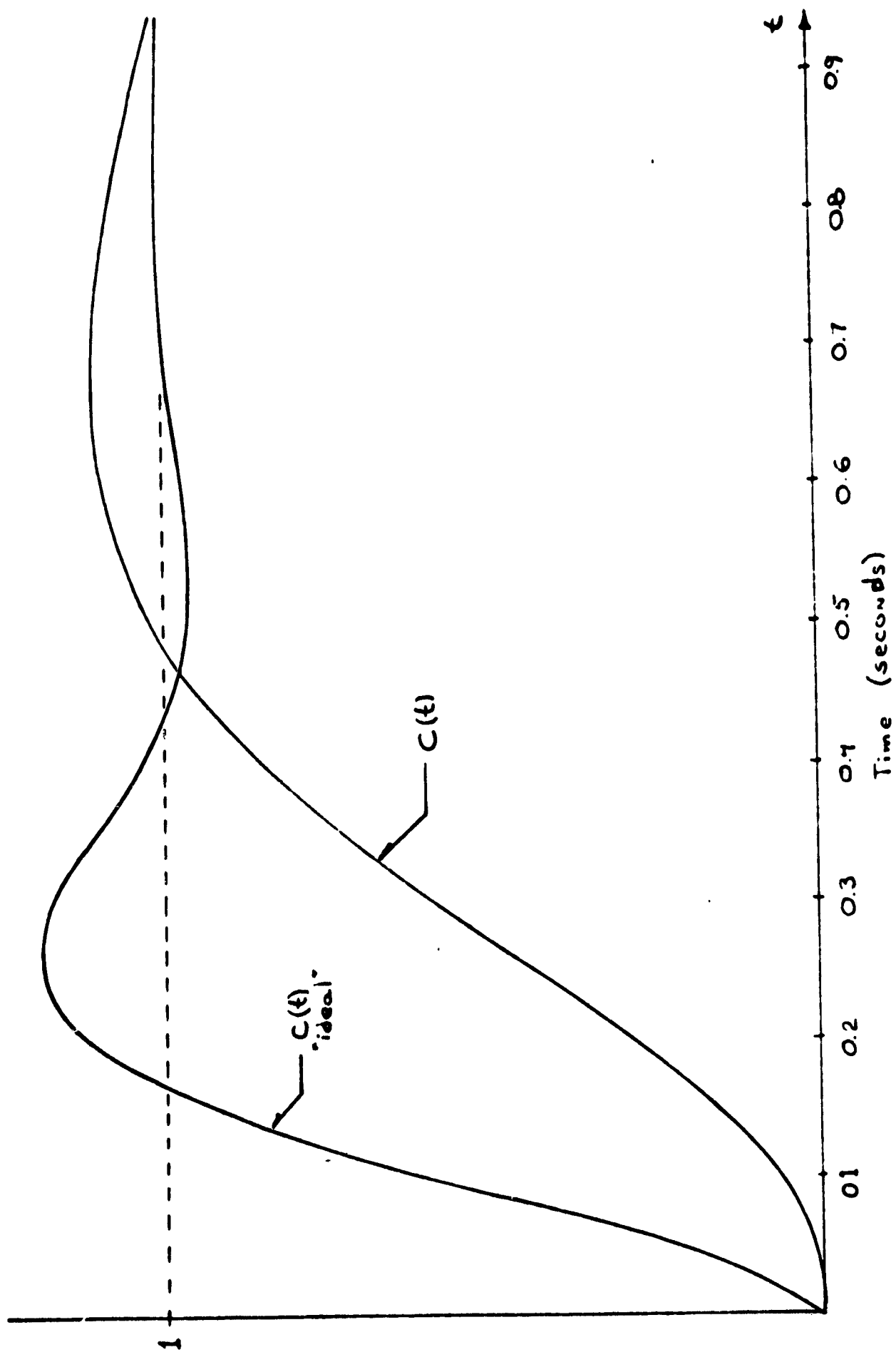


Fig. 17. Time Response of Third-Order System and "Ideal" Model

$$C(s)/R(s) = \frac{45 \cdot 10^6 (s+200)(s+49)}{(s^2 + 100s + 3850)(s+190)(s+300)(s+2000)}$$

and

$$G(s) = \frac{45 \cdot 10^6 (s+200)(s+49)}{s(s+100)(s+150)(s+300)(s+400)}$$

The block diagram for the system is shown in Figure 18.

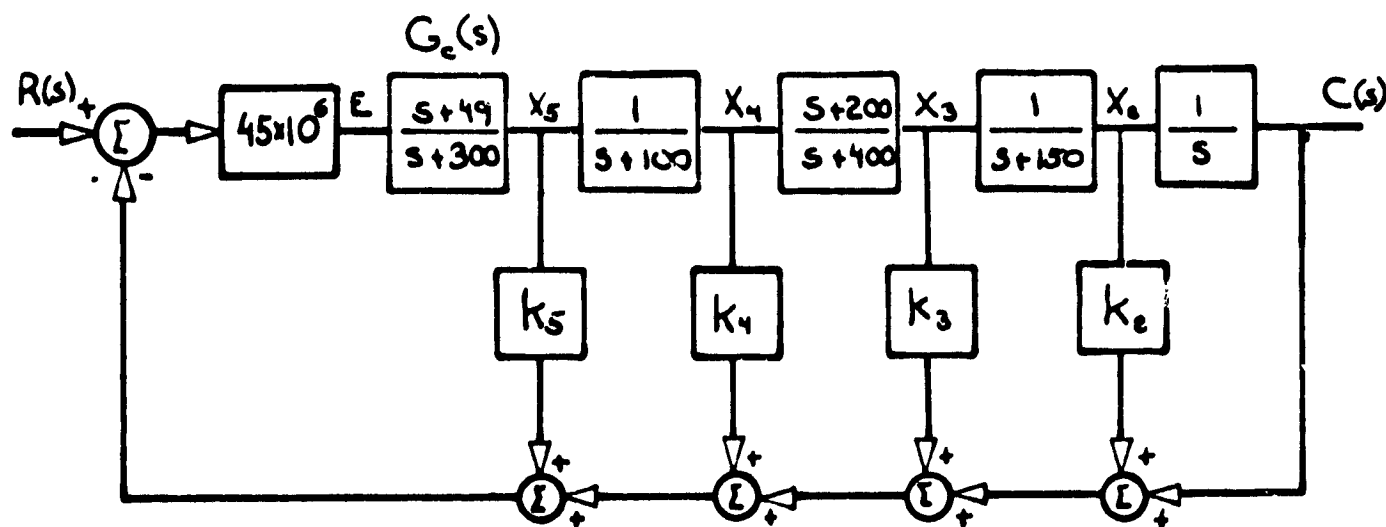


Fig. 18. Block Diagram of Fifth-Order Example

If $H_{eq}(s)$ is calculated using x_5 as a state variable, it does not have a pole at -49 . A new state variable, x'_5 , replacing x_5 can be fed back which places the desired pole in $H_{eq}(s)$. This is accomplished by building the compensator and picking the state variable as shown in Figure 19.

Before completing the design, a closer look should be taken at $C(s)/R(s)$. As noted in Chapter V, the zero at -49 does not affect the position of the root loci. The

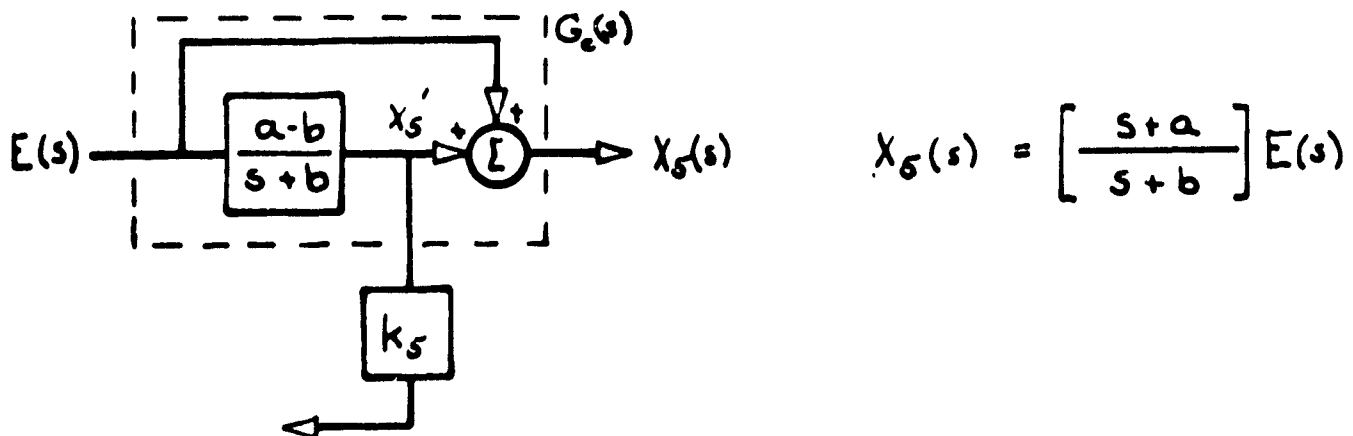


Fig. 19. Zeros in the First Block of a Block Diagram

zero was placed at -49 in the "ideal" model to increase K_v . If K_v is computed from its defining equation of Chapter III, repeated here as

$$\frac{1}{K_v} = \frac{2\zeta}{\omega_n} + \sum_{\text{poles of C/R}} \frac{1}{s} - \sum_{\text{zeros of C/R}} \frac{1}{s}$$

the K_v for the extended system is 125 rad/sec, less than its specified minimum of 200 rad/sec. The "ideal" model had a K_v of 280 rad/sec.

The other performance measures have also suffered by the extension, but there are no charts or formulas to determine their deterioration. Since the zero does not affect the root loci and a formula does exist for K_v , the zero is moved to regain an acceptable velocity error coefficient. A pole must be moved simultaneously so that the K_p remains infinite.

If the K_v specification requires a contribution, ψ , from the compensator zero and pole (select the largest pole in $C(s)/R(s)$, P), then

$$\psi = \frac{1}{a} - \frac{1}{p}$$

The position error constant is maintained as specified if

$$P_o/a_o = P/a$$

where a_o and P_o are the original positions ($a_o = 49$, $P_o = 2000$ in this example). Both equations are solved by placing the pole at

$$P = (P_o/a_o - 1)/\psi \quad (6.1)$$

and the zero at

$$a = a_o P/P_o \quad (6.2)$$

If $P_o \gg a_o$, the equations (6.1) and (6.2) reduce to

$$P \approx P_o/a_o \psi$$

$$a \approx 1/\psi$$

For this example $P_o \gg a_o$ and a ψ of 24.6×10^{-3} forces K_v to be 300, greater than the 200 of the ideal model. The zero and pole positions are then

$$a \approx 41$$

$$P \approx 1670$$

and the closed loop transfer function to be realized is

$$C(s)/R(s) = \frac{45 \cdot 10^6 (s+200)(s+41)}{(s^2 + 106s + 3850)(s+190)(s+300)(s+1670)}$$

The feedback function obtained by block diagram manipulation is

$$H_{eq}(s) = 1 + k_2 s + k_3 s(s+150) + k_4 \frac{s(s+150)(s+400)}{s+200} + k_5 \frac{-259s(s+150)(s+400)(s+100)}{(s+200)(s+41)}$$

Once again, $C(s)/R(s)$ is expressed in terms of $H_{eq}(s)$ and $G(s)$ and the coefficients of like powers equated to evaluate the k 's. After some straight forward algebra, \underline{k} is found to be

$$\underline{k} = \begin{bmatrix} 1 \\ 15 \cdot 2 \cdot 10^{-3} \\ -59 \cdot 10^{-6} \\ 34 \cdot 10^{-6} \\ 125 \cdot 10^{-9} \end{bmatrix}$$

The plant gains, especially around the x_1 feedback loop, are large. A large static-loop sensitivity leads to a close approximation of the "ideal" model as shown in Figure 20, but saturation is likely to occur if the system is driven hard. In the next section, a method is proposed which attempts to retain the optimum nature of $C(s)/R(s)$ without saturation.

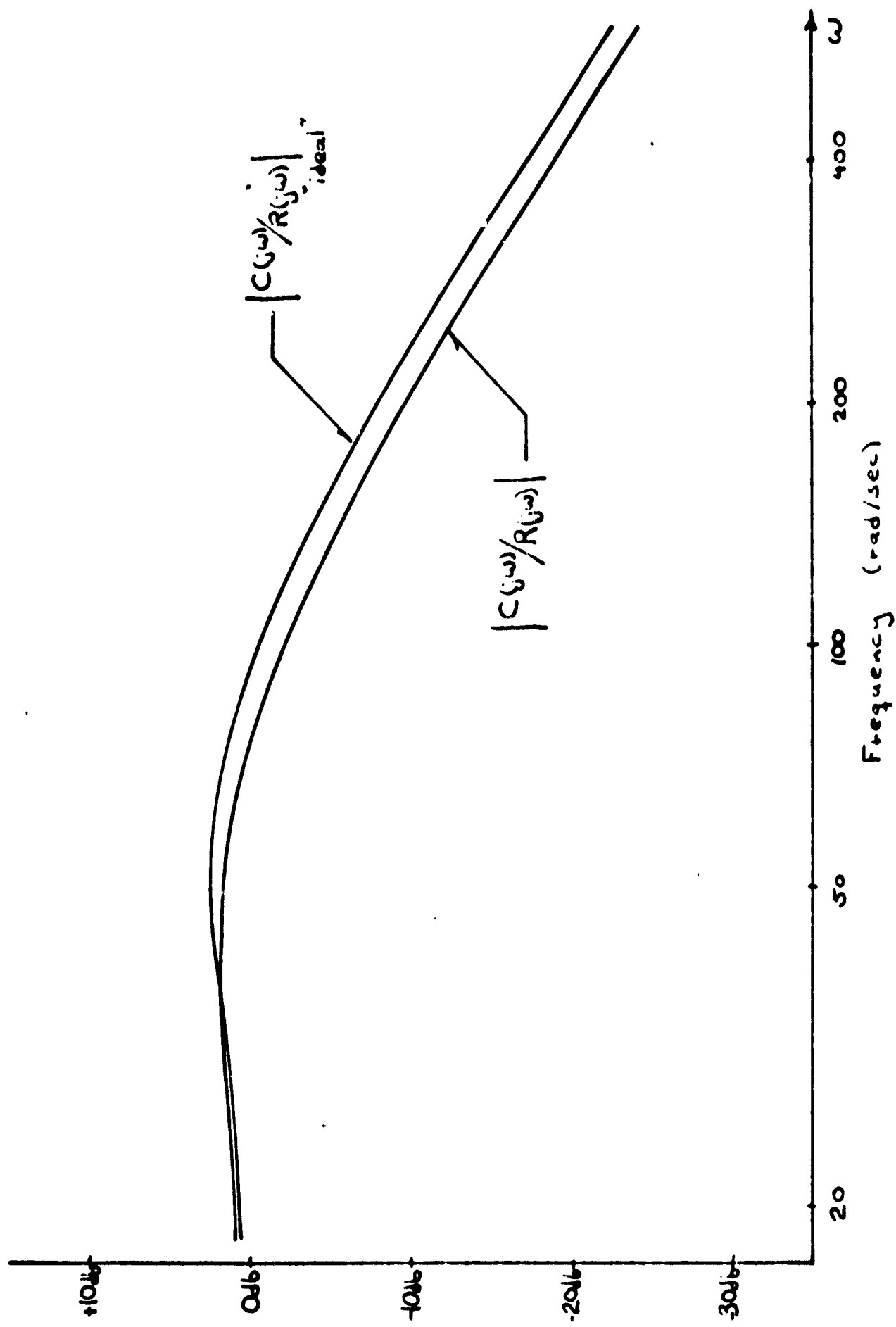


Fig. 20. Frequency Response of Fifth-Order System and "Ideal" Model

Saturation

The closed-loop poles are placed where specified by the zeros of H_{eq} for any gain. If saturation occurs in one of the state variables being fed back, at least one of the zeros and possibly the poles of $H_{eq}(s)$ move or vanish. When the gain is high, instability becomes inevitable.

Saturation in the system is not necessarily a bad feature if stability is maintained. Merriam (1964) states that for the simple system shown in Figure 21 ". . . the saturating controller with a linear zone . . . is the optimum controller for the error measure . . ." (p. 20).

$$PI = \int_t^\infty [e(\tau)^2 + pu(\tau)^2] d\tau$$

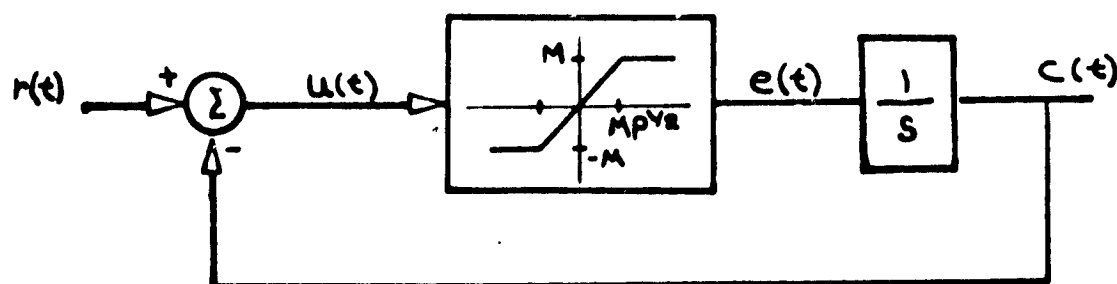


Fig. 21. Optimum Controller for First-Order System

Merriam shows that the optimum solution for this system is one with a linear region gain of $K = p^{-1/2}$ with velocity saturation occurring at $e(t) = M$ or $c(t) = M/K$. Thus, if $e(t)$ is kept as large as possible the system is driven with maximum velocity toward the desired output.

The extension of this to high-order systems is that it should be driven as hard as possible by keeping the gain large.

A possible method of obtaining an almost maximum effort system while maintaining optimality is suggested by the root locus of optimal models defined by Equation (5.5). If the state variables are fed back so that as the controller reaches saturation, the zeros of H_{eq} are still determined by \underline{k} , then the system remains stable.

The controller is built to saturate for excessive error signals, but this region can be extended by dividing the controller gain into two linear regions, $K_a K_b$ and K_b , as shown in Figure 22. The feedback loops are also split into two groups. When the first stage is saturated, the reduced gain and new zeros of $H_{eq}^b(s)$ can be made to force the closed-loop poles of $C(s)E_a(s)$ toward the plant's poles along the optimum root locus. If these poles are close to the poles of $G(s)$, the linear region is greatly extended and the optimum nature of the system maintained.

Summary

The specified closed-loop transfer function can be modified for improved system accuracy when an alterable, desired zero is present in the open-loop plant. If this zero is in the first block, care must be taken to insure that this zero is a pole of $H_{eq}(s)$.

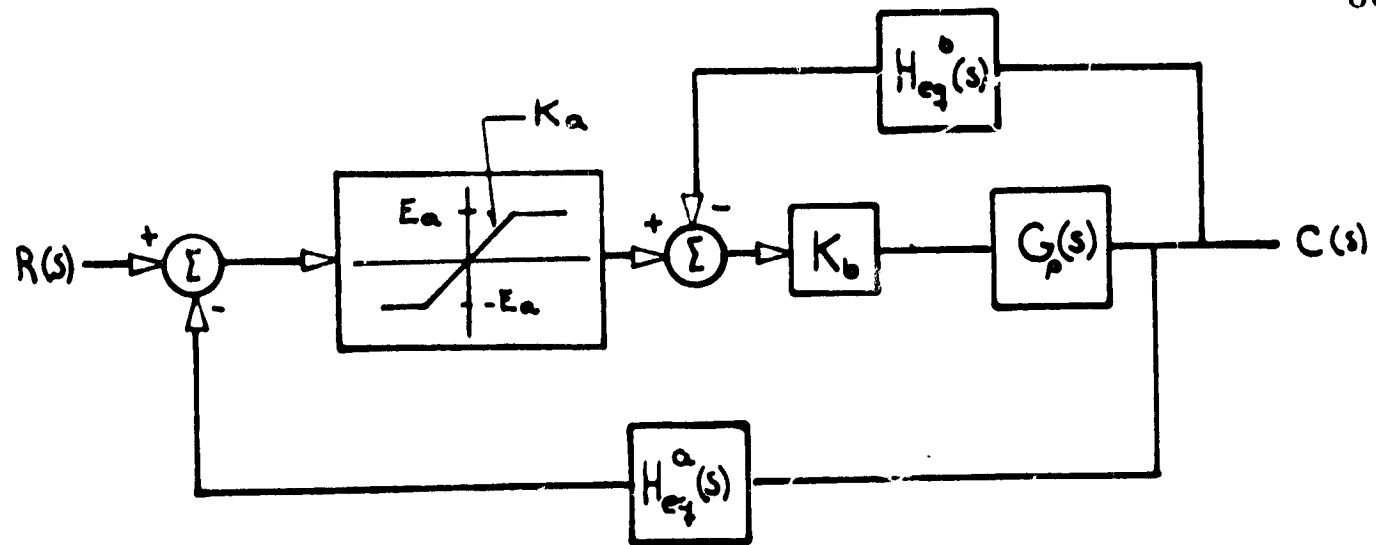


Fig. 22. Optimum Controller With Two Modes

The synthesis is completed by the calculation of \underline{k} which places the zeros of $H_{eq}(s)$ (or $H_{eq}^a(s)$ and $H_{eq}^b(s)$) so that the desired closed-loop poles are exactly realized.

CHAPTER VII

CONCLUSIONS

The methods of specifying closed-loop transfer functions of any order, coupled with the ability to realize that function using state variable feedback, make the synthesis of linear control systems straight forward. The synthesis proceeds from performance criteria to the calculation of the feedback coefficients in five steps.

1. Values are assigned to performance measures, making them performance specifications from the design criteria. A set of measures, sufficiently describing either the time or frequency response, includes BW, M_p , ω_p , T_d , T_r , T_s , PO, FVE (K_v), Z_o and DR.
2. An "ideal" model of low order (up to three poles and one zero) is specified from the design charts.
3. The "ideal" model is extended to be compatible with the gain, order and zeros of the compensated plant, $G(s)$, using the equation

$$\left| \frac{D_c(s)}{D(s)} \right|^2 = 1 + \left| \frac{G(s)}{[C(s)/R(s)] \text{"ideal"}} \right|^2$$

4. A pole and compensator zero are adjusted to improve K_v if necessary.
5. The state variables are then chosen and the \underline{k} vector calculated.

If the gain chosen for the plant is large, the closed-loop system response can be specified and realized independent of the plant. Saturation, however, places a limit on the gain and therefore on the extent of alteration of the open-loop performance using state variable feedback.

REFERENCES

Chen, K., "A Quick Method for Estimating Closed-Loop Poles of Control Systems," Trans. AIEE, Application and Industry, May, 1957, pp. 80-87.

D'Azzo, J. J. and C. H. Houpis, Feedback Control System Analysis and Synthesis, McGraw-Hill Book Company, Inc., New York, N. Y., 1960.

Gibson, J. E. et al., "Specification and Data Presentation in Linear Control Systems," A Technical Report, AFMDC-TR-60-2, Prepared for Air Force Missile Development Center, Holloman Air Force Base, New Mexico, Purdue University, 1960.

Graham, D. et al., "Performance Criteria for Linear Constant-Coefficient Systems with Deterministic Inputs," A Technical Report, ASD-TR-61-501, Prepared for Aeronautical Systems Division, Wright-Patterson Air Force Base, Ohio, Washington, Government Printing Office, 1962.

Hausbauer, C. R., "Synthesis of Feedback Systems," Ph.D. thesis, University of Missouri, Columbia, Missouri, 1957.

Merriam, C. W., Optimization Theory and the Design of Feedback Control Systems, McGraw-Hill Book Company, Inc., New York, N. Y., 1964.

Schultz, D. G. and J. L. Melsa, State Functions and Linear Control Systems, McGraw-Hill Book Company, Inc., New York, N. Y., 1967.

Thaler, G. J. and R. G. Brown, Servomechanism Analysis, McGraw-Hill Book Company, Inc., New York, N. Y., 1953.

Truxal, J. G., Automatic Feedback Control System Synthesis, McGraw-Hill Book Company, Inc., New York, N. Y., 1955.

PART II
SENSITIVITY AND STATE VARIABLE FEEDBACK

Prepared Under Grant NGR-03-002-115
National Aeronautics and Space Administration

by

Robert C. White
and
Donald G. Schultz

Electrical Engineering Department
The University of Arizona
Tucson, Arizona

ABSTRACT

Two new time-domain sensitivity measures, integral sensitivity and peak sensitivity, are defined in terms of the sensitivity function. A relation between integral sensitivity and classical frequency-domain sensitivity is established, and the generation of classical sensitivities, sensitivity functions, peak sensitivity, and integral sensitivity is discussed. Classical sensitivity is employed in a comparison of the sensitivity properties of linear control systems designed by two methods: series compensation and state-variable feedback. It is shown that under certain conditions the system designed by feeding back all of the state variables may be expected to be less sensitive than the series compensated system. A modification of state-variable feedback, the H-equivalent system, is considered in further attempt to reduce sensitivity to parameter changes. Several examples are presented to illustrate the theory.

TABLE OF CONTENTS

CHAPTER I	INTRODUCTION	1
CHAPTER II	SENSITIVITY MEASURES	5
2.1	Root Sensitivity	5
2.2	Classical Sensitivity	6
2.3	Sensitivity Functions	9
2.4	Peak Sensitivity and Integral Sensitivity	15
CHAPTER III	GENERATION OF SENSITIVITY MEASURES	17
3.1	The Relation between S_λ and S_λ^W	17
3.2	Generation of Classical Sensitivities	19
3.3	Generation of Sensitivity Functions, Peak Sensitivity, and Integral Sensitivity	26
CHAPTER IV	SENSITIVITY AND STATE-VARIABLE FEEDBACK	29
4.1	Series Compensation and State-Variable Feedback . .	29
4.2	Sensitivities	33
4.3	Restrictions Imposed by the Fixed Plant and the Closed-Loop Transfer Function	36
4.4	Modifications of State-Variable Feedback	40
4.5	A Note on Integral Sensitivity and the Poles of the Fixed Plant	42
4.6	Summary	44
CHAPTER V	EXAMPLES	45
Example 1.	45	
Example 2.	61	
Example 3.	63	
Example 4.	71	
CHAPTER VI	CONCLUSIONS	77
APPENDIX	80	
REFERENCES	82	

LIST OF FIGURES

Figure

2.1 A single-loop control system.	7
2.2 An experiment to illustrate the definition of the sensitivity function	7
2.3 A second order control system	11
2.4 A second order control system	11
2.5 Sensitivity functions for the example	13
2.6 The effects of parameter variations on the step response .	14
3.1 The block diagram of a control system	20
3.2 A reduced block diagram	21
3.3 A series compensated system	24
3.4 The generation of sensitivity functions and integral sensitivities	27
4.1 The series compensated system	30
4.2 The state-variable feedback system	31
4.3 A third order control system	38
4.4 The H-equivalent system	41
5.1 The fixed plant of Example 1	46
5.2 The compensated system of Example 1	46
5.3 Gain sensitivities for the state-variable feedback system of Example 1	48
5.4 Pole sensitivities for the state-variable feedback system of Example 1	50

LIST OF FIGURES

Figure

5.5 Feedback coefficient sensitivities for the state-variable feedback system of Example 1	52
5.6 The system of Example 1 compensated by the Guillemin-Truxal method	54
5.7 Pole sensitivities for the series compensated system of Example 1	55
5.8 Generation of sensitivity functions and integral sensitivities for the series compensated system	56
5.9 Generation of sensitivity functions and integral sensitivities for the state-variable feedback system	57
5.10 The sensitivity functions for the forward gains of the state-variable feedback system	58
5.11 The sensitivity functions for the poles of the fixed plant in the state-variable feedback system	59
5.12 The sensitivity functions for the feedback coefficients of the state-variable feedback system	60
5.13 The H -equivalent system of Example 2	62
5.14 The H' -equivalent system of Example 3	65
5.15 Generation of sensitivity functions and integral sensitivities for the $H'_{eq}(s)$ system	66
5.16 The closed loop poles and zeros for the $H'_{eq}(s)$ system	68
5.17 The step response of the $H'_{eq}(s)$ system	69
5.18 A table of sensitivities for Examples 1., 2., and 3.	70
5.19 The fixed plant of Example 4	72
5.20 The closed loop system of Example 4	72
5.21 Generation of sensitivity functions and integral sensitivities for the system of Example 4	75

CHAPTER I

INTRODUCTION

The need to consider the sensitivity properties of a control system arises from two general sources. While the system is in operation, there may be variations in components because of aging, environmental changes, etc. Secondly, it may be necessary to design a controller for a system without having an accurate knowledge of the parameters of the fixed plant. These problems have motivated a search for design methods that yield systems for which the performance is insensitive to variations in system parameters.

In order to evaluate these design methods, it is necessary to have quantitative sensitivity measures, many of which have been defined in the literature. The first definition of "classical sensitivity" was given in early work on the theory of feedback systems by Bode (1945). In fact, reduction of the effects of component variations on system performance was a primary motivation for the use of feedback. Variations of Bode's frequency domain definition of sensitivity have been used in further studies by Horowitz (1963) and Haddad and Truxal (1964). Kalman (1964) has used classical sensitivity to demonstrate a link between the theory of optimal control and classical control theory. Sensitivity in terms of pole and zero variations is discussed by Horowitz (1963), and has been used in the analysis of high order systems by Van Ness, et. al. (1965). A time-domain measure of sensitivity and its

application to control systems analysis is discussed by Tomovic (1964).

This thesis is an attempt to study the sensitivity properties of a class of linear systems. The systems to be considered are non-time varying and have a single input $R(s)$ and a single output $Y(s)$.

A vector differential equation of the form

$$\dot{\underline{x}}(t) = A \underline{x}(t) + b r(t) \quad (1.1)$$

may be used to characterize the dynamics of the system. However, the sensitivity properties of a system depend on its topology, which is not described by Eq. (1.1). Therefore, the systems to be studied are defined in terms of block diagrams.

The problem to be solved is of the following form. A given fixed plant, which is unalterable internally, is specified by a transfer function $G_p(s)$. It is assumed that the state variables of $G_p(s)$ are measurable. Also specified is a closed-loop transfer function, $Y(s)/R(s) = W(s)$, for the desired system. The general problem is to find a method for compensating the plant so as to yield $W(s)$ in such a way that the sensitivity of the system performance with respect to changes in the parameters of the system is a minimum.

The design procedure to be investigated here is the method of obtaining $W(s)$ by feeding back all of the state variables. A detailed discussion of this method is presented by Schultz and Melsa (1967). Here, the state-variable feedback system is compared to the system which realizes the same $W(s)$ by series compensation. The use of series compensation to realize a specific $W(s)$ is known as the Guillemin-Truxal

method, which is described in Chapter 5 of Truxal (1955). Thus, given a fixed plant $G_p(s)$ any specified closed-loop transfer function $W(s)$ may be obtained by either of the two methods. In this work the sensitivity properties of the resulting systems are examined. An extension of the state-variable feedback design is also investigated.

It is desired to find a general method of synthesis which yields $W(s)$ with minimum sensitivity of the system performance with respect to parameter variations. Hence, a single measure of sensitivity and a single criterion of system performance must be defined. Then the solution based strictly on these definitions may be sought. However, such a procedure may lead to solutions which are impractical. To illustrate, a system may be designed such that the sensitivity of its performance with respect to a differential change in some parameter is a minimum (in some sense). But a finite change in the same parameter may result in instability. Such a case is demonstrated in Chapter V. Therefore, while attempting to find a design method based on precise definitions of sensitivity and performance criteria, the engineer must keep in mind an overall view of the nature of the system.

In Chapter II several definitions of sensitivity from the literature are discussed, and two new sensitivity measures are defined. The generation of sensitivity measures is the subject of Chapter III. Chapter IV is a general discussion of the sensitivity properties of systems designed by cascade compensation, and by feeding back the state variables. In Chapter V several numerical examples are presented, and some conclusions are stated in Chapter VI.

It is found that a system designed by feeding back all of the state variables may be expected to be less sensitive to parameter changes than the series compensated system.

CHAPTER II

SENSITIVITY MEASURES

In this chapter several sensitivity measures are discussed in relation to the type of systems to be studied here. A sensitivity measure should incorporate two features. It should be mathematically tractable, in order that its usefulness is not limited by computational problems. Also, it must be physically meaningful in relation to the performance of the system. In particular, the sensitivity measure should relate to the performance criteria which are used to design the system. The systems to be discussed in this thesis are designed for a specific closed-loop transfer function, $W(s) = Y(s)/R(s)$. Since $W(s)$ is usually chosen so as to yield a desired response to a step input, a meaningful sensitivity measure for this type of system should indicate how the step response is affected by parameter changes.

2.1 Root Sensitivity

A sensitivity measure which has been used frequently in the analysis of control systems and circuits is root sensitivity. This measure estimates the effect of a change in a system parameter on the positions of the poles of the closed-loop system. The interpretation of the results of an analysis using root sensitivity depends on the correspondence between closed-loop pole locations and the characteristics of the transient response. The control engineer gains by experience an intuitive notion of this correspondence, but for a complicated system, where many

pole locations change with variations in a parameter, this correspondence may not be clear. Also, except in the simplest cases, the relation between the changes in pole locations and transient response, which one can obtain by inspection, is only qualitative. For these reasons root sensitivity was not used for the problems considered here.

2.2 Classical Sensitivity

The expression given here for classical sensitivity is the definition from Truxal (1955). The (classical) sensitivity of a function $T(s, \lambda)$ with respect to a parameter λ may be defined as:

$$S_\lambda^T = S_\lambda^T(s) = \frac{d \ln T}{d \ln \lambda} \quad (2.1)$$

$$= \frac{dT/T}{d\lambda/\lambda} \\ = \frac{\lambda}{T} \frac{dT}{d\lambda} \quad (2.2)$$

For $Y(s)/R(s) = W(s)$, $S_\lambda^W(s)$ is a measure of the percentage change in $W(s)$ for a percentage change in a parameter λ . A physical interpretation of S_λ^W is difficult, because S_λ^W is a function of the complex variable s . However, it is shown that $S_\lambda^W(j\omega)$ is related to a sensitivity measure which is used extensively in this study. Therefore, some formulas for classical sensitivity are presented here.

Consider the single-loop feedback system of Fig. 2.1. The (classical) sensitivity of the closed-loop transfer function with respect to G is:

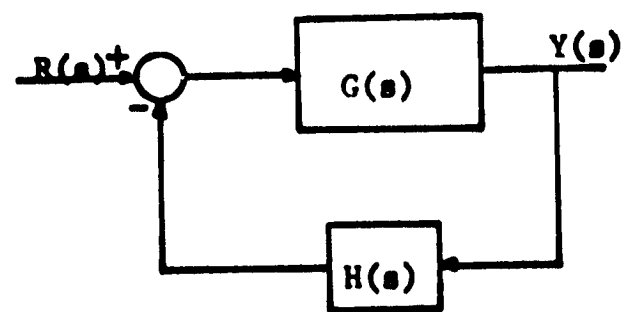


Figure 2.1 A single-loop control system.

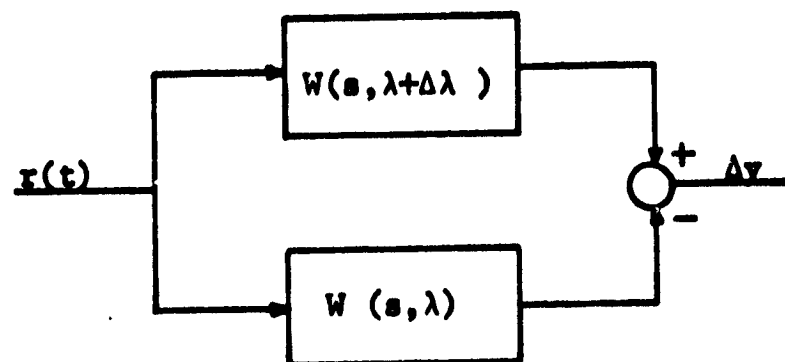


Figure 2.2 An experiment to illustrate the definition of the sensitivity function.

$$\begin{aligned}
 S_G^W &= \frac{G}{W} \frac{dW}{dG} \\
 &= \frac{G}{W} \frac{d}{dG} \left[\frac{G}{1 + GH} \right] \\
 &= \frac{1}{1 + GH} \\
 &\approx \frac{1}{GH} \text{ if } |GH| \gg 1.
 \end{aligned} \tag{2.3}$$

This result expresses the well-known fact that increasing the loop gain of a system reduces the effects of variations of elements in the forward path. This fact provides a precise link between classical control theory and the theory of optimal control. For the system of Fig. 2.1, the quantity $F(s) = 1 + GH(s)$ is called the return difference. Kalman (1964) has shown that the control law for a wide class of linear systems is optimal if and only if $|F(j\omega)| > 1$ for all real ω . Thus, it might be said that an optimal system is an insensitive system, and vice versa.

The sensitivity of $W(s)$ with respect to $H(s)$ is:

$$\begin{aligned}
 S_H^W &= \frac{W}{H} \frac{dW}{dH} \\
 &= \frac{GH}{1 + GH}
 \end{aligned} \tag{2.4}$$

It is seen that for a loop gain much greater than unity component variations in the feedback path are undiminished in their effect on $W(s)$.

Suppose λ is a parameter which appears only in a component block G .

$$\begin{aligned}
 S_{\lambda}^W &= \frac{\lambda}{W} \frac{dW}{d\lambda} \\
 &= \frac{\lambda}{W} \frac{dW}{dG} \frac{dG}{d\lambda} \frac{G}{G} \\
 &= \frac{G}{W} \frac{dW}{dG} \times \frac{\lambda}{G} \frac{dG}{d\lambda} \\
 &= S_G^W S_{\lambda}^G.
 \end{aligned}$$

Consider the function:

$$G(s) = \frac{K(s+z_1)(s+z_2)\dots(s+z_m)}{(s+p_1)(s+p_2)\dots(s+p_n)}$$

$$\text{Then } S_K^G = 1 \quad (2.5)$$

$$S_{p_1}^G = \frac{-p_1}{s + p_1} \quad (2.6)$$

$$S_{z_1}^G = \frac{z_1}{s + z_1} \quad (2.7)$$

It is clear from the above calculations that classical sensitivities are relatively easy to evaluate. This feature, along with the fact that they are related to another sensitivity measure which is closely connected with the step response of the system, makes classical sensitivity a useful tool in the analysis to follow.

2.3 Sensitivity Functions

The sensitivity measure discussed here is defined by Tomovic (1964). Let λ be a system parameter with a nominal value λ_0 . Let $y(t, \lambda)$ be the response of the system to a step input. Then for a change in the parameter λ , the step response may be expanded in a Taylor series.

$$y(t, \lambda_0 + \Delta\lambda) = y(t, \lambda_0) + \frac{dy(t, \lambda)}{d\lambda} \Big|_{\lambda_0} \Delta\lambda + \frac{d^2y(t, \lambda)}{d\lambda^2} \Big|_{\lambda_0} \frac{(\Delta\lambda)^2}{2!} + \dots$$

$\frac{dy(t, \lambda)}{d\lambda} \Big|_{\lambda_0}$, which is a function of time, is a linear approximation of

the change in $y(t, \lambda)$, at the time t , resulting from a change $\Delta\lambda$ in the parameter λ from its nominal value λ_0 . Usually it is desired to have an estimate of the change in $y(t, \lambda)$ for a percentage change in λ .

Therefore, the sensitivity of the system with respect to the parameter λ is defined as:

$$u_\lambda(t) = \frac{dy(t, \lambda)}{d\lambda} \Big|_{\lambda} \quad (2.8)$$

$u_\lambda(t)$ is called the sensitivity function for the parameter λ . The physical meaning of $u_\lambda(t)$ may become more concrete if the situation pictured in Fig. 2.2 is considered. A step input is applied simultaneously to two systems. In one system the parameter under consideration has a value λ , while in the other system the parameter has a value $\lambda + \Delta\lambda$. The difference between the outputs of the systems is:

$$\Delta y = y(t, \lambda + \Delta\lambda) - y(t, \lambda)$$

Division by the normalized change in the parameter yields:

$$\frac{\Delta y}{\Delta\lambda/\lambda} = \frac{y(t, \lambda + \Delta\lambda) - y(t, \lambda)}{\Delta\lambda/\lambda}$$

Under the assumption that the following limit exists,

$$\lim_{\Delta\lambda \rightarrow 0} \frac{\Delta y}{\Delta\lambda/\lambda} = \frac{dy(t, \lambda)}{d\lambda/\lambda} = u_\lambda(t).$$

A simple example illustrates the interpretation of sensitivity functions. Fig. 2.3 shows the block diagram for a control system for

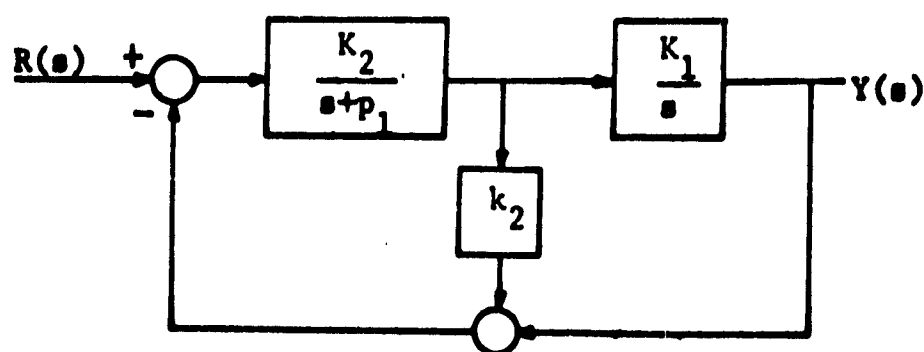


Figure 2.3 A second order control system.

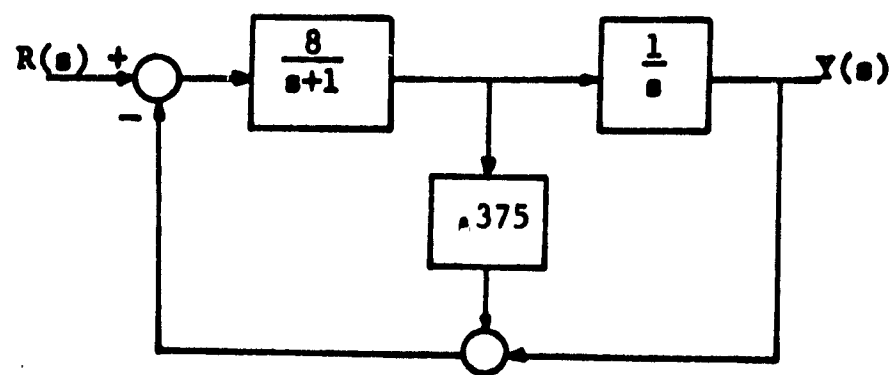


Figure 2.4 A second order control system.

which $W(s)$ is required to be:

$$W(s) = \frac{8}{s^2 + 4s + 8}$$

Fig. 2.4 is one possible realization of $W(s)$. The response ($y(t)$) of this system for a step input and the sensitivity functions ($u_{K_1}(t)$,

$u_{K_2}(t)$, $u_{k_2}(t)$) are plotted in Fig. 2.5. Since the sensitivity functions approach zero as $t \rightarrow \infty$, K_1 , K_2 , and k_2 have no effect on the final value of $y(t)$. From the fact that the magnitudes of $u_{K_1}(t)$ and $u_{K_2}(t)$ are largest during the time when the output is rising toward its final value, it may be concluded that K_1 and K_2 affect the rise time of the system, with an increase in K_1 or K_2 decreasing the rise time. Also, a change in K_2 has a smaller effect on the response than does a change in K_1 . The curve of $u_{k_2}(t)$ indicates that k_2 affects the response in the region close to its peak value, so that an increase in k_2 decreases the overshoot. This behavior should be expected, since k_2 is the coefficient of rate feedback. Fig. 2.6 shows the actual affects of 20% increases in K_1 and k_2 for the particular system of Fig. 2.4. From this figure it is seen that the qualitative effects of changes in K_1 and k_2 are as predicted.

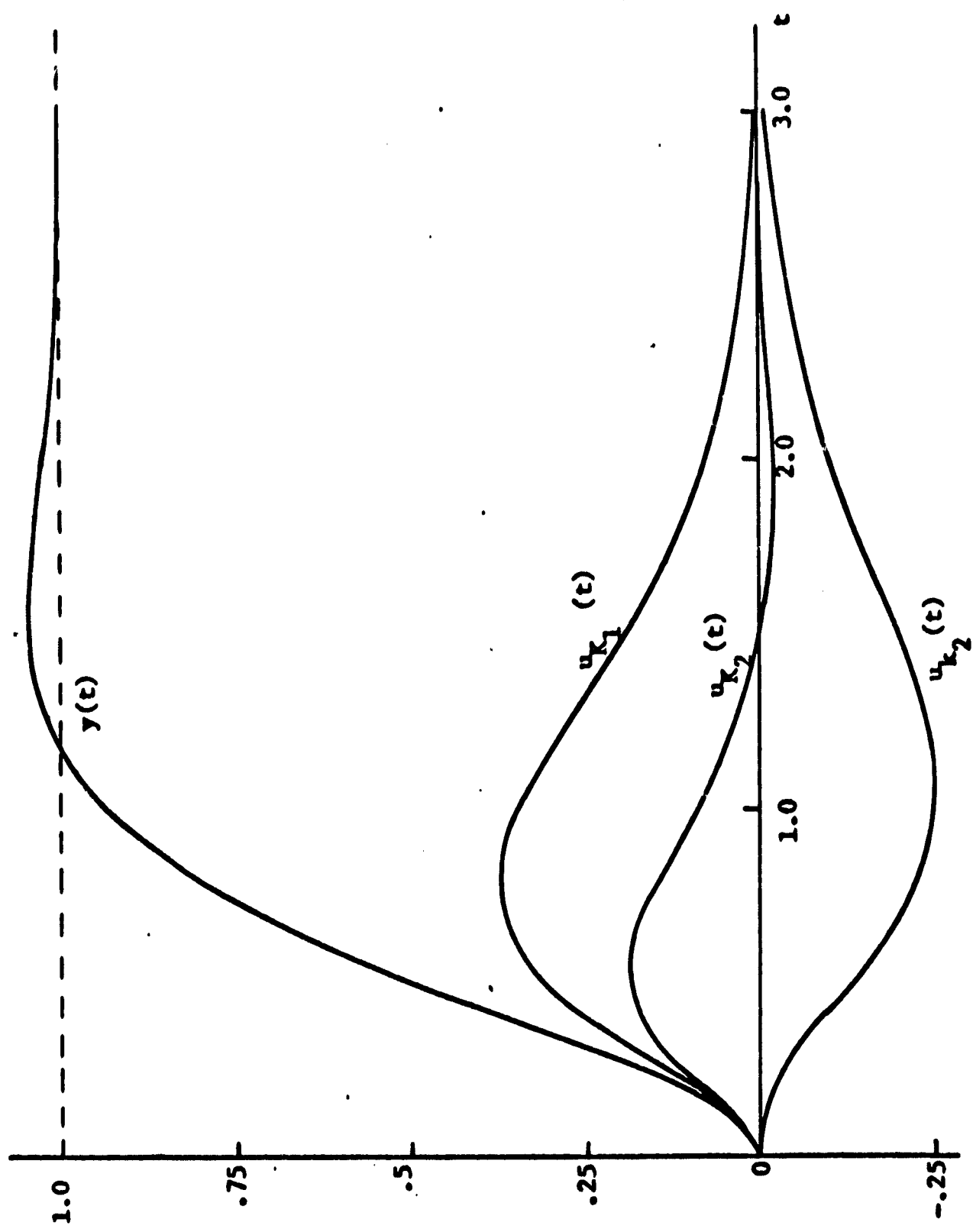


Figure 2.5 Sensitivity functions for the example.

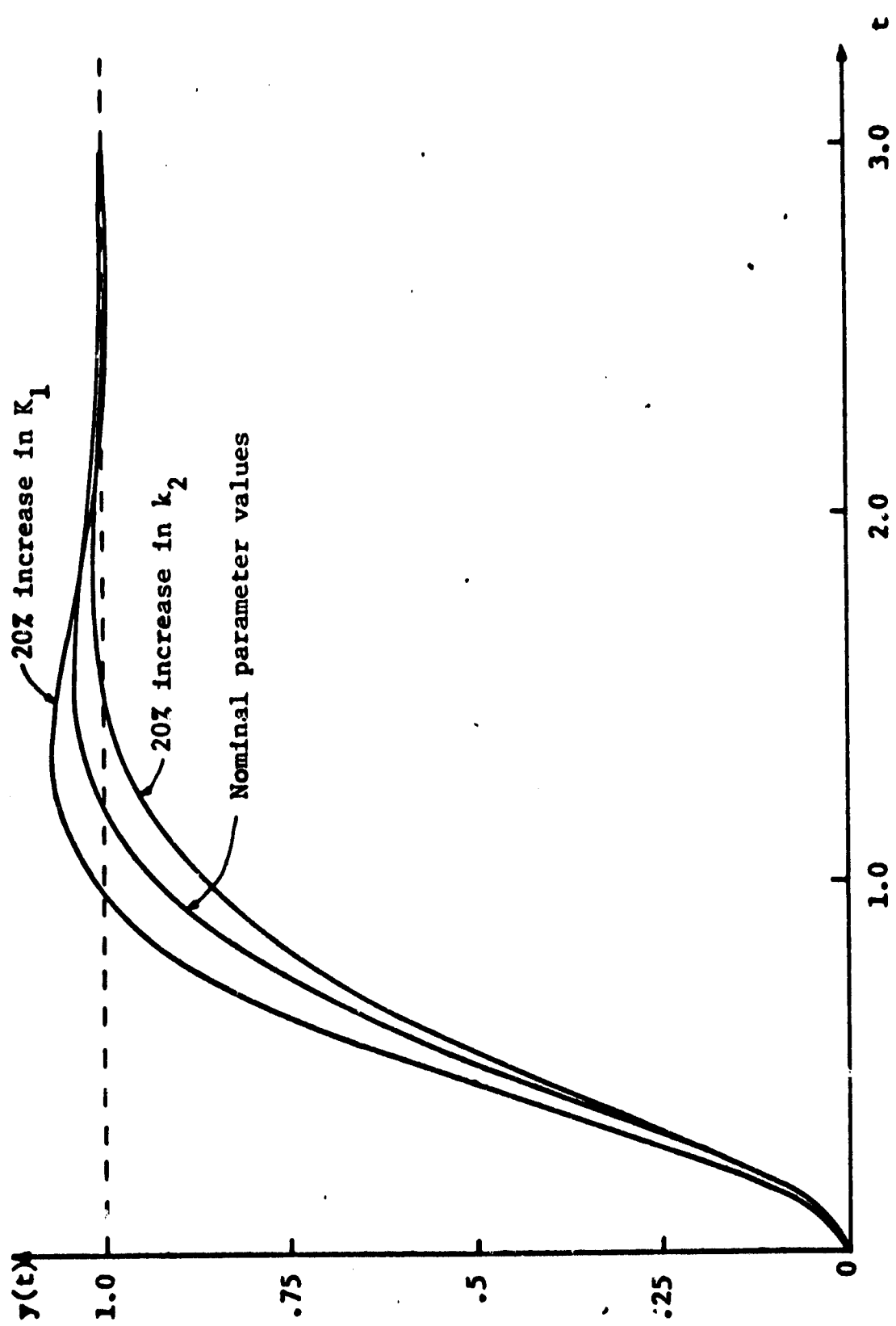


Figure 2.6 The effects of parameter variations on the step response.

2.4 Peak Sensitivity and Integral Sensitivity

The sensitivity functions have the desirable features of relating directly to transient response and indicating just how much each part of the response is affected by the parameters. However, this wealth of information is not in a compact form, since the sensitivity functions are functions of time. In an attempt to find a measure of sensitivity which relates directly to transient response and yet is more concise in form, two new sensitivity measures are defined here.

The peak sensitivity of the system with respect to a parameter is defined as

$$u_{\lambda}^* = u_{\lambda}(T) \quad (2.9)$$

where $T =$ the value of t such that $|u_{\lambda}(t)|$ is a maximum. u_{λ} gives an estimate of the maximum change in the response (at time T) for a $\pm 1\%$ change in λ .

The integral sensitivity of the system with respect to a parameter λ is defined as

$$S_{\lambda} = \int_0^{\infty} u_{\lambda}^2(t) dt \quad (2.10)$$

when this integral exists. Unless λ is a parameter affecting the final value of $y(t)$, $u_{\lambda}(t)$ approaches zero as $t \rightarrow \infty$. It is shown in Chapter III that $u_{\lambda}(t)$ is the response of a linear system. Then if $u_{\lambda}(t) \neq 0$ as $t \rightarrow \infty$, it approaches zero in an exponential fashion. In such a case $u_{\lambda}^2(t)$ is the sum of decaying exponentials, so that the above integral does exist. Therefore, it is concluded that S_{λ} exists if λ does not affect the final value of $y(t)$. If the final value of $y(t)$ does depend

on λ , the integral sensitivity with respect to λ is not defined. The sensitivity of the system with respect to such a parameter might be characterized by the peak sensitivity and the final value of the sensitivity function $u_\lambda(t)$.

The definition given for integral sensitivity was chosen as a measure of the overall influence of a parameter λ on the step response. For the integrand, $u_\lambda^2(t)$ was preferred over $|u_\lambda(t)|$ for two reasons. The squared quantity weights large values of $u_\lambda(t)$ more heavily than small values. Also, the integrand $u_\lambda^2(t)$ allows the use of Parseval's Theorem in the evaluation of the integral. This is discussed in the next chapter.

Clearly, in obtaining more concise sensitivity measures, some information as to the way in which λ affects the response is lost. The sensitivity functions are useful in particular cases where this information is important.

CHAPTER III

GENERATION OF SENSITIVITY MEASURES

The purpose of this chapter is to show how sensitivity functions, peak sensitivities, and integral sensitivities may be found. To generate these sensitivity measures, an analog or digital computer is required, while classical sensitivities can be found easily from a block diagram of the system. It is shown that classical sensitivity and integral sensitivity are connected by a relationship which enables one to predict the nature of sensitivity functions and integral sensitivity from a knowledge of classical sensitivity.

3.1 The Relation between S_λ and S_λ^W

From the definition of the sensitivity function,

$$u_\lambda(t) = \frac{dy(t)}{d\lambda}$$

$$L\{u_\lambda(t)\} = U_\lambda(s) = \frac{dY(s)}{d\lambda}$$

$$= R(s) \frac{d(Y(s)/R(s))}{d\lambda/\lambda}$$

for $R(s)$ not a function of λ . Since the sensitivity functions are defined in Chapter II for a step input, $R(s) = \frac{1}{s}$. Then,

$$\begin{aligned}
 u_\lambda(s) &= \frac{1}{s} \frac{dW(s)}{d\lambda} \frac{W(s)}{W(s)} \\
 &= \frac{1}{s} W(s) \frac{\lambda}{W(s)} \frac{dW(s)}{d\lambda} \\
 &= \frac{1}{s} W(s) S_\lambda^W
 \end{aligned} \tag{3.1}$$

For $s = j\omega$,

$$|u_\lambda(j\omega)| = \frac{|W(j\omega)|}{|\omega|} |S_\lambda^W(j\omega)|.$$

Now,

$$\begin{aligned}
 S_\lambda &= \int_0^\infty u_\lambda^2(t) dt \\
 &= \int_0^\infty u_\lambda^2(t) dt
 \end{aligned}$$

since $u(t) = 0$ for $t < 0$. Then using Parseval's Theorem,

$$S_\lambda = \frac{1}{2\pi j} \int_{-j\infty}^{j\infty} U(s) U(-s) ds \tag{3.2}$$

$$\begin{aligned}
 &= \frac{1}{2\pi} \int_{-\infty}^{\infty} |U(j\omega)|^2 d\omega \\
 &= \frac{1}{2\pi} \int_{-\infty}^{\infty} \frac{|W(j\omega)|^2}{\omega^2} |S_\lambda^W(j\omega)|^2 d\omega
 \end{aligned} \tag{3.3}$$

Eq. (3.3) shows the relation between integral sensitivity S_λ and classical sensitivity S_λ^W . Clearly, reducing $|S_\lambda^W(j\omega)|$ reduces S_λ .

In this thesis the systems to be studied have identical transfer functions $W(s)$, but different classical sensitivities with respect to the same parameter. Then from Eq. (3.3) it is seen that the differences between integral sensitivities for such systems are determined by differences in their classical sensitivities. This link between

classical and integral sensitivity is important, because classical sensitivities are easily found from a block diagram of the system, while the generation of S_λ requires a computer. For this reason it is desirable to have a method for finding classical sensitivities.

3.2 Generation of Classical Sensitivities

The procedure given here for finding classical sensitivities from the system block diagram is essentially the same as the method described by Tomovic (1964). The block diagram of a control system is shown in Fig. 3.1, where the component blocks of particular interest are $G_1(s)$ and $H_1(s)$. For the case where all of the $G_j(s)$ are first order and the $H_j(s) = k_j$ (constants), Fig. 3.1 is a block diagram of a system where all of the state variables are fed back. However, the expressions derived here for classical sensitivities are valid for $G_j(s)$ and $H_j(s)$ of any order. Fig. 3.2 shows a reduction of the block diagram for the purpose of calculating $S_{G_1}^W$ and $S_{H_1}^W$. $L(s)$ is the transfer function from E_1 to B_1 . (These variables are defined in Fig. 3.1.) $M(s)$ represents the sum of the feedback through the paths containing H_1, H_2, \dots, H_{i-1} when these paths are referred to the output. $N(s)$ is the transfer function from the output of G_1 to the system output. These quantities are defined by the following equations.

$$L(s) = \frac{B_1(s)}{E_1(s)} = \frac{\prod_{j=1}^n G_j}{1 + \sum_{j=1}^n (H_j \prod_{l=j}^n G_l)} \quad (3.4)$$

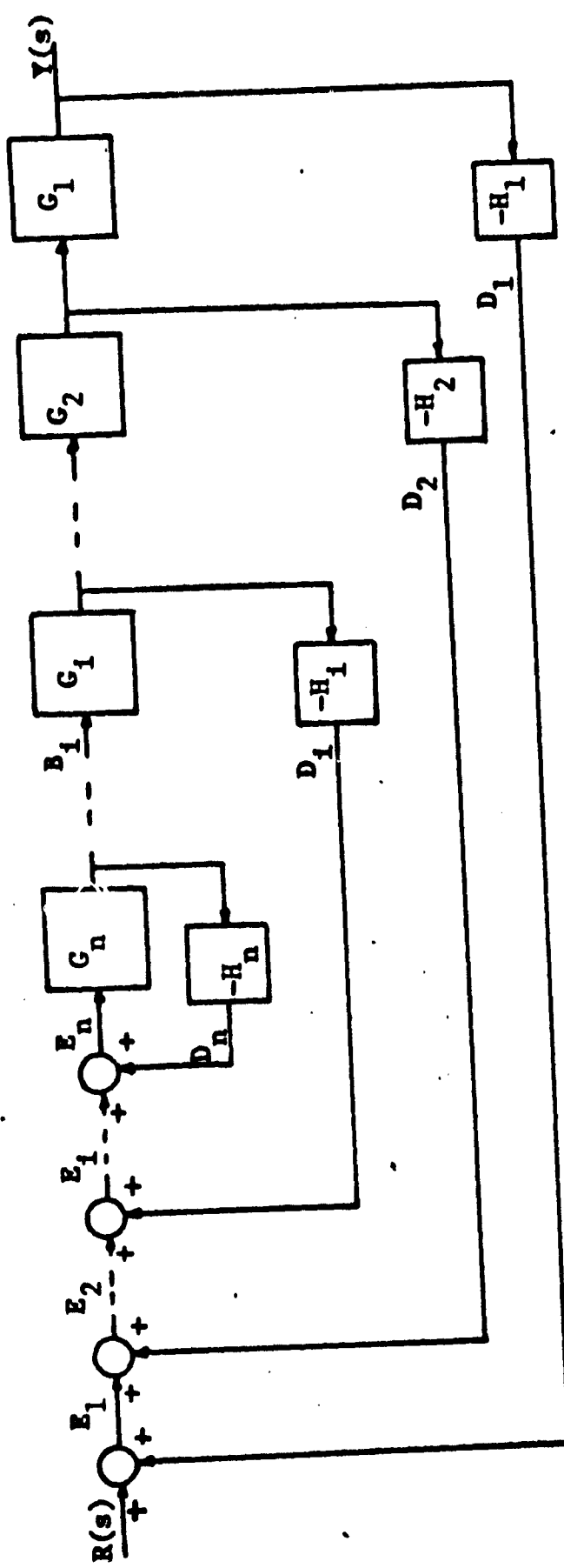


Figure 3.1 The block diagram of a control system.

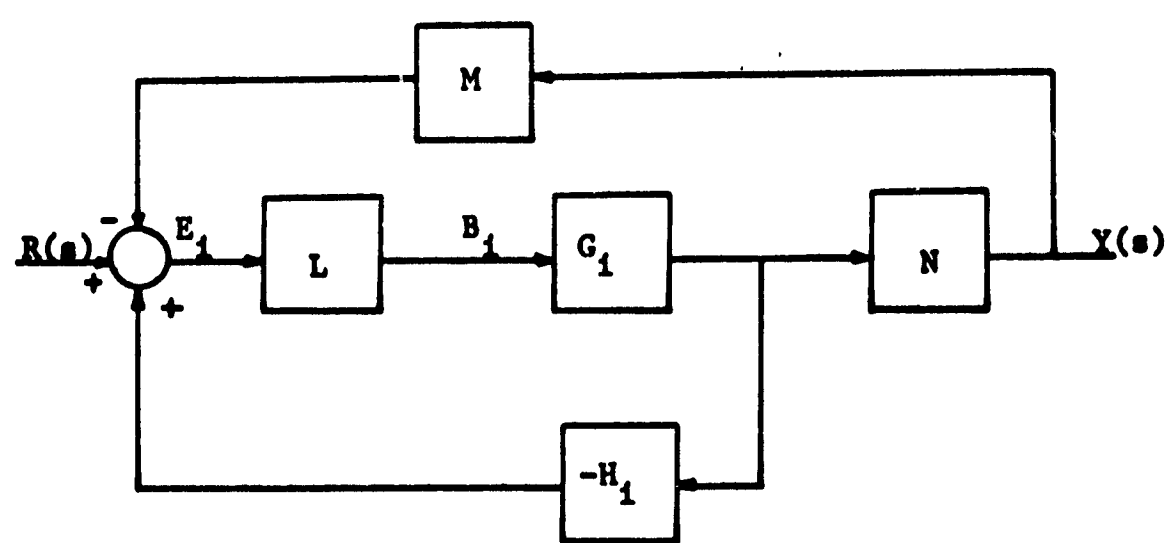


Figure 3.2 A reduced block diagram.

$$M(s) = H_1 + \sum_{j=2}^{i-1} (H_j \prod_{l=1}^{j-1} G_l) \quad (3.5)$$

$$N(s) = \prod_{j=1}^{i-1} G_j \quad (3.6)$$

Then,

$$\begin{aligned} \frac{Y(s)}{R(s)} = W(s) &= \frac{G_1 LN}{1 + G_1 L [H_1 + NM]} \\ &= \frac{G_1 LN}{1 + G_1 LF} \end{aligned} \quad (3.7)$$

where $F = H_1 + NM$.

Then the sensitivity of $W(s)$ with respect to $G_1(s)$ is

$$\begin{aligned} s_{G_1}^W &= \frac{G_1(s)}{W(s)} \frac{dW(s)}{dG_1(s)} \\ &= \frac{G_1}{W} LN \frac{1 + G_1 LF - G_1 LF}{[1 + G_1 LF]^2} \\ &= \frac{1}{1 + G_1 LF} \end{aligned}$$

The transfer function from the input to $E_1(s)$ is:

$$\begin{aligned} \frac{E_1(s)}{R(s)} &= \frac{1}{1 + G_1 LN [M + \frac{H_1}{N}]} \quad (3.8) \\ &= \frac{1}{1 + G_1 L [H_1 + NM]} \\ &= \frac{1}{1 + G_1 LF} \end{aligned}$$

$$= s_{G_1}^W \quad (3.9)$$

Thus, the classical sensitivity of the system with respect to $G_1(s)$ is just the transfer function from the input to $E_1(s)$. The sensitivity of $W(s)$ with respect to $H_1(s)$ is:

$$S_{H_1}^W = \frac{H_1(s)}{W(s)} \frac{dW(s)}{dH_1(s)}$$

In order to simplify calculations, let $G(s)$ be defined as:

$$G(s) = \frac{LG_1}{1 + LG_1 \frac{M}{N}}$$

$$\text{Then, } W(s) = N \frac{G}{1 + GH_1}$$

$$S_{H_1}^W = \frac{H_1}{W} NG \left[\frac{-G}{(1 + GH_1)^2} \right]$$

$$= \frac{-GH_1}{1 + GH_1}$$

$$= \frac{D_1(s)}{R(s)}$$

(3.10)

The classical sensitivity of the system with respect to $H_1(s)$ is the transfer function from the input to $D_1(s)$.

Eqs. (3.9) and (3.10) for classical sensitivities only apply to the system of Fig. 3.1. However, the series compensated system is easily treated as a special case. A unity feedback system with a fixed plant $G_p(s)$ and a series compensator $G_c(s)$ is shown in Fig. 3.3. Since there is no feedback from the output of $G_c(s)$, the transfer functions in the forward path may be combined. Let $G_1(s) = G_c(s) G_p(s)$. Then the

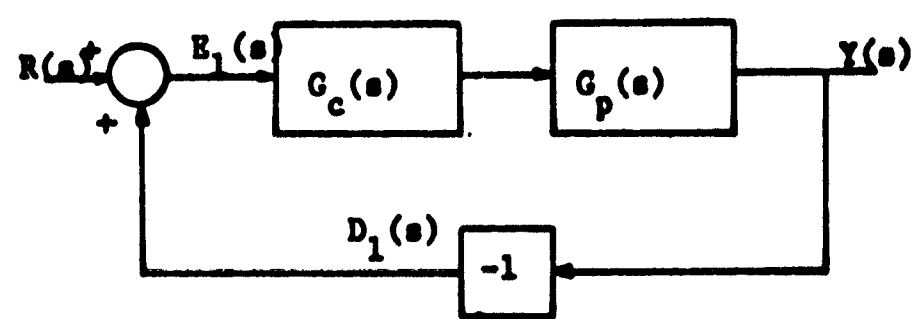


Figure 3.3 A series compensated system.

series compensated system of Fig. 3.3 is a special case of the system of Fig. 3.1, with only one block in the forward path ($G_1(s)$) and with $H_1(s) = 1$. Now, from Eqs. (3.9) and (3.10),

$$s_{G_1}^W = \frac{Z_1(s)}{R(s)} = \frac{1}{1 + G_1(s)}$$

$$= \frac{1}{1 + G_c(s)G_p(s)}$$

$$s_{H_1}^W = \frac{D_1(s)}{R(s)} = \frac{-G_1(s)}{1 + G_1(s)}$$

$$= \frac{-G_c(s) G_p(s)}{1 + G_c(s) G_p(s)}$$

For system configurations which are not special cases of the diagram in Fig. 3.1, the classical sensitivities can be found by direct application of the definition (Eq. (2.2)).

3.3 Generation of Sensitivity Functions, Peak Sensitivity, and Integral Sensitivity.

In Section 3.1 S_λ was expressed as an integral in the form of Eq. (3.2). For the case where $U(s)$ is a ratio of polynomials, the integral has been tabulated as a function of the coefficients of the polynomials (Newton, et.al. (1957)). However, the expressions for this integral become cumbersome rapidly as the order of $U(s)$ increases. Since for an n th order system the order of $U(s)$ is $2n$, the evaluation of S_λ by Eq. (3.2) is impractical.

The method presented in Section 3.2 for finding classical sensitivities and Eq. (3.1) for $U_\lambda(s)$ indicate how sensitivity functions may be generated. Eq. (3.1) is repeated here:

$$U_\lambda(s) = \frac{1}{s} W(s) S_\lambda^W$$

If α is a parameter only of $G_1(s)$, then

$$U_\alpha(s) = \frac{1}{s} W(s) S_{G_1}^W S_\alpha^{G_1} \quad (3.11)$$

If β is a parameter only of $H_1(s)$, then

$$U_\beta(s) = \frac{1}{s} W(s) S_{H_1}^W S_\beta^{H_1} \quad (3.12)$$

The generation of $U_\alpha(s)$ and $U_\beta(s)$ is shown in Fig. 3.4. A step input is applied to a system with the transfer function $W(s)$. The output is applied to the input of a second system (with transfer function $W(s)$) whose sensitivity is to be studied.

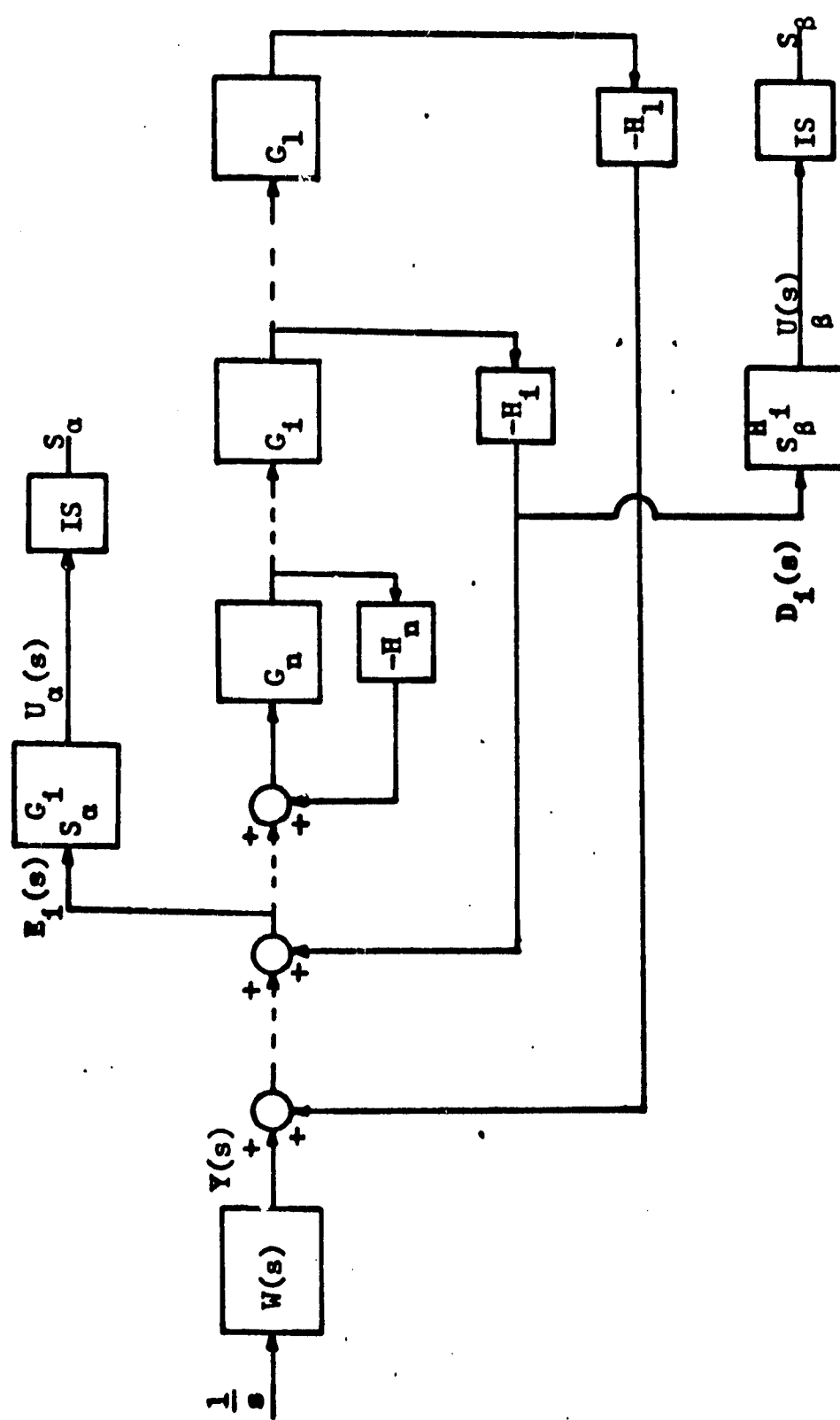


Figure 3.4 The generation of sensitivity functions and integral sensitivities.

The transfer functions $\frac{E_1(s)}{Y(s)}$ and $\frac{D_1(s)}{Y(s)}$ provide the terms $S_{G_1}^W$ and $S_{H_1}^W$ in Eqs. (3.11) and (3.12). The blocks labeled $S_a^{G_1}$ and $S_\beta^{H_1}$ provide the corresponding terms in Eqs. (3.11) and (3.12) to complete the generation of $U_a(s)$ and $U_\beta(s)$. For the cases where the parameters a and β are gains, poles, or zeros, $S_a^{G_1}$ and $S_\beta^{H_1}$ are simple functions, as shown in Chapter II. Finally, the blocks labeled I. S. (Integral Squared) square the time functions $u_a(t)$ and $u_\beta(t)$ and integrate to yield S_a and S_β . (The generation of the sensitivity functions is carried out in the time domain by a computer, but for convenience, the method is discussed using the transformed variables.)

For the example systems of Chapter V, a digital computer is used to generate the sensitivity functions, peak sensitivities, and integral sensitivities. For the 5th order system of Example 3 in Chapter V, the sensitivities with respect to eight parameters are found. The generation of the sensitivity functions, peak sensitivities, and integral sensitivities for each parameter leads to a system of equations of order 23. The computer time required for the solution is approximately 4 minutes.

It has been pointed out that the evaluation of S_λ from tables of the integral (Eq. (3.2)) is usually impractical. However, for the third order system of Example 1 in Chapter V, the integral sensitivities were found by this method. These results were compared to those obtained from a digital computer program, which approximately solves the differential equations for the integral sensitivities. The values obtained by the two methods agreed to within 0.3%.

CHAPTER IV

SENSITIVITY AND STATE-VARIABLE FEEDBACK

The sensitivity measures which have been discussed are used in this chapter and in Chapter V to study the sensitivity of some linear control systems. In the present chapter a slightly general discussion of the problem is attempted. Because sensitivity analysis in terms of sensitivity functions and integral sensitivity is practically limited to specific cases, much use is made of classical sensitivity.

4.1 Series Compensation and State Variable Feedback

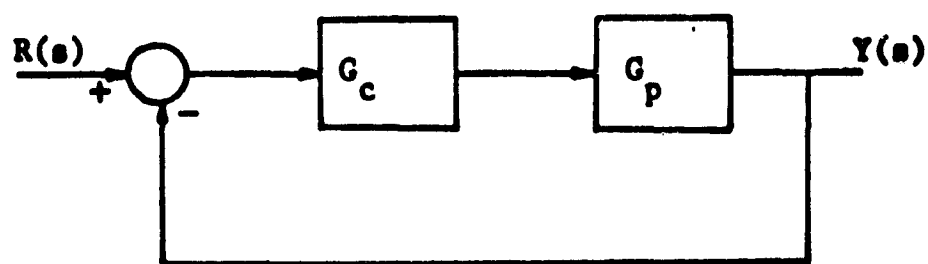
It is assumed that a given fixed plant is to be compensated in order to yield a desired closed-loop response. Figs. 4.1 and 4.2 indicate two approaches which may be used to solve the problem. The fixed plant is of order m , and has a transfer function

$$G_p(s) = G_1(s)G_2(s)\dots G_m(s)$$

where the $G_i(s)$ are first order. In Fig. 4.1 a cascade compensator $G_c(s)$ has been used to realize the required $W(s)$, which is of order n .

$$W(s) = \frac{G_c G_p}{1 + G_c G_p} \quad (4.1)$$

$G_c(s)$ may be found by the Guillemin-Truxal method discussed in Truxal (1955). In Fig. 4.2 $W(s)$ is obtained by feeding back the state variables of the fixed plant and, if necessary, by adding first order series



$$G_p(s) = G_1(s)G_2(s)\dots G_m(s) \quad (\text{order } m)$$

$$G_{eq}(s) = G_c(s)G_p(s) \quad (\text{order } n)$$

Figure 4.1 The series compensated system.

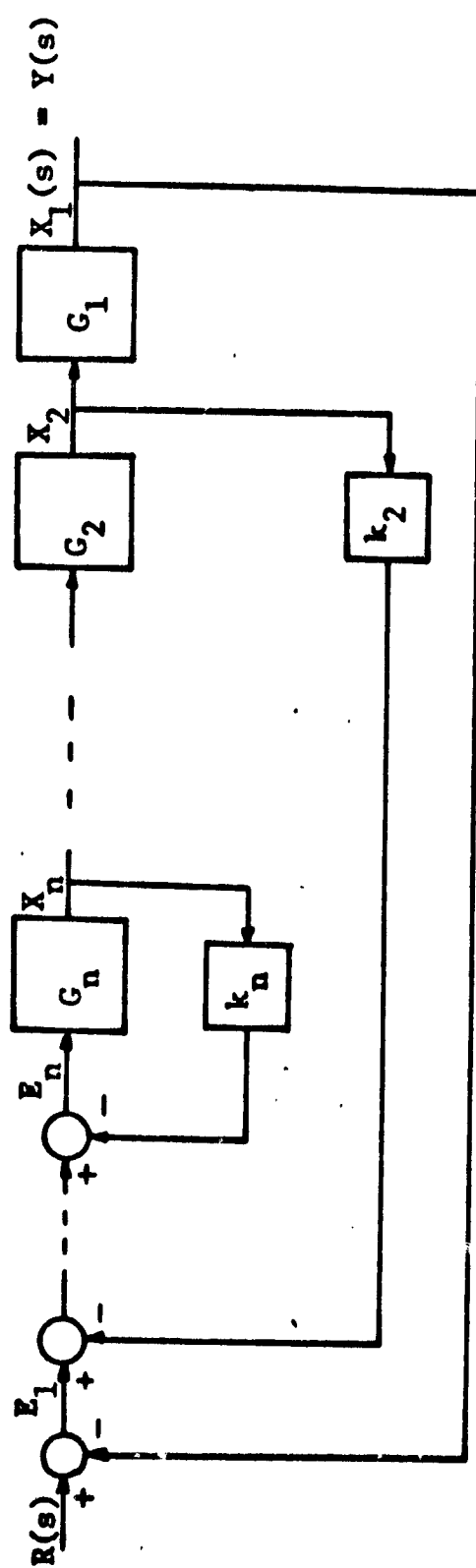


Figure 4.2 The state-variable feedback system.

compensating elements, whose state variables are also fed back. This method of design is described in detail by Schultz and Melsa (1967). The resulting system has the same nth order, closed-loop transfer function $W(s)$ as the series compensated system. The following expression for $W(s)$ of the state-variable feedback system is derived in the Appendix.

$$W(s) = \frac{G_1 G_2 \dots G_n}{1 + k_1 G_1 G_2 \dots G_n + k_2 G_2 \dots G_n + \dots + k_n G_n} \quad (4.2)$$

$$= \frac{\prod_{i=1}^n G_i}{1 + \sum_{i=1}^n \left[\prod_{j=i}^n G_j \right]} \quad (4.3)$$

4.2 Sensitivities

The sensitivities of the two systems with respect to parameters in both the forward paths and the feedback paths are studied in this section. However, more attention is focused on the parameters in the forward path, especially those in the fixed plant. This is because in most cases the designer is able to select compensating components with production tolerances which are small enough to avoid problems of sensitivity with respect to these components. Sensitivities with respect to the compensating elements should still be checked, however, in order to avoid a situation where the tolerances required are impractical.

Consider the state variable feedback system. Using Eq. (3.9),

$$S_{G_1}^W = \frac{E_1(s)}{R(s)}$$

It is shown in the Appendix that

$$S_{G_1}^W = \frac{1 + \sum_{j=1}^{n-1} \left[k_j + \sum_{l=j+1}^n G_l \right]}{1 + \sum_{j=1}^n \left[k_j + \sum_{l=j+1}^n G_l \right]} \quad (4.4)$$

For example in a third order system these sensitivities are:

$$S_{G_1}^W = \frac{1 + k_2 G_2 G_3 + k_3 G_3}{1 + k_1 G_1 G_2 G_3 + k_2 G_2 G_3 + k_3 G_3} \quad (4.5a)$$

$$S_{G_2}^W = \frac{1 + k_3 G_3}{1 + k_1 G_1 G_2 G_3 + k_2 G_2 G_3 + k_3 G_3} \quad (4.5b)$$

$$S_{G_3}^W = \frac{1}{1 + k_1 G_1 G_2 G_3 + k_2 G_2 G_3 + k_3 G_3} \quad (4.5c)$$

The denominators of $S_{G_i}^W$ do not depend on i , so the magnitudes of the $S_{G_i}^W$ may be compared by examining the numerators. For this discussion let

$$S_{G_i}^W = \frac{A_i(s)}{B(s)}$$

$$= \frac{A_i(j\omega)}{B(j\omega)} \quad \text{for } s = j\omega.$$

For frequencies less than the system bandwidth, and if all $k_i > 0$, it may be expected that $|A_i(j\omega)|$ is smaller for larger values of i . In this case, from the discussion of the relation between classical sensitivity and integral sensitivity, it is expected that the $S_{G_i}^W$ are smaller for larger values of i . Intuitively, one might predict this behavior from noticing that the $G_i(s)$ are more imbedded in feedback loops for larger values of i . For all of the examples studied with $k_i > 0$, it was found that $S_{G_i}^W$ decreased as i increased. However, it is not always true that all of the k_i are positive. If one or more of the feedback coefficients are negative, it may be expected that for some value of i , $S_{G_{i+1}}^W > S_{G_i}^W$. An example of this situation is shown in Chapter V.

Consider now the series compensated system. Let $G_{eq}(s) = G_c(s) G_p(s)$. Then using the fact that the sensitivities for all blocks in cascade are equal,

$$S_{G_{eq}}^W = S_{G_c}^W = S_{G_i}^W = \frac{E(s)}{R(s)} \text{ for all } i.$$

Since the closed-loop transfer functions for the two systems are the same,

$$S_{G_{eq}}^W = \frac{E(s)}{R(s)} = \frac{E_1(s)}{R(s)} = S_{G_1}^W$$

where $E_1(s)$ is defined in Fig. 4.2, and $S_{G_1}^W$ refers to the state feedback system. Thus, the sensitivity of $W(s)$ with respect to any block in the forward path of the series compensated system is equal to the sensitivity of $W(s)$ with respect to G_1 in the system using state-variable feedback. Then for most cases $S_{G_1}^W$ is smaller for the state variable feedback system, since $S_{G_1}^W$ decreases as i increases in that system.

The sensitivities of the state-variable feedback system with respect to the feedback coefficients, k_i , are now considered. In the Appendix it is shown that

$$S_{k_1}^W = \frac{-k_1 \prod_{j=1}^n G_j}{1 + \sum_{j=1}^n \left[k_j \prod_{l=j}^n G_l \right]} \quad (4.6)$$

$$= \frac{-k_1 \prod_{j=1}^n G_j}{B(s)} \quad (4.7)$$

For the case of a third order system these sensitivities are:

$$\begin{aligned} S_{k_1}^W &= \frac{-k_1 G_1 G_2 G_3}{B(s)} \\ &= \frac{-G_1 G_2 G_3}{B(s)} = \frac{-Y(s)}{R(s)} \end{aligned} \quad (4.8a)$$

for $k_1 = 1$

$$s_{k_2}^W = \frac{-k_2 G_2 G_3}{B(s)} \quad (4.8b)$$

$$s_{k_3}^W = \frac{-k_3 G_3}{B(s)} \quad (4.8c)$$

For the series compensated system let $k = 1$ be the unity gain of the single feedback path. Then,

$$s_k^W = \frac{-G_c G}{1 + G_c G} = \frac{-Y(s)}{R(s)}$$

$$= s_{k_1}^W \quad \text{for } k_1 = 1$$

Thus, the sensitivity of the state-variable feedback system with respect to the unity feedback gain from the output is the same as for the series compensated system. The relative magnitudes of $s_{k_1}^W(j\omega)$, for different values of i , depend on the magnitudes of the $G_i(j\omega)$.

If $|G_1(j\omega)| > 1$ and if the k_i are of the same order of magnitude, it would appear that $|s_{k_1}^W(j\omega)|$ decreases as i increases. In such cases the state-variable feedback system would not be more sensitive with respect to changes in the feedback coefficients than would the series compensated system with respect to a change in the single unity feedback gain.

4.3 Restrictions Imposed by the Fixed Plant and the Closed-Loop Transfer Function.

From the comparisons made above between the series compensated system and the state-variable feedback system, it is seen that

decreased sensitivity may be obtained by a change in the system configuration. However, it appears that the minimum sensitivity that can be achieved is limited by the fact that the fixed plant and the closed-loop response are specified. An example which illustrates this is the system of Fig. 4.3. The closed loop transfer function is

$$W(s) = \frac{K_1 K_2 K_3}{s^3 + (p_2 + p_3 + k_3 K_3)s^2 + (p_2 p_3 + p_2 k_3 K_3 + k_2 K_2 K_3)s + K_1 K_2 K_3}$$

If k_2 and k_3 are positive, it may be expected that G_3 is the least sensitive block. From Eq. (4.5c),

$$S_{G_3}^W = \frac{s(s + p_2)(s + p_3)}{s^3 + (p_2 + p_3 + k_3 K_3)s^2 + (p_2 p_3 + p_2 k_3 K_3 + k_2 K_2 K_3)s + K_1 K_2 K_3}$$

The examples of Chapter V show that the low frequency asymptote of S_{λ}^W is important in determining S_{λ} . Here, for small values of ω ,

$$|S_{G_3}^W(j\omega)| \approx \frac{p_2 p_3 \omega}{K_1 K_2 K_3}$$

The product $p_2 p_3$ is determined by the fixed plant, while the product $K_1 K_2 K_3$ is specified by the closed-loop transfer function. Decreasing $S_{G_3}^W$ by specifying a new closed loop response with a larger constant term, $K_1 K_2 K_3$, is usually not feasible, since the constant term determines the loop gain of the system; the loop gain is usually

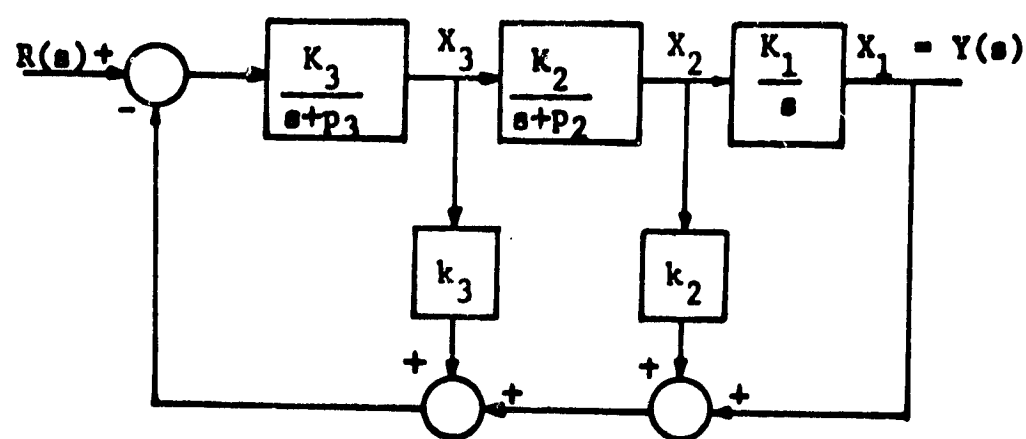


Figure 4.3 A third order control system.

restricted so that the system remains in a linear region of operation for some expected input.

The dependence of sensitivity on the fixed plant and the closed-loop transfer function is currently being investigated by Dial (1967).

4.4 Modifications of State Variable Feedback

Earlier in this chapter it was found that, under certain conditions, one would expect the system using state-variable feedback to be the least sensitive to the $G_1(s)$ nearest the input. In an attempt to extend this minimum value of sensitivity to the other $G_i(s)$, modifications of the feedback structure are investigated.

If in the system of Fig. 4.2 all the feedback paths are referred to the output, then the resulting system has the form of Fig. 4.4 where

$$H_{eq}(s) = 1 + \frac{k_2}{G_1} + \frac{k_3}{G_1 G_2} + \dots + \frac{k_n}{G_1 \dots G_{n-1}} \quad (4.9)$$

The system in this form is referred to as the "H-equivalent" system. The transfer function $Y(s)/R(s)$ is unchanged. The H-equivalent system is often used as a block diagram reduction of the state-variable feedback system for the purpose of calculating the closed-loop transfer function. However, the H-equivalent system here is intended as an actual physical system; that is, the output is fed back through $H_{eq}(s)$, and no other state variables are fed back. For the H-equivalent system,

$$\begin{aligned}
 S_G^W &= \frac{E'(s)}{R(s)} = \frac{1}{1 + GH_{eq}} \\
 &= \frac{1}{1 + G_1 G_2 \dots G_n [1 + \frac{k_2}{G_1} + \dots + \frac{k_n}{G_1 \dots G_{n-1}}]} \\
 &= \frac{1}{1 + G_1 G_2 \dots G_n + k_2 G_2 \dots G_n + \dots + k_n G_n} \\
 &= S_{G_n}^W
 \end{aligned} \quad (4.10)$$

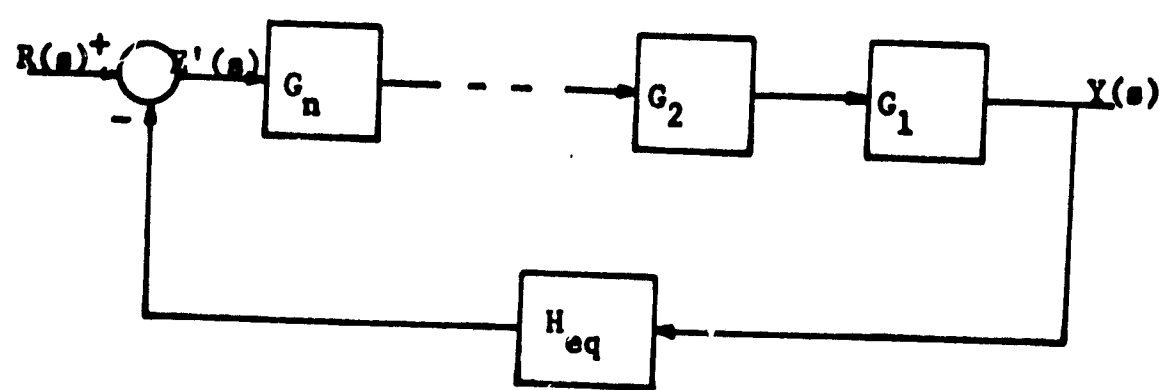


Figure 4.4 The H -equivalent system.

Thus, the sensitivity of the H-equivalent system with respect to any block in the forward path is equal to the sensitivity of the state-variable feedback system with respect to $G_n(s)$. This is the "minimum sensitivity" which was sought.

With regard to the construction of a system, the H-equivalent configuration has both advantages and disadvantages in comparison to the state-variable feedback system. For the H-equivalent system only the output is actually measured. This is an advantage when measurement of all of the state variables is difficult. However, unless the numerator and denominator of $G(s)$ are of the same order, the numerator of $H_{eq}(s)$ is of higher order than the denominator. Then in order to realize $H_{eq}(s)$ approximately, poles must be added. This problem is treated in an example in Chapter V.

4.5 A Note on Integral Sensitivity and the Poles of the Fixed Plant

Consider again Eqs. (4.2) and (4.3) for $W(s)$ of the state-variable feedback system. It is assumed that the functions $G_i(s)$ are of the form:

$$G_i(s) = \frac{K_i(s + z_i)}{s + p_i} \quad (4.11)$$

The factor $(s + z_i)$ is not always present. If the functions in the numerator and denominator of $W(s)$ are cleared by multiplying by $\prod_{i=1}^n (s + p_i)$, $W(s)$ may be written as:

$$W(s) = \frac{P(s)}{Q(s)} = \frac{a_m s^m + a_{m-1} s^{m-1} + \dots + a_0}{s^n + b_{n-1} s^{n-1} + \dots + b_0} \quad (4.12)$$

where the roots of $Q(s)$, the characteristic polynomial, are the closed-loop poles of the system. Similarly, if the expressions for the

classical sensitivities, $S_{G_1}^W$, are cleared of fractions, the sensitivities may be written as:

$$S_{G_1}^W = \frac{N_1(s)}{Q(s)}$$

$$= \frac{c_1 s^k + c_{k-1} s^{k-1} + \dots + c_0}{s^n + b_{n-1} s^{n-1} + \dots + b_0} \quad (4.13)$$

From Eqs. (4.12) and (4.13) it is seen that the denominators of the $S_{G_1}^W$ are the characteristic polynomial, which is specified by the required closed-loop response.

The sensitivity with respect to $G_n(s)$ is:

$$S_{G_n}^W = \frac{\prod_{i=1}^n (s + p_i)}{Q(s)} \quad (4.14)$$

Recall that the integral sensitivity, S_λ , depends on the magnitude of S_λ^W . Now,

$$|S_{G_n}^W|^2 = \frac{\prod_{i=1}^n (s + p_i)(-s + p_i)}{Q(s) Q(-s)} \quad (4.15)$$

From Eq. (4.15) it is clear that the integral sensitivity, $S_{G_n}^W$, is the same for two systems which have the same closed-loop response, but whose open loop poles are symmetrical with respect to the $j\omega$ -axis.

Thus, one or more of the open loop poles could be located in the RHP, and $S_{G_n}^W$ would remain the same. This emphasizes the fact that the sensitivity function, $u_\lambda(t)$, and therefore S_λ , are defined in terms of an incremental change in the parameter λ . Clearly, for sufficiently

large changes in the gain K_n , a system with open-loop poles in the RHP behaves very differently from a system with only LHP open-loop poles.

The discussion above indicates that in addition to compensating the system for the desired closed-loop response and evaluating sensitivities, it is necessary to retain a wider view of the system design - for example, in terms of a root locus.

4.6 Summary

From the analysis in section 4.2 it is seen that, under certain conditions, the state-variable feedback system is less sensitive to parameter changes as compared to the series compensated system with the same closed-loop transfer function $W(s)$. However, it appears that the minimum sensitivity attainable is restricted by the fixed plant and by the required $W(s)$. The H -equivalent system, or a system using an approximation to $H_{eq}(s)$, might be used to extend this minimum value of sensitivity to all of the blocks in the forward path. Chapter V consists of a series of examples which illustrate the ideas discussed here.

CHAPTER V

EXAMPLES

This chapter consists of several examples to illustrate the sensitivity properties of systems designed by the methods discussed in Chapter IV. In Example 1 a fixed plant is compensated by feeding back all of the state variables and by the Guillemin-Truxal method. The sensitivities of the two resulting systems are compared. The same fixed plant is compensated with H-equivalent feedback in Example 2., and a system with an approximation of $H_{eq}(s)$ is discussed in Example 3. In Example 4, a zero, which is not desired in $W(s)$, is included in the fixed plant. Sensitivity analysis is used to determine the parameters of a cascade compensator which provides for cancellation of the zero in the closed-loop response.

Example 1. Figure 5.1 shows the fixed plant of a control system which is required to have the following closed-loop transfer function.

$$W(s) = \frac{80}{s^3 + 14s^2 + 48s + 80}$$
$$= \frac{80}{(s + 10)(s^2 + 4s + 8)}$$

$W(s)$ is obtained in two ways. One system is synthesized using state-variable feedback, while the Guillemin-Truxal method is used to design

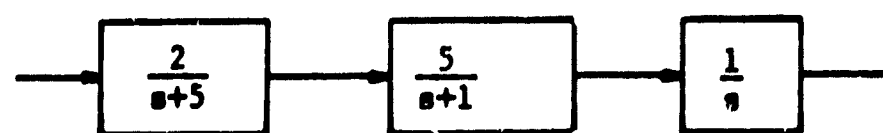


Figure 5.1 The fixed plant of Example 1.

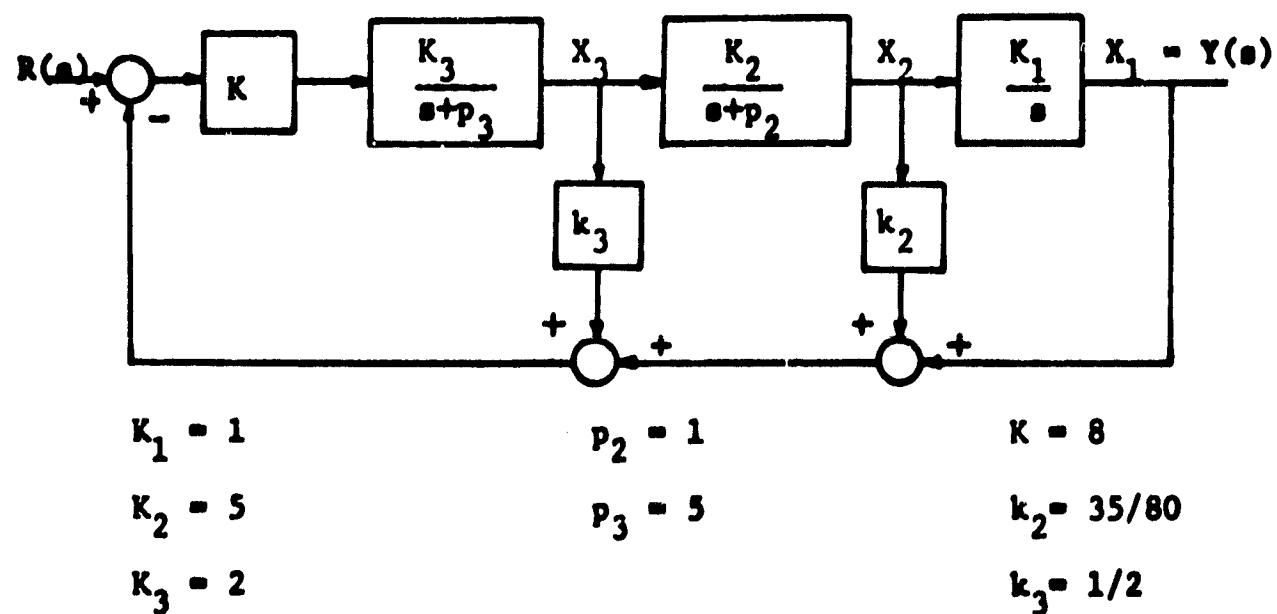


Figure 5.2 The compensated system of Example 1.

the second system. For both systems in this example classical sensitivities and sensitivity functions, as well as peak sensitivities and integral sensitivities, are found in order to show the connection between the different sensitivity measures.

For the state variable feedback system (Fig. 5.2) the sensitivities with respect to the blocks in the forward path are given by Eqs. (4.5). For this example the equations become:

$$s_{G_1}^W = \frac{s^3 + 14s^2 + 48s}{s^3 + 14s^2 + 48s + 80}$$

$$= \frac{3}{5} \frac{s(\frac{s}{6} + 1)(\frac{s}{8} + 1)}{(\frac{s}{10} + 1)(\frac{s}{8} + \frac{s}{2} + 1)}$$

$$s_{G_2}^W = \frac{s^3 + 14s^2 + 13}{s^3 + 14s^2 + 48s + 80}$$

$$= \frac{13}{80} \frac{s(\frac{s}{13} + 1)}{(\frac{s}{10} + 1)(\frac{s}{8} + \frac{s}{2} + 1)}$$

$$s_{G_3}^W = \frac{s^3 + 6s^2 + 5s}{s^3 + 14s^2 + 48s + 80}$$

$$= \frac{1}{16} \frac{s(s + 1)(\frac{s}{5} + 1)}{(\frac{s}{10} + 1)(\frac{s}{8} + \frac{s}{2} + 1)}$$

Asymptotic Bode plots for these sensitivities are shown in Fig. 5.3.

There is also in Fig. 5.3 a Bode plot of $G_{eq}(s)$, which is included in order to indicate the bandwidth of the system. It may be noted that

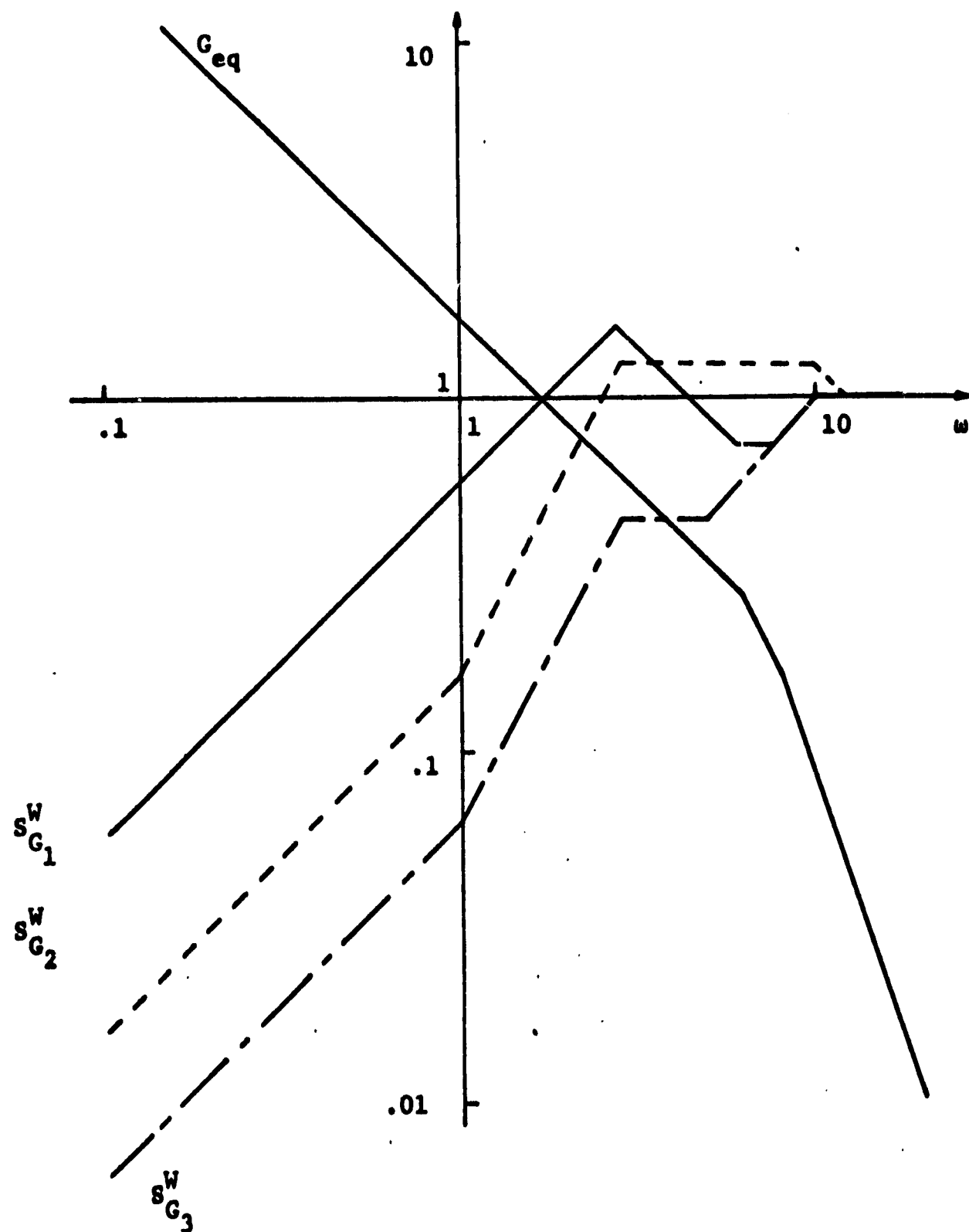


Figure 5.3 Gain sensitivities for the state-variable feedback system of Example 1.

for frequencies less than the gain crossover frequency, $S_{G_3}^W < S_{G_2}^W < S_{G_1}^W$.

The classical sensitivities with respect to the specific parameters in the forward path are:

$$S_{K_1}^W = S_{G_1}^W$$

$$S_{K_2}^W = S_{G_2}^W$$

$$S_{K_3}^W = S_K^W = S_{G_3}^W$$

$$S_{P_2}^W = S_{G_2}^W \frac{-p_2}{s + p_2}$$

$$= \frac{-13}{80} \frac{s(\frac{s}{13} + 1)}{(\frac{s}{10} + 1)(\frac{s}{8} + \frac{s}{2} + 1)}$$

$$S_{P_3}^W = S_{G_3}^W \frac{-p_3}{s + p_3}$$

$$= \frac{-1}{16} \frac{s(s + 1)}{(\frac{s}{10} + 1)(\frac{s}{8} + \frac{s}{2} + 1)}$$

Asymptotic Bode plots for $S_{P_2}^W$ and $S_{P_3}^W$ are in Fig. 5.4.

The sensitivities with respect to the feedback coefficients are given by Eqs. (4.8).

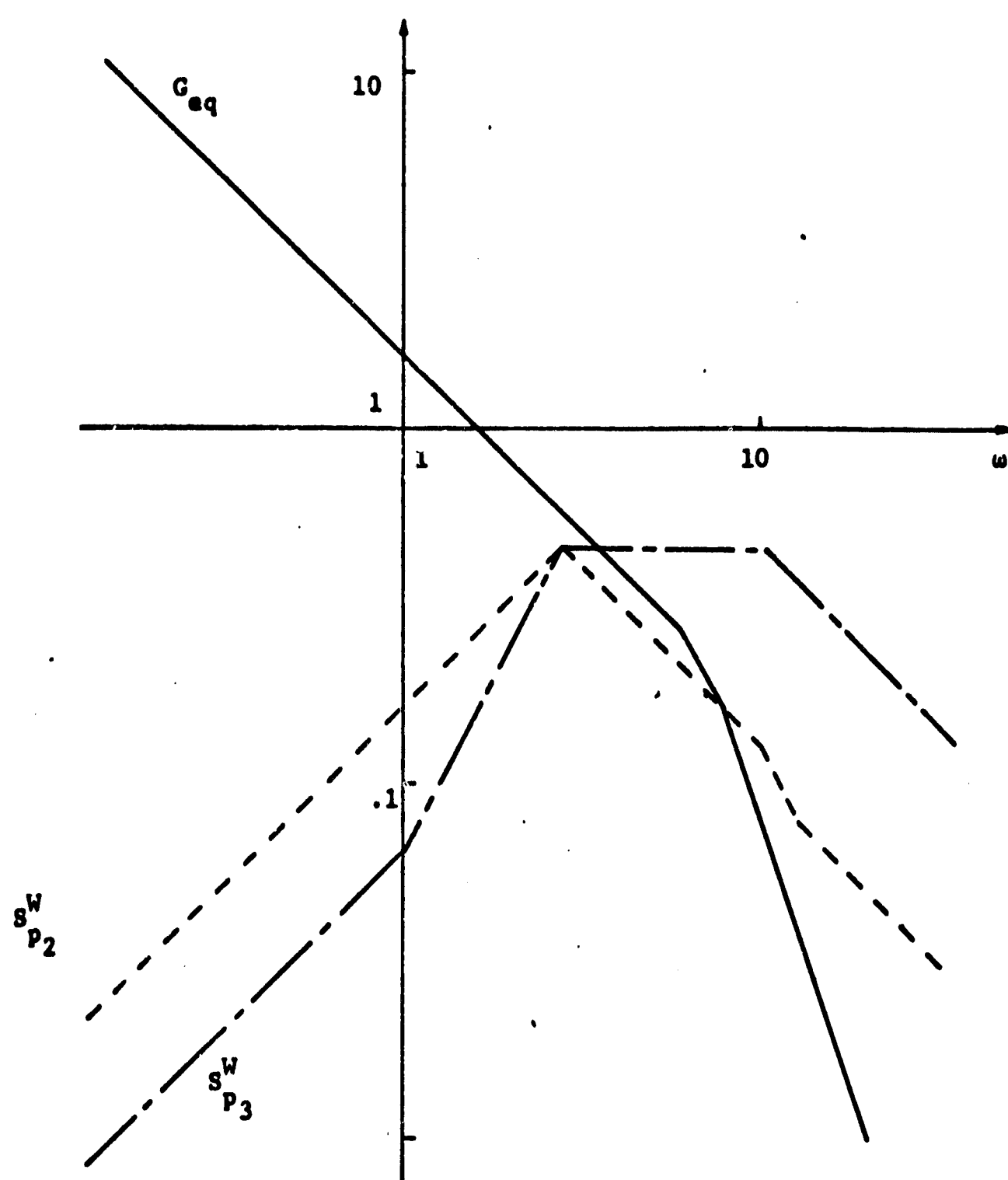


Figure 5.4 Pole sensitivities for the state-variable feedback system of Example 1.

$$s_{k_1}^W = \frac{-1}{\frac{s^2}{10} + 1} \frac{s^2}{(\frac{s}{8} + 1)(\frac{s}{2} + 1)}$$

$$s_{k_2}^W = \frac{-7}{16} \frac{s^2}{\frac{s^2}{10} + 1} \frac{s^2}{(\frac{s}{8} + 1)(\frac{s}{2} + 1)}$$

$$s_{k_3}^W = \frac{-1}{10} \frac{s(s+1)}{\frac{s^2}{10} + 1} \frac{s^2}{(\frac{s}{8} + 1)(\frac{s}{2} + 1)}$$

Fig. 5.5 shows Bode plots of these functions.

If the Guillemin-Truxal method is used to compensate the plant, the final closed-loop system is as shown in Fig. 5.6. For this system s_K^W , the sensitivity with respect to any gain in the forward path, is equal to $s_{k_1}^W$ for the state-variable feedback system. Similarly, the sensitivity of the series compensated system with respect to the unity feedback coefficient is equal to $s_{k_1}^W$ for the state-variable feedback system. The sensitivities of the series compensated system with respect to the poles of the fixed plant are:

$$s_{p_2}^W = s_K^W \left[\frac{-p_2}{s + p_2} \right]$$

$$= \frac{-3}{5} \frac{s(\frac{s}{6} + 1)(\frac{s}{8} + 1)}{\frac{s^2}{10} + 1} \frac{s^2}{(\frac{s}{8} + 1)(\frac{s}{2} + 1)(s + 1)}$$

$$s_{p_3}^W = s_K^W \left[\frac{-p_3}{s + p_3} \right]$$

$$= \frac{-3}{5} \frac{s(\frac{s}{6} + 1)(\frac{s}{8} + 1)}{\frac{s^2}{10} + 1} \frac{s^2}{(\frac{s}{8} + 1)(\frac{s}{2} + 1)(\frac{s}{5} + 1)}$$

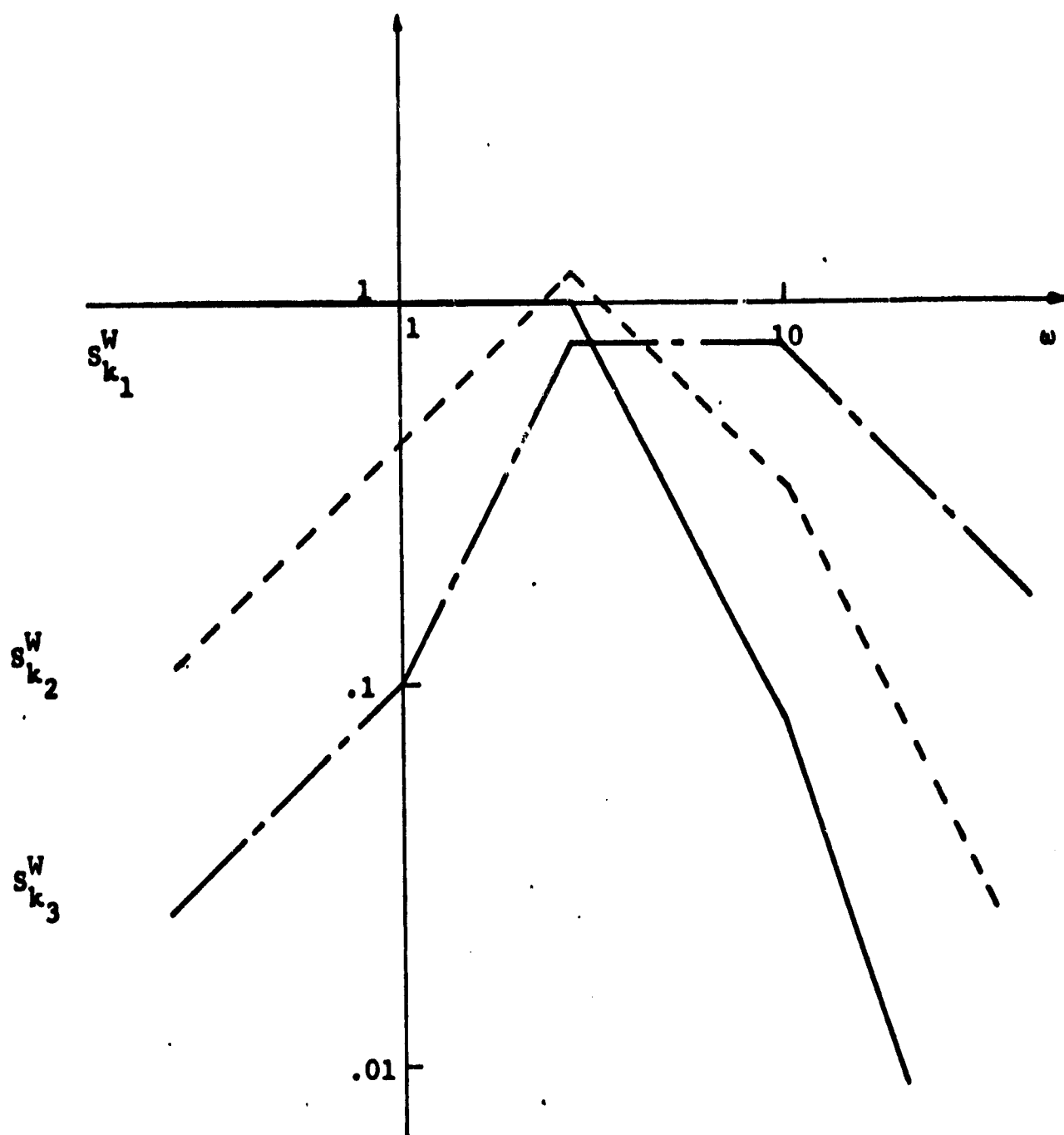


Figure 5.5 Feedback coefficient sensitivities for the state-variable feedback system of Example 1.

The Bode plots for these functions are shown in Fig. 5.7.

A comparison of the Bode plots of the classical sensitivities of the two systems shows that for all parameters, the magnitudes of the classical sensitivities for the state-variable feedback system are less than or equal to those for the series compensated system for frequencies less than the gain crossover frequency.

A similar comparison may be made in terms of sensitivity functions and integral sensitivities.

Figs. 5.8 and 5.9 show block diagrams for the generation of sensitivity functions for both systems. Plots of the sensitivity functions are shown in Figs. 5.10, 5.11, and 5.12, and a table listing peak sensitivities and integral sensitivities is in Fig. 5.18.

From these results it is clear that a reduction in sensitivity with respect to the parameters K_2 , K_3 , p_2 , and p_3 has been obtained using the state-variable feedback method of design.

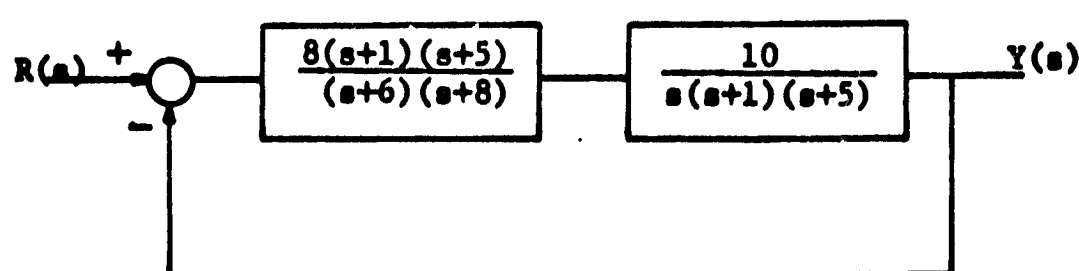


Figure 5.6 The system of Example 1 compensated by the Guillemin-Truxal method.

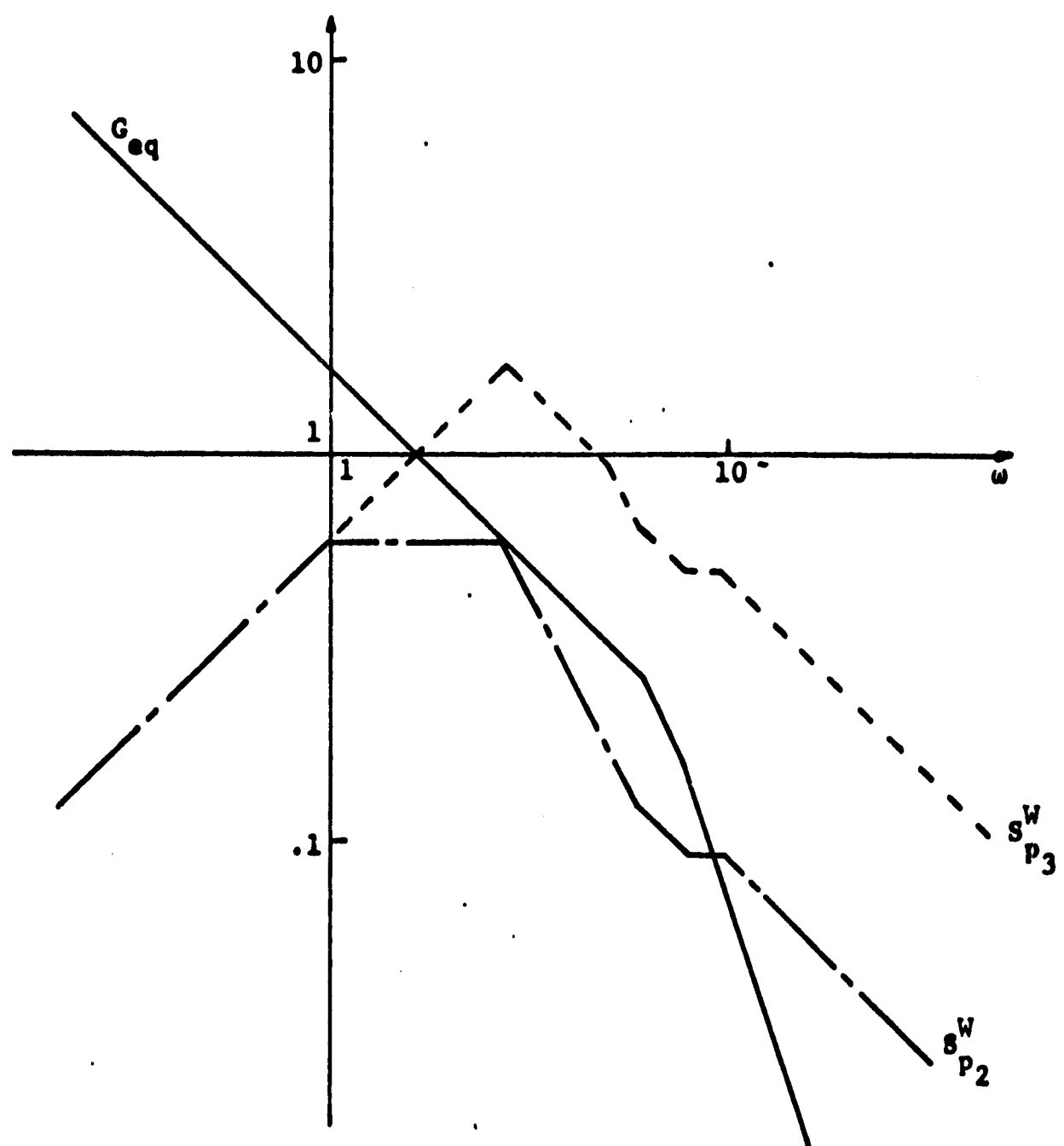


Figure 5.7 Pole sensitivities for the series compensated system of Example 1.

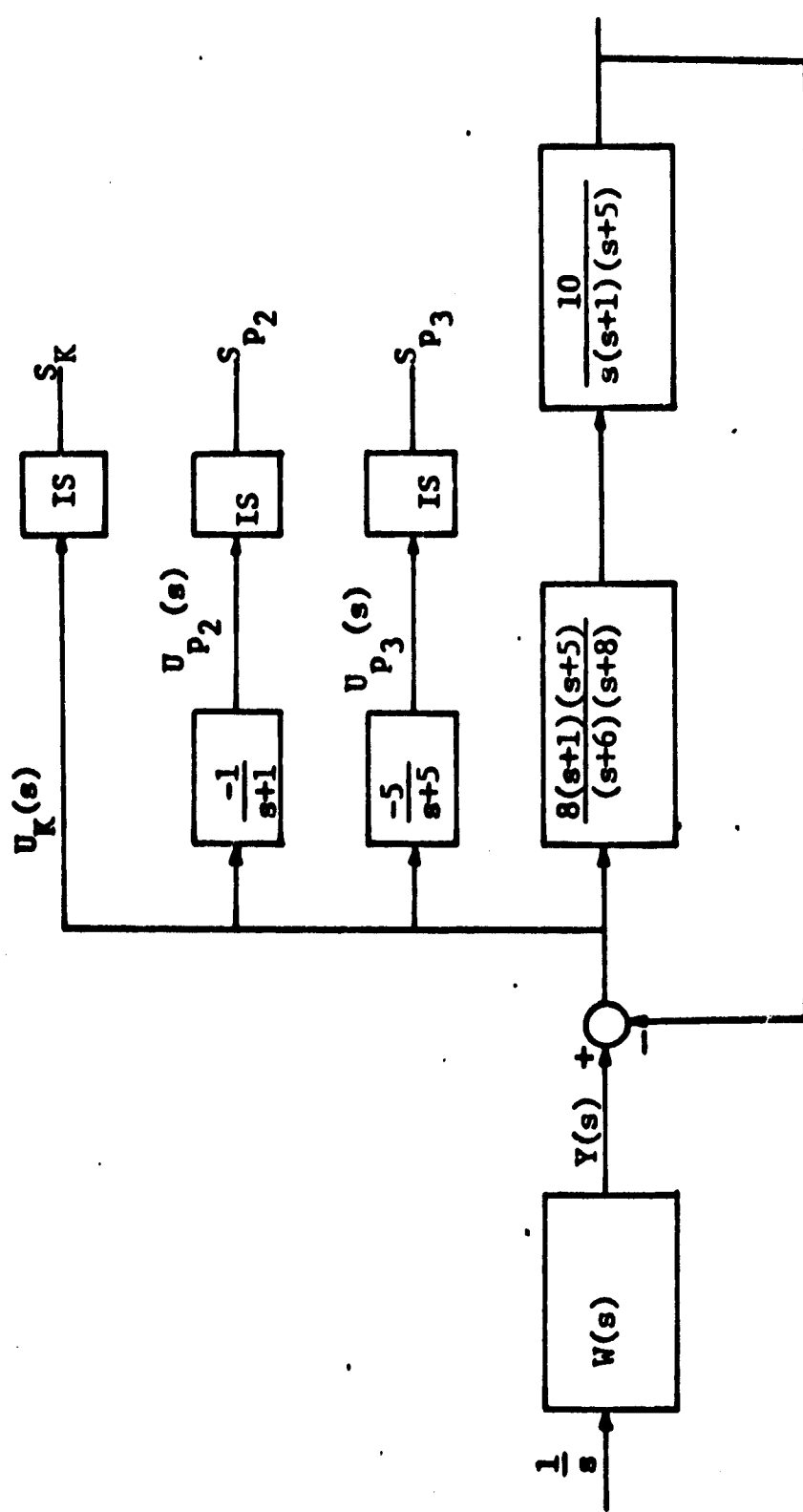


Figure 5.8 Generation of sensitivity functions and integral sensitivities for the series compensated system.

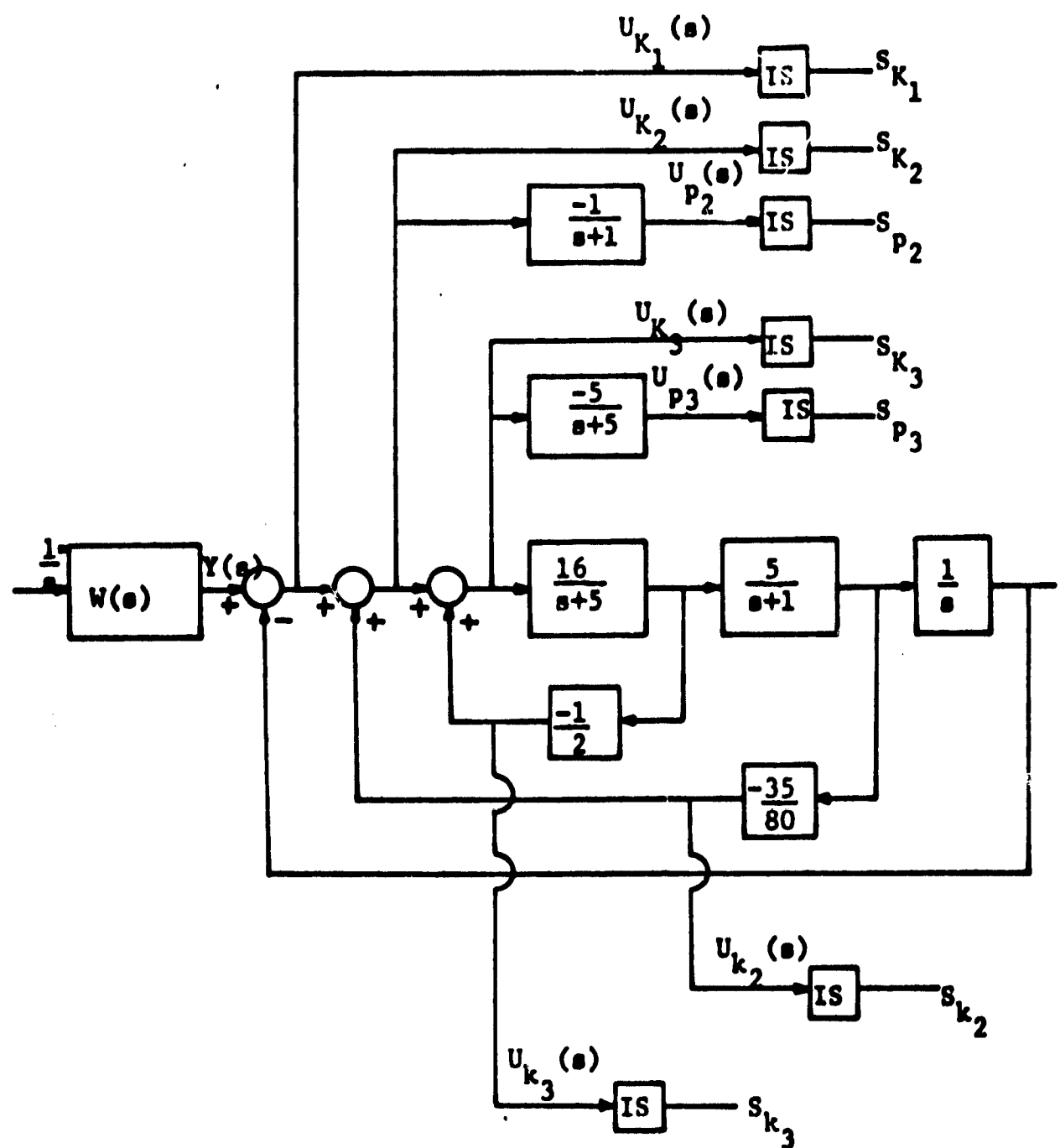


Figure 5.9 Generation of sensitivity functions and integral sensitivities for the state-variable feedback system.

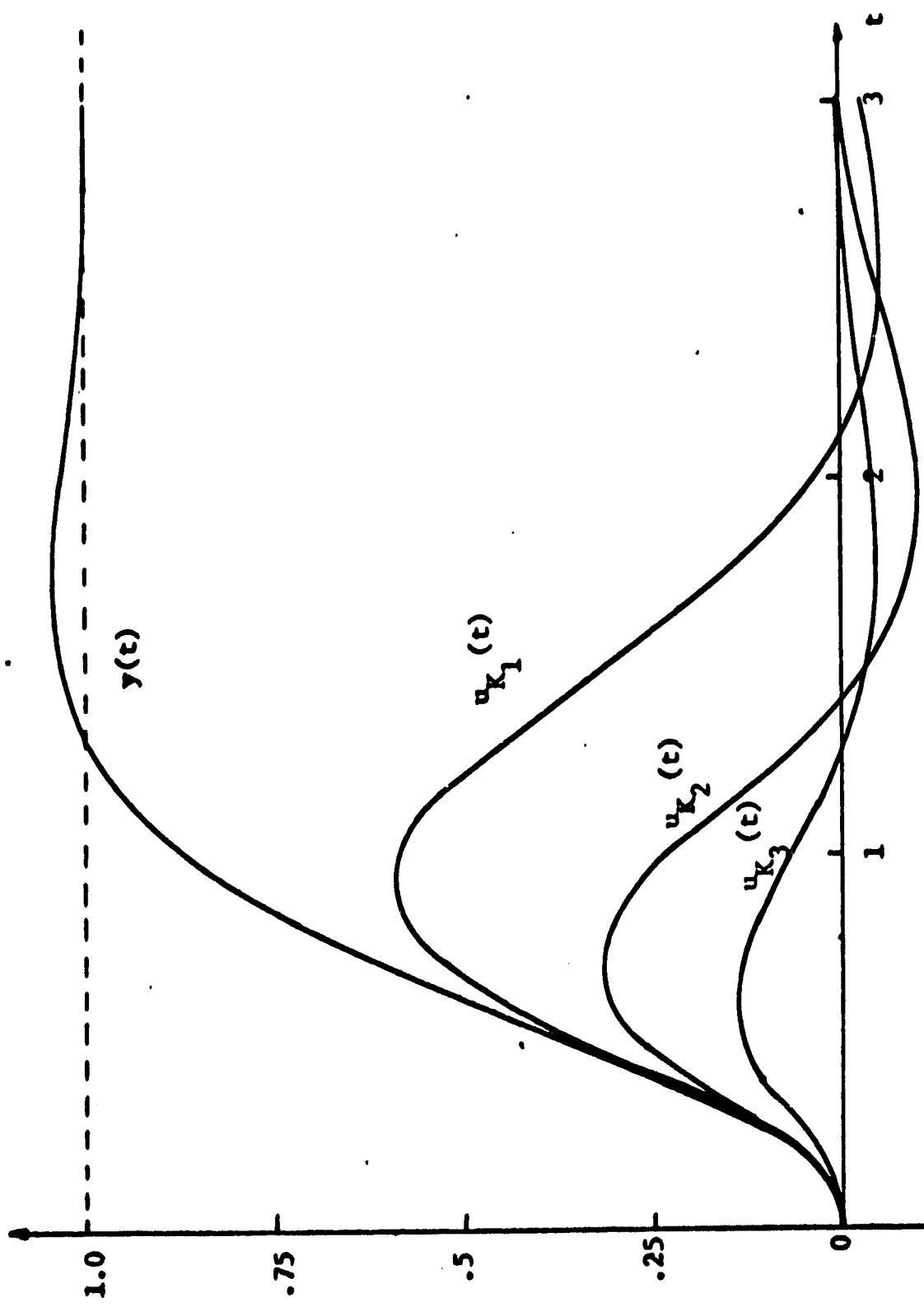


Figure 5.10 The sensitivity functions for the forward gains of the state-variable feedback system.

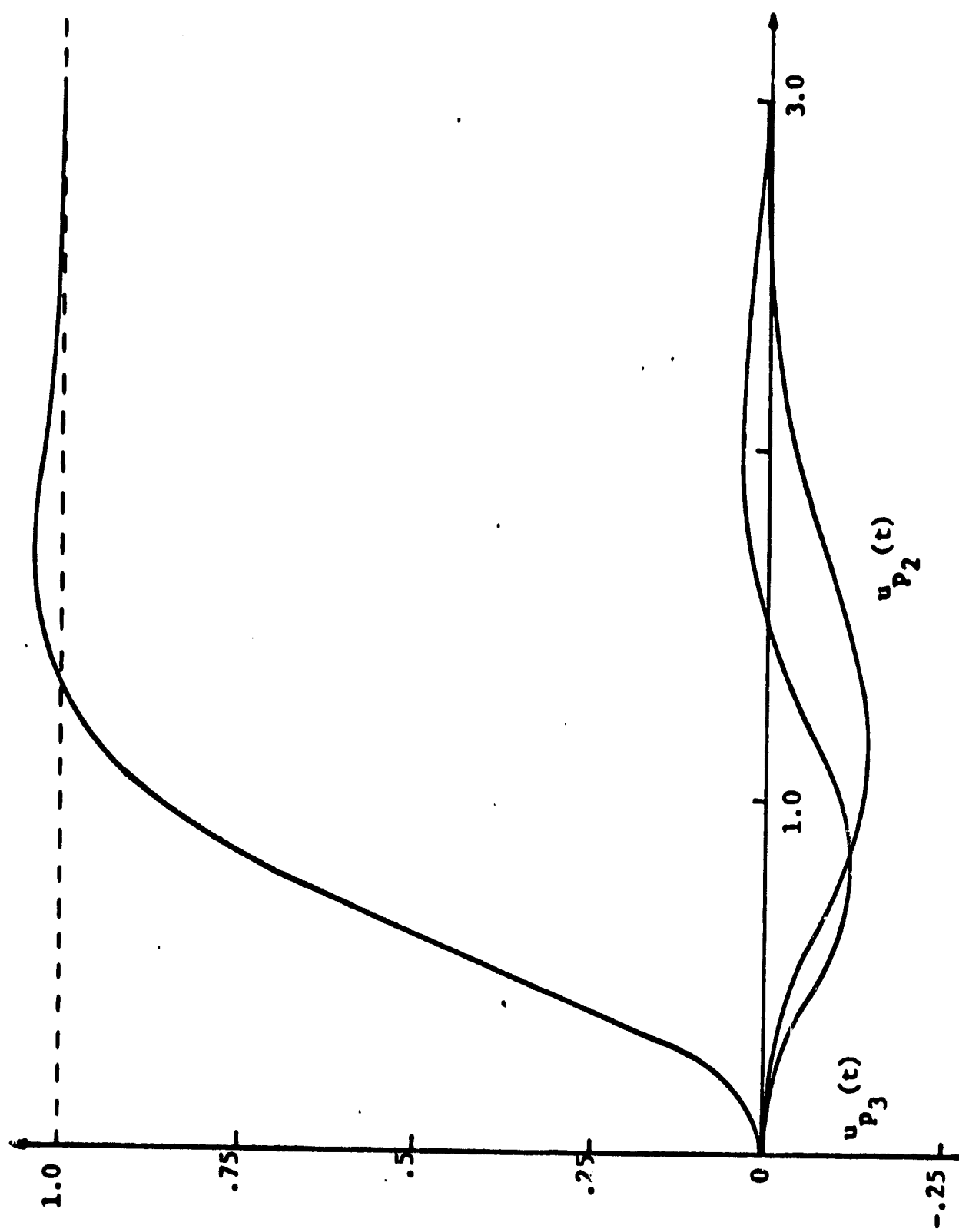


Figure 5.11 The sensitivity functions for the poles of the fixed plant in the state-variable feedback system.

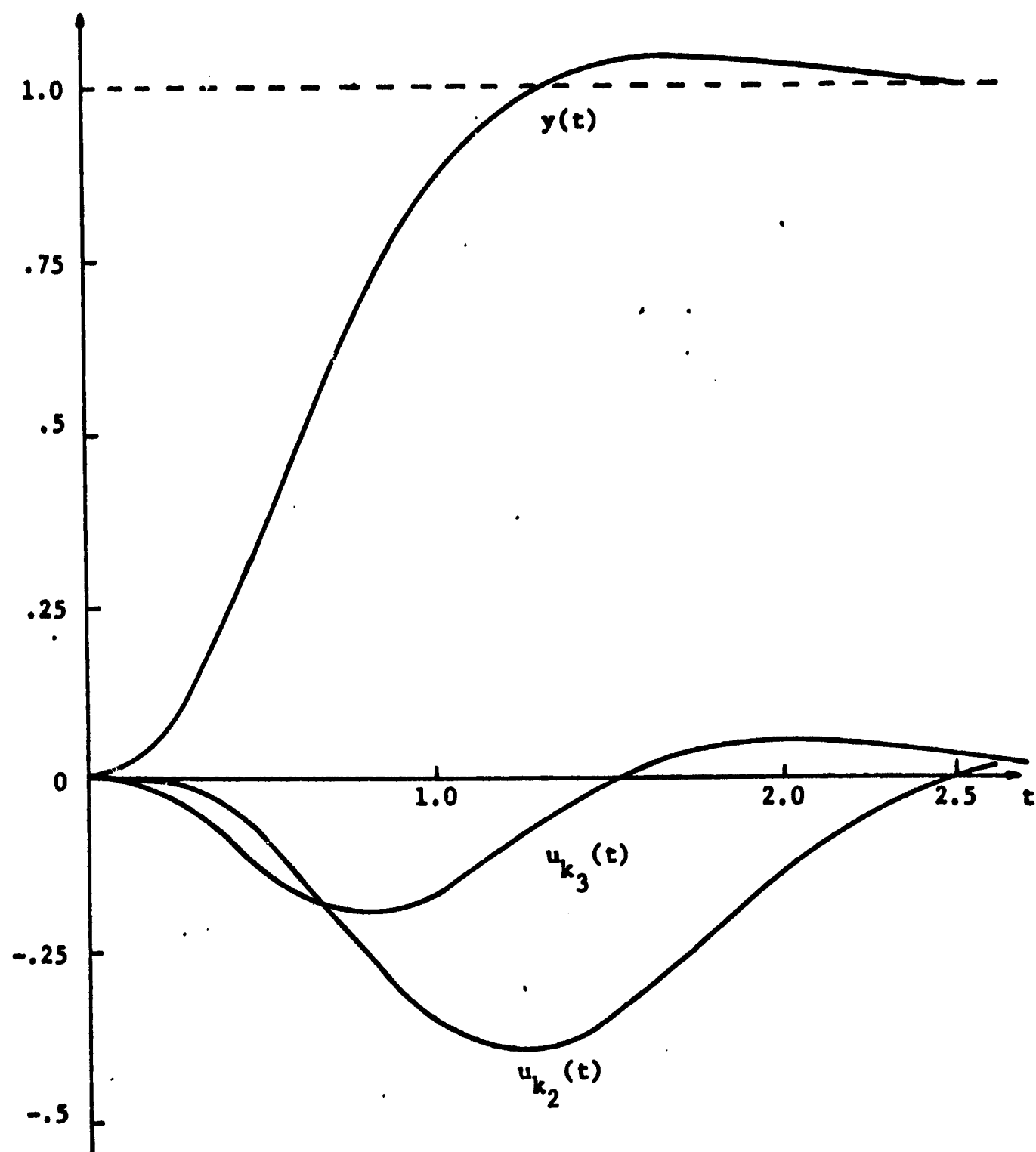


Figure 5.12 The sensitivity functions for the feedback coefficients of the state-variable feedback system.

Example 2. For the state-variable feedback system of Example 1. the sensitivities with respect to K_1 , K_2 , and p_2 may be reduced by using H-equivalent feedback. The $H_{eq}(s)$ system is shown in Fig. 13.

From Eq. (4.10) the sensitivity of the $H_{eq}(s)$ system with respect to any block in the forward path is:

$$S_G^W = S_{G_n}^W = S_{G_3}^W$$

where $S_{G_n}^W$ is the sensitivity of the state-variable feedback system with respect to G_n ($n = 3$). The sensitivities with respect to p_2 and p_3 are:

$$S_{p_2}^W = S_G^W \left(\frac{-1}{s+1} \right)$$

$$S_{p_3}^W = S_G^W \left(\frac{-5}{s+5} \right)$$

$S_{p_3}^W$ is the same as for the state-variable feedback system. The sensitivity with respect to p_2 has been reduced, since $|S_G^W| < |S_{G_2}^W|$, where $S_{G_2}^W$ is the sensitivity with respect to G_2 for the state-variable feedback system.

The peak sensitivities and integral sensitivities for the H-equivalent system are listed in the table of Fig. 5.18.

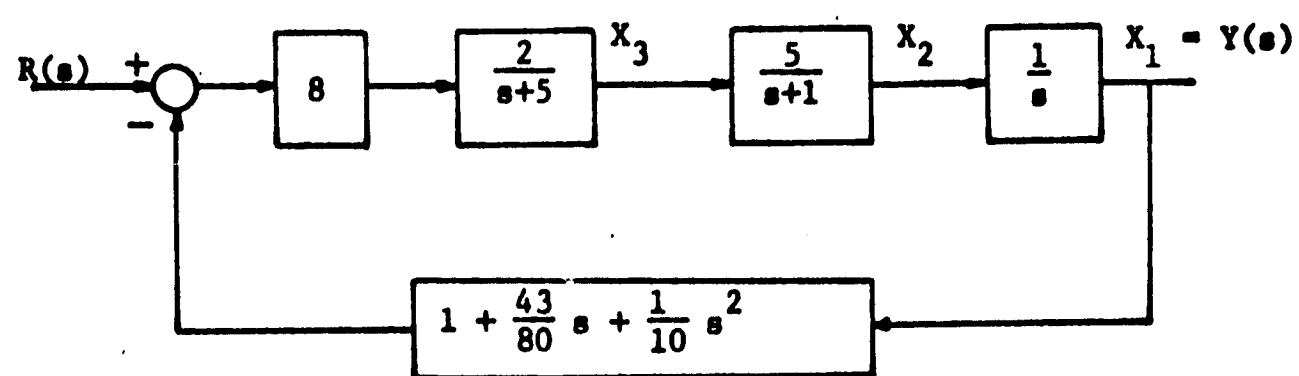


Figure 5.13 The H-equivalent system of Example 2.

Example 3. In Example 2. a reduction in sensitivity was obtained by using H-equivalent feedback. However, $H_{eq}(s)$ is not in a form which is easily realizable. It is desirable to approximate $H_{eq}(s)$ by a transfer function which is realizable by RC elements and a gain factor.

$$H_{eq}(s) = 1 + \frac{43}{80} s + \frac{1}{10} s^2$$

$$= 1 + \frac{5}{10}(s + 5.38)$$

In order to make the second term realizable, poles are added at $s = -40$ and $s = -50$, while preserving the low frequency gain.

$$H'_{eq}(s) = 1 + \frac{200 s(s + 5.38)}{(s + 40)(s + 50)} \quad (5.1)$$

There are several factors to be considered in choosing the approximation of $H_{eq}(s)$. The large gain of $H_{eq}(s)$ at high frequencies is undesirable if there is noise at the system output. The addition of low frequency poles to $H_{eq}(s)$ alleviates this problem. However, two other considerations make the use of high frequency poles desirable. The poles of $H'_{eq}(s)$, which become zeros of $W(s)$, have less effect on $y(t)$ if they are placed at high frequencies. Secondly, the addition of poles in the manner shown in Eq. (5.1) causes the zeros of $H'_{eq}(s)$ to be different from those of $H_{eq}(s)$. This error in zero locations, which also affects $y(t)$, is smaller for high frequency poles. Thus, a compromise must be made between the filtering of output noise and the approximation of $H_{eq}(s)$. Another possibility is to approximate $H_{eq}(s)$ by:

$$H'_{eq}(s) = \frac{2000 (1 + .538s + .1s^2)}{(s + 40)(s + 50)}$$

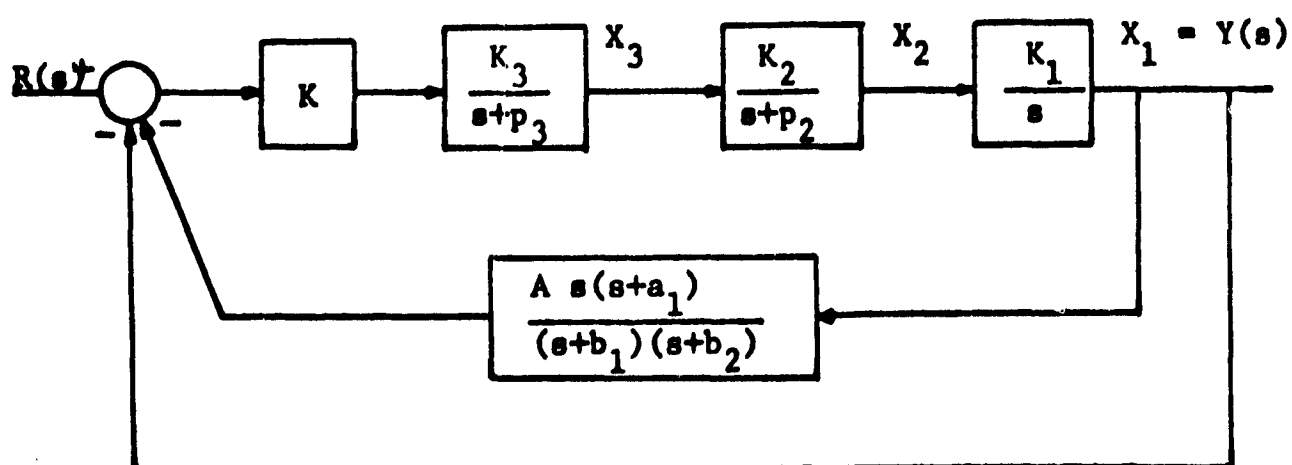
However, with this approximation a change in the pole location or the gain constant of $H'_{eq}(s)$ results in a steady-state error at the output.

One other idea in the approximate realization of $H'_{eq}(s)$ is to obtain a system which has zero steady-state error for a ramp input. For such a system the velocity error constant, K_v , is infinite. K_v may be expressed (Truxal, 1955) as:

$$\frac{1}{K_v} = \sum_{j=1}^n \frac{1}{p_j} - \sum_{j=1}^n \frac{1}{z_j}$$

where the p_j and z_j are the poles and zeros of the closed-loop transfer function. Since K_v is determined by the closed-loop poles and zeros, the poles added to $H'_{eq}(s)$ might be placed in such a way that $K_v = \infty$. This is a topic for further investigation.

The structure of the system with $H'_{eq}(s)$ feedback is shown in Fig. 5.14, and a block diagram for the generation of sensitivity functions is in Fig. 5.15. The table of Fig. 5.18 lists the peak sensitivities and integral sensitivities. For the parameters in the fixed plant, the sensitivities are approximately equal to those of the $H'_{eq}(s)$ system. The sensitivities with respect to the parameters of $H'_{eq}(s)$ are reasonably small (less than S_{K_1} for the state variable feedback system).



$$K_1 = 1$$

$$p_2 = 1$$

$$K = 8$$

$$K_2 = 5$$

$$p_3 = 5$$

$$A = 200$$

$$K_3 = 2$$

$$a_1 = 5.38$$

$$b_1 = 40$$

$$b_2 = 50$$

Figure 5.14 The H'-equivalent system of Example 3.

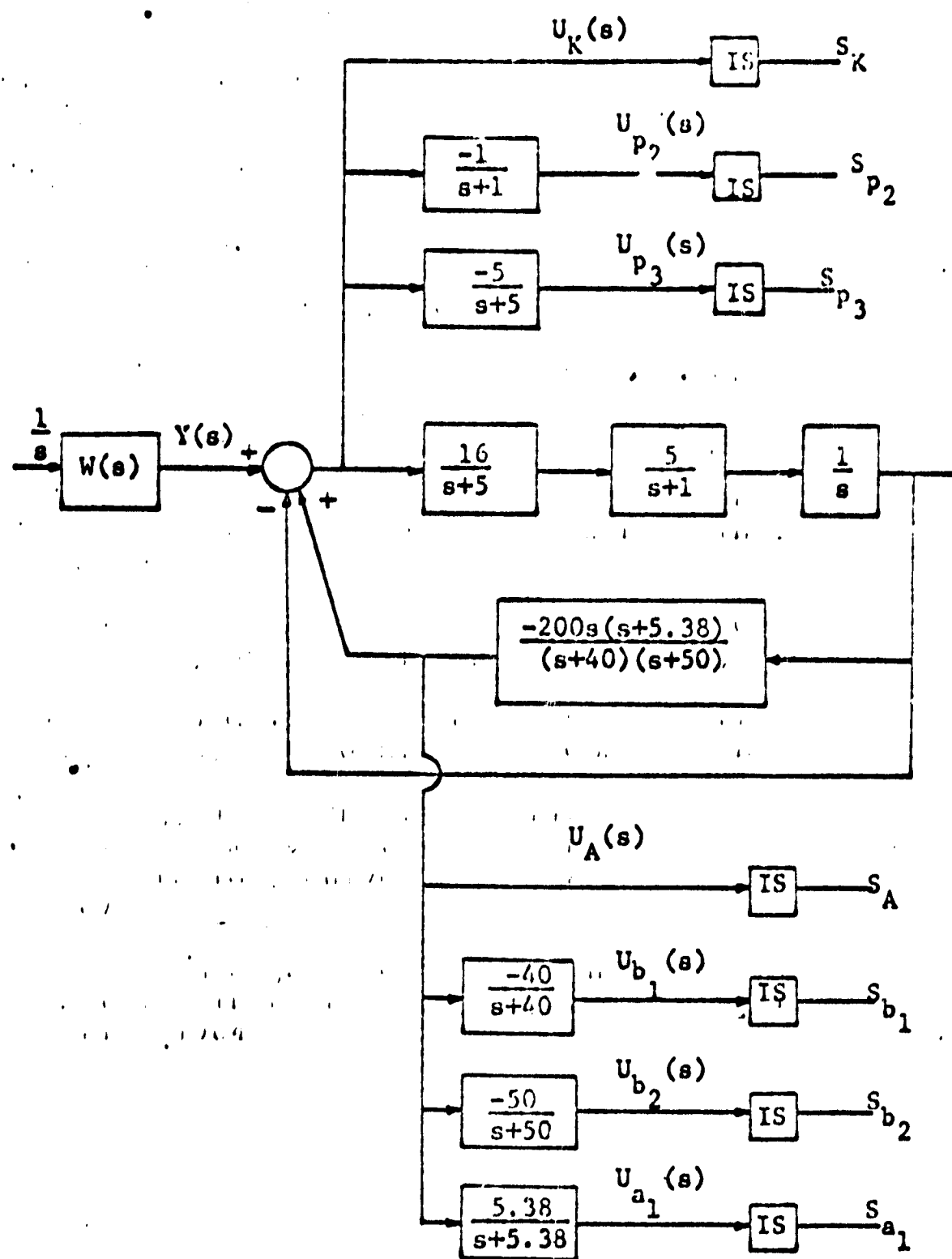


Figure 5.15 Generation of sensitivity functions and integral sensitivities for the $H'_{eq}(s)$ system.

For the $H'_{eq}(s)$ system the new closed-loop transfer function is

$$W(s) = \frac{80(s + 40)(s + 50)}{(s + 61.9)(s^2 + 29.4s + 287)(s^2 + 4.81s + 9.05)}$$

The pole and zero locations are shown in Fig. 5.16, and a graph of $y(t)$ is in Fig. 5.17. It is seen that the addition of poles in the feedback structure has altered the step response. This example demonstrates that while a system using an approximation to $H_{eq}(s)$ may show an improvement in sensitivity over a system with state-variable feedback, two new problems are introduced. The addition of poles to $H_{eq}(s)$ affects the closed-loop response, and the high gain of $H'_{eq}(s)$ at high frequencies is undesirable if there is noise at the output.

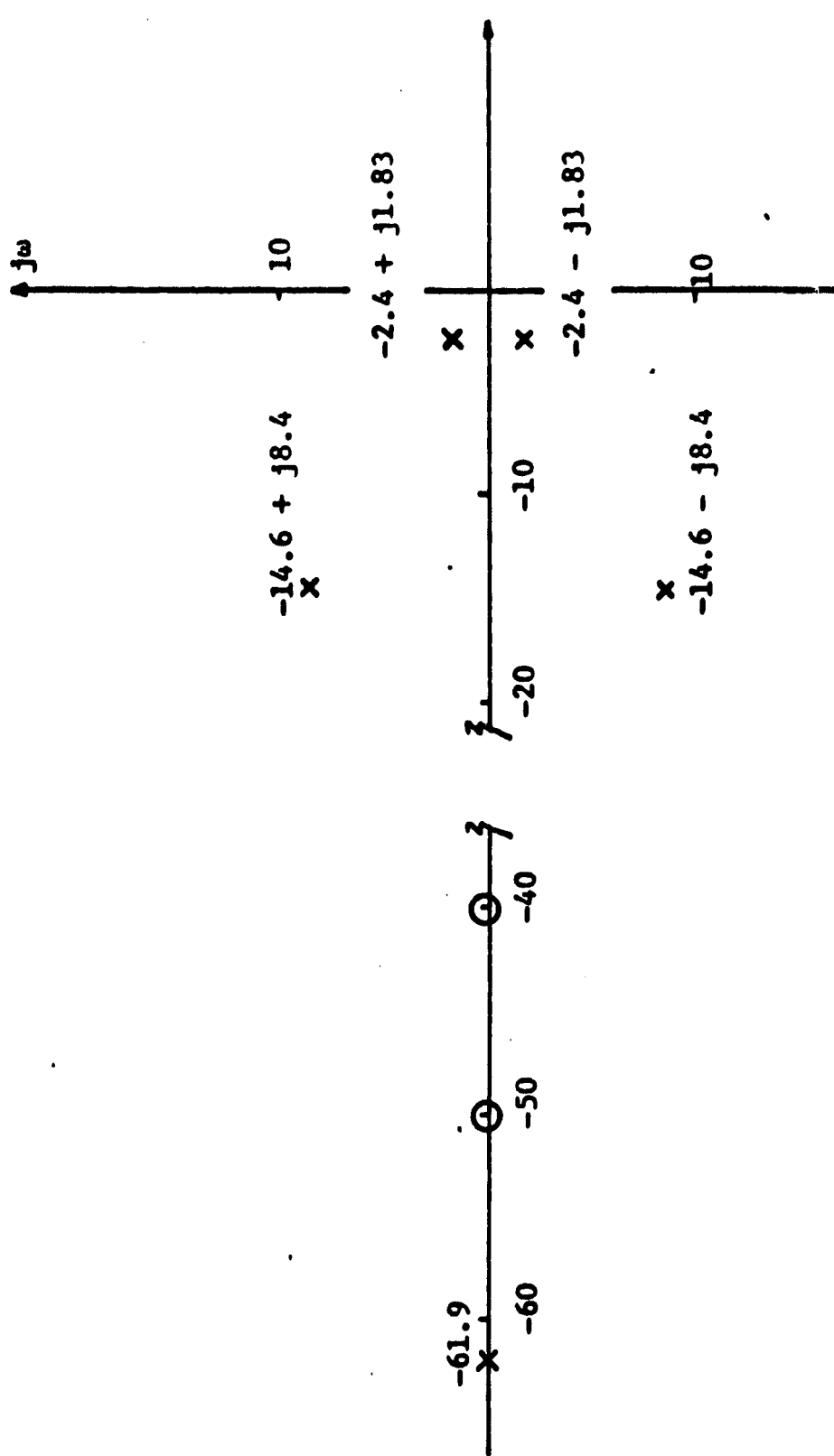


Figure 5.16 The closed loop poles and zeros for the $H'_{\text{eq}}(s)$ system.

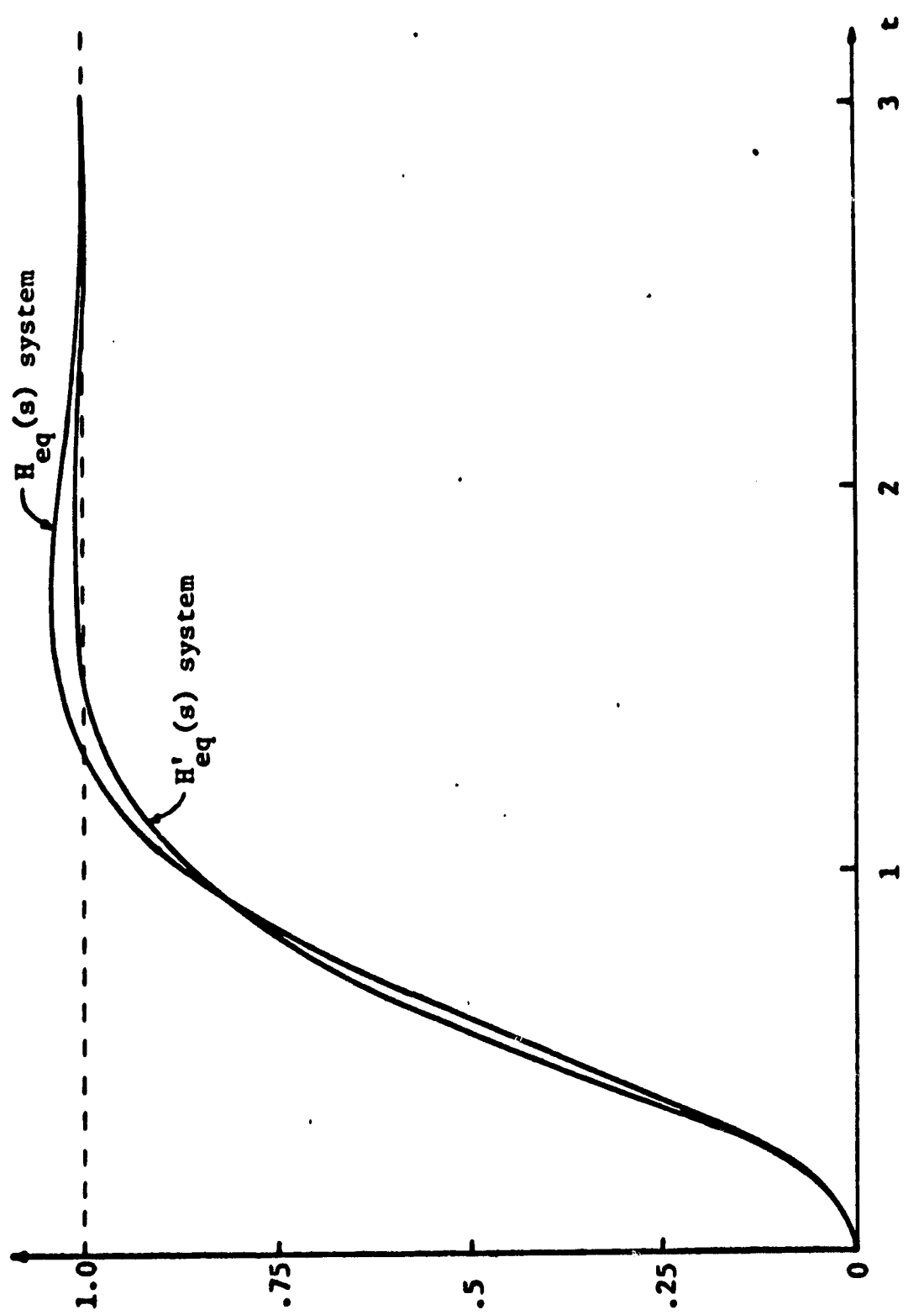


Figure 5.17 The step response of the $H'_{eq}(s)$ system.

parameter	series compensated system			state-variable feedback system			$H_{eq}(s)$ system			$H'_{eq}(s)$ system		
	u_{λ}^*	s_{λ}	u_{λ}^*	s_{λ}	u_{λ}^*	s_{λ}	u_{λ}^*	s_{λ}	u_{λ}^*	s_{λ}	u_{λ}^*	s_{λ}
k_1	0.593	0.286	0.593	0.286	0.140	0.0117	0.149	0.0112	0.149	0.0112	0.149	0.0112
k_2	0.593	0.286	0.321	0.0669	0.140	0.0117	0.149	0.0112	0.149	0.0112	0.149	0.0112
k_3	0.593	0.286	0.140	0.0117	0.140	0.0117	0.149	0.0112	0.149	0.0112	0.149	0.0112
p_2	-0.329	0.133	-0.148	0.0190	-0.0610	0.0031	-0.0595	0.0028	-0.0595	0.0028	-0.0595	0.0028
p_3	-0.548	0.260	-0.120	0.0096	-0.120	0.0096	-0.124	0.0089	-0.124	0.0089	-0.124	0.0089
k_2			-0.396	0.136								
k_3			-0.193	0.0245								
A									-0.505	0.205		
s_1									-0.469	0.189		
b_1									0.505	0.205		
b_2									0.505	0.205		

Figure 5.18 A table of sensitivities for Examples 1., 2., and 3.

Example 4. Fig. 5.19 shows the block diagram of a fixed plant for which the transfer function is

$$G_p(s) = \frac{5(s + 2)}{s(s + 1)(s + 5)}$$

The desired closed-loop transfer function is

$$W(s) = \frac{80}{(s + 10)(s^2 + 4s + 8)}$$

In order to realize $W(s)$, the zero of the fixed plant must be cancelled, and it is assumed that it is impossible to insert a pole immediately preceding this zero.

Since direct series cancellation is impossible, the zero appears as a zero of $W(s)$. Thus, $W(s)$ is also required to have a pole at $s = -2$. That is,

$$W(s) = \frac{80(s + 2)}{(s + 2)(s + 10)(s^2 + 4s + 8)}$$

To accomplish this, the order of the system is increased by inserting a series compensator as shown in Fig. 5.20, and the new state variable x_4 is fed back. The parameters k_2 , k_3 , k_4 , K , and p_4 are then chosen so as to realize $W(s)$. The values of k_2 , k_3 , and K are found to be:

$$K = 16, \quad k_2 = 7/16, \quad k_3 = -3/4$$

To obtain the specified $W(s)$, the values of k_4 and p_4 must be chosen such that the transfer function $\frac{x_4(s)}{z(s)}$, as defined in Fig. 5.20, is:

$$\frac{x_4(s)}{z(s)} = \frac{16}{s + p_4 + 16k_4} = \frac{16}{s + 10}$$

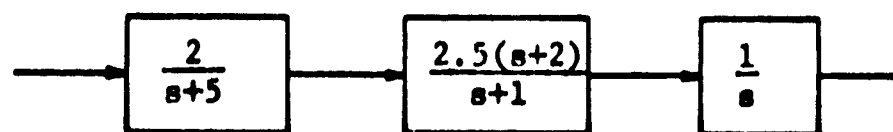


Figure 5.19 The fixed plant of Example 4.

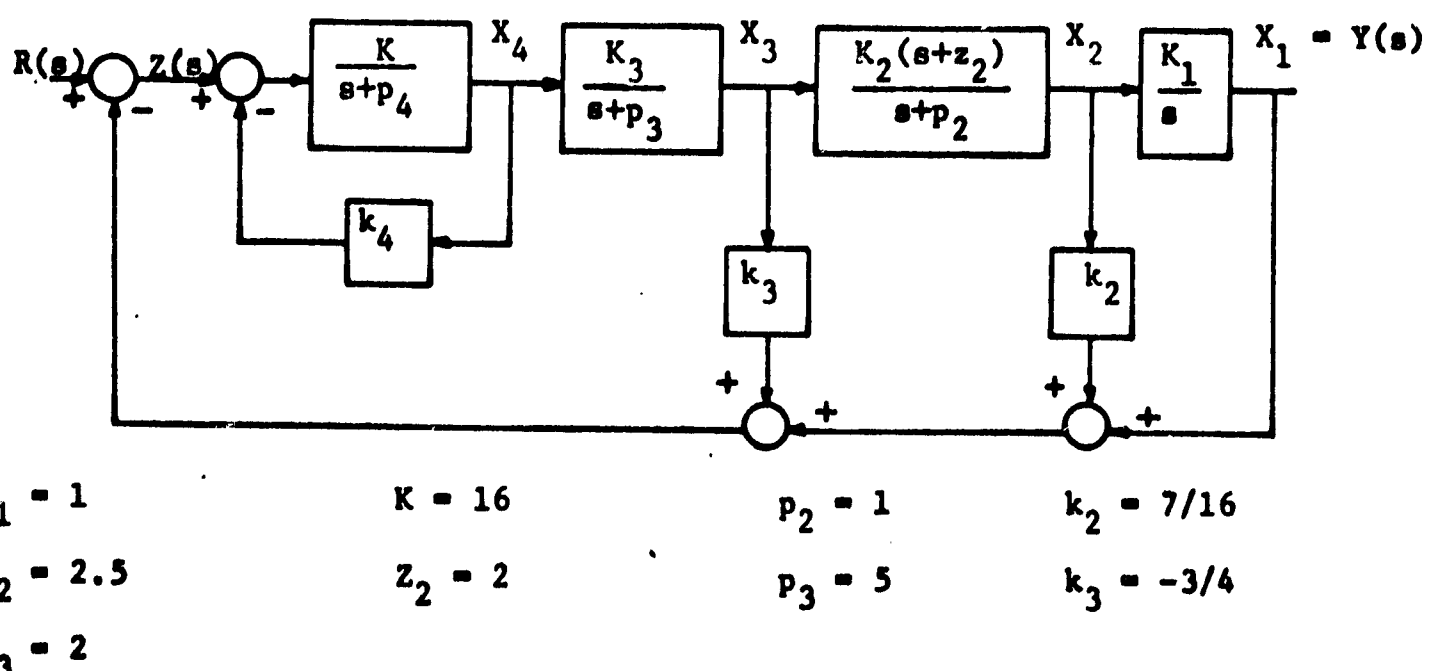


Figure 5.20 The closed-loop system of Example 4.

Any values of k_4 and p_4 satisfying $p_4 + 16k_4 = 10$ produce the required pole at $s = -2$ in the closed loop transfer function.

Bounds on a desirable value of p_4 may be obtained from stability considerations (Schultz and Melba 1967). If $p_4 = 0$, the system has two open-loop poles at the origin, and the root locus, as a function of the gain K , is in the RHP for small values of K . Another possible choice is $p_4 = 10$, which requires $k_4 = 0$. Since the state variable x_4 is not fed back when $k_4 = 0$, a zero of $H_{eq}(s)$ is lost. Therefore, as $K \rightarrow \infty$, two closed-loop poles (instead of only one) approach infinity. This is a disadvantage with regard to stability for high gain.

An intermediate value of p_4 may be obtained by considering the sensitivity of $W(s)$ with respect to p_4 and k_4 . From Eq. (4.14),

$$s_{G_4}^W = \frac{(s + p_4)(s + 5)(s + 1)s}{Q(s)}$$

Therefore,

$$\begin{aligned} s_{p_4}^W &= s_{G_4}^W \frac{-p_4}{s + p_4} \\ &= \frac{-p_4(s + 5)(s + 1)s}{Q(s)} \end{aligned} \tag{5.2}$$

From Eq. (4.7),

$$\begin{aligned} s_{k_4}^W &= \frac{-k_4 G_4}{B(s)} \\ &= \frac{-k_4 K(s + 5)(s + 1)s}{Q(s)} \end{aligned} \tag{5.3}$$

It is seen that $|S_{p_4}^W|$ and $|S_{k_4}^W|$ are proportional to $|p_4|$ and $|k_4|$ respectively. Usually it is desirable to decrease the sensitivity with respect to elements in the forward path and to accept higher sensitivities for the feedback coefficients, because the tolerances for the k_i 's may be controlled. However, in this case the series compensator is also selected by the designer. A possible solution is to choose p_4 such that the sensitivities with respect to p_4 and k_4 are equal. From Eqs. (5.2) and (5.3) this requires $16k_4 = p_4$.

We have

$$p_4 + 16k_4 = 10 \quad (5.4)$$

Therefore,

$$p_4 = 5, \quad k_4 = 5/16$$

It should be noted that the sensitivities with respect to the other parameters of the system do not depend on the values of k_4 and p_4 , as long as these values satisfy Eq. (5.4). This is seen from the fact that the transfer functions used to calculate the sensitivities for the other parameters involve p_4 and k_4 only through the function $\frac{x_4(s)}{z(s)}$.

A block diagram for the generation of sensitivity functions for this example is shown in Fig. 5.21, and the results are listed below.

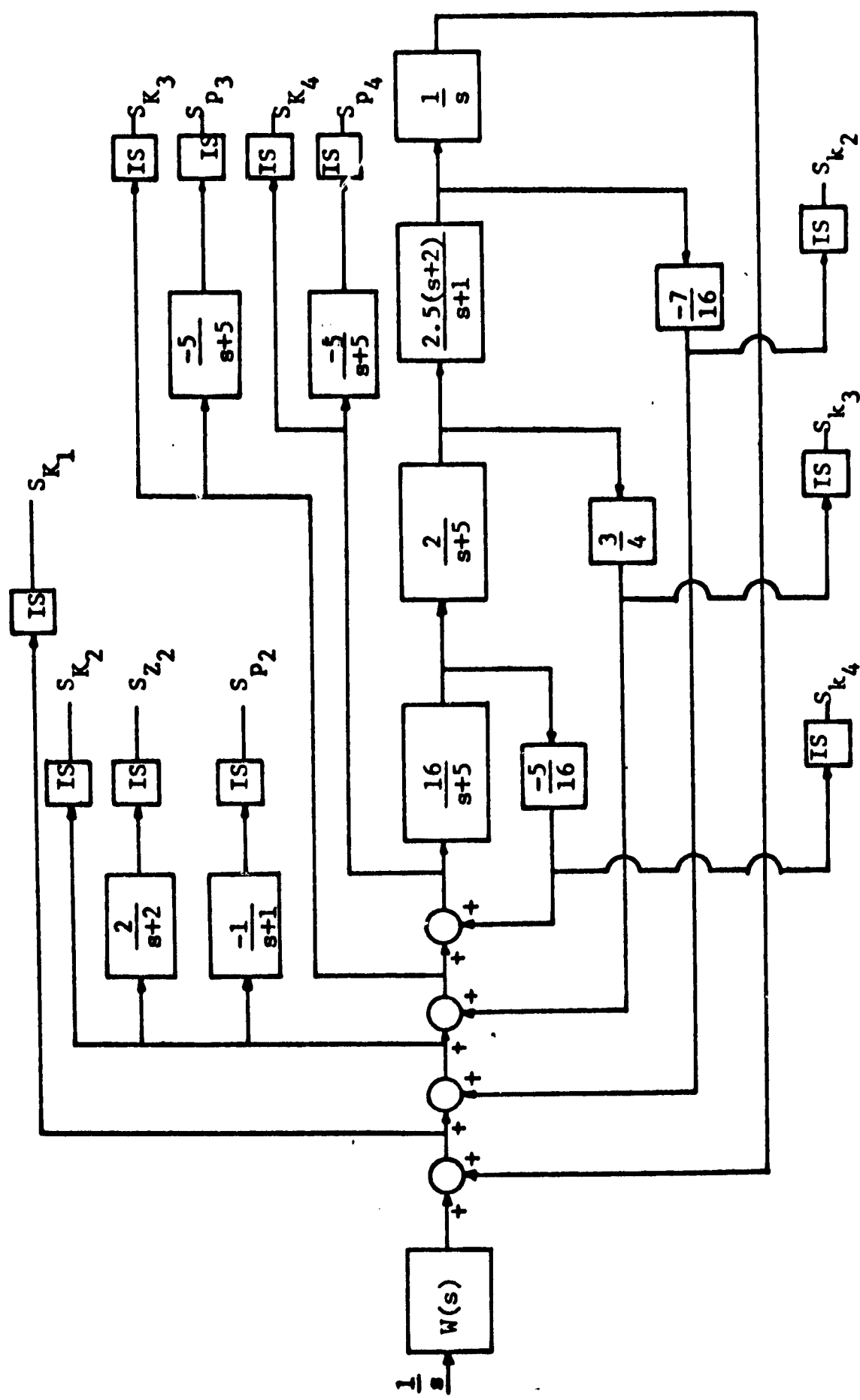


Figure 5.21 Generation of sensitivity functions and integral sensitivities for the system of Example 4.

<u>Parameter</u>	<u>Peak Sensitivity</u>	<u>Integral Sensitivity</u>
K_1	0.593	0.286
K_2	0.321	0.0670
K_3	0.458	0.152
K	0.248	0.0424
z_2	0.213	0.0354
p_2	-0.148	0.0191
p_3	-0.415	0.132
p_4	-0.223	0.0366
k_2	-0.396	0.1366
k_3	0.194	0.0295
k_4	-0.223	0.0366

It is seen that the peak and integral sensitivities with respect to p_4 and k_4 are equal, which follows from the equality of their classical sensitivities. It should also be noted that $S_{K_3} > S_{K_2}$. This occurs because the feedback coefficient k_3 is negative.

It may be noted that $|S_{p_4}^W| \rightarrow 0$ as $p_4 \rightarrow 0$. Thus, for minimum sensitivity with respect to p_4 , the best choice is $p_4 = 0$. However, as mentioned above, this value of p_4 leads to instability for small values of K . This illustrates the need to maintain an overall view of the system behavior when a solution for minimum sensitivity is being sought.

CHAPTER VI

CONCLUSIONS

In this thesis a new sensitivity measure, integral sensitivity (s_λ), has been defined in terms of the sensitivity function ($u_\lambda(t)$).

$$s_\lambda = \int_0^\infty u_\lambda^2(t) dt$$

where $u_\lambda(t) = \frac{dy(t, \lambda)}{d\lambda}$, and $y(t, \lambda)$ is the response of the system to a step input. Although the integral sensitivity contains less information than the sensitivity function, it does, along with the peak sensitivity (u_λ^*), provide a quantitative measure of sensitivity in a concise form. Peak sensitivity is defined as:

$$u_\lambda^* = u_\lambda(T)$$

where T = the value of t such that $|u_\lambda(t)|$ is a maximum. Integral sensitivity is a measure of the overall effect on the system step response of a parameter variation, while the peak sensitivity is an estimate of the maximum change in $y(t)$ for a $\pm 1\%$ change in the parameter. Part of the value of integral sensitivity is derived from its close connection to classical sensitivity ($s_\lambda^W = \frac{\lambda}{W} \frac{dW}{d\lambda}$) by the equation

$$s_\lambda = \frac{1}{2\pi} \int_{-\infty}^{\infty} \frac{|W(j\omega)|}{\omega^2} |s_\lambda^W(j\omega)| d\omega$$

From this relation the relative magnitudes of classical sensitivities, which may be found without the use of a computer, can be used to predict the relative magnitudes of integral sensitivities. Furthermore, integral sensitivities can be computed for practical cases only in a numerical fashion, while classical sensitivities can be evaluated in terms of the literal parameters of the system. In this way sensitivity considerations are included early in the design process.

In Chapter IV a comparison is made between the sensitivity properties of state-variable feedback systems and series compensated systems. It is seen that, under certain conditions, the sensitivities with respect to most of the system parameters may be expected to be smaller for the state-variable feedback system, and that the sensitivities with respect to blocks in the state feedback system are less for the blocks closer to the system input. This behavior is demonstrated by the examples of Chapter V.

The use of H -equivalent feedback is seen to be advantageous with regard to sensitivities for parameters in the forward path. However, in order to make the feedback transfer function realizable, it is necessary to add poles to $H_{eq}(s)$. The locations of these poles must be chosen with attention to their effects on $W(s)$ and the filtering of output noise. There is also the possibility of choosing the poles such that the resulting system has zero steady-state error for a ramp input. The judicious choice of these pole locations as

an integral part of the system design appears to be a subject for future work.

The following observations seem to indicate another topic for further research. By feeding back the state variables, a reduction in sensitivity for parameters in the forward path is obtained, but the feedback coefficients which are introduced represent a new source of sensitivity. Also, it was seen by an example calculation in section 4.3 that the sensitivity value of the least sensitive component depends entirely on the given fixed plant and the specified closed-loop response. These considerations lead to the conjecture that, given a fixed plant which constitutes the forward path, and a specified closed-loop response, there may exist a law of "conservation of sensitivity" for the system. That is, reduction of the sensitivity with respect to certain parameters may lead to increased sensitivity due to other parameters, and the total sensitivity is, in some sense, a constant.

APPENDIX

For the system of Fig. 4.2, Eqs. (4.4) and (4.6) are given for the sensitivities with respect to $G_j(s)$ and k_j respectively. The closed loop transfer function $W(s)$ is given by Eq. (4.3). These expressions are derived here.

The system of Fig. 3.1 is the same as that of Fig. 4.2 for the case where $H_j = k_j$ for all j . Consider the reduced block diagram of Fig. 3.2. An expression for $S_{G_1}^W = E_1(s)/R(s)$ is given by Eq. (3.8).

$$S_{G_1}^W = \frac{1}{1 + G_1 L N [M + k_1/N]} = \frac{1}{1 + G_1 L [NM + k_1]}$$

Substitution for $L(s)$, $M(s)$ and $N(s)$ from Eqs. (3.4), (3.5) and (3.6), and multiplication of the numerator and denominator of $S_{G_1}^W$ by the denominator of $L(s)$ yields:

$$\begin{aligned} S_{G_1}^W &= \frac{1 + k_{i+1} G_{i+1} \dots G_n + k_{i+2} G_{i+2} \dots G_n + \dots + k_n G_n}{1 + k_{i+1} G_{i+1} \dots G_n + \dots + k_n G_n + [k_1 G_1 \dots G_n + k_2 G_2 \dots G_n + \dots + k_n G_n]} \\ &+ \frac{\dots + k_1 G_1 \dots G_n}{1 + k_{i+1} G_{i+1} \dots G_n + \dots + k_n G_n} \\ &= \frac{1 + k_{i+1} G_{i+1} \dots G_n + k_{i+2} G_{i+2} \dots G_n + \dots + k_n G_n}{1 + k_1 G_1 \dots G_n + k_2 G_2 \dots G_n + \dots + k_n G_n} \\ &= \frac{1 + \sum_{j=1}^n k_{i+j} \sum_{l=1+j}^n G_l}{1 + \sum_{j=1}^n k_j \sum_{l=j}^n G_l} \end{aligned}$$

This is Eq. (4.4). $W(s)$ may be found from $S_{G_n}^W$.

$$\begin{aligned}
 W(s) &= \frac{Y(s)}{R(s)} = \frac{E_n(s)}{R(s)} G_1(s) \dots G_n(s) = s_{G_n}^W G_1 \dots G_n \\
 &= \frac{G_1 \dots G_n}{1 + k_1 G_1 \dots G_n + k_2 G_2 \dots G_n + \dots + k_n G_n} \\
 &= \frac{\prod_{i=1}^n G_i}{1 + \sum_{l=1}^n k_l \prod_{j=l}^n G_j}
 \end{aligned}$$

This is Eq. (4.3).

From Eq. (3.10) and with reference to Fig. (3.2),

$$\begin{aligned}
 s_{k_1}^W &= \frac{D_1(s)}{R(s)} = -k_1 \frac{1}{N(s)} \frac{Y(s)}{R(s)} \\
 &= \frac{-k_1}{G_1 G_2 \dots G_{i-1}} W(s) \\
 &= \frac{-k_1 G_1 G_{i+1} \dots G_n}{1 + k_1 G_1 \dots G_n + k_2 G_2 \dots G_n + \dots + k_n G_n} \\
 &= \frac{-k_1 \prod_{j=1}^n G_j}{1 + \sum_{j=1}^n k_j \prod_{l=j}^n G_l}
 \end{aligned}$$

This is Eq. (4.6).

REFERENCES

H.W. Bode, Network Analysis and Feedback Amplifier Design, Van Nostrand, 1945.

J.H. Dial, "The Specification and Synthesis of High-Order Control Systems," M.S. Thesis, The University of Arizona, June 1967.

R.A. Haddad and J.G. Truxal, "Sensitivity and Stability in Multiloop Systems," Joint Automatic Control Conference, 1964.

I.M. Horowitz, Synthesis of Feedback Systems, Academic Press, 1963.

R.E. Kalman, "When Is a Linear Control System Optimal?" Journal of Basic Engineering, March 1964.

G.C. Newton, L.A. Gould and J.F. Kaiser, Analytical Design of Linear Feedback Controls, Wiley, 1957.

D.G. Schultz and J.L. Melsa, State Functions and Linear Control Systems, McGraw-Hill, 1967.

R. Tomovic, Sensitivity Analysis of Dynamic Systems, McGraw-Hill, 1964.

J.G. Truxal, Automatic Feedback Control System Synthesis, McGraw-Hill, 1955.

J.E. Van Ness, J.M. Boyle and F.P. Imad, Sensitivities of Large, Multiple-Loop Control Systems, IEEE Transactions on Automatic Control, July 1965.

PART III

**INTENTIONAL NONLINEARITY IN A
STATE VARIABLE FEEDBACK SYSTEMS**

**Prepared Under Grant NGR-03-002-115
National Aeronautics and Space Administration**

by

Hasmukhrai Bhawanidas Parekh

and

Donald G. Schultz

**Electrical Engineering Department
The University of Arizona
Tucson, Arizona**

ABSTRACT

In this work a particular type of nonlinear state variable feedback system is discussed. The system contains a single nonlinearity, and it is shown by describing function techniques and examples that the optimum location of the nonlinear element for maximum control is at the left end. A method for designing gain-insensitive systems is presented, and it is shown by simple reasoning and examples that the system response for the gain-insensitive design is better than that of systems designed by conventional state variable feedback.

A method is given to overcome the effects of saturation within the fixed plant by introducing an intentional nonlinearity to limit the saturating elements to their linear regions of operation. This makes it possible to apply the above gain-insensitive design technique so that the nonlinear plant can be made absolutely stable for all gain. The proposed method is then applied to improve the response of a fuel valve servomechanism, and the system is evaluated using an analog computer.

TABLE OF CONTENTS

Chapter	Page
Acknowledgment.....	iv
List of Figures.....	vi
Abstract.....	ix
I Introduction.....	1
II General Theory.....	6
III Design of Nonlinear Gain-Insensitive Systems.....	31
IV Design of a Fuel Valve Servomechanism...	54
V Summary and Conclusions.....	69
Appendix.....	72
References.....	82

LIST OF FIGURES--Continued

Number		Page
2-14	Polar Plot of $G(j\omega)$ and $-1/k_{eq}$ for Case III	29
3-1	A Linear Gain-Insensitive System, where $G(s)H_{eq}(s) = k'/(s+a)$	33
3-2	Nonlinear Gain-Insensitive System and Modified Block Diagram	35
3-3	Plant and Characteristic of N for Example 1	38
3-4	Gain-Insensitive and Non-Gain-Insensitive Systems with Their Root Locus Sketch in the Linear Region	41
3-5	Time Response for the System of Example 1	42
3-6	Explains the Decrease in k' When N Operates in the Nonlinear Region	43
3-7	Plant and Characteristic of N for Example 2	45
3-8	Gain-Insensitive and Non-Gain-Insensitive Systems Along with Their Root Locus Sketch in the Linear Region	47
3-9	Plant and Characteristic of N for Example 3	48
3-10	Gain and Non-Gain-Insensitive Systems Along with Their Root Locus Sketch in the Linear Region	49
3-11	Time Response for the System of Example 3	50
3-12	Time Response Showing Oscillations for Example 3	52
4-1	Linearized Plant of Physical System . .	55
4-2	Open-Loop and Closed-Loop Pole Location for the Linear System	59

LIST OF FIGURES--Continued

Number		Page
4-3	Modification of Plant by Feeding Back Variables x_2 Through x_7	62
4-4	Realization of Closed-Loop Transfer Function by Feeding Back Variables x_1 Through x_7	63
4-5	Time Responses of the 7th Order Linear Gain-Insensitive System	65
4-6	Time Response for the Nonlinear System .	67
A-1	Linearized Plant of Physical System . . .	73
A-2	Analog Computer Wiring Diagram for Simulation	79
A-3	The Details of the Bridge Circuit Realizing Limiter and its Input-Output Characteristic	81

LIST OF FIGURES

Number		Page
2-1	Basic Configuration for a Linear State Variable Feedback System	8
2-2	G_{eq} and H_{eq} Method of Representing a Linear System	10
2-3	A State Variable Feedback System with the Nonlinearity N in the Forward Path .	11
2-4	Block Diagram Reduction for the System Shown in Fig. 2-3	12
2-5	Equivalent or Reduced Form of Fig. 2-4(b) with $r(t) = 0$	14
2-6	Characteristic and the Polar Plot of Equivalent Gain for the Nonlinearity . .	17
2-7	The System of Fig. 2-4(b)	19
2-8	Various Types of $G(j\omega)$ Functions Showing the Possibility of Oscillations and the Polar Plot of $-1/k_{eq}$ for the Nonlinearity	19
2-9	Plant Showing Saturation at Different Points in the System	21
2-10	Nonlinear System Designed by State Variable Feedback Method	23
2-11	Polar Plot of $G(j\omega)$ and $-1/k_{eq}$ for Case I	24
2-12	Polar Plot of $G(j\omega)$ and $-1/k_{eq}$ for the System Shown in Fig. 2-12(a)	26
2-13	Polar Plot of $G(j\omega)$ and $-1/k_{eq}$ for Case II	27

I. Introduction

The application of modern control theory to linear control systems with constant coefficients is quickly developing into an efficient and powerful theory. The key idea is the use of state variable feedback, and it is initially assumed that all of the state variables are available for measurement and control. An effective synthesis technique using state variable feedback is known as the H equivalent method (Schultz and Melsa, 1967). The basic assumption of the H equivalent method is that the desired closed loop transfer function is specified in advance, and by feeding back all of the state variables, this desired transfer function can be realized exactly for a range of inputs for which the system remains linear. The method is attractive because all manipulations and calculations are done in the frequency domain with Laplace transforms.

The basic assumption of state variable feedback methods is that the system remains linear during its entire period of operation. In particular, for large inputs one or more of the internal state variables

may saturate. The resulting behavior of the system may then be different than predicted by the linear theory, and, in fact, may even become unstable. In this work the H_2 equivalent synthesis procedures are extended to systems in which an intentional nonlinearity has been introduced to insure that no saturation occurs in the internal state variables. The technique is combined with the gain insensitive design of Herring (1967) to insure that the resulting system is not only stable, but that the dynamics of the saturated and unsaturated systems are very much alike.

In the general case minor loop feedback is applied to the open loop system to force all but one of the open loop poles to lie at desired closed loop pole positions. The poles of the closed loop system are fixed at the desired locations by placing zeros of $H_{eg}(s)$ at the same places. In the case of the fuel valve servomechanism with seven open loop poles, this task was simplified by retaining four of the complex poles of the plant unchanged. This was possible because the natural frequencies involved were far greater than the desired band width of the closed loop system.

The use of a gain insensitive, saturating controller for the fuel valve system results in a

marked improvement in overall system performance.

When the system is operating in the linear region, the second order desired response is almost exactly realized by the seventh order system. For larger inputs, the system exerts maximum effort, and for small inputs the system responds in the desired linear fashion.

The improvements obtained in the fuel valve servomechanism using this approach are appreciable. The table shown below compares the results of the design discussed in this work with both a conventional lead-lag compensated system and with a system designed by linear state variable feedback methods.

Conventional	Heg (linear)	Heg/Sat. controller
Bandwidth BW	220 Hz	700 Hz
Percent PO	10%	10%
Overshoot		8.2%
Small inputs		
Stability	Stable	Extensive overshoot
For	decreased	PO = 10%
Large inputs	bandwidth	decreased bandwidth

Outline of Thesis

In the following chapters it is shown how the introduction of an intentional nonlinearity can be combined with state variable feedback to overcome the effects of saturation. A step-by-step development is presented with illustrative examples, and the method is applied to improve the response of a practical problem.

Chapter II deals with the representation of linear and nonlinear state variable feedback systems. Stability criteria for nonlinear systems are presented along with a brief description of describing function theory. The effect of the location of the nonlinearity is investigated, and it is concluded that the optimum location is at the left most end for maximum control over the system. Finally, the chapter is concluded with illustrative examples.

In Chapter III the effect of saturation in a system is discussed and the idea of introducing an intentional, saturation type of nonlinearity is described. The concept of gain-insensitive systems is presented for linear as well as nonlinear systems. Two systems, gain-insensitive and non-gain-insensitive, are compared and discussed. It is shown that the gain-insensitive system

is absolutely stable and has a satisfactory step response when the gain is varied or operates in the nonlinear region. Finally, a design technique is given for overcoming the effects of saturation by introducing an intentional nonlinearity.

In Chapter IV the techniques developed in Chapter II and III are applied to improve the response of a fuel valve servomechanism. The design is evaluated using both digital and analog computers, and the results are presented in recorded form.

The final chapter presents the conclusions and suggestions for further investigation.

CHAPTER II

GENERAL THEORY

In this chapter the modern representation of linear systems is discussed and state variable feedback methods are presented; general expressions for the transfer functions $G_{eq}(s)$, $H_{eq}(s)$, $Y/R(s)$, etc., are given in matrix form. It is shown that for systems which contain a single nonlinearity but are otherwise linear, the corresponding expressions for $G_{eq}(s)$, $H_{eq}(s)$, etc., depend on the location of the nonlinearity in the forward path.

The effects of the location of the nonlinear element in a system are further investigated by applying describing function theory; and it is concluded that, when the nonlinearity is located at the left end of the system, desirable stability properties and maximum control over the system are achieved. Finally, the results are illustrated with a third-order system having a single nonlinearity.

Representation of Linear Systems

There are two different ways to represent control systems: the input-output form and the modern

state variable method. Here the latter one is of prime interest and hence is presented in detail.

Consider Fig. 2-1, showing a general representation of a linear system. G_p represents the plant and is described by the following set of n first-order linear differential equations:

$$\dot{x} = Ax + bu \quad (Ab)$$

$$y = c^T x \quad (c)$$

where

A is the $n \times n$ plant matrix

b is the $n \times 1$ control vector

c is the $n \times 1$ output vector

k is the $n \times 1$ column matrix of feedback coefficients

x is the $n \times 1$ state vector

u is the input to the plant

r is the input to the system

I is the $n \times n$ identity matrix

The transfer function $G_p(s)$ relating the control function u and the output of the system y is given by

$$G_p(s) = y/u(s) = c^T \Phi(s) b \quad (2-1)$$

where $\Phi(s)$ is called the resolvent matrix and is given by $(sI - A)^{-1}$ (Schultz and Melsa, 1967). The input and output of the system are related by

$$Y/R(s) = c^T \Phi_k b \quad (2-2)$$

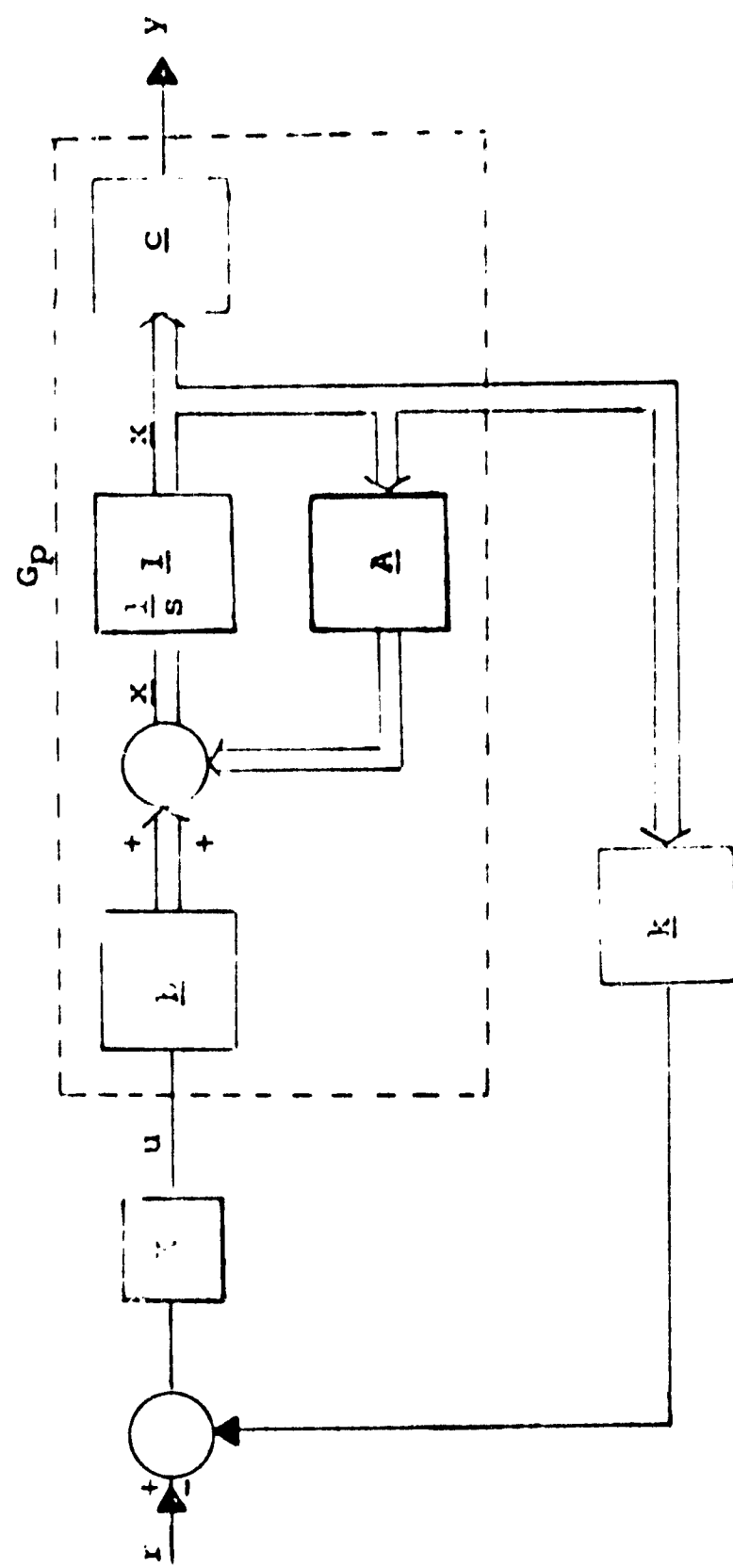


Fig. 2-1 Basic Configuration for a Linear State Variable Feedback System

where $\underline{\Delta}_k$ is the closed-loop resolvent matrix, given by $(s\underline{I} - \underline{\Delta}_k)^{-1}$ or $(s\underline{I} - \underline{\Delta} + \underline{b}\underline{k}^T)^{-1}$.

The system of Fig. 2-1 can be represented by two alternate block diagram configurations, the $G_{eq}(s)$ and $H_{eq}(s)$ representations shown in Fig. 2-2(a) and (b), respectively. General expressions for $H_{eq}(s)$, $G_{eq}(s)$, and $G_p(s)H_{eq}(s)$ are given below.

$$H_{eq}(s) = (\underline{k}^T \underline{\Phi}(s) \underline{b}) / (\underline{c}^T \underline{\Phi}(s) \underline{b}) \quad (2-3)$$

$$G_{eq}(s) = (\underline{c}^T \underline{\Phi}(s) \underline{b}) / (1 + (\underline{k} - \underline{c})^T \underline{\Phi}(s) \underline{b}) \quad (2-4)$$

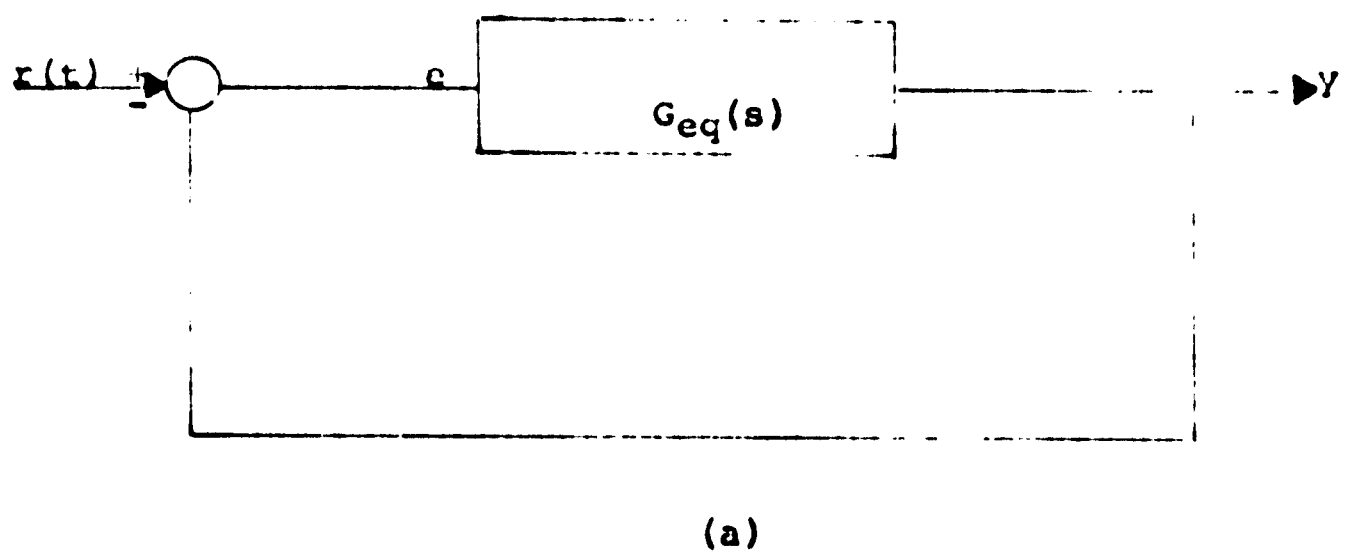
$$G_p H_{eq}(s) = \underline{k}^T \underline{\Phi}(s) \underline{b} \quad (2-5)$$

All the above expressions can be found in terms of $\underline{\Delta}_k$ (Schultz and McIsaac, 1967).

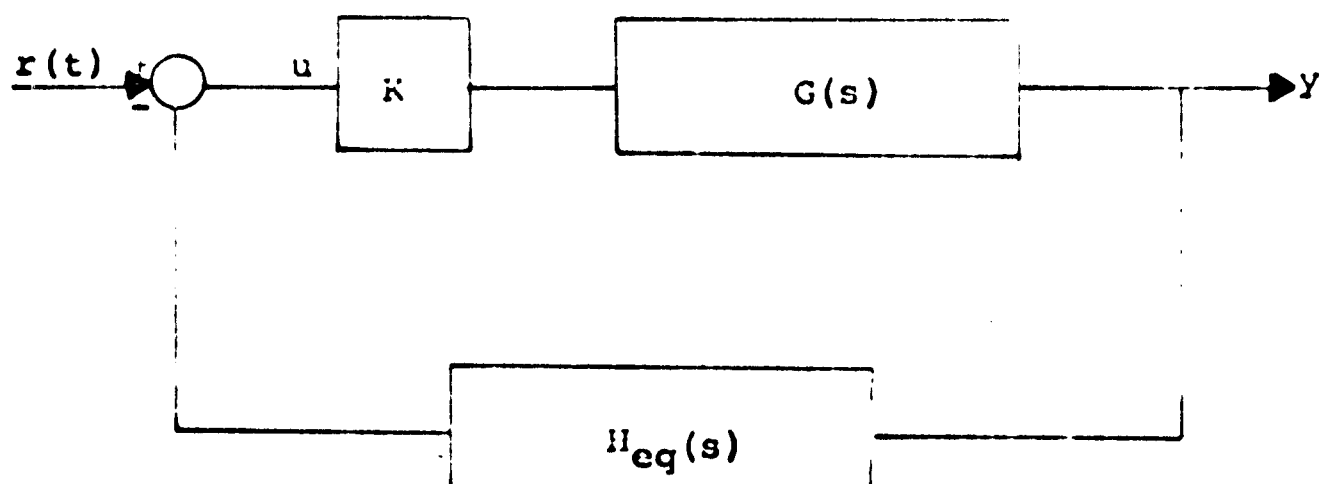
State Variable Representation of a Particular Type of Nonlinear System

Consider the configuration shown in Fig. 2-3 and having the single nonlinearity represented by the block labelled N. G^1, G^2, \dots, G^n each represents a first-order transfer function; i.e., $G^i = k_i(s + z_i)/(s + p_i)$. Block diagram manipulation yields the modified diagram shown in Fig. 2-4(a), where $G_1(s)$ and $G_2(s)$ represent $(n - 1)^{th}$ and i^{th} order linear transfer functions, respectively, and $H_{1eq}(s)$ and $H_{2eq}(s)$ are of order $(n - i - 1)$ and $(i - 1)$, respectively. Further

10



(a)



(b)

Fig. 2-2 G_{eq} and H_{eq} Method of Representing a Linear System

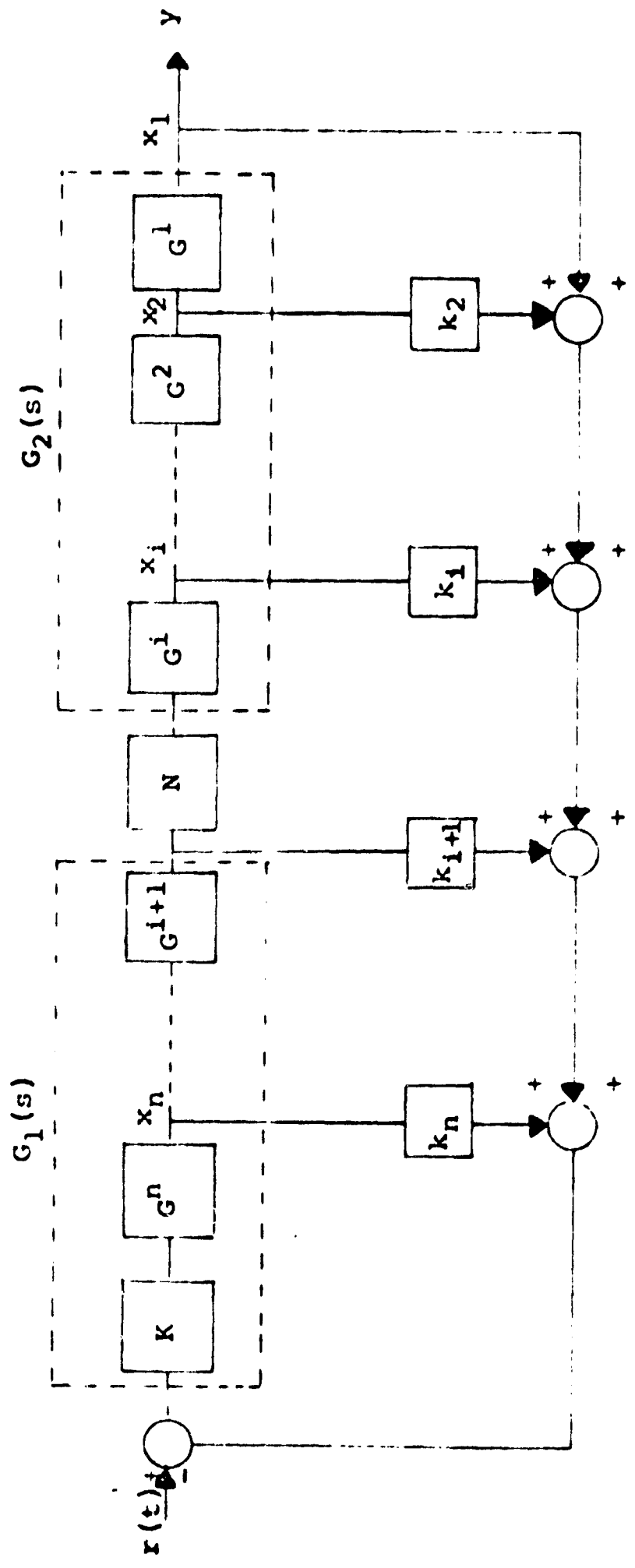
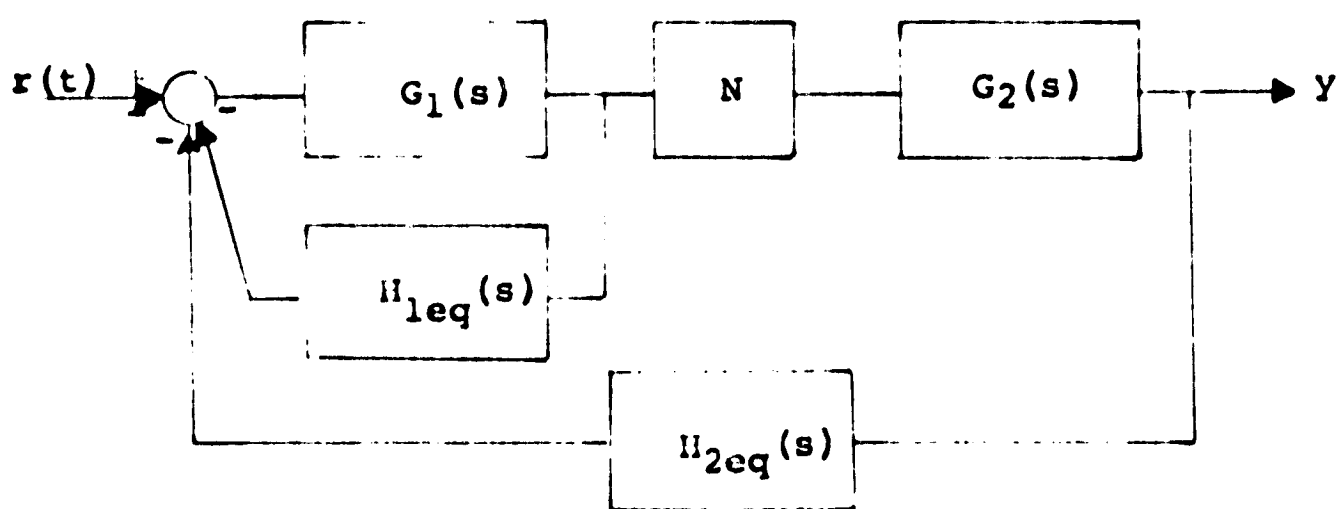
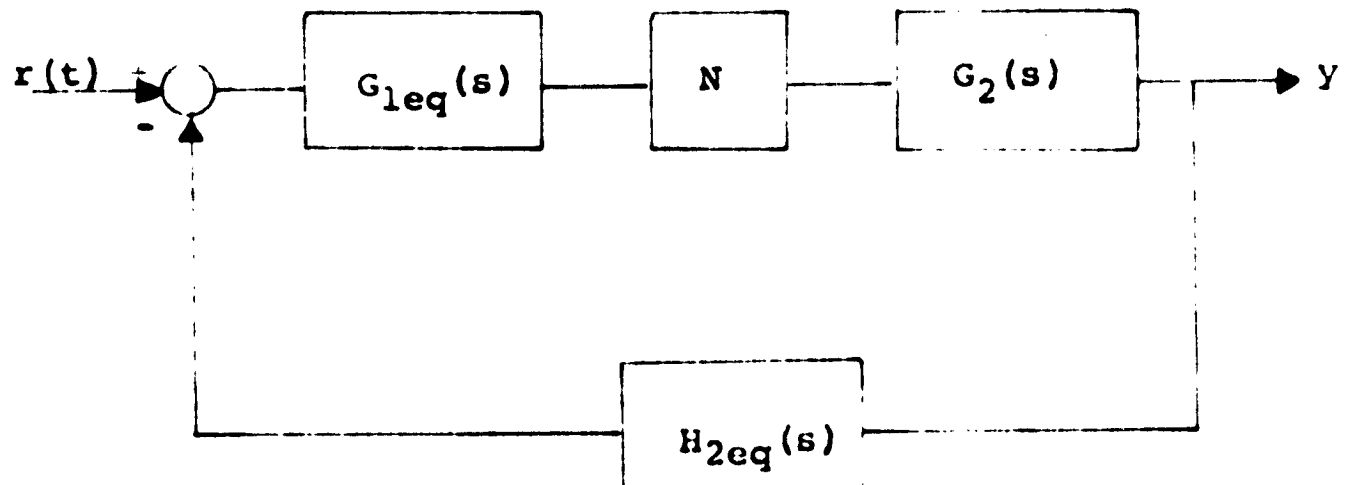


Fig. 2-3 A State Variable Feedback System with the Nonlinearity N in the Forward Path



(a)



(b)

Fig. 2-4 Block Diagram Reduction for the System Shown in Fig. 2-3

reduction of the block diagram shows the system in final form in Fig. 2-4(b).

Now comparing the representations for linear systems and nonlinear systems, one can observe that nonlinear systems cannot be represented in the simplest G_{eq} or H_{eq} form (as can linear systems) unless the nonlinearity is located at the left most end. In the general case (see Fig. 2-4(b)) linear transfer functions and characteristics of the nonlinearity are required to describe the nonlinear system. $H_{eq}(s)$ has $n - 1$ zeros while $H_{2eq}(s)$ has $i - 1$ zeros. As the nonlinearity is shifted towards the left side, the number of zeros in $H_{2eq}(s)$ increases and finally becomes $n - 1$ when it is located at the left end.

Describing Function Theory

The describing function method is based on an analysis which neglects the effects of harmonics in the system, so that the accuracy of technique increases with the order of the system. The system configuration shown in Fig. 2-5 represents the reduced form of Fig. 2-4(b) and is in the correct form for applying the describing function method. N is the single nonlinearity of the system and is assumed to be insensitive

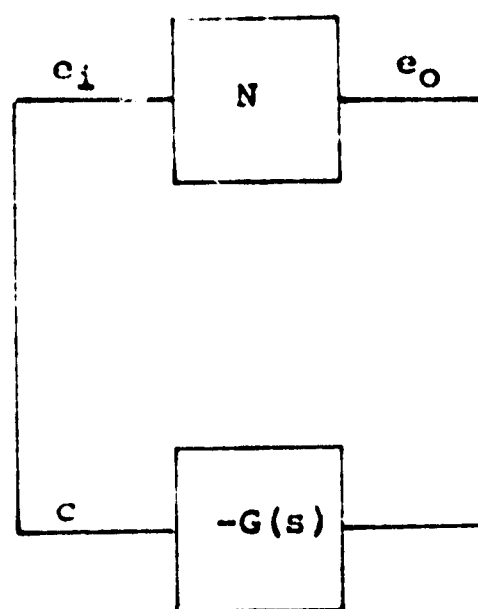


Fig. 2-5 Equivalent or Reduced Form
of Fig. 2-4(b) with $r(t) = 0$

to frequency. It is desired to determine whether a sustained oscillation of sinusoidal form exists in the system when there is no external input.

The output of the nonlinear element when its input is a sinusoidal wave having an amplitude E is written in the form

$$c_o = k_{eq}e + f_d(e) \quad (2-6a)$$

The first term on the right-hand side is the fundamental while the second term represents harmonic distortion and is neglected. Hence

$$c_o \approx k_{eq}e \quad (2-6b)$$

k_{eq} is known as the equivalent gain, or the describing function, and it is a function of input-signal amplitude E . The describing function for the nonlinearity can be found as follows (Gibson, 1963):

$$k_{eq} = g(E) + jb(E) \quad (2-7)$$

where

$$g(E) = \frac{1}{\pi E} \int_0^{2\pi} f(E \sin \theta) \sin \theta d\theta \quad (2-8a)$$

$$b(E) = \frac{1}{\pi E} \int_0^{2\pi} f(E \sin \theta) \cos \theta d\theta \quad (2-8b)$$

From Fig. 2-5

$$\frac{c(j\omega)}{c_o(j\omega)} = -G(j\omega) \quad (2-9)$$

Referring to the equations (2-6b) and (2-9), one can see that for the existence of sustained oscillations

there must exist a simultaneous solution which satisfies both equations; i.e.,

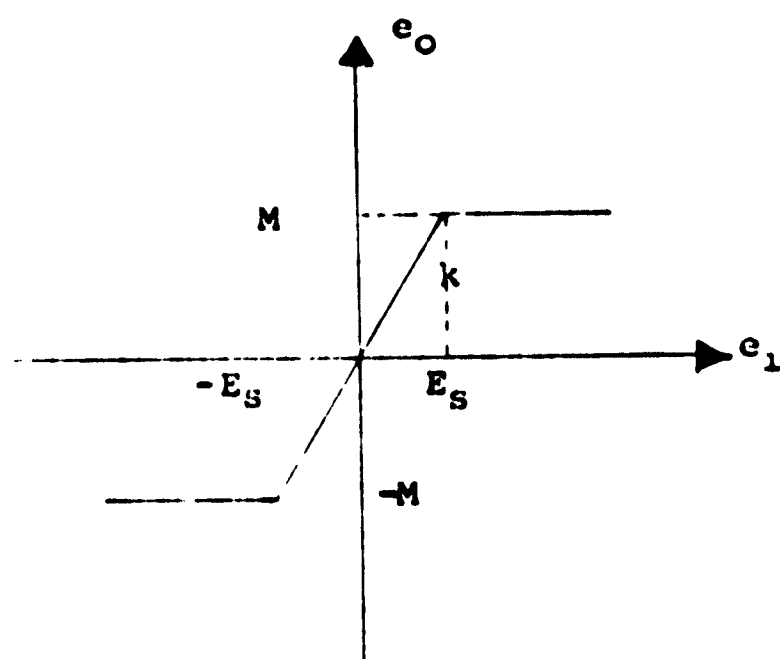
$$G(j\omega) = -\frac{1}{k_{eq}} \quad (2-10)$$

A convenient way of investigating equation (2-10) is to draw polar plots of both sides and check for an intersection; the point of intersection gives the frequency and amplitude of oscillation. The oscillations may be stable or unstable depending on whether the amplitude of oscillation decreases or increases as the operating point on $-1/k_{eq}$ locus moves within the frequency-sensitive locus of $G(j\omega)$; i.e., the Nyquist plot.

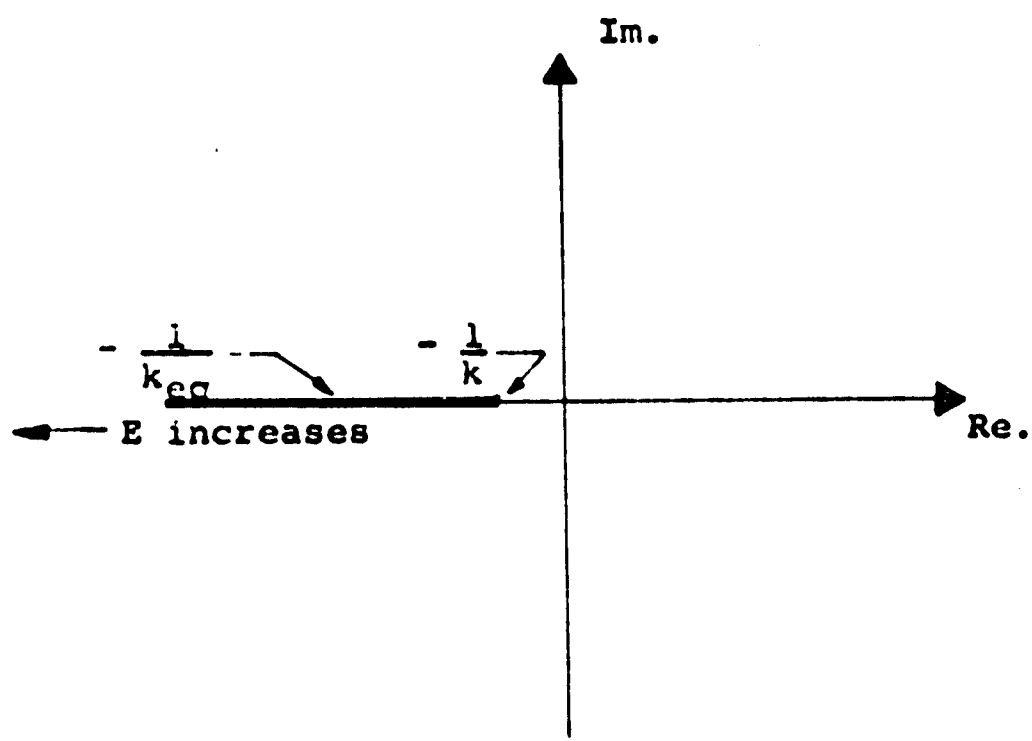
One can apply the describing function method to check the stability of a system having a particular type of nonlinearity N . N is single-valued and symmetric, lying in first and third quadrants. The describing function for this type nonlinearity will always be real and non-negative (Gibson, 1963). Fig. 2-6(a) shows a saturation type nonlinearity, a representative of the class we are considering. The equivalent gain for such a nonlinearity is given by (Thaler and Pastel, 1962)

$$k_{eq} = \frac{2k}{\pi} \left(\sin^{-1} \frac{E_S}{E} + \frac{E_S}{E} \sqrt{\left(1 - \frac{E_S}{E}\right)^2} \right) \quad (2-11)$$

which is always real and non-negative, as expected. The polar plot is shown in Fig. 2-6(b).



(a)



(b)

Fig. 2-6 Characteristic and the Polar Plot of Equivalent Gain for the Nonlinearity

Consider the system whose block diagram is shown in Fig. 2-7(a) which is similar to Fig. 2-4(b). It was stated previously that $G_{1eq}(s)$ has $n - i$ poles, $G_2(s)$ has i poles, and $H_{2eq}(s)$ has $i - 1$ zeros. Hence

$$G(j\omega) = G_{1eq}(s)G_2(s)H_{2eq}(s) \quad (2-12)$$

has n poles and $i - 1$ zeros. Now to check for the existence of oscillations, the polar plot of $- \frac{1}{k_{eq}}$ for a single-valued, symmetric nonlinearity is plotted in Fig. 2-8. For oscillations

$$G(j\omega) \Big|_{\omega = \omega_c} \leq -\frac{1}{k} \quad (2-13)$$

where ω_c is a frequency for which $G(j\omega)$ is real. This is possible if and only if $G(j\omega)$ is inherently unstable in the linear region or $G(j\omega)$ is conditionally stable as shown in Fig. 2-8, labelled $G''(j\omega)$ and $G'(j\omega)$, respectively.

From Equation (2-13) it can be seen that oscillations can exist for some value of gain k as long as the polar plot of $G(j\omega)$ crosses the negative real axis. Thus to avoid oscillations $G(j\omega)$ should not cross the negative real axis for any value of gain; i.e., $G(j\omega)$ should have the form shown by the curve in Fig. 2-8 and labelled $G'''(j\omega)$. This is possible if $G(j\omega)$ has a pole-zero excess of < 2 and if the zeros of $G(j\omega)$ are located at proper places. Thus it is desired to have

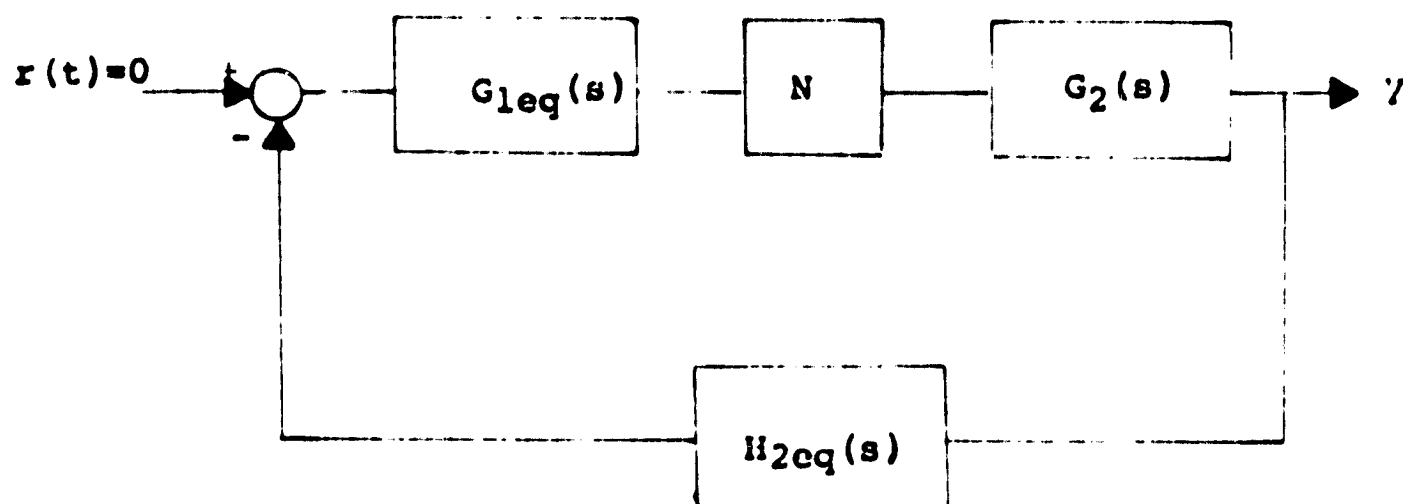
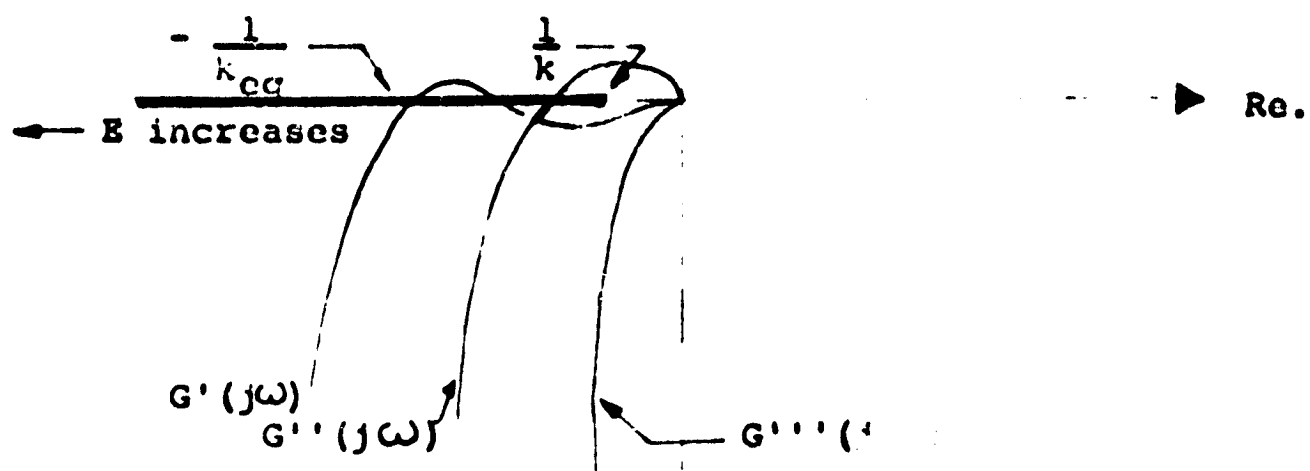


Fig. 2-7 The System of Fig. 2-4(b)

▲ Im.

Fig. 2-8 Various Types of $G(j\omega)$ Functions
Showing the Possibility of Oscillations
and the Polar Plot of $-1/k_{eq}$ for the
Nonlinearity

$$\begin{aligned} n - i + 1 &\leq 2 \\ i &> n - 1 \end{aligned} \quad (2-14)$$

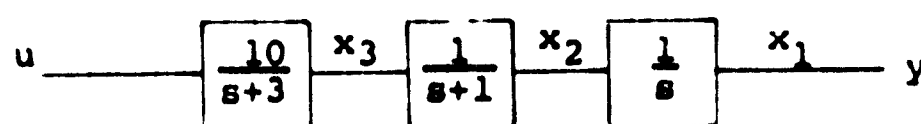
in order to prevent oscillations. Also, it is known that the more zeros there are in $H_{2eq}(s)$, the better a system can be controlled, so that the optimum choice for i would be n ; that is, the best location for the nonlinearity is at the left most end of the system. It should be noted that stability of the system still depends upon the zeros of $H_{2eq}(s)$ and hence the feedback coefficients.

Example

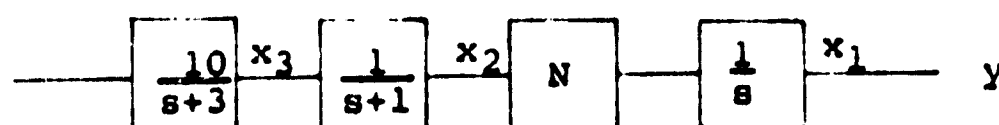
Consider the plant shown in Fig. 2-9(a) which is to be controlled by state variable feedback. All systems saturate at one or another point. Here saturation is accounted for by the nonlinearity labelled N , which is presumed to be of the type shown in Fig. 2-6(a). Different possibilities for saturation are shown in Fig. 2-9(b), (c), and (d). It is the purpose of this example to investigate what happens when the system saturates at these different points.

Case I

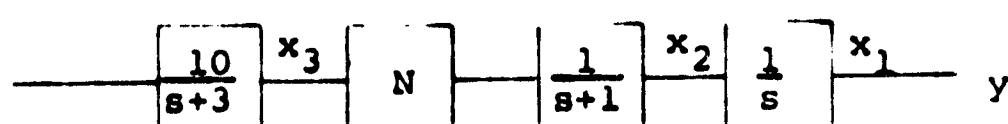
Let N be located as in Fig. 2-9(b). State variable feedback is to be used to achieve the closed-loop transfer function



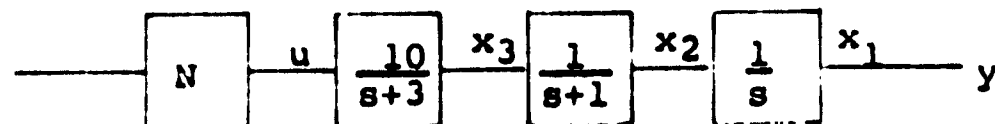
(a)



(b)



(c)



(d)

Fig. 2-9 Plant Showing Saturation at Different Points in the System

$$\frac{Y(s)}{R} = \frac{10}{s^3 + 5.25s^2 + 8s + 10}$$

when operating in the linear region. The result is shown in Fig. 2-10(a). When the system operates in the nonlinear region, the input-output relation does not hold; but some aspects of the behavior can be investigated by the describing function method. By block diagram reduction of Fig. 2-10(a)

$$G_{1eq} = \frac{10}{s^2 + 5.25s + 8}$$

$$G_2(s) = \frac{1}{s}$$

$$H_{2eq}(s) = 1$$

so that

$$\begin{aligned} G(s) &= G_{1eq}(s) \cdot H_{2eq}(s) \cdot G_2(s) \\ &= \frac{10}{s(s^2 + 5.25s + 8)} \end{aligned}$$

The polar plots of $G(j\omega)$ and $-\frac{1}{k_{eq}}$ as given by Equation (2-12) are shown in Fig. 2-11. The point at which $G(j\omega)$ intersects with the negative real axis can be found very easily to be -0.238 at $\omega = 2\sqrt{2}$.

That is,

$$\begin{aligned} G(j\omega) \Big|_{\omega = 2\sqrt{2}} &= \frac{10}{2\sqrt{2}(-8 + j5.25 \cdot 2\sqrt{2} + 8)} \\ &= -0.238 \end{aligned}$$

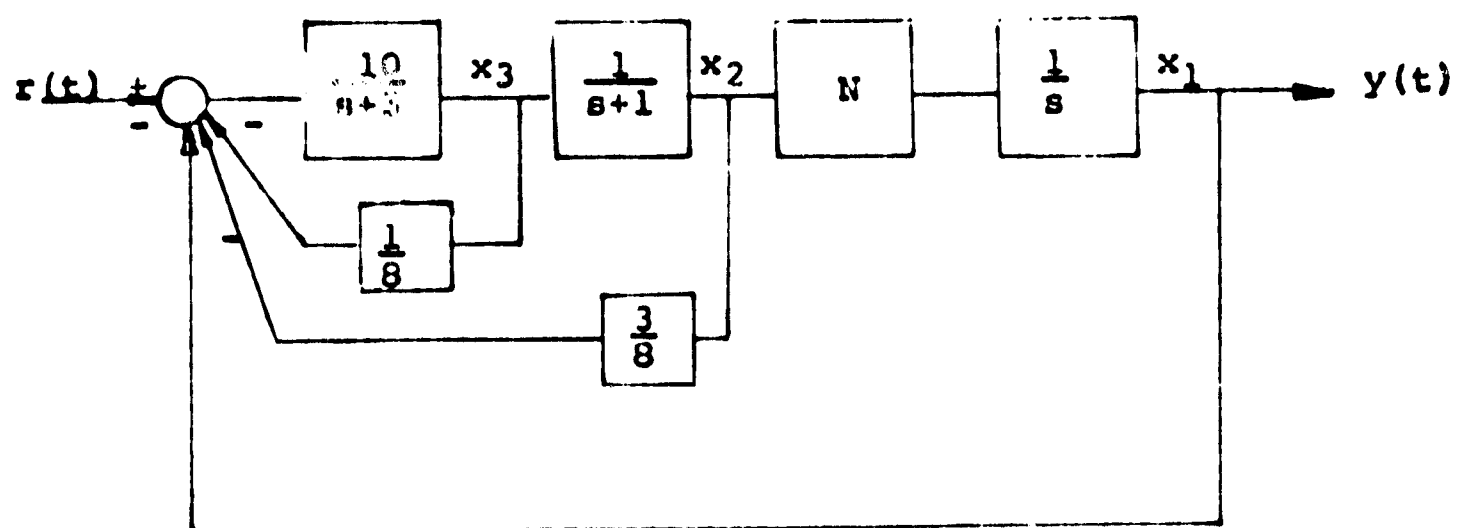


Fig. 2-10 Nonlinear System Designed by State Variable Feedback Method

▲ Im.

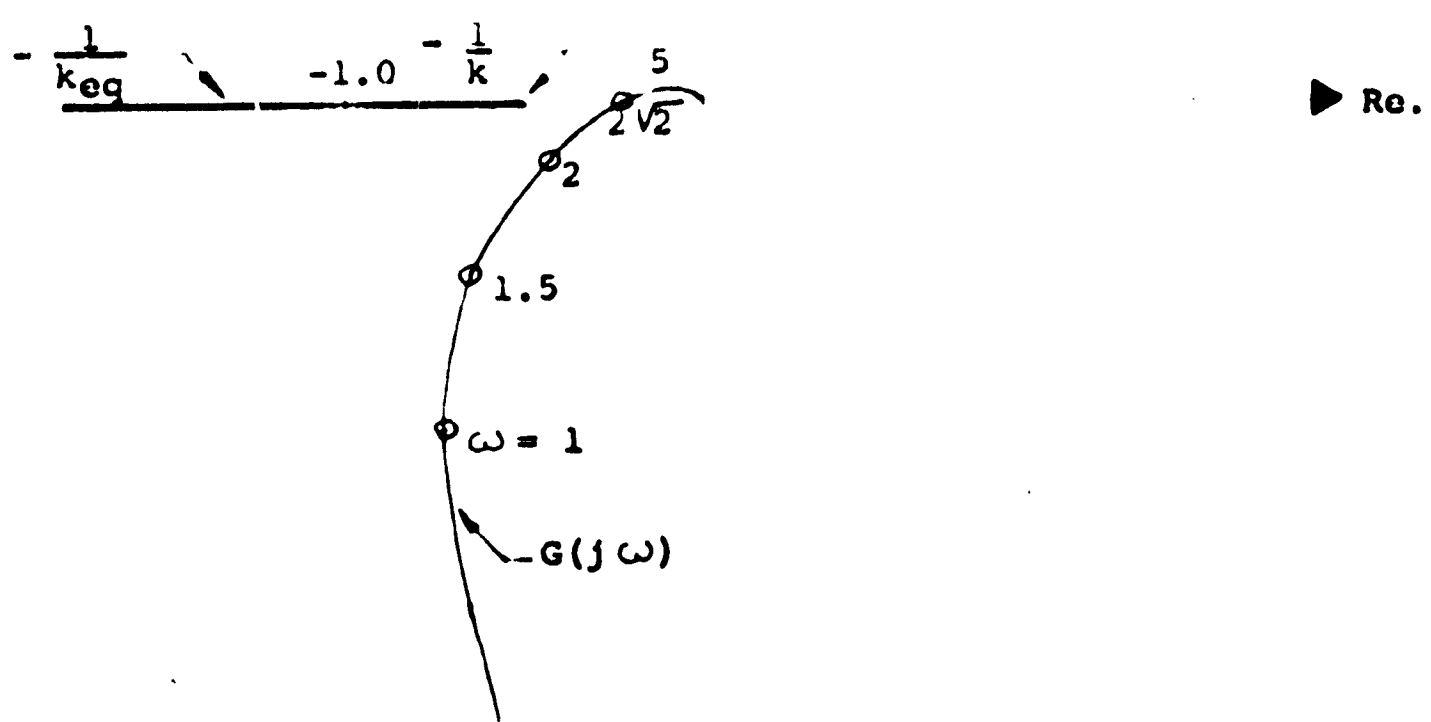


Fig. 2-11 Polar Plot of $G(j\omega)$ and $-1/k_{eq}$ for Case I

Thus for oscillation $(-\frac{1}{k_{eq}})_{max} = -0.238$, which gives the maximum value of k , the linear gain, which the nonlinearity can have. In this case oscillations will occur when k is increased beyond 1/0.238; however, examples can be found where even without variation of k , the system can show oscillations. One such system is shown in Fig. 2-12(a) along with its polar plot in Fig. 2-12(b).

Case II

Let N be located as in Fig. 2-9(c). The system still has the same configuration when operating in the linear region. When operating in the nonlinear region

$$G_{eq}(s) = \frac{10}{s + 4.25}$$

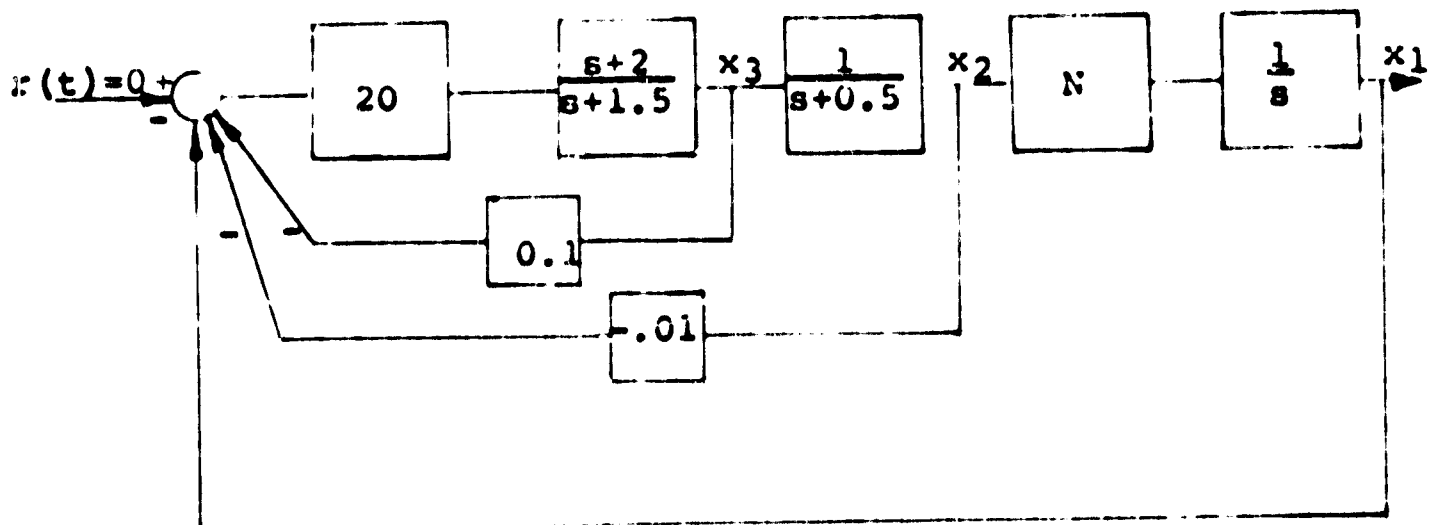
$$H_{2eq}(s) = \frac{3}{8}(s + 2.66)$$

$$G_2(s) = \frac{1}{s(s + 1)}$$

so that

$$G(s) = \frac{3.75(s + 2.66)}{s(s + 1)(s + 4.25)}$$

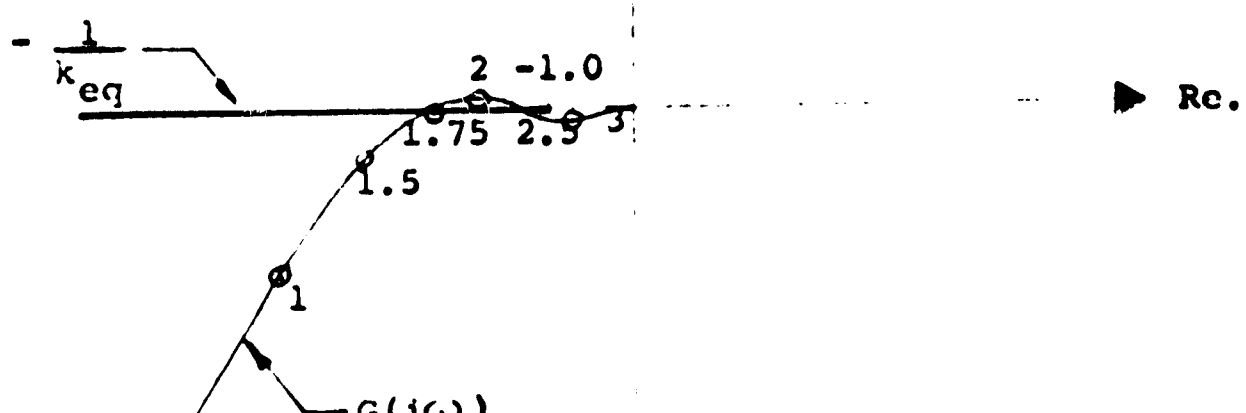
The polar plot for $G(j\omega)$ and $-\frac{1}{k_{eq}}$ are shown in Fig. 2-13, and it can be seen that there cannot be an intersection for any value of gain k of the nonlinearity or for any gain associated with $G(j\omega)$. Thus there is no oscillation and the system is stable for all gain.



$$G(s) = \frac{20(s + 2)}{3s(s^2 + 2.0266s + 0.783)}$$

(a)

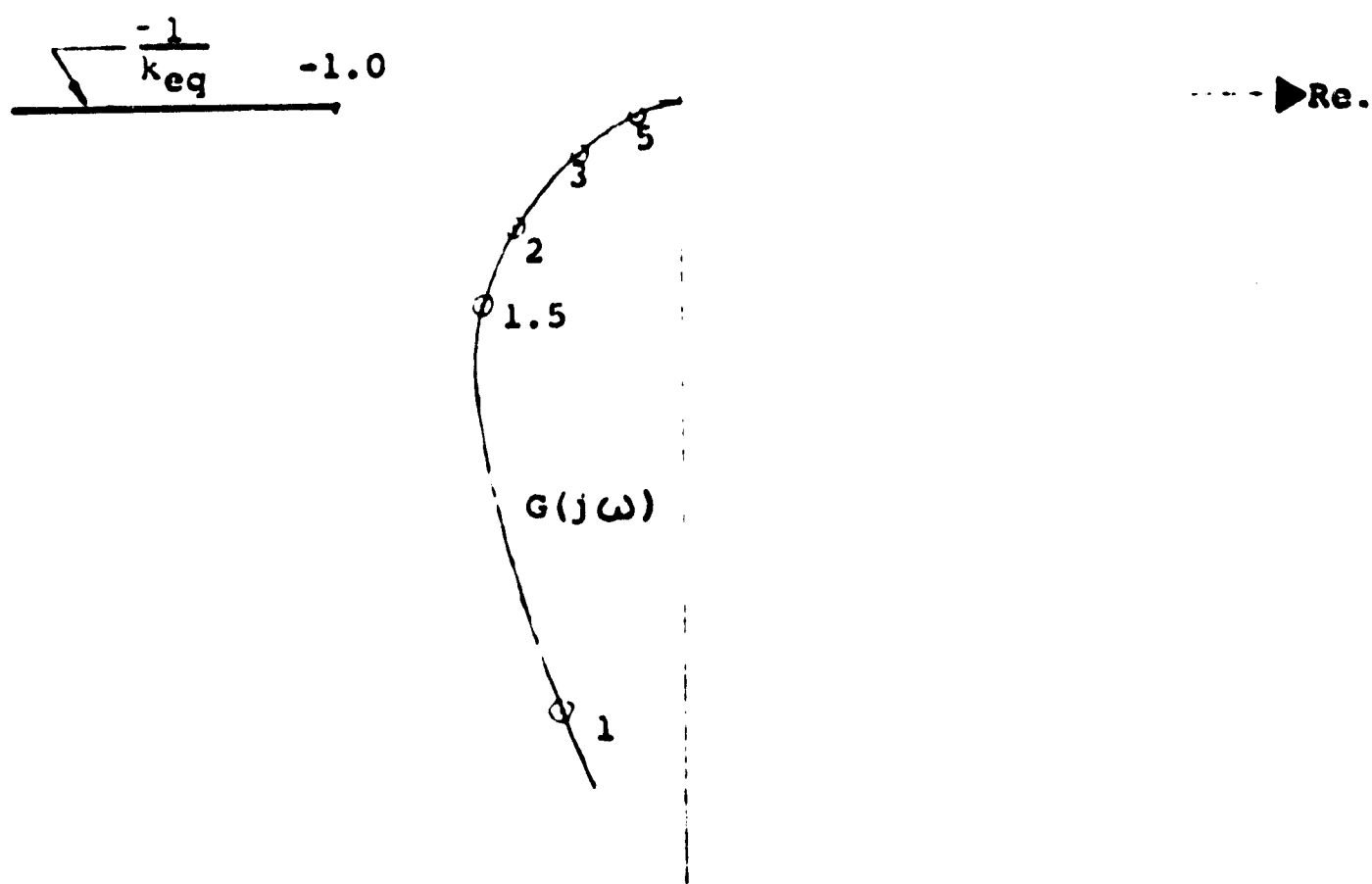
▲ Im.



(b)

Fig. 2-12 Polar Plot of $G(j\omega)$ and $-1/k_{eq}$ for the System Shown in Fig. 2-12(a)

▲ Im.

Fig. 2-13 Polar Plot of $G(j\omega)$ and $-1/k_{eq}$ for Case II

Case III

Let N be located as in Fig. 2-9(d). In the nonlinear region

$$G_{1eq}(s) = 1$$

$$G_2(s) = \frac{10}{s(s + 1)(s + 3)}$$

$$H_{2eq}(s) = \frac{1}{8}(s^2 + 4s + 8)$$

so that

$$G(s) = \frac{1.25(s^2 + 4s + 8)}{s(s + 3)(s + 1)}$$

Again, it can be seen from the polar plot of Fig. 2-14 that the system is stable for all gain whether it be associated with the nonlinearity or with any other gain in the forward loop.

Comparing all three cases, one can see that as the N is moved towards the left end the number of zeros of $H_{2eq}(s)$ increases, forcing the polar plot of $G(j\omega)$ to approach the origin at a lower multiple of 90° . Finally, when saturation takes place at the left most state variable, $G(j\omega)$ approaches the origin at -90° , and the example system becomes stable for all gain. Still, placing nonlinearity at the left end does not give assurance of stability if the system is conditionally stable in the linear region, as the location of zeros of

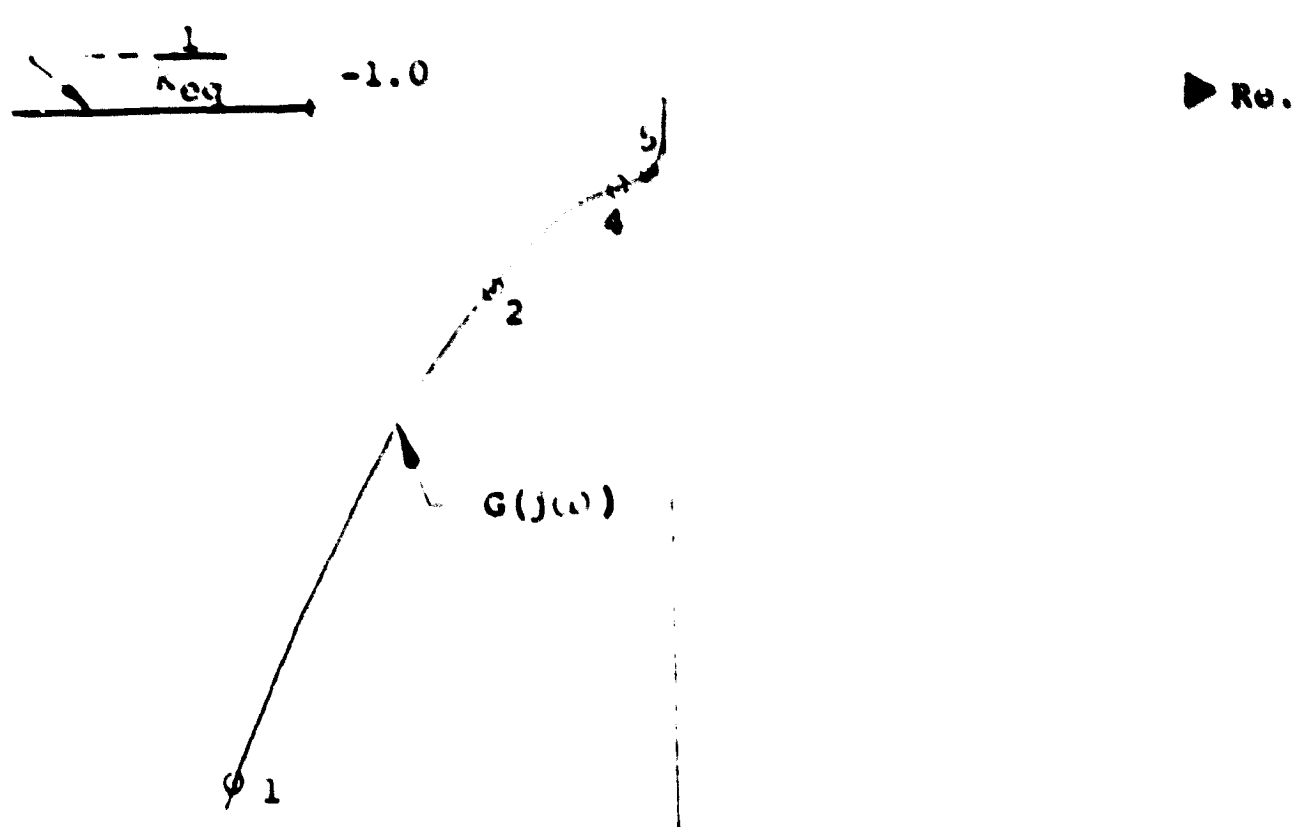


Fig. 2-14 Polar Plot of $G(j\omega)$ and $-1/k_{eq}$ for Case III

$H_{2eq}(s)$ influences the shape of the polar plot of $G(j\omega)$ and hence helps to determine whether or not there are any intersections with the plot of $-\frac{1}{k_{eq}}$.

To assure the absolute stability for all values of gain, a method of designing a system is presented in the next chapter. Thus it can be concluded if N is located at the left end, the number of zeros of $H_{2eq}(s)$ to control the system is at a maximum; and the system can be made stable for all gain by placing these zeros at proper places.

Although the conclusions derived above were discussed for the system having a saturation type nonlinearity, they also hold for any frequency-insensitive, single-valued, and symmetrical nonlinearity, as k_{eq} for such nonlinearity is always real and non-negative.

CHAPTER III

DESIGN OF NONLINEAR GAIN-INSENSITIVE SYSTEMS

In Chapter II it was shown that the stability of systems containing a single nonlinearity and designed by using state variable feedback depends upon the location of both the nonlinearity and the zeros of $H_{2eq}(s)$. In this chapter the same type of system is studied further and a method of making the system gain-insensitive to ensure stability is presented. Systems designed by the proposed method are shown to have absolute stability for any value of gain associated with the linear part of the system or with the nonlinearity.

Next, gain-insensitive and non-gain-insensitive systems having the same closed-loop transfer function in the linear region are compared and significant features of gain-insensitive systems are presented. One can show how the introduction of an additional intentional nonlinearity and state variable feedback can be combined to design systems to have both absolute stability and satisfactory transient response. The technique utilizes the results of Herring (1967), who

has suggested a method of designing systems which are absolutely stable for all values of gain. He has shown that a system can be made absolutely stable and insensitive to gain if $n - 1$ of the n open-loop poles are placed where $n - 1$ of the n closed-loop poles are required. In other words, in terms of Fig. 3-1, the zeros of $H_{eq}(s)$ are placed at the same places where $n - 1$ of the n poles of $G(s)$ are located.

A step-wise procedure for designing a gain-insensitive system is given below.

1. Describe the system in physical variables and assume all the variables are available for control purposes.
2. Choose the desired locations of the n closed-loop poles of Y/R .
3. Modify the plant, or open-loop system, with series or feedback compensation such that $n - 1$ open-loop poles are located at the positions of $n - 1$ of the desired poles of Y/R .
4. Use state variable feedback to force the $n - 1$ zeros of H_{eq} to coincide with $n - 1$ of the new poles of $G(s)$.

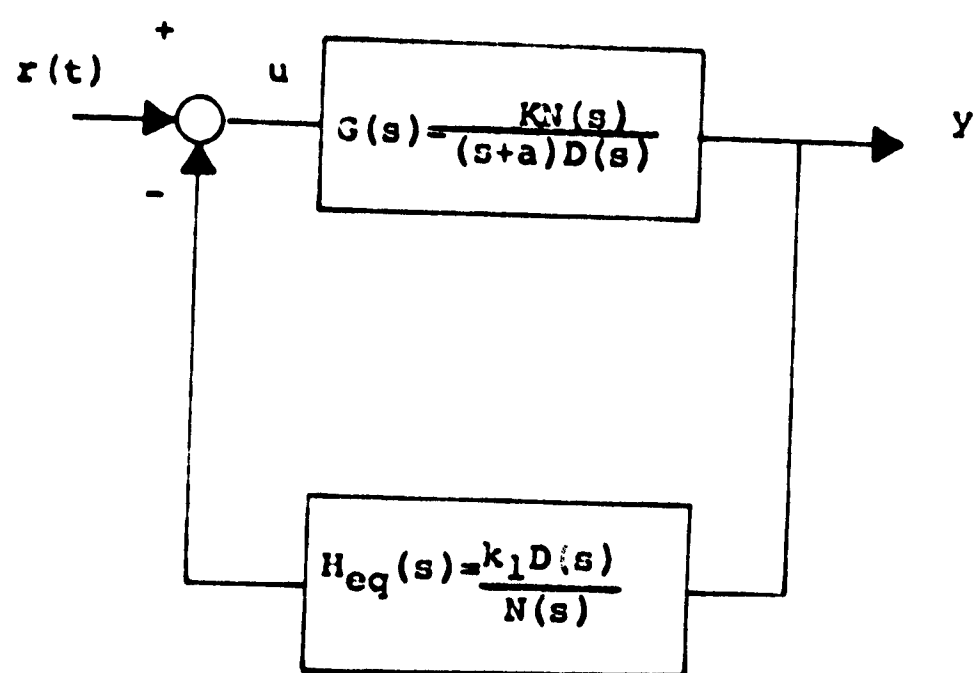
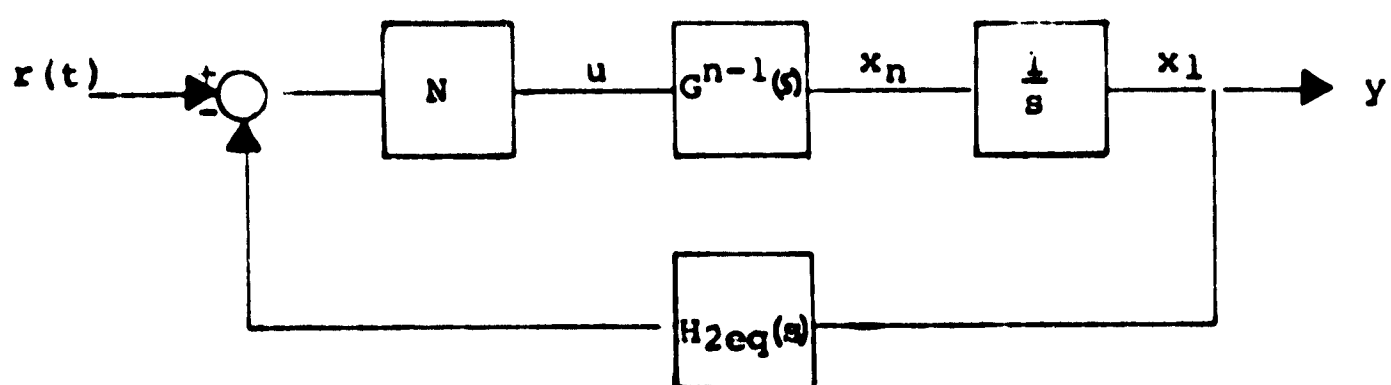


Fig. 3-1 A Linear Gain-Insensitive System,
Where $G(s)H_{eq}(s) = k'/s+a$

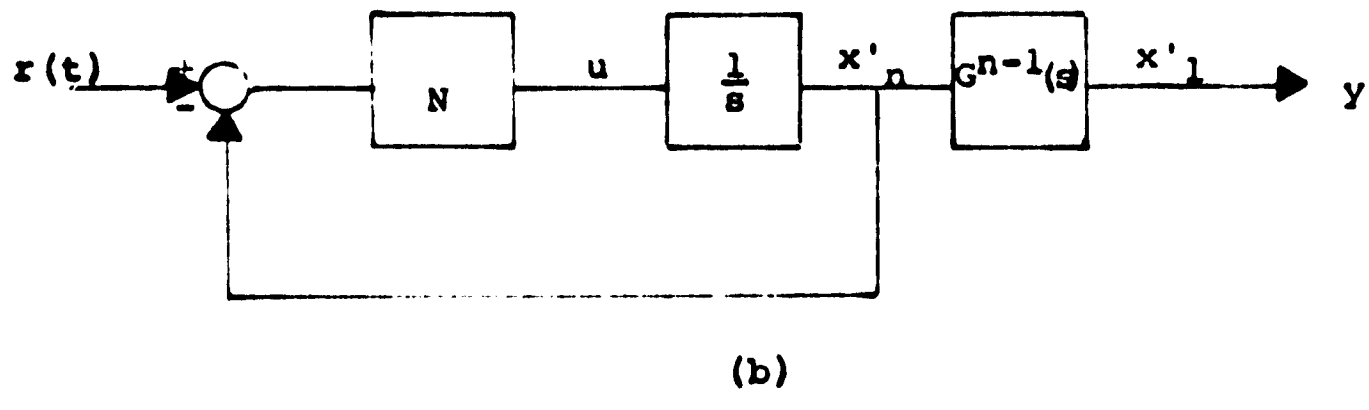
5. If all the variables are not available, use the calculated values of the feedback coefficients to determine the required minor-loop compensation (Schultz and Melsa, 1967).

A system designed by the gain-insensitive method has only 1 out of the n closed-loop poles as a function of gain, whereas a non-gain-insensitive system has all n of its closed-loop poles as a function gain. Thus when the gain varies, the response of the gain-insensitive system is likely to change very little; however, the response of the non-gain-insensitive system can change significantly, and the system may even become unstable. Also, the gain-insensitive system always satisfies the frequency criteria for optimal control as the polar plot for open-loop gain never crosses the unit circle, while the non-gain-insensitive system does not.

Consider a nonlinear system shown in Fig. 3-2(a) where N is of the specific type considered in Chapter II; namely, N is frequency-insensitive, single-valued, and symmetrical. The system is designed such that $n - 1$ zeros of $H_{2eq}(s)$ lie at the same places where $n - 1$ of the n open-loop poles are located. Such a system can be reduced to a simple first-order nonlinear system in series with an $(n - 1)^{\text{st}}$ order system as shown in



(a)



(b)

Fig. 3-2 Nonlinear Gain-Insensitive System and Modified Block Diagram

Fig. 3-2(b). It is easy to analyze such a system by graphical methods such as the like isocline method. The system designed by the non-gain-insensitive method is of n^{th} order and cannot be reduced to any such simple form and hence cannot be analyzed as easily by graphical methods.

Although the gain-insensitive method of designing a system is superior to other techniques in many respects, it is difficult to put the zeros of $H_{2\text{eq}}(s)$ exactly on top of the poles of $G(s)$. If cancellation does not take place, then the system has n poles which vary with the gain, possibly even becoming unstable if the poles are near the $j\omega$ -axis (Herring, 1967).

The results of this and the previous chapter are now used to design a system which saturates at a certain point. It was mentioned previously that all systems saturate; typical physical components having saturating characteristics are an amplifier in the forward loop and the movement of some mechanical part which is restricted to a certain range. In Chapter II it was shown that the saturating element might cause the system to oscillate if it is not located at the proper place within the loop. The locations of such elements are not controllable as they are part of the physical system.

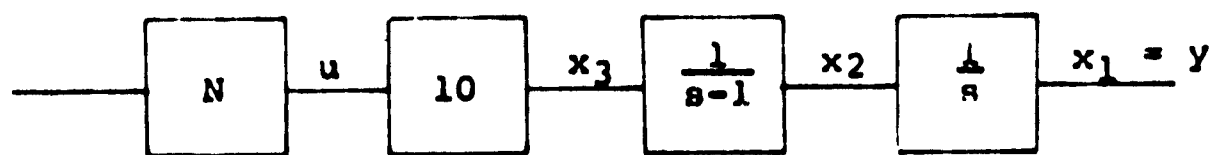
A way to prevent saturation of such an element is to control the input signal to that element; this can be done by introducing an intentional nonlinearity having a limiter type characteristic with the proper limiting values. With the introduction of such an element the system following the nonlinearity always operates in its linear region since the nonlinearity input is always restricted to the range of linear operation for the nonlinearity.

In Chapter II it was shown that if the location of the nonlinear element is at the left most end and state variable feedback is used, there are $n - 1$ zeros of $H_{2eq}(s)$ to control the plant. Thus it can be seen that if a limiter is introduced at the left end and if state variable feedback is used, then saturation in other parts of the system can be prevented and the system can be made stable for all gain, even insensitive to gain.

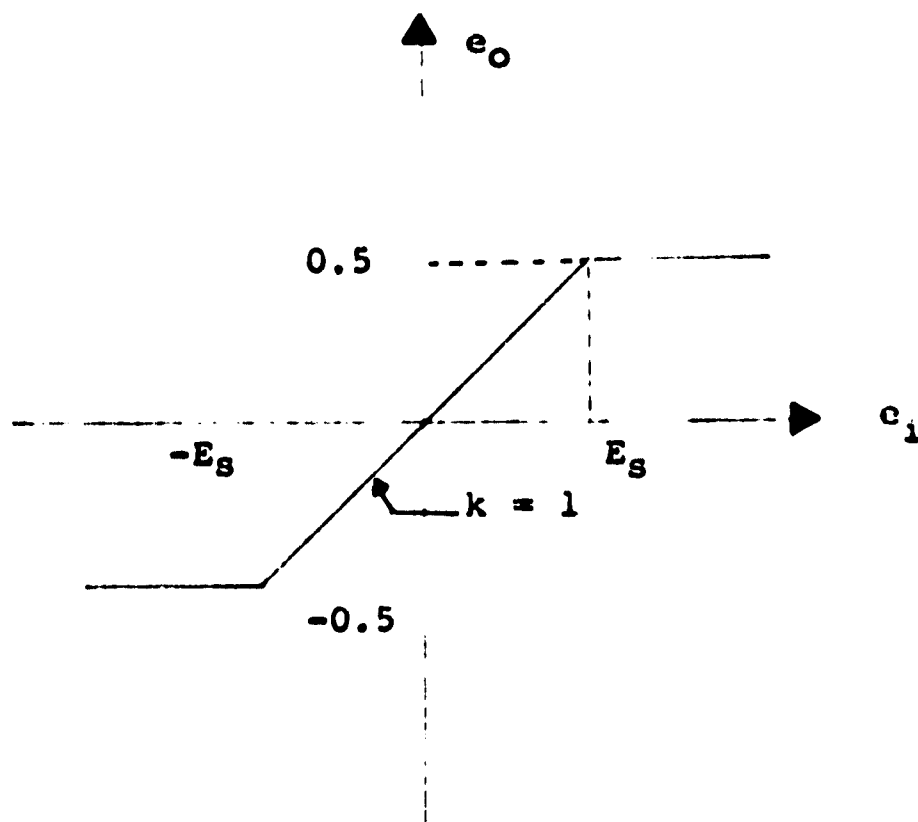
The technique is illustrated in the following example where two methods of designing the same system are presented for comparison.

Example 1

Consider the plant shown in Fig. 3-3(a) and having an intentionally introduced nonlinear element



(a)



(b)

Fig. 3-3 Plant and Characteristic of N for Example 1

of the saturation type whose characteristic is shown in Fig. 3-3(b). When operating in the linear region

$$G_p = \frac{10}{s(s - 1)}$$

and the required closed-loop transfer function is chosen to be

$$\frac{Y}{R}(s) = \frac{10}{(s + 2)(s + 5)}$$

Gain-Insensitive Design

Now feeding back x_2 to modify the plant so that $n - 1$ (1) of the open-loop poles lie at the same place as $(n - 1)$ one of the closed-loop poles, gives the modified open-loop plant, as

$$G(s) = \frac{10}{s - 1 + 10k_2'} \cdot \frac{1}{s}$$

The value of k_2' that places one of the poles of $G(s)$ at the closed-loop pole location $s = -2$ is $k_2' = .3$.

Next, both x_1 and x_2 are fed back from the modified $G(s)$ to realize the desired closed-loop transfer function when operating in the linear region. By block diagram manipulation

$$\frac{Y}{R} = \frac{10}{s^2 + 2s + 10(k_2s + k_1)}$$

Equating the denominators of the required and the designed closed-loop transfer functions, k_1 and k_2 are found to be $k_1 = 1.0$ and $k_2 = 0.5$.

Non-Gain-Insensitive Design

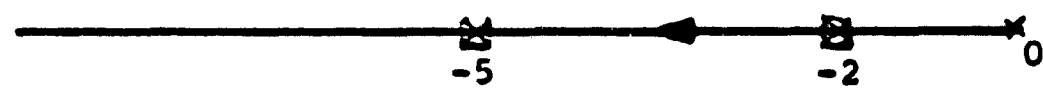
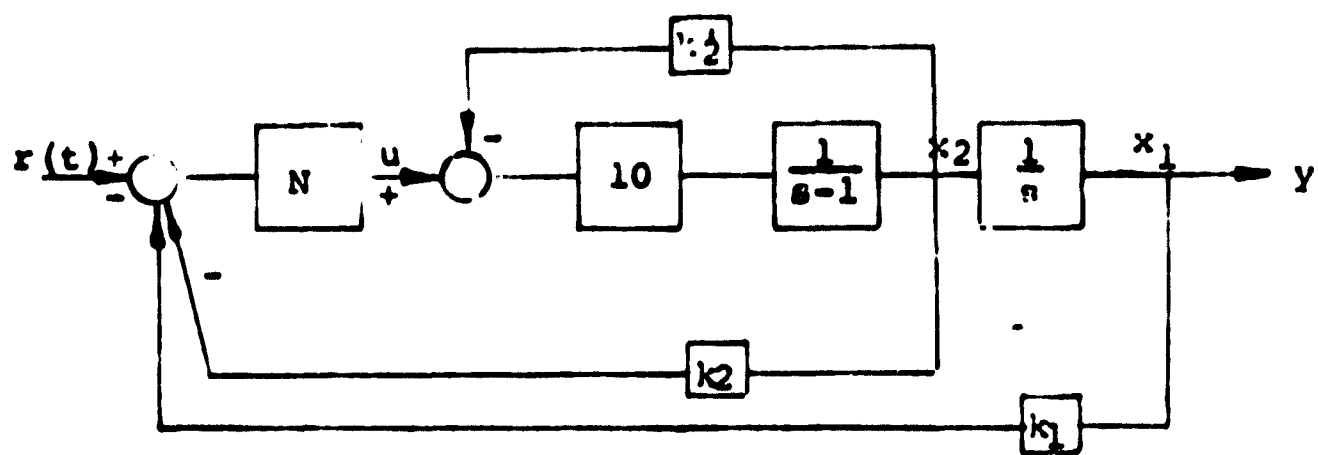
Here both x_1 and x_2 are fed back directly from $G_p(s)$. Block diagram manipulation yields

$$\frac{Y}{R} = \frac{10}{s^2 - s + 10(k_2 s + k_1)}$$

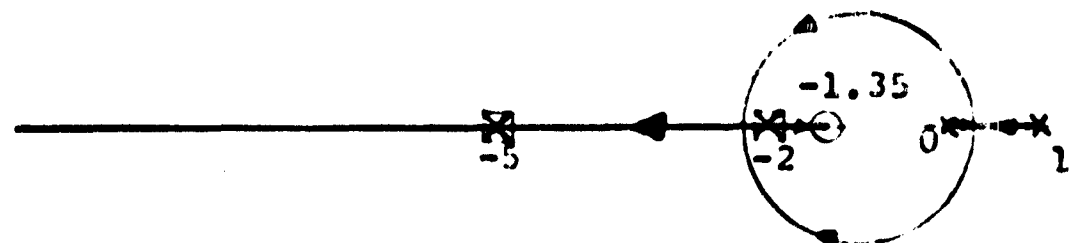
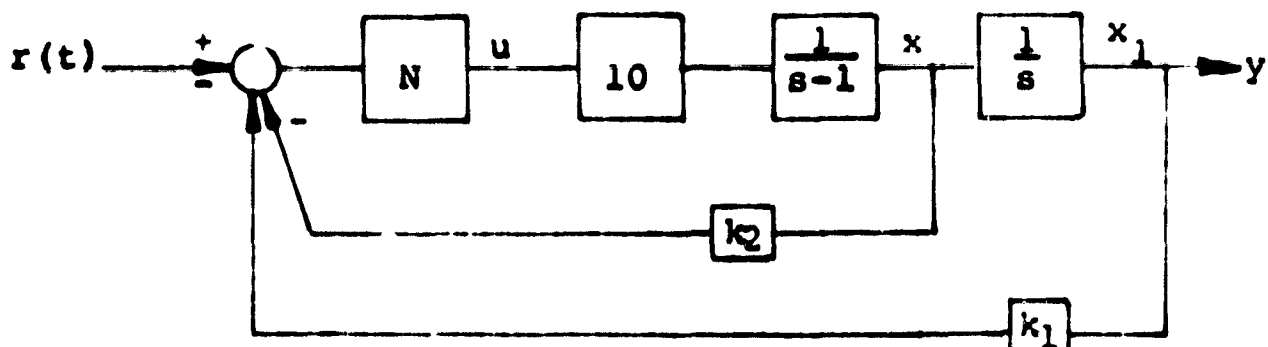
Comparing the denominator of the required and designed expression for Y/R , k_1 and k_2 are found to be $k_1 = 1.0$, $k_2 = 0.800$.

Both systems are shown with their root locus in the linear region of operation in Fig. 3-4(a) and 3-4(b). Both systems were simulated on an analog computer, and the step responses are presented in Fig. 3-5(a) and 3-5(b), respectively. It can be seen that for a step input, in the linear region of operation, both systems respond in the same way. However, when the input is increased so that the systems operate in nonlinear region of N, the non-gain-insensitive system gives an overshoot while the other system does not; in fact, the response of the gain-insensitive system does not differ very much from its response in the linear region.

The behavior of the non-gain-insensitive system in the nonlinear region can be explained as follows. Consider the characteristic of a general saturation type nonlinearity shown in Fig. 3-6. e_1 is the input to the nonlinearity, e_0 represents the output, and k is

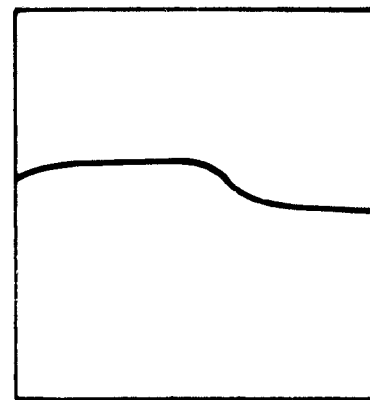
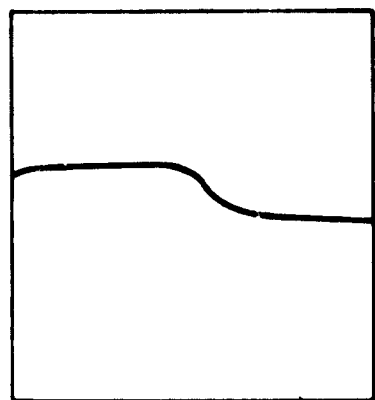


(a)

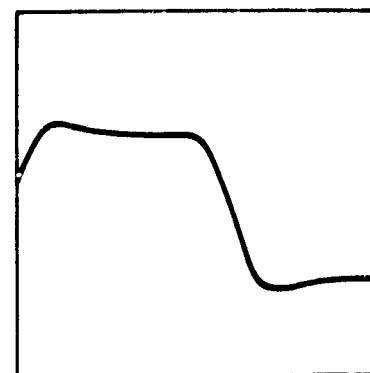
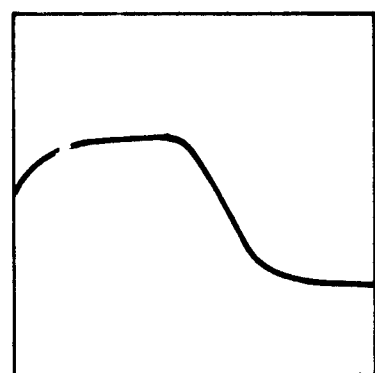


(i)

Fig. 3-4 Gain-Insensitive and Non-Gain-Insensitive Systems with Their Root Locus Sketch in the Linear Region



Operation in the Linear Region

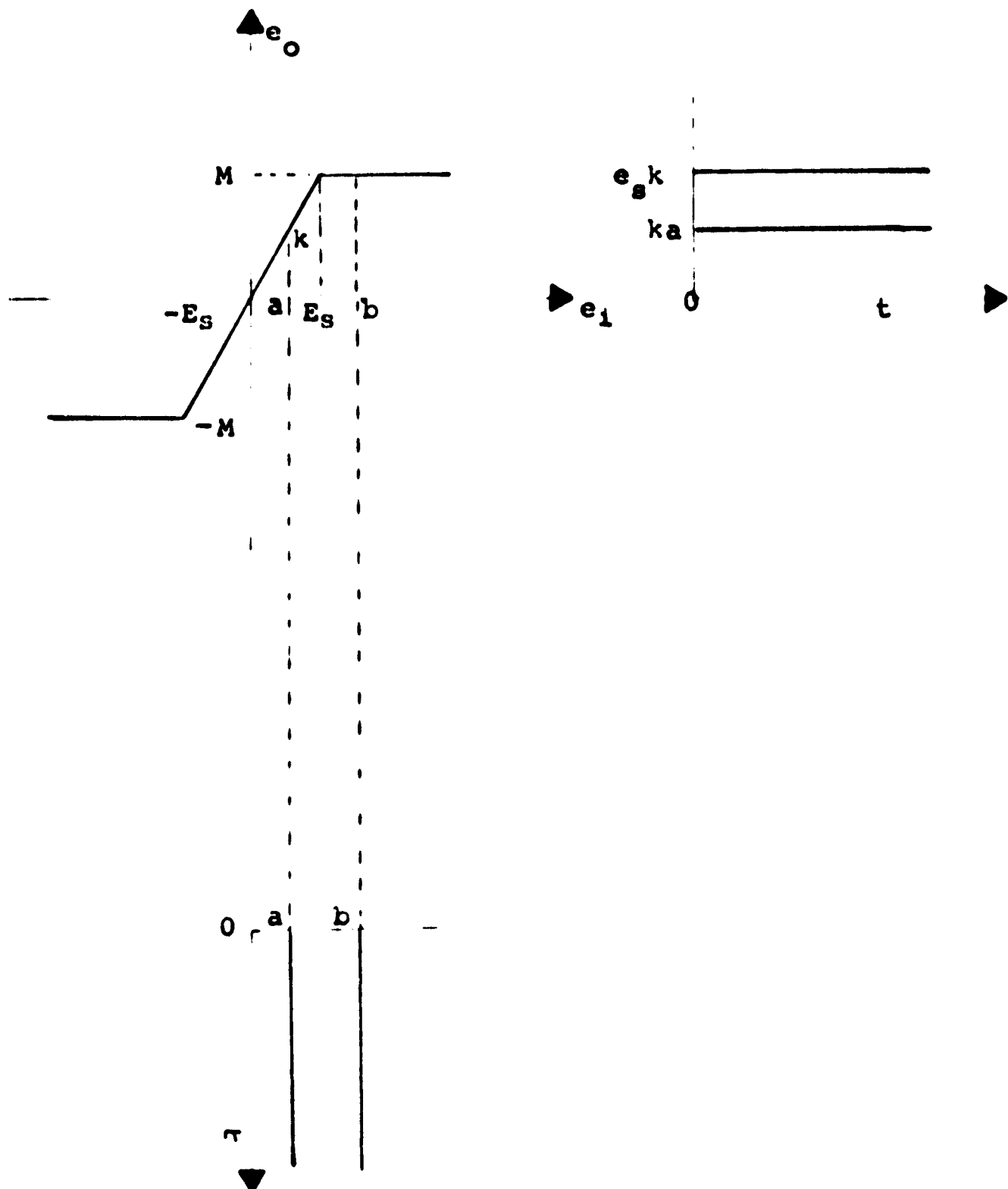


Operation in the Nonlinear Region

(a)

(b)

Fig 3-5 Time Response for the System of Example 1



$$k' = \frac{\text{Output}}{\text{Input}}$$

Fig. 5-6 Explains the Decrease in k' When N Operates in the Nonlinear Region

the gain in the linear region of operation. When the input has a magnitude less than e_s , the output is k times the input and the equivalent gain is

$$k' = \frac{\text{output}}{\text{input}} = k$$

When $|e_i| > e_s$, the output is $\pm e_s k$ and k' becomes

$$k' = \frac{\pm e_s k}{\text{input}} < k$$

Thus it can be seen that as the input amplitude increases k_{eq}' decreases. In Example 1 when the input amplitude is increased, so that the input to N is greater than $e_s = 0.5$, k' decreases and hence the total gain in the loop decreases, causing the n poles of non-gain-insensitive system to assume a different configuration. The new closed-loop configuration can be a pair of complex conjugate poles (see root locus sketch Fig. 3-5(b)), which causes overshoot in the output of the system.

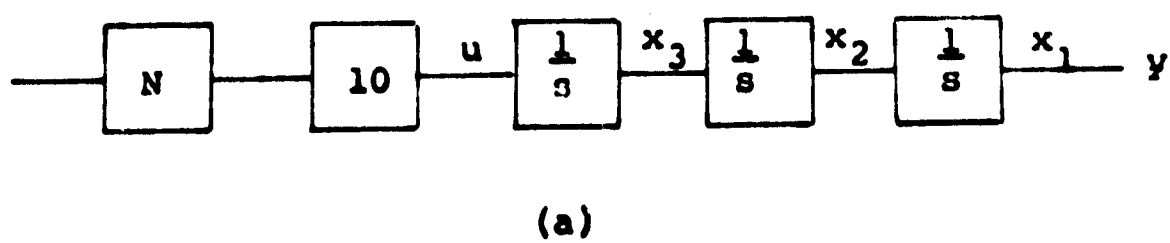
Example 2

Consider the plant shown in Fig. 3-7(a). The nonlinearity N is of the saturation type as shown in Fig. 3-7(b). In the linear region

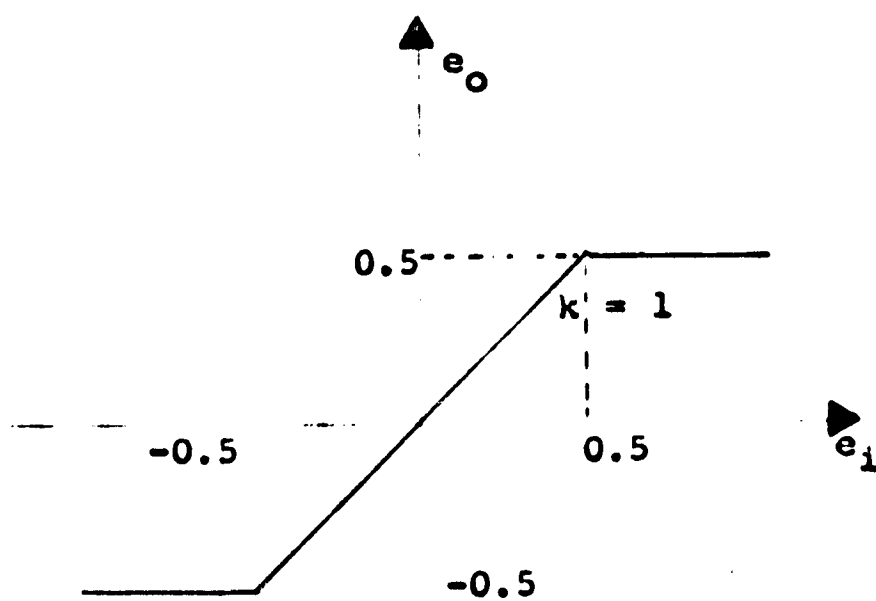
$$G_p = \frac{1}{s^3}$$

and the desired closed-loop transfer function is chosen to be

$$\frac{Y(s)}{R(s)} = \frac{10}{(s + 10)(s^2 + s + 1)}$$



(a)



(b)

Fig. 3-7 Plant and Characteristic of N for Example 2

Two designs, gain-insensitive and non-gain-insensitive, are shown with their root locus plots for linear operation in Fig. 3-8(a) and (b), respectively. In the linear region both systems respond in the same way, but when operating in the nonlinear region, as the step-input amplitude is increased, the non-gain-insensitive system gives more and more overshoot and finally becomes unstable. This does not happen with the gain-insensitive system. The above phenomenon can again be explained by the same reasoning given in the previous example and also can be seen from the root locus diagram.

Example 3

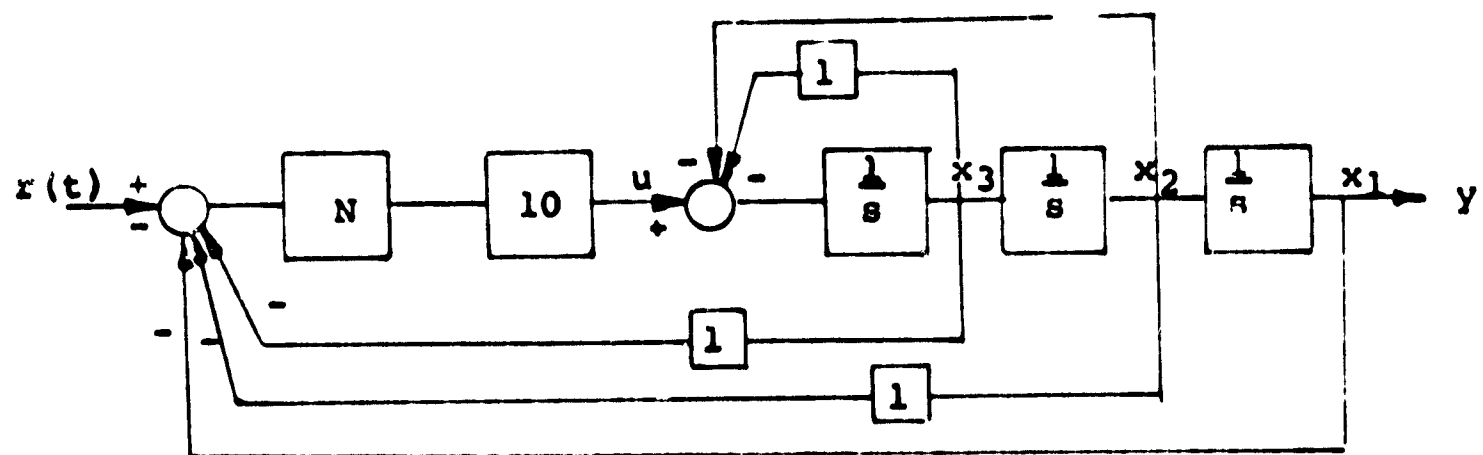
The last example has the plant shown in Fig. 3-9(a) and the nonlinearity shown in Fig. 3-9(b). In the linear region

$$G_p(s) = \frac{20}{(s^2 + 0.2s + 1)s}$$

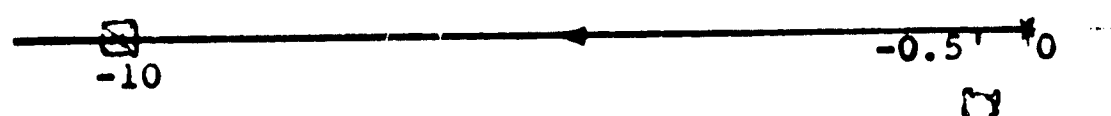
and the desired closed-loop transfer function is

$$\frac{Y(s)}{R(s)} = \frac{20}{(s + 10)(s^2 + 0.4s + 2)}$$

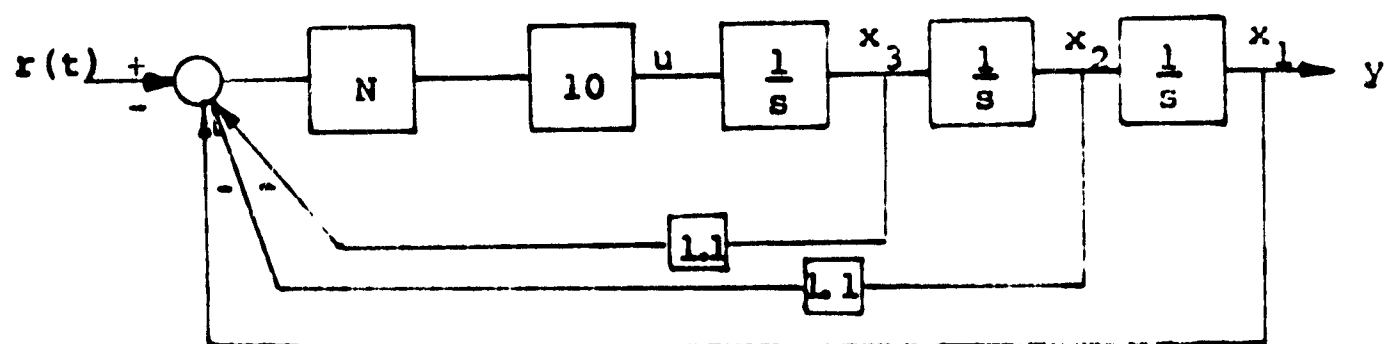
Gain-insensitive and non-gain-insensitive designs are shown in Fig. 3-10(a) and 3-10(b) along with their root locus diagrams for linear operation. Both systems were simulated on the analog computer and the response to a step input is presented in Fig. 3-11(a) and 3-11(b).



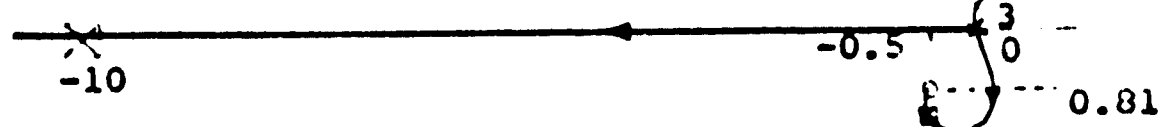
$\bullet \dots \dots 0.866$



(a)

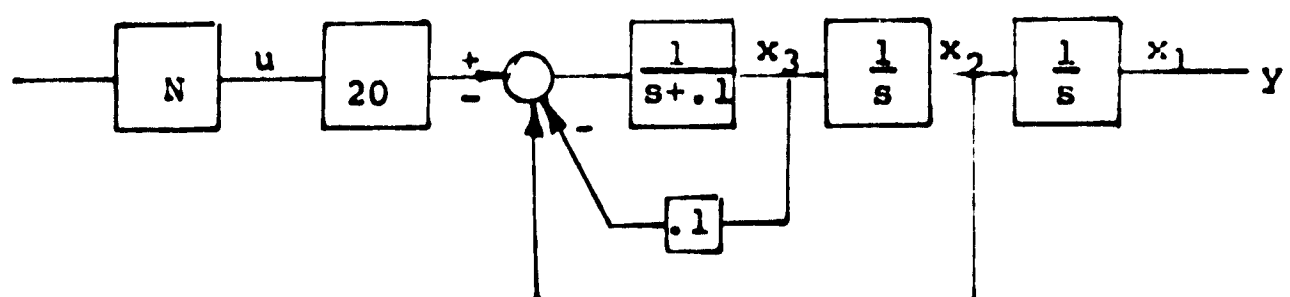


$\bullet \dots \dots 0.866$

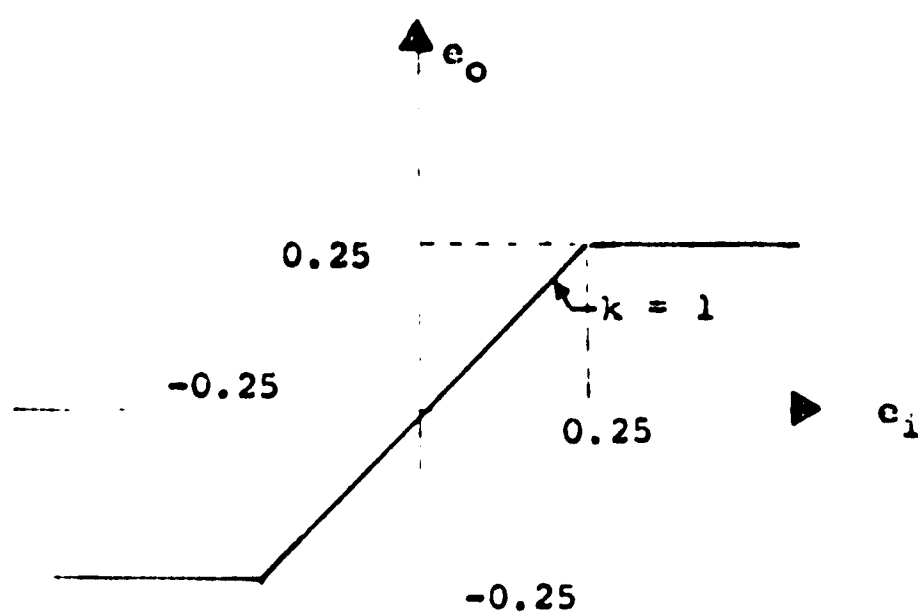


(b)

Fig. 3-8 Gain-Insensitive and Non-Gain-Insensitive Systems Along with Their Root Locus Sketch in the Linear Region

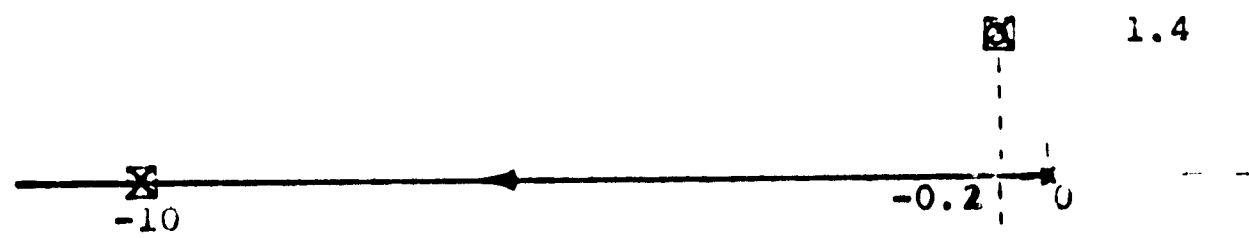
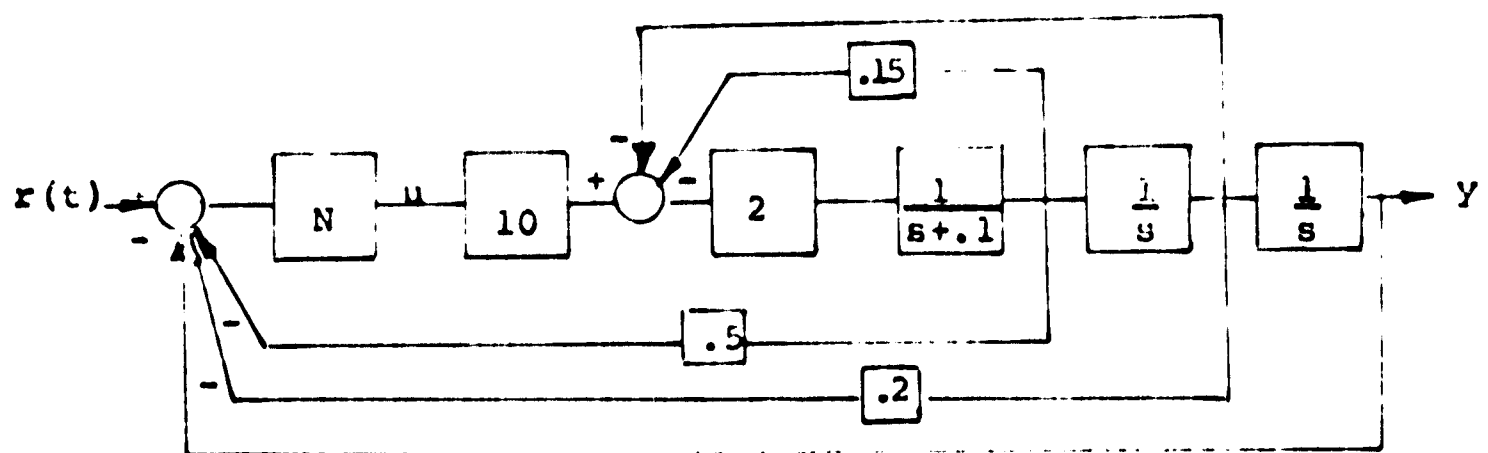


(a)

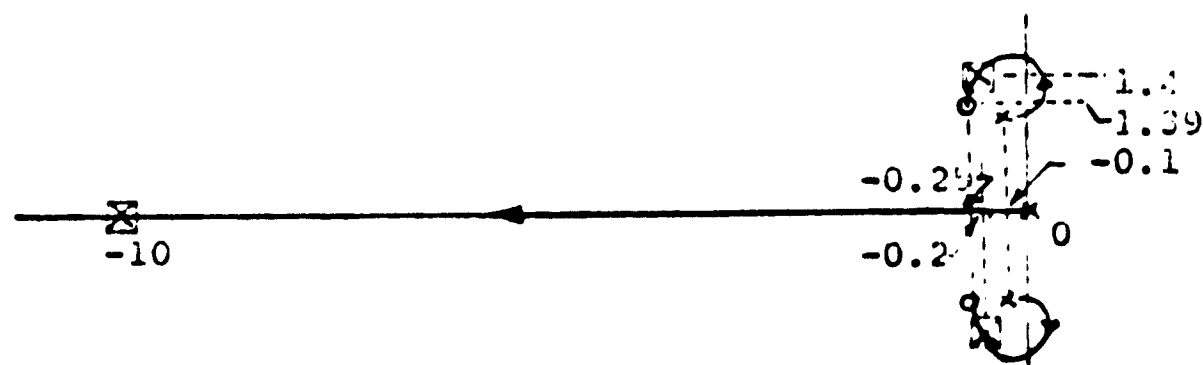
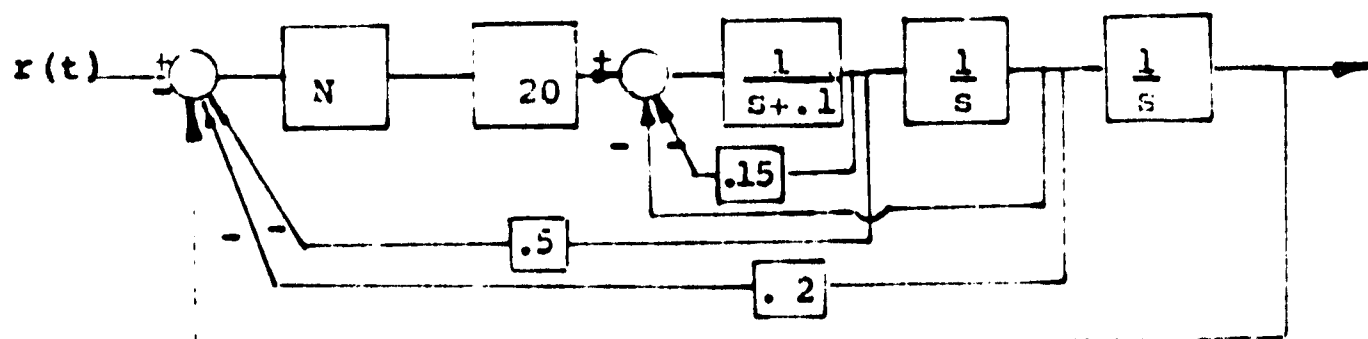


(b)

Fig. 3-9 Plant and Characteristic of N for Example 3

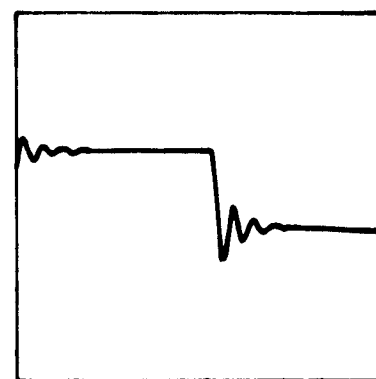
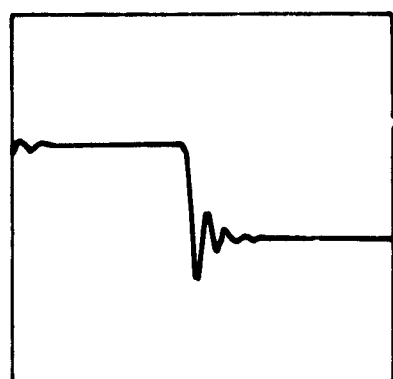


(a)

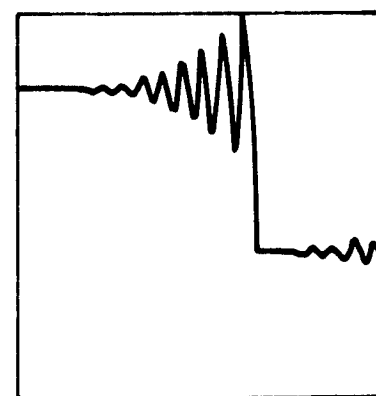
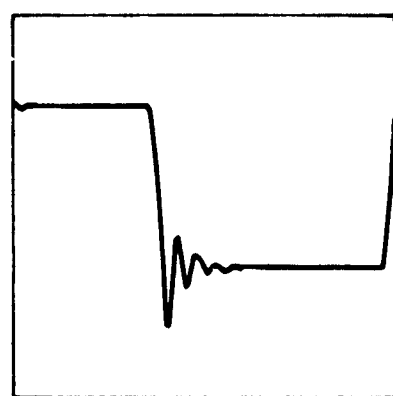


(b)

Fig. 3-10 Gain and Non-Gain-Insensitive Systems Along With Their Root Locus Sketch in the Linear Region



Operation in the Linear Region



Operation in the Nonlinear Region

(a)

(b)

Fig 3-11 Time Response for the System of Example 3

When operating in the linear region, the response to a step input is the same for both systems. When the input is increased so that the systems operate in the region in which the nonlinearity is saturated, the results show that the non-gain-insensitive system gives more overshoot than when operating in the linear region and that the transient takes a relatively long time to die down. Also, when the magnitude of the input step to the system is increased more and more, a point is reached where there are sustained oscillations; these oscillations die down when the input magnitude is further increased. If the input amplitude is further increased, it again gives sustained oscillations as can be seen from Fig. 3-12. As in the previous examples, the response of the gain-insensitive system does not differ much from the linear response when operating in the nonlinear region.

From the above three examples, it can be seen that for the same closed-loop transfer function in the linear region, the system designed by the gain-insensitive method is absolutely stable and almost insensitive to gain; its response is good even when operating in the saturated region. For the system designed by the non-gain-insensitive method there is more overshoot and

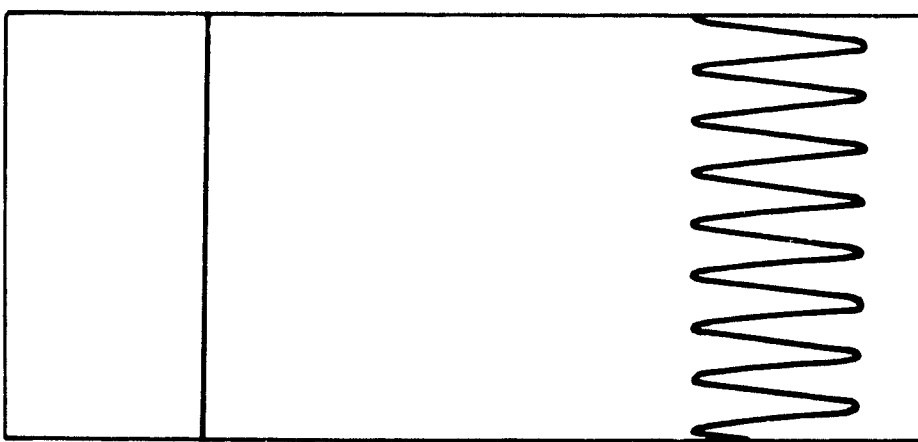
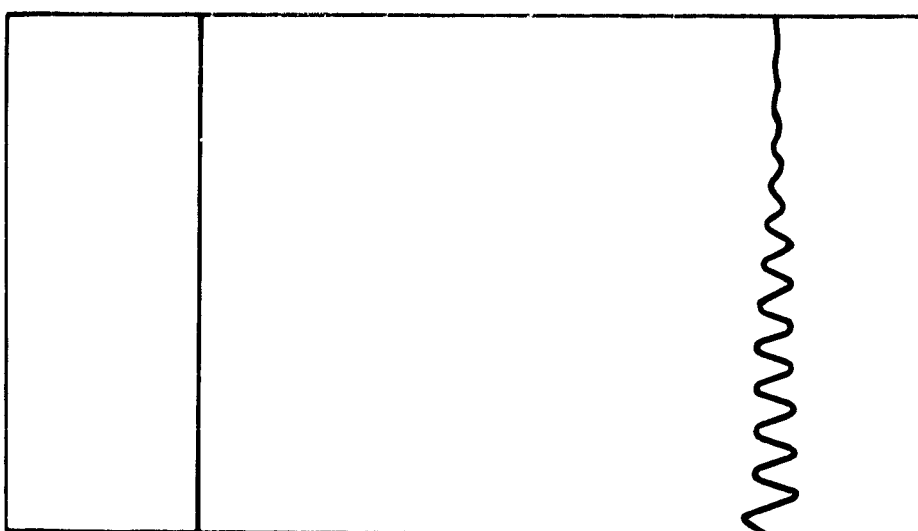
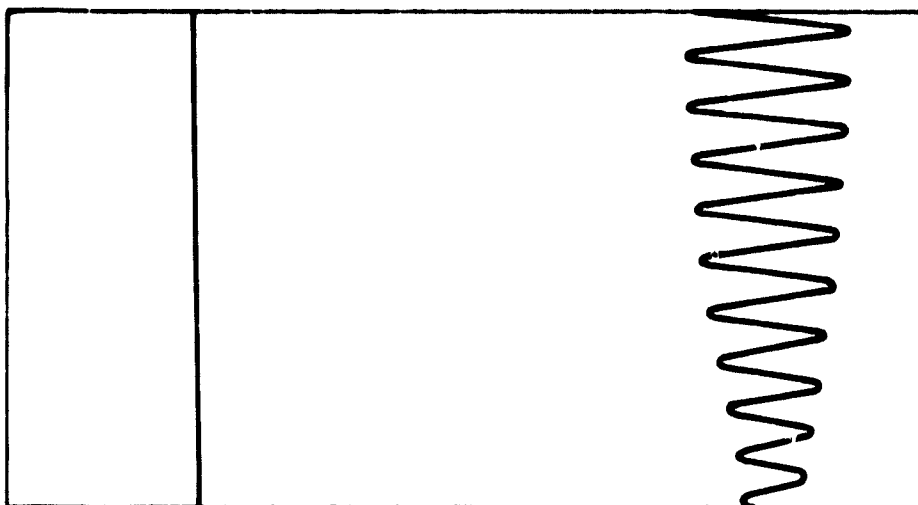


Fig. 3-12 Time Response Showing Oscillations
for Example 3

sustained oscillations if the plant is unstable or conditionally stable. Thus from the above observations it can be seen that the system stabilized by introducing an intentional nonlinearity and designed by the gain-insensitive method gives a more satisfactory performance although it increases the complexity of the system.

In the next chapter the gain-insensitive design technique is applied to a practical, high-order design problem.

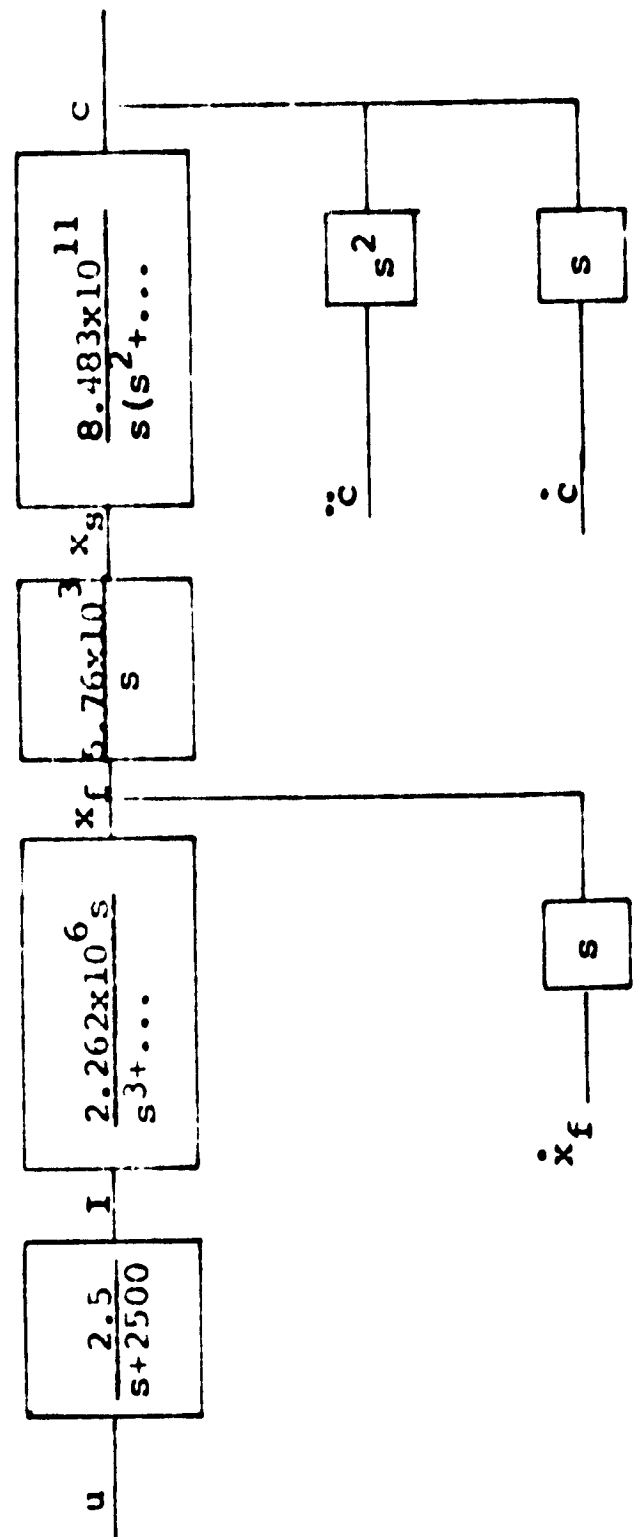
CHAPTER IV

DESIGN OF A FUEL VALVE SERVOMECHANISM

In this chapter the results of the previous two chapters (that is, an intentional nonlinearity can be introduced at the left end of the plant to prevent saturation of signals further down in the system, and using state variable feedback a system can be made absolutely stable and insensitive to gain) are applied to improve the performance of a fuel valve servomechanism for a General Electric J-85 jet engine. The engine is being used at Lewis Research Center, a NASA facility, for studying engine and inlet controls for the supersonic transport.

In order to apply the design technique it is necessary to start with a linear model of the physical system. Fig. 4-1 shows the block diagram of the 7th order linearized plant where the state variables are

- c Actuator position
- \dot{c} Actuator velocity
- \ddot{c} Actuator acceleration
- x_s Spool valve displacement
- x_f Flapper valve displacement



Third-Order Polynomial: $s^3 + 3.66937 \times 10^3 s^2 + 2.1038 \times 10^7 s + 1.7617 \times 10^{10}$

$$\text{Second-Order Polynomial: } s^2 + 6.6831 \times 10^3 s + 3.28 \times 10^8$$

Fig. 4-1 Linearized Plant of Physical System

\dot{x}_f Flapper valve velocity

I Torque motor current

Let $c = x_1$, $\dot{x}_1 = x_2$, $\dot{x}_2 = x_3$, $x_s = x_4$, $x_f = x_5$, $\dot{x}_5 = x_6$, and $I = x_7$. Then the plant can be described by 7 first-order differential equations as shown in the Appendix and can be represented by equations (Ab) and (c)

$$\dot{x} = Ax + bu \quad (\text{Ab})$$

$$y = \underline{\omega}^T x \quad (\text{c})$$

where

$$A = \begin{bmatrix} 0 & 1 & 0 & 0 & 0 & 0 & 0 \\ 0 & 0 & 1 & 0 & 0 & 0 & 0 \\ 0 & -3.28 \times 10^8 & -6.68 \times 10^3 & 8.48 \times 10^{11} & 0 & 0 & 0 \\ 0 & 0 & 0 & 0 & 5.76 \times 10^3 & 0 & 0 \\ 0 & 0 & 0 & 0 & 0 & 1 & 0 \\ 0 & 0 & 0 & -3.05 \times 10^6 & -2.10 \times 10^7 & -3.66 \times 10^3 & 2.26 \times 10^6 \\ 0 & 0 & 0 & 0 & 0 & 0 & -2.5 \times 10^3 \end{bmatrix}$$

$$b^T = [0 \quad 0 \quad 0 \quad 0 \quad 0 \quad 0 \quad 2.5 \times 10^0]$$

$$\underline{\omega}^T = [1 \quad 0 \quad 0 \quad 0 \quad 0 \quad 0 \quad 0]$$

In the actual physical system the signals x_f , x_s , and c are limited to magnitudes less than 0.0012 inches, 0.015 inches, and 0.125 inches, respectively.

There have been at least two previous compensation schemes to improve the performance of this control system,

both of which utilized the above linear model. One scheme was to use conventional lead-lag compensation; the resulting system had a bandwidth of 220 hertz and a step response with an overshoot of 10% for small size step inputs. For input amplitudes of over 10% full scale the effects of the saturation limits caused an unsatisfactory deterioration of the response.

The second scheme utilized state variable feedback and sought to achieve a much faster response than that resulting from the lead-lag compensation. The resulting design required feedback from 5 of the 7 state variables and had a bandwidth of 700 hertz and an overshoot of less than 10% in the step response. Unfortunately, when the saturation limits on the system variables were introduced, for disturbances of any reasonable magnitude the system per cent overshoot in the transient response was excessive; and the system bandwidth decreased to approximately 100 hertz (Slivinsky, Dellner, Aparasi, 1967).

In this chapter the linearized system is first designed by the gain-insensitive method for a bandwidth of about 350 hertz and an overshoot less than 10%. Then an intentional nonlinearity of the saturation type is introduced whose saturating limits are found experimentally

on an analog computer so that the signals at x_f , x_g , and the output do not saturate when the full-scale input is applied.

Design of Gain-Insensitive System

The gain-insensitive design is carried out in three steps: selecting the desired closed-loop transfer function, modifying the plant so that 6 of the 7 closed-loop poles are achieved, and finding the feedback coefficients so that the closed-loop transfer function is realized.

As an aid in carrying out the first step one can refer to the pole-zero configuration for the original plant as shown in Fig. 4-2. Studying this plot and the normalized step-and frequency-response curves satisfying the ITAE performance index (integral of time multiplied absolute error, Graham and Lathrop, 1955) a second-order model is chosen with $\omega_n = 2250$ radians/second and $\zeta = 0.7$ to realize a bandwidth of about 350 hertz and an overshoot of less than 10%. Thus the second-order model has the transfer function

$$\left(\frac{Y}{R}\right)_{\text{model}} = \frac{5.0625 \times 10^6}{s^2 + 3.15 \times 10^3 s + 5.0625 \times 10^6} \quad (4-1)$$

The model is extended to the seventh order by choosing 2 of the seven poles to be located as in

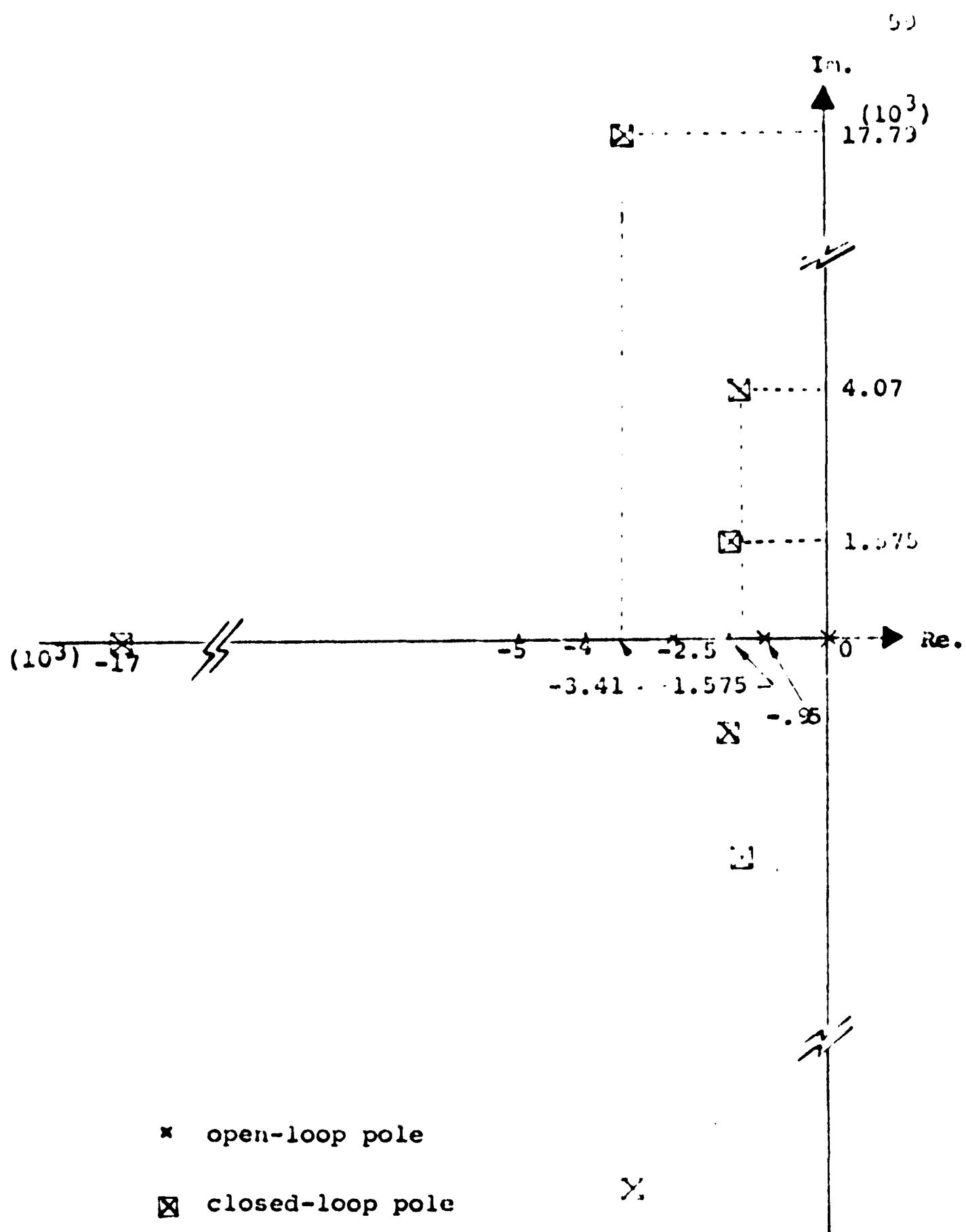


Fig. 4-2 Open-Loop and Closed-Loop Pole Location for the Linear System

Equation 4-1, 1 at the location $s = -1.7 \times 10^4$, and the remaining 4 at the same positions as the complex conjugate poles of the fixed plant. The resulting configuration is shown in Fig. 4-2, and the closed-loop transfer function is given by

$$\frac{Y}{R}_{\text{extended}} = \frac{5.0995 \times 10^{26}}{(s+3.34149 \times 10^3 + j1.77998 \times 10^4) \cdot \frac{(s+1.3556 \times 10^3 + j4.07384 \times 10^3)}{(s+1.575 \times 10^3 + j1.575 \times 10^3)(s+1.7 \times 10^4)}} \quad (4-2)$$

Note that Y/R approaches 1 as s approaches 0 so that that system has 0 steady-state error for step inputs.

The extended model was checked for time response and frequency response, and it was found that the results were almost the same as for the simple second-order system; i.e., the bandwidth was 350 hertz, and the overshoot was 8.4% with a rise time of about .0011 seconds.

To carry out the second step it is necessary to put $n - 1$ (6) of the open-loop poles where 6 of the closed-loop poles are located. The plant is modified such that the new open-loop transfer function is

$$G(s) = \frac{2.997 \times 10^{24}}{s(s+3.34149 \times 10^3 + j1.77998 \times 10^4) \cdot \frac{(s+1.3556 \times 10^3 + j4.07384 \times 10^3)(s+1.575 \times 10^3 + j1.575 \times 10^3)}{(s+1.575 \times 10^3 + j1.575 \times 10^3)}} \quad (4-3)$$

This is done by feeding back the state variables x_2 through x_7 as shown in Fig. 4-3. With the help of the IBM 7072 digital computer, using the program of Melsa (1967) and the \underline{A} , \underline{B} , and \underline{C} matrices given above with the slight modification given in the Appendix, the coefficients were found to be

$$k_2' = -4.6774 \times 10^{-5}$$

$$k_3' = -1.7077 \times 10^{-9}$$

$$k_4' = 1.57057 \times 10^1$$

$$k_5' = 1.272 \times 10^1$$

$$k_6' = 4.66671 \times 10^{-3}$$

$$k_7' = -1.13557$$

and the gain k is 1.0839.

Now the modified plant is used in feeding back the variables x_1 through x_7 to realize the closed-loop transfer function given in Equation 4-2. The system is as shown in Fig. 4-4. Again, Melsa's program was used to perform the calculations, this time with the \underline{A} , \underline{B} , and \underline{C} matrices corresponding to the modified plant. These matrices are given below, and the details of the derivation of the differential equations can be found in the Appendix.

$$\underline{L}^T = \begin{bmatrix} 0 & 0 & 0 & 0 & 0 & 0 & 2.70982 \times 10^2 \end{bmatrix}^T$$

$$\underline{C}^T = \begin{bmatrix} 1 & 0 & 0 & 0 & 0 & 0 & 0 \end{bmatrix}^T$$

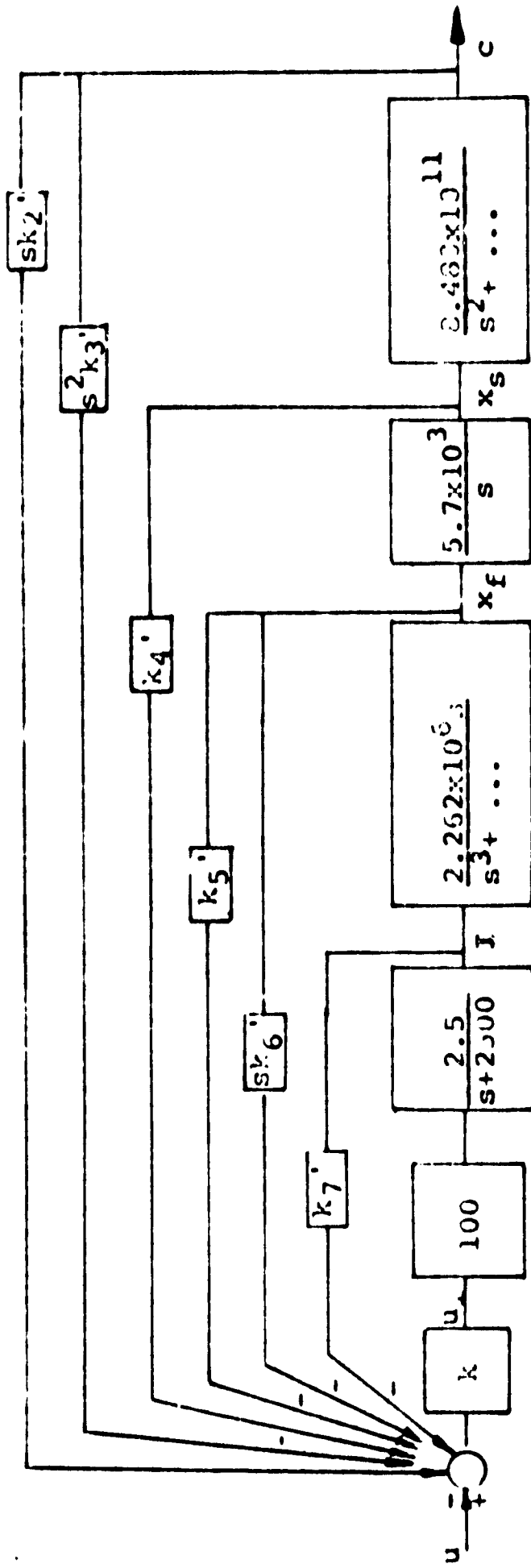


Fig. 4-3 Modification of Plant by Feeding Back Variables x_2 Through x_7

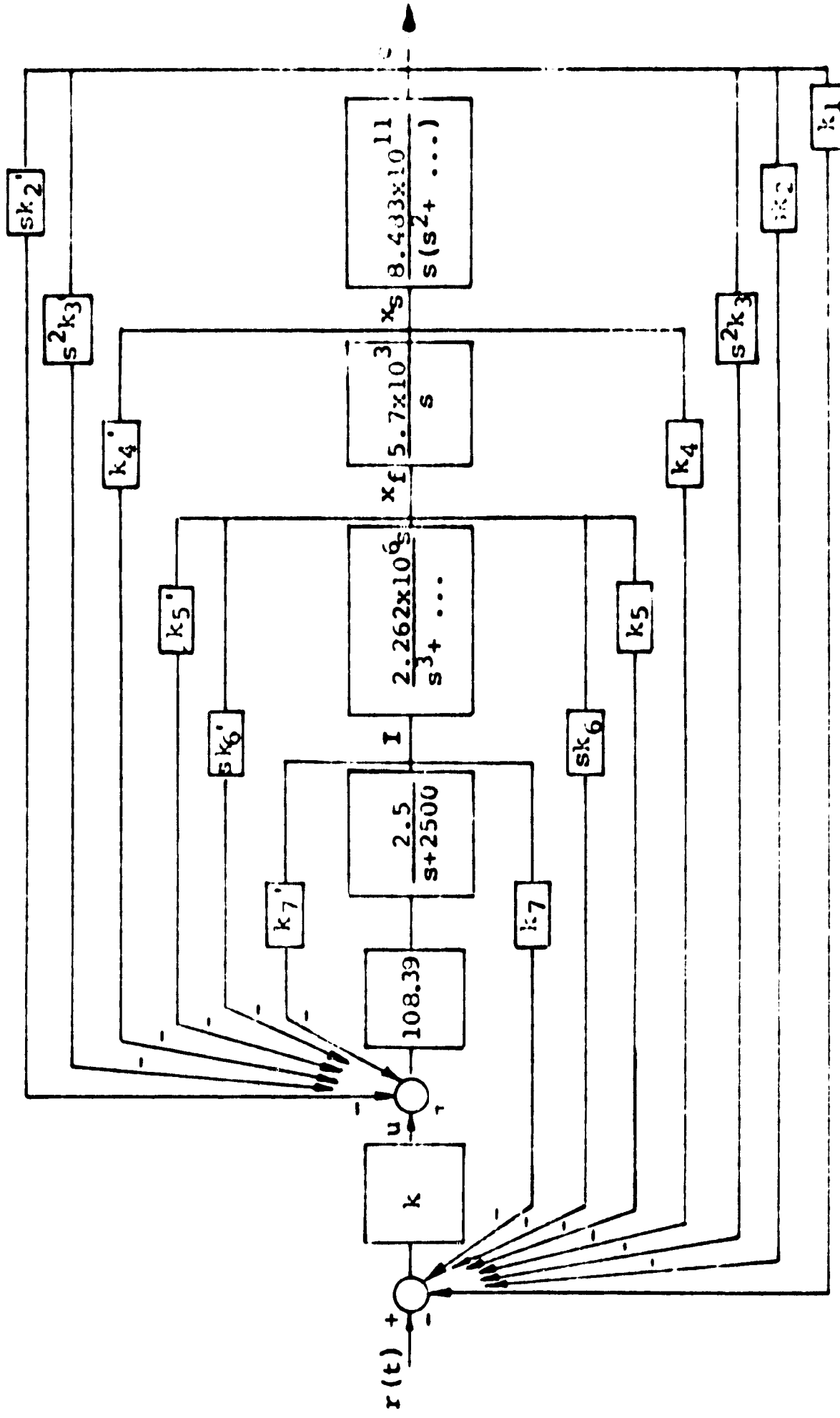


Fig. 4-1 Realization of Closed-Loop Transfer Function
by Feeding Back Variables x_1 Through x_7

$$A = \begin{bmatrix} 0 & 1 & 0 & 0 & 0 & 0 & 0 \\ 0 & 0 & 1 & 0 & 0 & 0 & 0 \\ 0 & 0 & -3.28 \times 10^8 & -6.68 \times 10^3 & -8.48 \times 10^{11} & 0 & 0 \\ 0 & 0 & 0 & 0 & 5.76 \times 10^3 & 0 & 0 \\ 0 & 0 & 0 & 0 & 0 & 1 & 0 \\ 0 & 0 & 0 & -3.05 \times 10^6 & -2.10 \times 10^7 & -3.66 \times 10^3 & 2.26 \times 10^6 \\ 0 & 1.36 \times 10^{-2} & 4.62 \times 10^{-7} & -4.08 \times 10^3 & -3.44 \times 10^3 & -1.20 & 12.19 \times 10^3 \end{bmatrix}$$

The feedback coefficients for this second application of state variable feedback are given by

$$k_1 = 1.000$$

$$k_2 = 2.03317 \times 10^{-5}$$

$$k_3 = 3.06212 \times 10^{-9}$$

$$k_4 = 1.5242$$

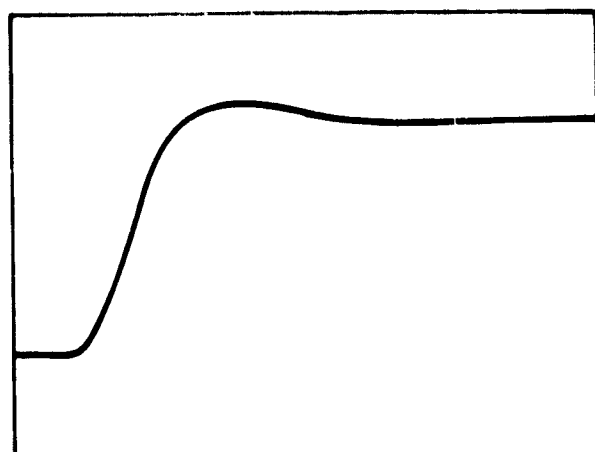
$$k_5 = 1.77896$$

$$k_6 = 3.57654 \times 10^{-4}$$

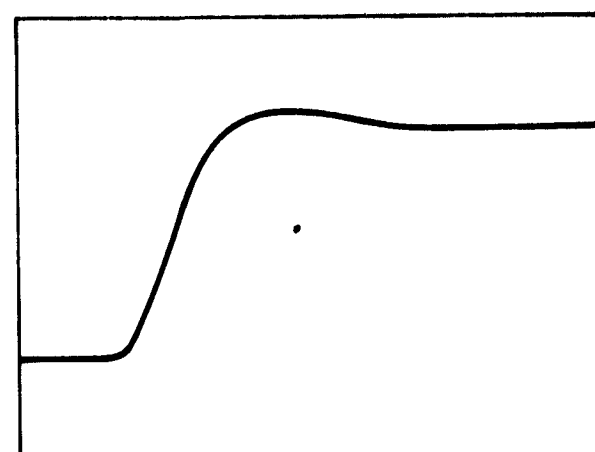
$$k_7 = 3.690275 \times 10^{-1}$$

and the gain is 1.7×10^2 .

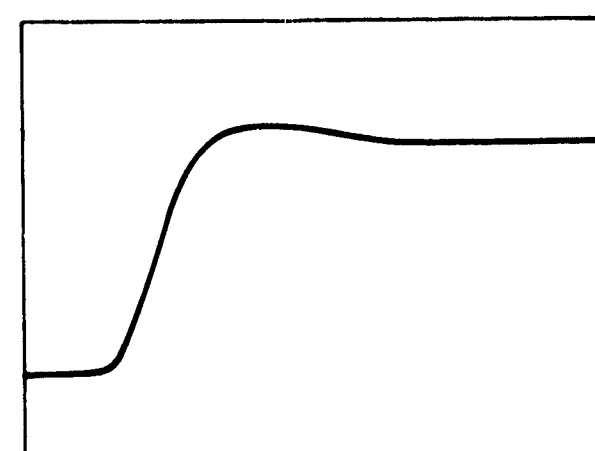
The system was simulated on an analog computer (the details of the simulation are given in the Appendix), and the time response for a step of 5 volts is given in Fig. 4-5(a) showing an overshoot of about 8.2% and a rise time of 0.00115 seconds. The feedback coefficients from different states were removed individually, and it was found that the removal of the two feedback signals from both 'c' and 'd' does not effect



(a)



(b)



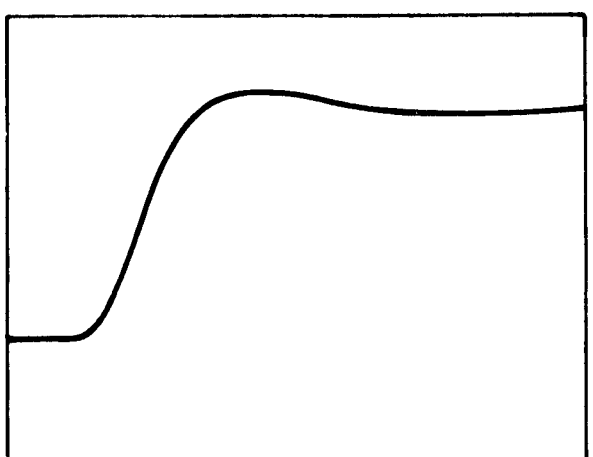
(c)

Fig 4-5 Time Responses of the 7th Order
Linear Gain-Insensitive System

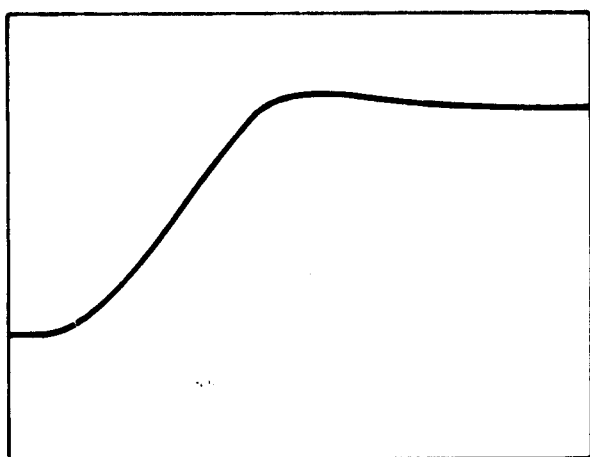
the system response very much as can be seen from Fig. 4-5(b). To check the property of gain-insensitivity the gain was varied from 100 to 250, and it was found that the effect is negligible as can be seen from Fig. 4-5(c). Thus we can conclude that the system is gain-insensitive, with a bandwidth of 350 hertz, an overshoot of 8.2% with a rise time of .00115 seconds and is unaffected by removing the feedback from c and \dot{c} .

In a more realistic model of the system saturation at x_s , x_f , and c must be taken into account. Here the technique of Chapters II and III is used, and an intentional nonlinearity of the saturation type is introduced, whose saturating limits were found experimentally to be ± 0.595 volts so that the signals at x_f and x_s never exceed their saturation limits.

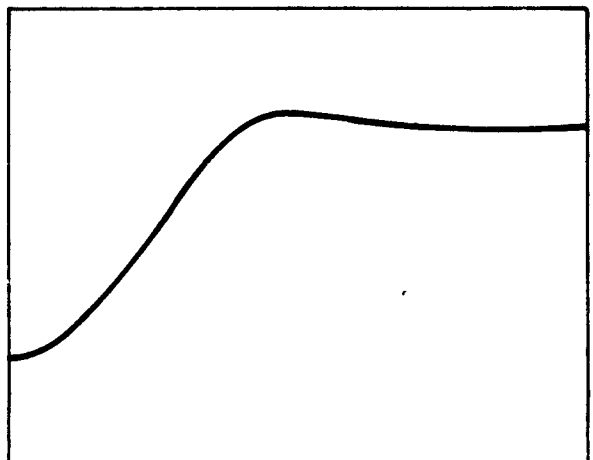
To check whether the nonlinear system is correct or not, the system response was found for the small input of 0.5 volts, and it was found to be the same as that of the linear system as shown in Fig. 4-6(a). The step response for a step size of 5 volts is shown in Fig. 4-6(b). Comparing this response with that of the linear system, one can see that the former has a large rise time because the system operates in part in the



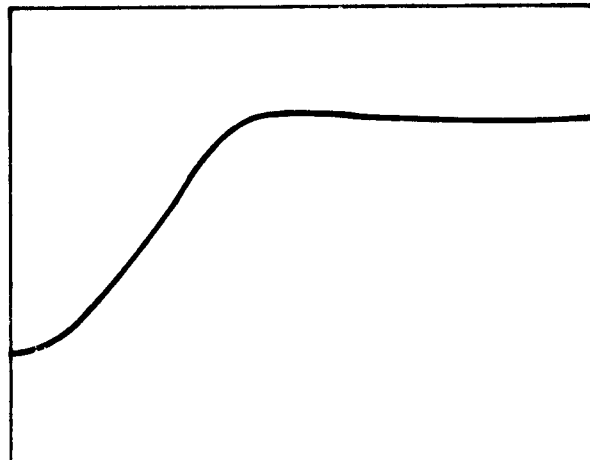
(a)



(b)



(c)



(d)

Fig. 5-6 Time Response for the Nonlinear System

saturated region. The overshoot is about the same as for the linear system.

The system response was checked with the feedback signals removed from \dot{c} and \ddot{c} , and it was found that the response is not much affected. The signals x_f and x_s do not exceed their saturating limits; and the per cent overshoot is in the same range as previously, as can be seen from the time response shown in Fig. 4-6(c). Also, the effects of varying the gain, which was varied from 100 to 255, were checked; and the response was found to be almost unaltered, as can be seen from Fig. 4-6(d). The system sensitivity was evaluated by varying the feedback coefficients by $\pm 25\%$, and it was found that this variation of the feedback coefficients does not cause any serious problems. Thus it can be concluded that the nonlinear system is insensitive to gain variations in feedback coefficients, and the removal of the feedback signals from \dot{c} and \ddot{c} . When the input is such that the system operates in the nonlinear range, the step response is slower than that of the linear system but the per cent overshoot is almost the same.

CHAPTER V

SUMMARY AND CONCLUSIONS

The representations of linear and a certain class of nonlinear state variable feedback systems have been presented. The nonlinear system was assumed to have a single nonlinear element of the non-memory type which was symmetric and had its characteristic lying in the first and third quadrant. The G_{eq} and H_{eq} representation was used to show that the optimum location for the nonlinear element is at the left end, although stability depends on both location of the nonlinearity and the locations of the zeros of $H_{2eq}(s)$.

To ensure absolute stability for all gain, the gain-insensitive method of design was proposed; and a step-by-step procedure was presented. Systems designed by the gain-insensitive method are absolutely stable and insensitive to gain. In the case of nonlinear systems, an n^{th} order system can be reduced to a first-order nonlinear system in series with the $(n-1)^{st}$ -order nonlinear system which is easy to analyze. Also, even when working in the nonlinear region the response of the nonlinear system is not degraded as much

as that of the same system designed by non-gain-insensitive methods. Thus the linear and nonlinear gain-insensitive systems are better in certain respects than non-gain-insensitive systems.

The property of inherent saturation in a plant was discussed along with effects which may cause instability. Saturation in the fixed plant can be prevented by introducing an intentional, saturation type nonlinear element with the proper limits. By combining this idea with the gain-insensitive method using state variable feedback, a system not only can be made stable but also absolutely stable for all gain.

The technique was used in improving the response of a fuel valve servomechanism which saturates at three different points. The resulting system has a large bandwidth and a low overshoot in response to a step input when operating in the linear region; in the nonlinear region, the response was better than that achieved in two previous design attempts.

Although the method worked well in the design example, there are several things yet to be investigated in connection with the design of the fuel valve servomechanism. The sensitivity of the system can be investigated further, perhaps even incorporating sensitivity requirements as one of the design criteria.

Also, whether the system response can be improved by using the conventional series compensation in combination with the gain-insensitive design technique can be investigated. A systematic method is still not available for choosing the closed-loop transfer function so that the unavailable feedback coefficients can be made negligibly small. The technique of introducing an intentional nonlinearity has been discussed for a particular type of system. It still has to be determined whether the technique is applicable to systems having other types of nonlinearities, such as a relay with dead space.

APPENDIX

Here the derivations of three sets of the (Ab) and (c) system equations are presented for the fuel valve servomechanism. Also, details of the analog computer simulations are given for this same system.

The differential equations describing the fuel valve servomechanism are derived with the aid of the block diagram presented in Fig. A-1. Let $c = x_1$, $\dot{x}_1 = x_2$, $\dot{x}_2 = x_3$, $x_s = x_4$, $x_f = x_5$, $\dot{x}_5 = x_6$, and $I = x_7$. Assuming all initial conditions to be zero, the first two equations describing the plant are

$$\dot{x}_1 = x_2 \quad (A-1)$$

$$\dot{x}_2 = x_3 \quad (A-2)$$

From the figure the transfer function relating x_1 to x_4 can be used to find \dot{x}_3

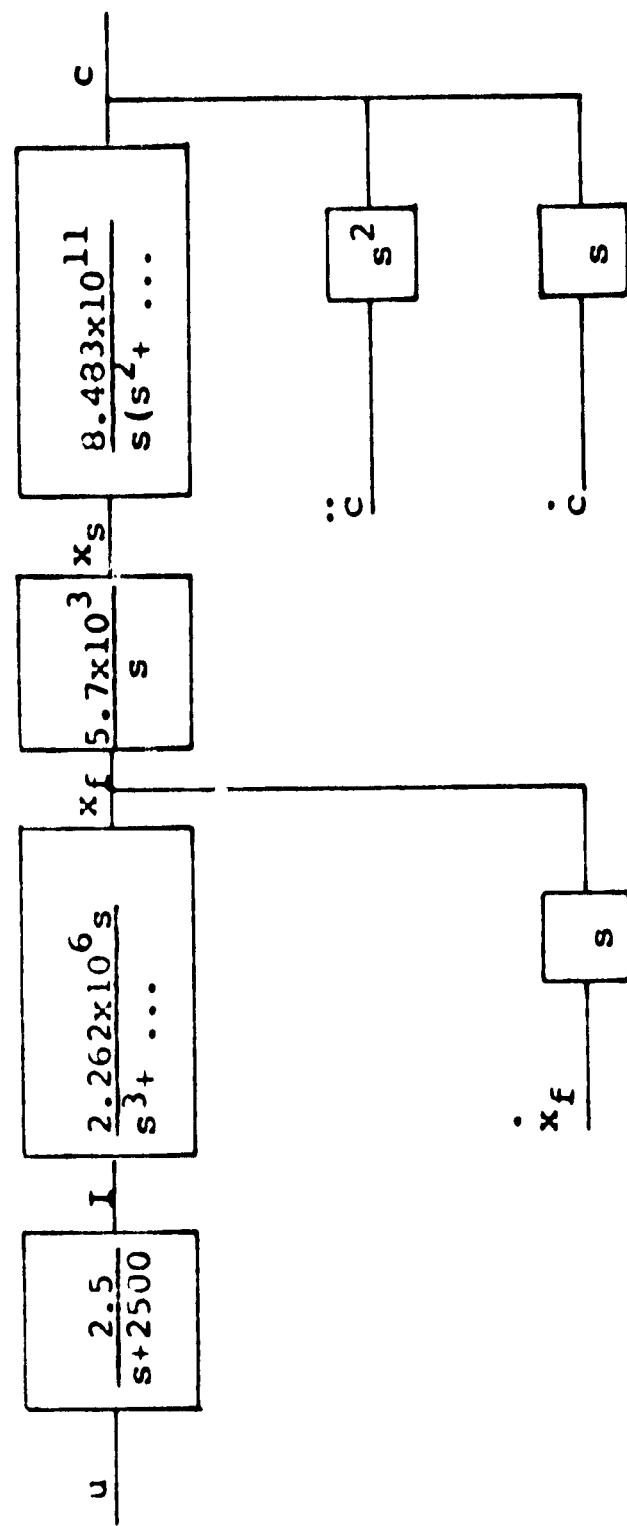
$$\frac{x_1}{x_4} = \frac{8.483 \times 10^{11}}{s^3 + 6.683 \times 10^3 s^2 + 3.28 \times 10^8 s}$$

Cross-multiplying and transferring to the time domain, one gets

$$\dot{x}_3 = -3.28 \times 10^8 x_2 - 6.683 \times 10^3 x_3 + 8.483 \times 10^{11} x_4 \quad (A-3)$$

Also from the relationship

$$\frac{x_4}{x_5} = \frac{5.769 \times 10^3}{s}$$



Third-Order Polynomial: $s^3 + 3.66937 \times 10^3 s^2 + 2.1033 \times 10^7 s + 1.7617 \times 10^{10}$

Second-Order Polynomial: $s^2 + 6.6331 \times 10^3 s + 3.23 \times 10^3$

Fig. A-1 Linearized Plant of Physical System

one gets

$$\dot{x}_4 = 5.769 \times 10^3 x_5 \quad (A-4)$$

and by definition

$$\dot{x}_5 = x_6 \quad (A-5)$$

The transfer function relating x_4 and x_7 can be used to find \dot{x}_6

$$\frac{x_4}{x_7} = \frac{2.262 \times 5.769 \times 10^9}{(s^3 + 3.669 \times 10^5 s^2 + 2.103 \times 10^7 s + 1.761 \times 10^{10})}$$

Cross-multiplying and transferring to the time domain,

one gets

$$\ddot{x}_4 = -3.669 \times 10^3 \ddot{x}_4 - 2.103 \times 10^7 \dot{x}_4 - 1.761 \times 10^{10} x_4 + 2.262 \times 5.769 \times 10^9 x_7$$

Substituting for \dot{x}_4 and \dot{x}_5

$$\dot{x}_6 = -3.055 \times 10^6 x_4 - 2.103 \times 10^7 x_5 - 3.669 \times 10^3 x_6 + 2.262 \times 10^6 x_7 \quad (A-6)$$

From the block diagram

$$\frac{x_7(s)}{u} = \frac{2.5}{s + 2.5 \times 10^3}$$

which gives

$$\dot{x}_7 = -2.5 \times 10^3 x_7 + 2.5u \quad (A-7)$$

Also

$$y = x_1 \quad (A-8)$$

Thus using Equations (A-1) to (A-8), the plant equations (Ab) and (c) can be written in matrix form.

For modifying the part of the plant from \dot{c} to u_1 as shown in Fig. 4-3, the required equations (Ab) and (c) can be found as follows. The equations for \dot{x}_2 , \dot{x}_3 , \dot{x}_4 , \dot{x}_5 , and \dot{x}_6 are the same as those of Equations (A-2, 3, 4, 5, and 6). From Fig. 4-3

$$\frac{x_7}{u_1} = \frac{2.5 \times 10^2}{s + 2500}$$

Cross-multiplying and transforming to the time domain, one gets

$$\dot{x}_7 = -2.5 \times 10^3 x_7 + 2.5 \times 10^2 u_1 \quad (\text{A-9})$$

and

$$y = x_2 \quad (\text{A-10})$$

Thus the modified matrices are

$$\underline{A} = \begin{bmatrix} 0 & 1 & 0 & 0 & 0 & 0 \\ -3.2 \times 10^8 & -6.5 \times 10^3 & 8.4 \times 10^{11} & 0 & 0 & 0 \\ 0 & 0 & 0 & 5.7 \times 10^3 & 0 & 0 \\ 0 & 0 & 0 & 0 & 1 & 0 \\ 0 & 0 & -3.0 \times 10^6 & -2.1 \times 10^7 & -3.6 \times 10^3 & 2.2 \times 10^6 \\ 0 & 0 & 0 & 0 & 0 & 2.5 \end{bmatrix}$$

$$\underline{b}^T = [0 \quad 0 \quad 0 \quad 0 \quad 0 \quad 2.5 \times 10^2]$$

$$\underline{c}^T = [1 \quad 0 \quad 0 \quad 0 \quad 0 \quad 0]$$

To realize the closed-loop transfer function by feeding back all the variables, the differential

equations describing the modified plant are used. The differential equations for \dot{x}_1 , \dot{x}_2 , \dot{x}_3 , \dot{x}_4 , \dot{x}_5 , and \dot{x}_6 are the same as Equations (A-1, 2, 3, 4, 5, and 6), respectively. Again, from the block diagram shown in Fig. 4-3

$$\dot{x}_7 = -2.5 \times 10^3 x_7 + 2.5 \times 10^2 u_1$$

Substituting for u_1 in the above equation gives

$$\begin{aligned} \dot{x}_7 = & 1.3675 \times 10^{-2} x_2 + 4.6277 \times 10^{-7} x_3 \\ & -4.0828 \times 10^3 x_4 - 3.4700 \times 10^3 x_5 \\ & -2.1923 \times 10^3 x_7 + 2.70982 \times 10^2 u \end{aligned} \quad (A-11)$$

Equations (A-1, 2, 3, 4, 5, 6, 11, and 8) are sufficient to describe the modified plant in matrix form to be used on the digital computer.

Details of the Analog Computer Simulations

To evaluate the designed gain-insensitive linear and nonlinear systems an analog computer of ± 100 v. was used. The systems were simulated using the differential equation approach. The different variables were scaled using the following scale factors

$$\begin{array}{cccc} x_1(2 \times 10^2) & x_2(1) & x_3(2.35 \times 10^3) & x_5(10^4) \\ x_6(1) & x_7(2 \times 10^3) & u(2 \times 10^3) & r(4 \times 10^2) \end{array}$$

The limits of the saturating states x_1 , x_4 , and x_5 have the magnitudes 5 volts, 35 volts, and 12 volts, respectively. The scaled differential equations are as follows:

$$\begin{aligned}
 \dot{x}_1 &= 2 \times 10^2 x_2 \\
 \dot{x}_2 &= 10^4 x_3 \\
 \dot{x}_3 &= -3.28 \times 10^4 x_2 - 6.683 \times 10^3 x_3 + 3.60978 \times 10^4 x_4 \\
 \dot{x}_4 &= 1.3557 \times 10^3 x_5 \\
 \dot{x}_5 &= 10^4 x_6 \\
 \dot{x}_6 &= -1.3 \times 10^3 x_4 - 2.1030 \times 10^3 x_5 - 3.669 \times 10^3 x_6 + 1.131 \times 10^3 x_7 \\
 \dot{x}_7 &= 2.7350 \times 10^1 x_2 + 3.2554 x_3 - 3.4747 \times 10^3 x_4 - 6.894 \times 10^2 x_5 \\
 &\quad - 2.5294 \times 10^3 x_6 - 2.1923 \times 10^3 x_7 + 4.60669 \times 10^4 u \\
 u &= (5r(t) - 2 \times 10^{-3} k^T x)
 \end{aligned}$$

The feedback coefficients are $k_1 = 10$, $k_2 = 4.066 \times 10^{-2}$,
 $k_3 = 6.124 \times 10^{-2}$, $k_4 = 1.297188$, $k_5 = 3.55792 \times 10^{-1}$,
 $k_6 = 7.15308 \times 10^{-1}$, and $k_7 = 3.690275 \times 10^{-1}$.

In order to facilitate the recording of step responses, the system was time-scaled by the factor 10^4 which gives the new differential equations

$$\begin{aligned}
 \dot{x}_1 &= 0.02 x_1 \\
 \dot{x}_2 &= x_3 \\
 \dot{x}_3 &= -3.28 x_2 - 0.6683 x_3 + 3.60978 x_4 \\
 \dot{x}_4 &= 0.13557 x_5 \\
 \dot{x}_5 &= x_6 \\
 \dot{x}_6 &= -0.13 x_4 - 0.2103 x_5 - 0.3669 x_6 + 0.1131 x_7 \\
 \dot{x}_7 &= 0.002735 x_2 + 0.00093 x_3 - 0.34747 x_4 - 0.06894 x_5 \\
 &\quad - 0.25294 x_6 - 0.21923 x_7 + 4.60669 u
 \end{aligned}$$

Using the above equations and the feedback coefficients the system circuit diagram is formed as

shown in the Fig. A-2 for the linear system. For the nonlinear system an intentional nonlinearity is introduced, whose characteristic is shown in Fig. A-3 along with the diode bridge to realize it.

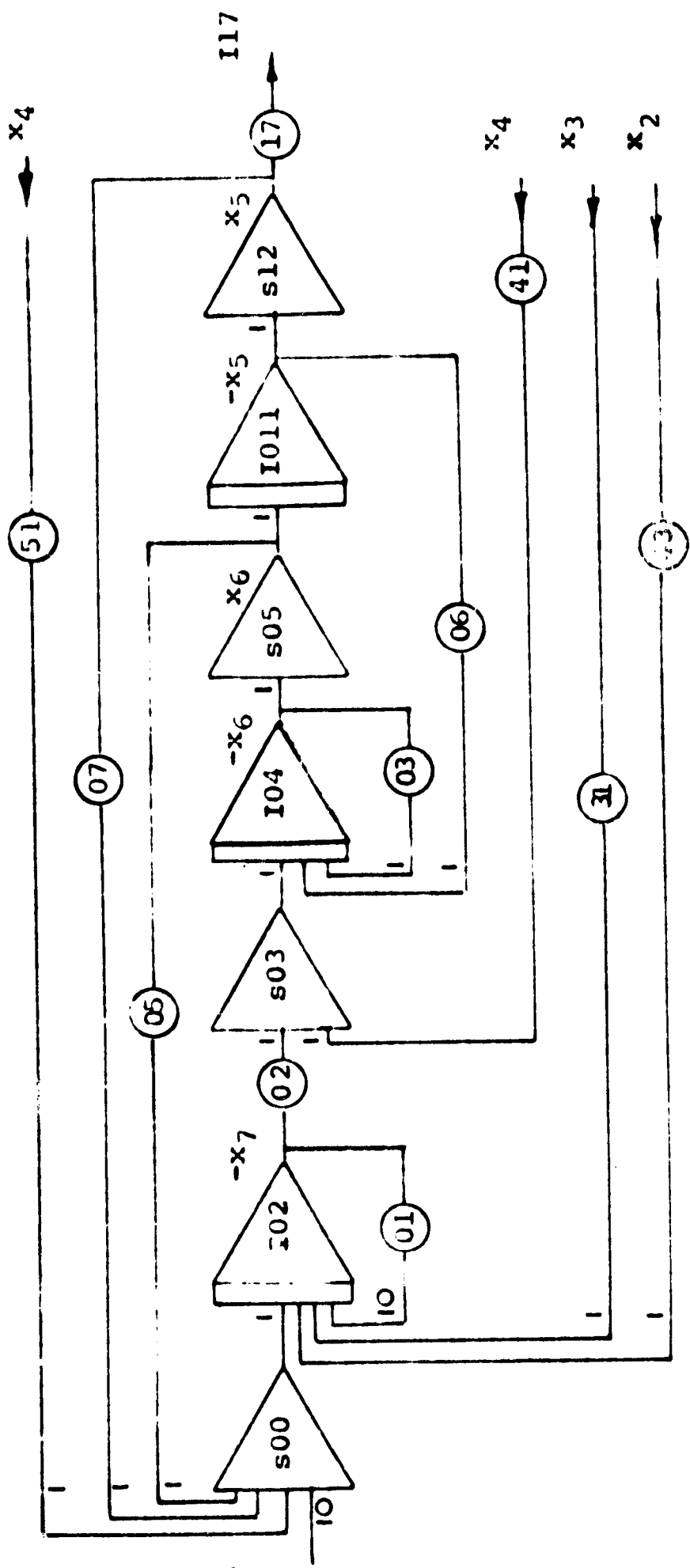


Fig. A-2 Analog Computer Wiring Diagram for Simulation (Continued on Next Page)

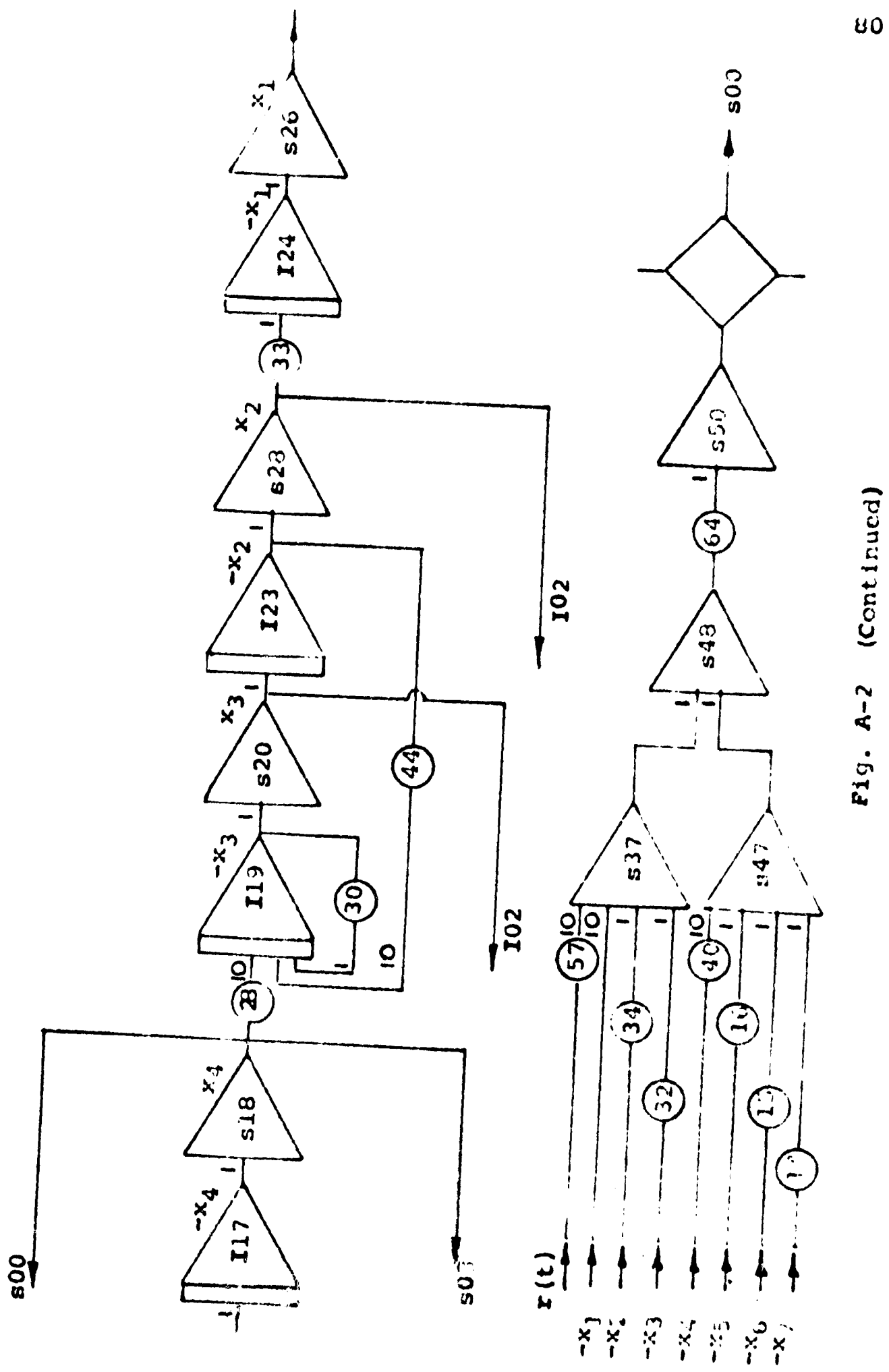


Fig. A-2 (Continued)

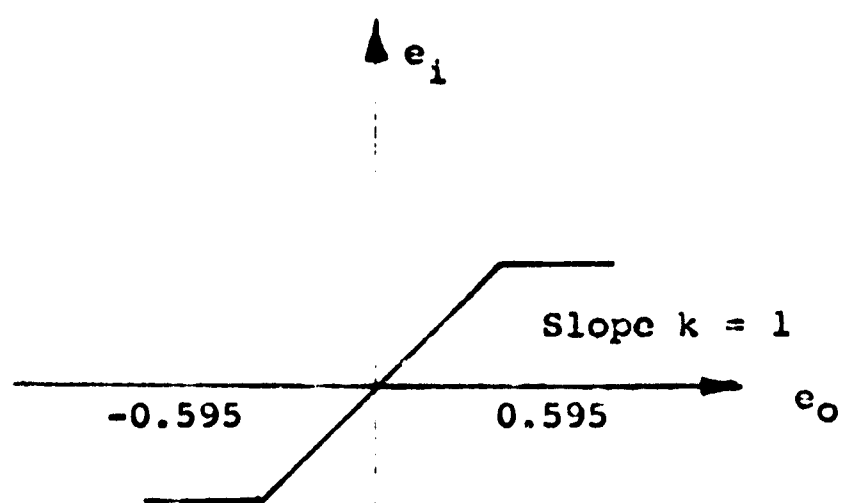
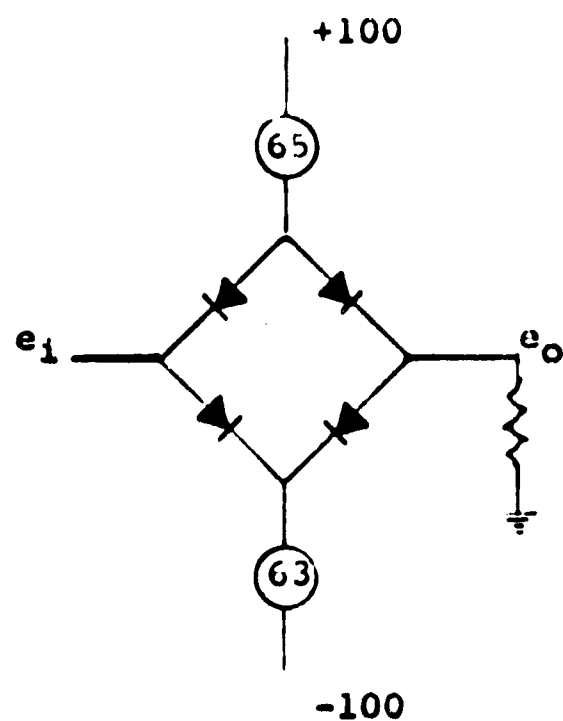


Fig. A-3 Details of the Bridge Circuit Realizing the Limiter and its Input-Output Characteristic

REFERENCES

Bower, J. L. and Schultheiss, P. M. Introduction to the Design of Servomechanisms. John Wiley & Sons, New York, 1959.

Gibson, J. E. Nonlinear Automatic Control. McGraw Hill, New York, 1963.

Graham, D. and Lathrop, R. C. The Synthesis of "Optimum" Transient Response: Criteria and Standard Forms. AIEE Trans. Part II, Application and Industry, Vol. 72, No. 9, pp. 273-288, November 1953.

Herring, J. W.; Schultz, D. G.; Weaver, L. E.; Vanasse, E. R. Design of Linear and Nonlinear Control Systems via State Variable Feedback, With Applications in Nuclear Reactor Control, University of Arizona (NASA NSG-490) 1967.

Melsa, J. L. A Digital Computer Program for the Analysis and Design of State Variable Feedback Systems, University of Arizona (NASA NSG-490) 1967.

Schultz, D. G. and Melsa, J. L. State Functions and Linear Control Systems. McGraw Hill, New York, 1967.

Schultz, D. G. The Generation of Liapunov Functions. Advances in Control Systems. Vol. 2, Academic Press Inc., New York, 1965.

Slivinsky, C. R.; Dellner, L. T.; and Arpasi, D. J. Formac Program to Assist in Analysis of Linear Control Systems Using State Variable Feedback Design Technique, Technical Memorandum, NASA TM X-1443.

Thaler, G. J. and Pastel, M. P. Analysis and Design of Nonlinear Feedback Control Systems. McGraw Hill, New York, 1962.

PART IV
STATE VARIABLE FEEDBACK AND UNAVAILABLE STATES

Prepared under Grant NGR-03-002-115
National Aeronautics and Space Administration

by

Milo E. Muterspaugh
and
Donald G. Schultz

Electrical Engineering Department
The University of Arizona
Tucson, Arizona

ABSTRACT

Three techniques are presented for generating unavailable states to realize a desired closed-loop response. Since all configurations realize the same closed-loop response, they are compared on the basis of peak and integral sensitivity. The system that is the least sensitive to changes in plant parameters is considered the best. The first two techniques discussed result in undesirable systems. The third system results in a new control system configuration that is a compromise between a state-variable feedback system and the corresponding $H_{eq}(s)$ system.

TABLE OF CONTENTS

	Page
LIST OF ILLUSTRATIONS	v
LIST OF TABLES	vii
ABSTRACT	viii
CHAPTER	
I INTRODUCTION	4
II GENERAL THEORY	4
2.1 State-Variable Feedback	4
2.2 Sensitivity Measures	14
III PARALLEL SIMULATION	19
IV OBSERVER SYSTEM	29
4.1 Observer Theory	29
4.2 An Example	33
4.3 Closed-Loop System	39
4.4 Closed-Loop Example	41
4.5 Sensitivity Example	46
V MODIFIED OBSERVER SYSTEM	51
5.1 System Configuration	51
5.2 Example One	57
5.3 Example Two	64
5.4 Physical Realizability	71
5.5 Summary	74
VI CONCLUSIONS	75
REFERENCES	79

LIST OF ILLUSTRATIONS

Figure	Page
2.1 General Plant	6
2.2 Representation of Complex Conjugate Roots . .	6
2.3 Plant with State-Variable Feedback	10
2.4 $H_{eq}(s)$ Configuration	10
2.5 Plant for Third-Order Example	11
2.6 State-Variable Feedback System	11
2.7 System with Feedback Moved to x_1 Node	11
2.8 Classical Control System Configuration . . .	16
3.1 Plant and Parallel Simulation	21
3.2 Closed-Loop System	21
3.3 Series Compensated System	22
3.4 Open-Loop Plant	24
3.5 Series Compensated System	24
3.6 Parallel Simulation System	24
3.7 Third-Order System	26
4.1 Open-Loop Plant	34
4.2 Observer	34
4.3 Plant and Observer with Generated States . .	36
4.4 Closed-Loop System	42
4.5 Steps in Solving Closed-Loop Problem	42
4.6 Plant and Observer	43

LIST OF ILLUSTRATIONS--Continued

LIST OF TABLES

CHAPTER I INTRODUCTION

Modern control theory states that the optimal control law should be a function of all the state variables. Schultz and Melsa (1967) develop this state-variable feedback configuration in detail for linear systems. White (1967) has shown that the state-variable feedback configuration has sensitivity advantages over a system using series compensation, designed by the Guillemin-Truxal technique discussed in Chapter 5 of Truxal (1955). In addition, any desired response can be achieved by feeding back all the states in the proper combination.

In most practical problems, all the states are not available for control, and in some cases, only the output is available. Schultz and Melsa (1967) describe how unavailable states can be generated by block diagram manipulations. These techniques are limited and do not always realize the sensitivity advantages. White (1967) moves all the feedback to the output by block diagram manipulation, resulting in the $H_{eq}(s)$ configuration. He then shows that for the $H_{eq}(s)$ configuration the sensitivities of plant parameters are as good as or better

than the state-variable feedback configuration. However, the resulting system is not realizable, except for the special case where the plant has the same number of poles and zeroes.

The problem attacked in this work is to find a way to generate these unavailable states while retaining some of the sensitivity advantages of state-variable feedback. Three techniques for generating unavailable states are discussed. These three configurations and state-variable feedback are discussed on the basis of sensitivity largely through the use of examples. Sensitivity is used as the criterion since all the techniques realize the same closed-loop transfer function.

Only linear, noiseless, time-invariant systems with single input and output are considered. It is also assumed that a desired closed-loop response has been specified in terms of a desired transfer function. Dial (1967) has shown a correspondence between a quadratic performance index and the specification of a closed-loop response.

Chapter II contains background material. State-variable feedback is discussed, and it is shown how to solve for the required feedback coefficients, given a plant and a desired response. Different sensitivity measures are also discussed briefly.

Chapter III explains the parallel simulation configuration, where the unavailable states are fed back from a parallel simulation of the plant. It is shown how this configuration is nothing more than series compensation, and an example is presented.

In Chapter IV, the observer system of Luenberger (1963) is used to feed back the unavailable states. Here another linear system, whose order is equal to the number of unavailable states of the plant, is introduced into the problem. This new system is driven by the available states and the input to the plant. The states of the new system are a linear transformation of the unavailable states of the plant. New feedback coefficients are defined for the available states of the plant and the states of the new system. Examples of the technique are given.

Chapter V develops a new control system configuration that is a modification of the observer system of Chapter IV. This new configuration is a compromise between a state-variable feedback system and the corresponding $H_{eq}(s)$ system. It is shown how this new system may be synthesized directly from the desired closed-loop response. Examples are presented that show how the technique may be applied when only the output is available, or when additional states are also available.

The final chapter contains a conclusion, and offers suggestions for further work.

CHAPTER II

GENERAL THEORY

This chapter discusses pertinent background material. State-variable feedback and the determination of the feedback coefficients to realize a given closed-loop response are described. Sensitivity measures are discussed briefly.

2.1 State-Variable Feedback

It is assumed that the given linear plant is represented in block diagram form. A typical plant is shown in Figure 2.1. The plant transfer function, $G_p(s)$, is given by

$$G_p(s) = G_1(s) G_2(s) \dots G_n(s)$$

and

$$\frac{y(s)}{u(s)} = G(s) = K G_p(s)$$

If the plant transfer function possesses a pair of complex conjugate poles, it is represented as two integrators with feedback. For example, the open-loop transfer function

$$G(s) = \frac{1}{s^2 + 3s + 6}$$

can be represented in block diagram form as in Figure 2.2.

If a state is associated with each block of the plant, as in Figure 2.1, the plant can be represented as a system of first-order linear differential equations. In matrix notation, these equations are

$$\begin{aligned}\dot{\underline{x}} &= \underline{A}\underline{x} + \underline{b}u \\ \underline{y} &= \underline{c}^T \underline{x}\end{aligned}\tag{2.1}$$

where

- \underline{x} is an $(n \times 1)$ state vector
- \underline{A} is an $(n \times n)$ plant matrix
- \underline{b} is an $(n \times 1)$ input vector
- \underline{c} is an $(n \times 1)$ output vector
- u is the scalar input
- y is the scalar output

The open-loop transfer function in matrix notation can be found by taking the Laplace transform of equation (2.1) with zero initial conditions, as

$$s\underline{x}(s) = \underline{A}\underline{x}(s) + \underline{b}u(s)$$

$$y(s) = \underline{c}^T \underline{x}(s)$$



Figure 2.1 General Plant

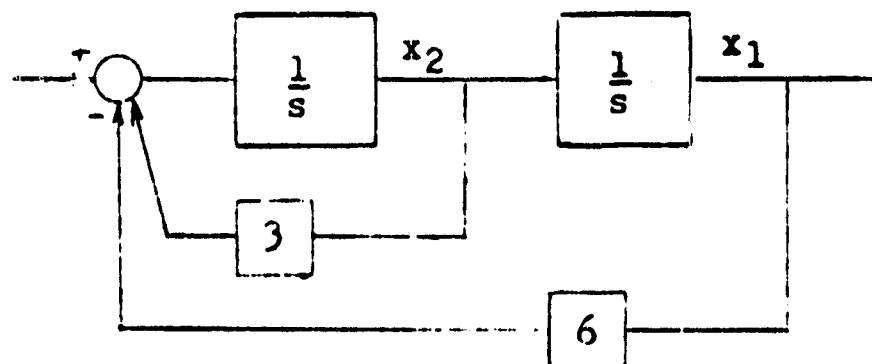


Figure 2.2 Representation of Complex Conjugate Roots

?

This may be rearranged to give

$$(sI - \underline{A})\underline{x}(s) = \underline{b}u(s)$$

such that

$$\underline{x}(s) = (sI - \underline{A})^{-1} \underline{b}u(s)$$

or

$$\underline{x}(s) = \underline{\Phi}(s) \underline{b}u(s) \quad (2.2)$$

where

$$\underline{\Phi}(s) = (sI - \underline{A})^{-1}$$

The open-loop transfer function is

$$G(s) = \frac{y(s)}{u(s)} = \frac{\underline{c}^T \underline{x}(s)}{u(s)} = \frac{\underline{c}^T \underline{\Phi}(s) \underline{b}u(s)}{u(s)}$$

or

$$G(s) = \underline{c}^T \underline{\Phi}(s) \underline{b} \quad (2.3)$$

Schultz and Melsa (1967) show that any closed-loop response of the same order as the plant can be achieved by feeding back all the states with the proper weighting. The zeroes of the plant show up as zeroes of the closed-loop response. If zeroes other than the inherent zeroes of the plant are desired, they are added to the plant using a series compensator that contains

the desired zeroes and additional poles. The order of the plant is then increased by the order of the compensator, and additional states are created that should also be used for control. The control input, u , for state-variable feedback is given by

$$u = r - \underline{k}^T \underline{x} \quad (2.4)$$

where

r is the closed-loop system input

\underline{k} is an $(n \times 1)$ vector of feedback coefficients

Substituting equation (2.4) into (2.1) for u , the closed-loop system can be represented by the set of equations

$$\begin{aligned} \dot{\underline{x}} &= (\underline{A} - \underline{b} \underline{k}^T) \underline{x} + \underline{b} r \\ y &= \underline{c}^T \underline{x} \end{aligned} \quad (2.5)$$

where

$(\underline{A} - \underline{b} \underline{k}^T)$ is the closed-loop system matrix

Equation (2.5) may be transformed to the frequency-domain and solved for $y(s)/r(s)$. This expression for $y(s)/r(s)$ in terms of the feedback coefficients is then equated to a desired response and the feedback coefficients found by simple algebraic manipulations.

It is simpler to convert the representation of Figure 2.3 to the H_{equivalent}(s) configuration as shown

in Figure 2.4. The expression below can be used to find $H_{eq}(s)$

$$H_{eq}(s) = \frac{\underline{k}^T \underline{p}(s) \underline{b}}{\underline{c}^T \underline{p}(s) \underline{b}}$$

Well known block diagram manipulations may also be used to find $H_{eq}(s)$ by moving the origins of the feed-back paths to the output. The closed-loop response for $H_{eq}(s)$ configuration is given by

$$\frac{y(s)}{r(s)} = \frac{G(s)}{1 + G(s) H_{eq}(s)} \quad (2.6)$$

Equation (2.6) may be equated to the desired response and the feedback coefficients found. The output block, G_1 , often contains an integrator, and in this case, k_1 is set equal to one to insure zero steady-state position error for step function inputs.

As an example of the technique, consider the plant shown in Figure 2.5. It is desired to realize the closed-loop transfer function

$$\frac{y(s)}{r(s)} = \frac{80}{s^3 + 14s^2 + 48s + 80} \quad (2.7)$$

Figure 2.6 shows the plant with feedback. The forward gain, K , is assumed adjustable, and k_1 is set equal to

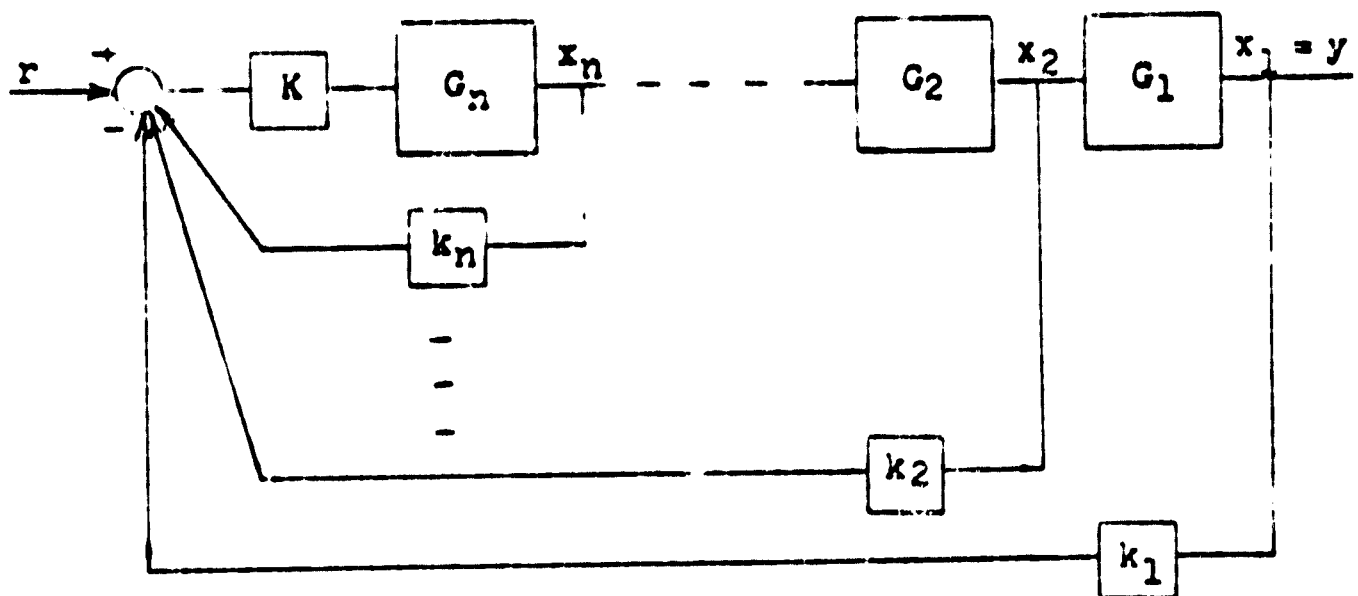


Figure 2.3 Plant with State-Variable Feedback

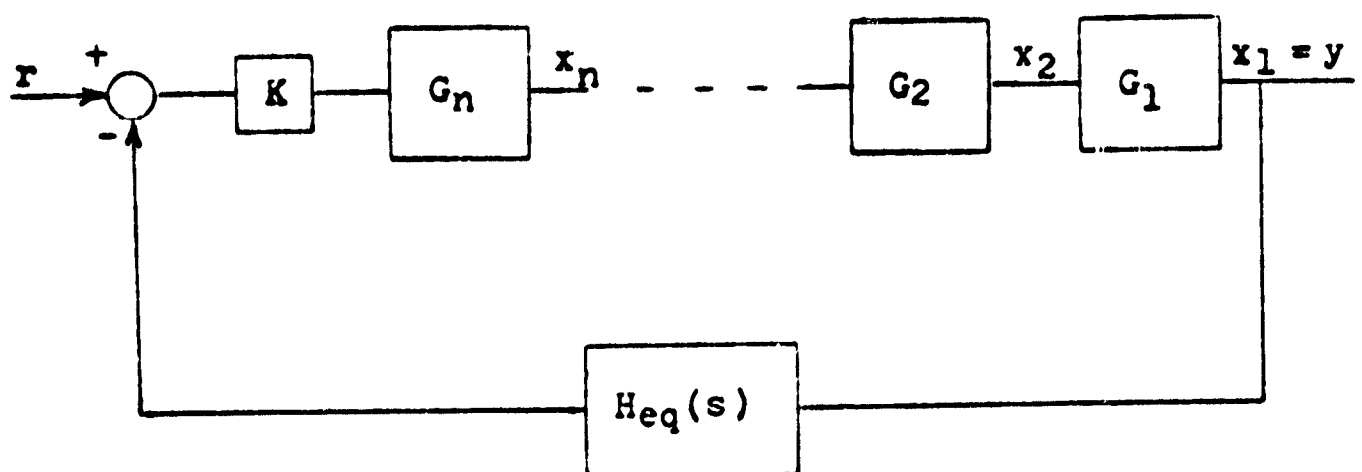


Figure 2.4 $H_{eq}(s)$ Configuration

11

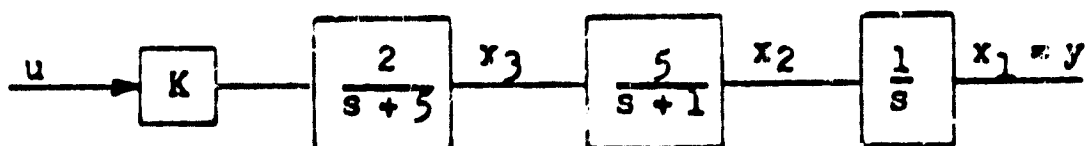


Figure 2.5 Plant for Third-Order Example

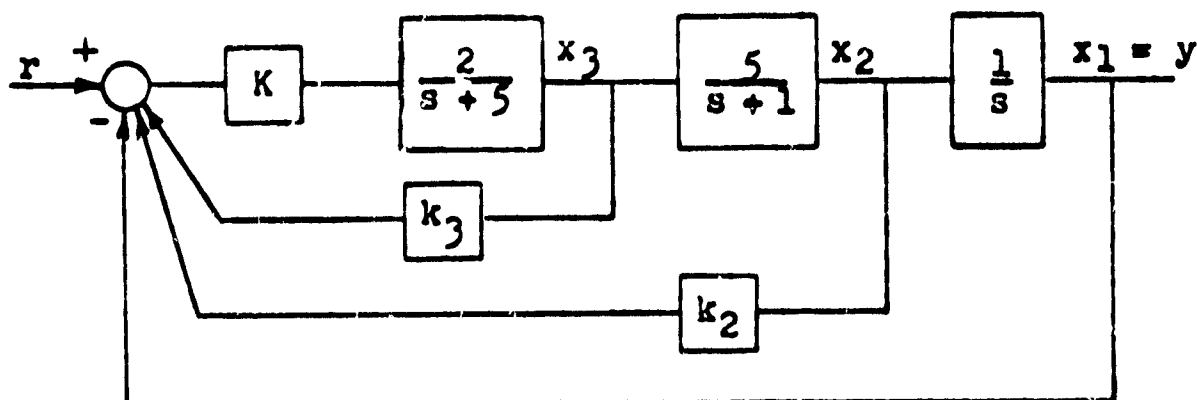


Figure 2.6 State-Variable Feedback System

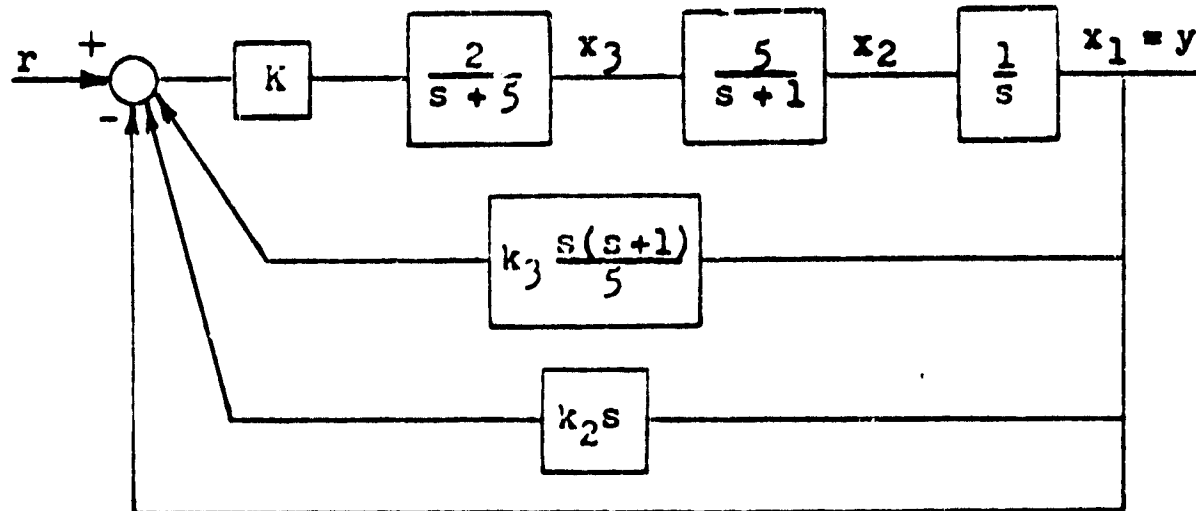


Figure 2.7 System with Feedback Moved to x_1 Node

one to realize the desired zero steady-state position error for step function inputs. In Figure 2.7, all the feedback has been moved to the x_1 node. $H_{eq}(s)$ is found by combining the three feedback paths to be

$$H_{eq}(s) = 1 + k_2 s + \frac{1}{5} k_3 s(s + 1)$$

or

$$H_{eq}(s) = \frac{k_3}{5} s^2 + \left(\frac{k_3}{5} + k_2\right) s + 1 \quad (2.8)$$

The open-loop transfer function is given by

$$G(s) = \frac{10K}{s(s + 1)(s + 5)} \quad (2.9)$$

Substituting equation (2.8) and (2.9) into equation (2.6) gives the overall response in terms of the feedback coefficients as

$$\frac{y(s)}{r(s)} = \frac{10K}{s^3 + (6 + 2Kk_3)s^2 + (5 + 2Kk_3 + 10Kk_2)s + 10K} \quad (2.10)$$

Equating coefficients in equation (2.10) with the desired response equation (2.7) gives the following equations:

$$10K = 80$$

$$2Kk_3 = 8$$

and

$$2Kk_3 + 10Kk_2 = 43$$

Solving the first for K, the remaining equations become linear with the solution.

$$K = 8$$

$$k_2 = 7/16$$

$$k_3 = 1/2$$

The closed-loop system is now realized as shown in Figure 2.6.

It would be ideal if all the state variables were always available for control, so that state-variable feedback could be applied directly. Often, however, this is not the case. The state variables may be too difficult or too costly to measure, or the measurements may be corrupted by an excess amount of noise. In these cases, the state variables can not be measured, and alternate means must be used to realize the desired closed-loop transfer function. In each case, the alternate means described here realize the same closed-loop transfer function. Hence, they can not be compared on an input to output or transfer function basis. The method of comparison used here is that of sensitivity.

2.2 Sensitivity Measures

It is important to have measures of how the response or overall system transfer function changes with system parameters. Several sensitivity measures are described here that may be applied to this problem.

The definition of classical sensitivity given here is from Truxal (1955). The sensitivity of a frequency function, $T(s, p)$, with respect to a parameter, p , is defined as

$$S_p^T = \frac{d \ln T}{d \ln p} = \frac{p}{T} \frac{dT}{dp}$$

The classical sensitivity expresses the percentage change in T for a percentage change in a parameter, p . Here, T is indicated as a function of s as well as p because the application usually involves transfer functions.

An application of classical sensitivity to the comparison of the sensitivities of plant parameters for two control system configurations results in two frequency functions that must be compared. If the magnitude of one classical sensitivity were smaller for all frequencies, then the corresponding system would be the least sensitive. Usually, the magnitude of one classical sensitivity is smaller for some frequency range, and it is not clear what system is the least sensitive; that is, interpretation is difficult.

For an example of classical sensitivity, consider the classical control system configuration of Figure 2.8. The overall response is given as

$$\frac{y(s)}{r(s)} = W(s) = \frac{G(s)}{1 + G(s) H(s)}$$

The sensitivity of $W(s)$ with respect to $G(s)$ is given by

$$S_G^W = \frac{G}{W} \frac{dW}{dG} = \frac{G}{W} \frac{d}{dG} \left(\frac{G(s)}{1 + G(s) H(s)} \right)$$

$$= \frac{1}{1 + G(s) H(s)}$$

which is approximately equal to

$$\approx \frac{1}{G(s) H(s)} \quad \text{if } |G(s) H(s)| \gg 1$$

By making the loop gain large, the effect of parameter variations in the forward path is made small.

Classical sensitivities are relatively easy to calculate. Unfortunately, they are a function of frequency and are difficult to interpret. In order to avoid the frequency dependence of classical sensitivity, three time-domain measures of sensitivity may be utilized.

The sensitivity function, $U_p(t)$, is defined by Tomovic (1964) as the change in the response, $y(t)$, to a

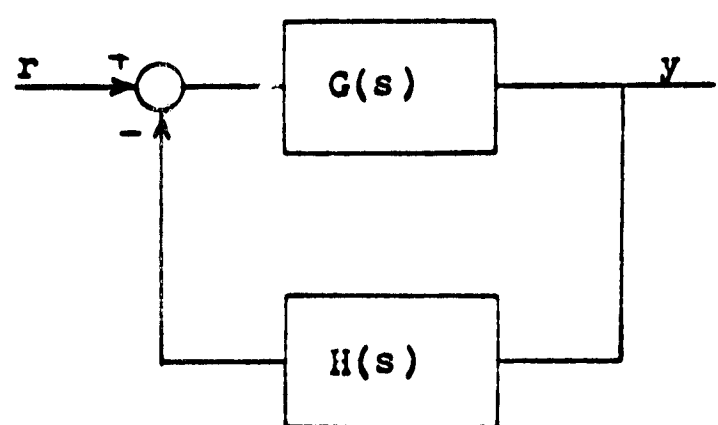


Figure 2.8 Classical Control System Configuration

step input, for a percentage change in a system parameter p .

$$U_p(t) = \frac{dy(t, p)}{dp/p}$$

Here $U_p(t)$ is a function of time, and this is also difficult to interpret.

White (1967) discusses two new sensitivity measures that give a number that can be used to compare the different control system configurations. He defines the peak sensitivity, U_p^* , of a parameter, p , as

$$U_p^* = U_p(T)$$

where T equals the value of t such that $|U_p(t)|$ is a maximum. Also defined is the integral sensitivity of the system with respect to a parameter, p , as

$$S_p = \int_0^\infty U_p(t) dt$$

when this integral exists. White shows that integral sensitivity is related to classical sensitivity by the relationship

$$S_p = \frac{1}{2\pi} \int_{-\infty}^{\infty} \left| \frac{w(jw)}{w^2} \right|^2 \left| S_p^W(jw) \right|^2 dw$$

where $w(jw)$ is the overall transfer function with s replaced by jw .

Peak and integral sensitivities give a number as a sensitivity measure, rather than a frequency or time function. Thus, peak and integral sensitivities are easy to interpret and will be used to compare the examples of the following chapters. However, except for simple cases, a computer is required for the generation of U_p^* and S_p (see White, 1967).

CHAPTER III

PARALLEL SIMULATION

This chapter and the following two describe three alternate means of realizing a desired closed-loop transfer function when all the state variables are not available. The technique used in this chapter is that of parallel simulation, and only single-input, single-output systems are discussed. The case where only the output is available is stressed as a "worst" case.

The plant and parallel simulation for generating the unavailable states in the worst case is shown in Figure 3.1. Stars are used to denote the generated states, which are only estimates of the actual states. Assume $G_p(s)$ is the unalterable plant of n th-order, where

$$G_p(s) = G_1 G_2 \dots G_n$$

It is only necessary to simulate $n-1$ of the states since the output is assumed available for feedback. The blocks, G_2^* through G_n^* , are simulations of the corresponding G_2 through G_n of the plant. Each G_i contains one pole, or one pole and a zero. If $G_p(s)$ contains complex conjugate roots, these can be simulated using two integrators with feedback, as discussed in Chapter II. If $G_p(s)$ is a

linearized model of the actual plant, the simulated states are only equal to the actual states near some operating point where the linear model is valid.

The state-variable feedback coefficients may be found as if all the states were available, but the unavailable states are fed back from the parallel simulation. Figure 3.2 shows the closed-loop system with the unavailable states generated by the parallel simulation. The transfer function from node e_2 to e_1 in Figure 3.2 is equivalent to the Guillemin-Truxal series compensator as discussed in Truxal (1955). Assuming the desired closed-loop response, $y(s)/r(s)$, is known, the Guillemin-Truxal compensator, G_c , is found from the relation

$$G_c = \frac{y/r}{G_p(1 - y/r)} \quad (3.1)$$

The Guillemin-Truxal configuration is shown in Figure 3.3.

White (1967) has shown that the sensitivities, both classical and sensitivity functions, for a state-variable feedback configuration are considerably better than those achieved using series compensation. Although sensitivities do vary in general with the system configuration, the sensitivities of the plant parameters in Figure 3.2 are only dependent on the overall function, G_c , and not how it is realized. This is true in general

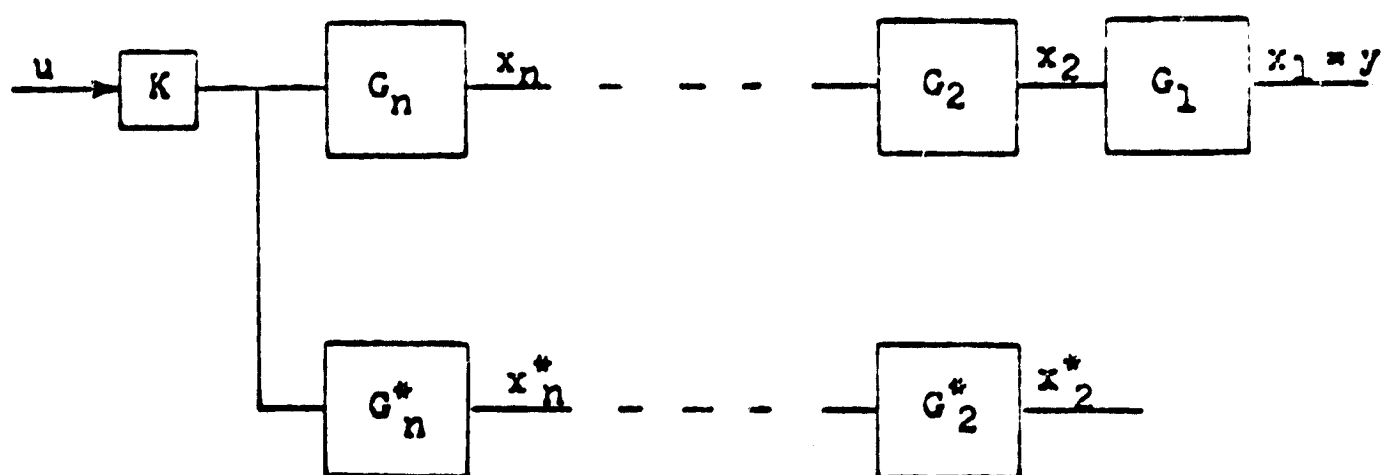


Figure 3.1 Plant and Parallel Simulation

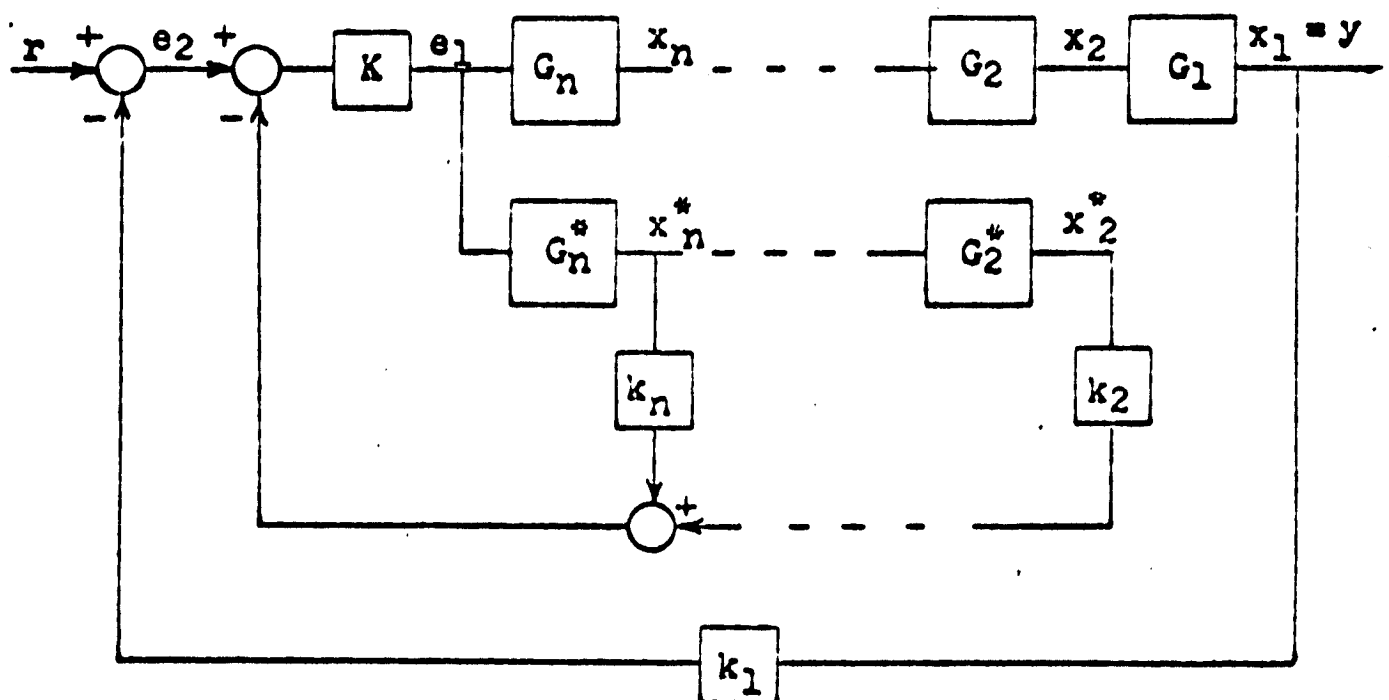


Figure 3.2 Closed-Loop System

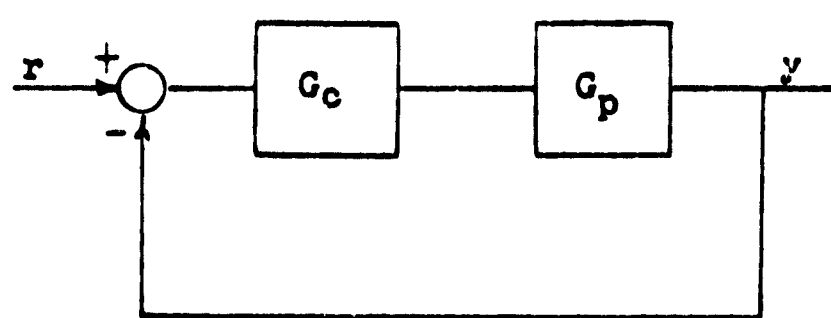


Figure 3.3 Series Compensated System

since any system compensated by the parallel simulation technique can always be reduced to the configuration of Figure 3.3. Here, G_u must equal the Guillemin-Truxal equalizer, since if two systems are identical except for one block, then that block must also be the same.

As an example, consider the third-order plant of Figure 3.4. It is assumed that only the output is available for control, and zero steady-state position error is desired. The desired closed-loop response is

$$\frac{y(s)}{r(s)} = \frac{80}{(s + 10)(s^2 + 4s + 8)}$$

The problem is first solved using the Guillemin-Truxal approach and then using a parallel simulation.

The desired series compensator is found using equation (3.1) as

$$G_c = \frac{8(s + 1)(s + 5)}{(s + 6)(s + 8)}$$

The closed-loop system is shown in Figure 3.5.

The feedback coefficients and forward gain for the parallel simulation system were found in Chapter II as

$$K = 8.0$$

$$k_1 = 1.0$$

$$k_2 = 7/16$$

$$k_3 = 1/2$$

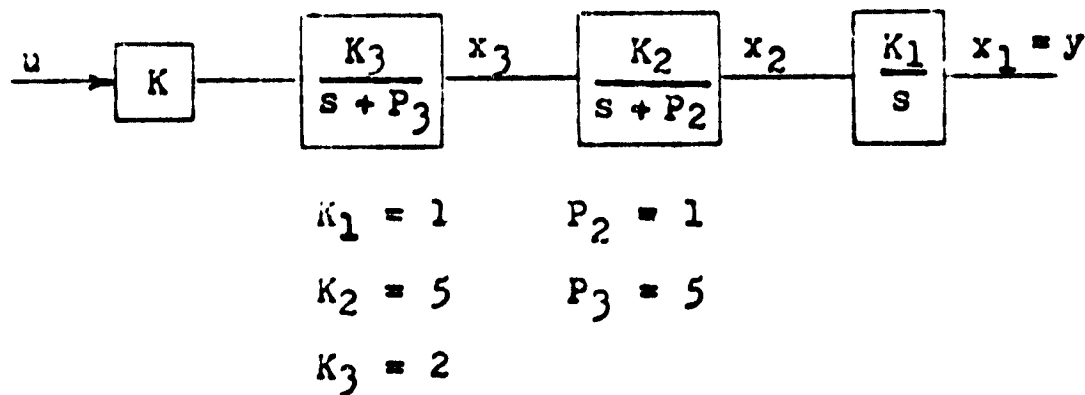


Figure 3.4 Open-Loop Plant

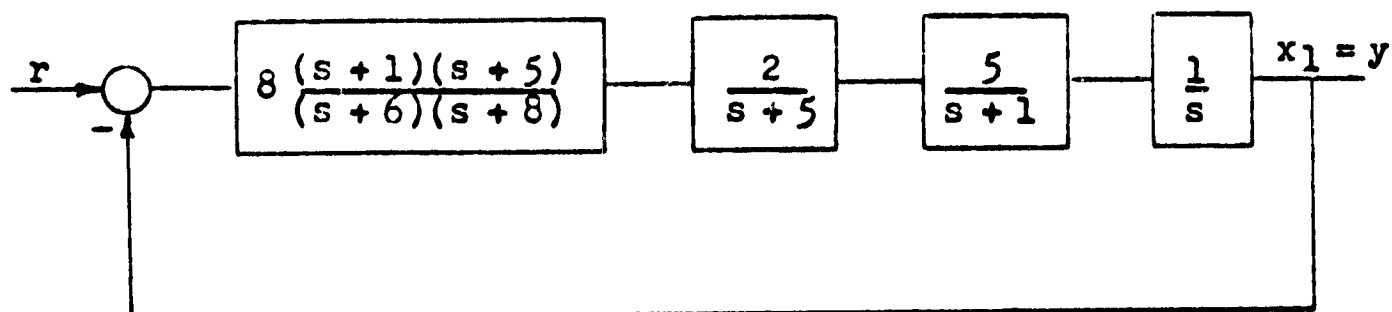


Figure 3.5 Series Compensated System

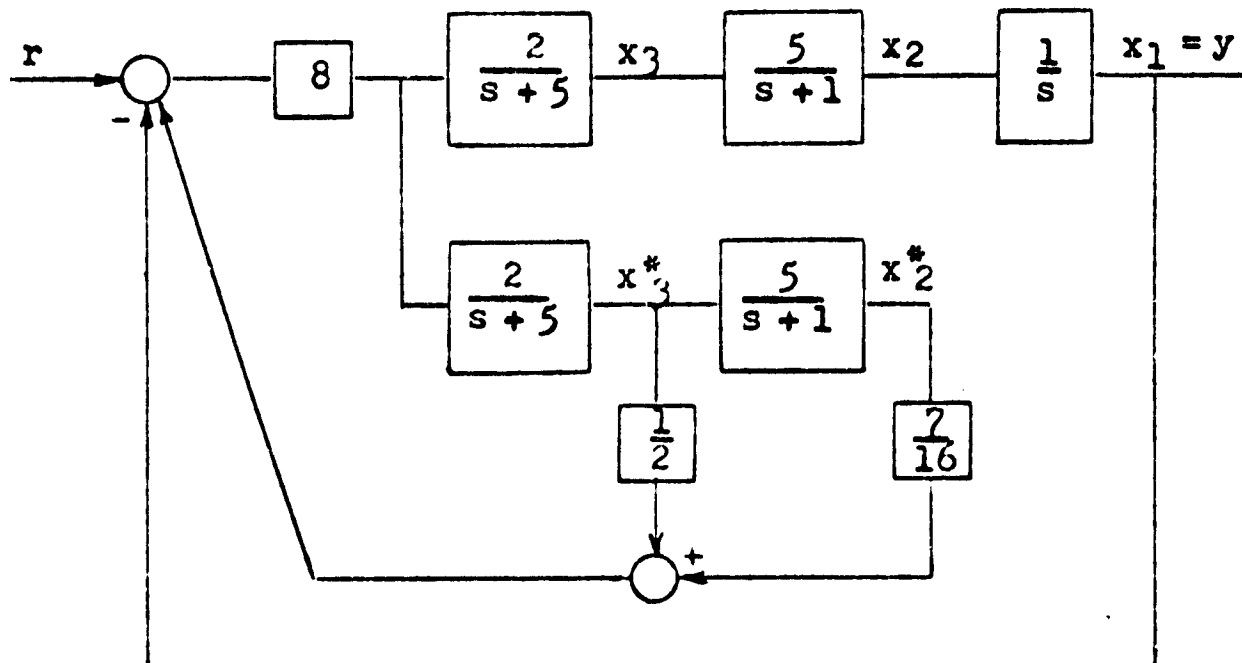


Figure 3.6 Parallel Simulation System

The parallel simulation system is shown in Figure 3.6. The corresponding series compensator calculated from this configuration is

$$G_c = \frac{8(s + 5)(s + 1)}{(s + 6)(s + 8)}$$

This is the same as was found using the Guillemin-Truxal approach, and the parallel simulation scheme is simply a way of mechanizing the required equalizer. Of course, the sensitivity of the closed-loop system to plant parameter variations is unaffected by how G_c is realized.

The peak and integral sensitivities of the plant parameters for the series-compensated (or parallel simulation) system were calculated. Also calculated were the sensitivities for the state-variable feedback configuration and the corresponding $H_{eq}(s)$ system of Chapter II. A computer program, written from White's (1967) thesis, was utilized to obtain the sensitivities which are listed in Table 3.1.

The sensitivities of the gain, K_1 , in the output block are the same for the series-compensated system and for the state-variable feedback configuration. The sensitivities of the parameters in the inner blocks are reduced appreciably for the state variable system. The inner most block of the state-variable feedback system is the least sensitive, because it is surrounded by the greatest number of feedback paths. All blocks of the $H_{eq}(s)$ system exhibit

Table 3.1 Sensitivities for Parallel Simulation Example

Param- eter	System		
	1	2	3
K_1	.593	.140	.593
K_2	.321	.140	.593
K_3	.140	.140	.593
P_2	.148	.061	.329
P_3	.120	.120	.548

Peak Sensitivity

Param- eter	System		
	1	2	3
K_1	.286	.012	.286
K_2	.067	.012	.286
K_3	.012	.012	.286
P_2	.019	.0031	.133
P_3	.0096	.0096	.260

Integral Sensitivity

System	Description
1	State-Variable Feedback
2	$H_{eq}(s)$ System
3	Series Compensation or Parallel Simulation

sensitivities of the same order of magnitude as the innermost block of the state-variable feedback configuration, but, unless the plant has the same number of poles as zeroes, the resulting $H_{eq}(s)$ is not physically realizable.

Observe that $H_{eq}(s)$ is driven only by the output of the system, and not by the input. Therefore, the system used to generate the unavailable states should be weighted heavily on the output of the plant. The next two chapters look at schemes for generating unavailable states that are dependent on both the input and the output of the plant.

An intuitive feeling for the poor sensitivity characteristics associated with the parallel simulation configuration can be obtained by considering Figure 3.7. If a parameter in one of the blocks of the plant is perturbed, say G_3 , the control, u , is not affected immediately, as it would be if the states were fed back directly from the plant. By using state-variable feedback, the control always knows what the plant is doing.

The parallel simulation configuration may be looked at as merely a block diagram manipulation where the origins of all the feedback coefficients (except the output) are moved to the input of the plant. This technique may be of value when a small percentage of the states are unavailable, as discussed in Chapter 9 of Schultz and Melsa (1967). However, it should not be considered when only the output is available for control.

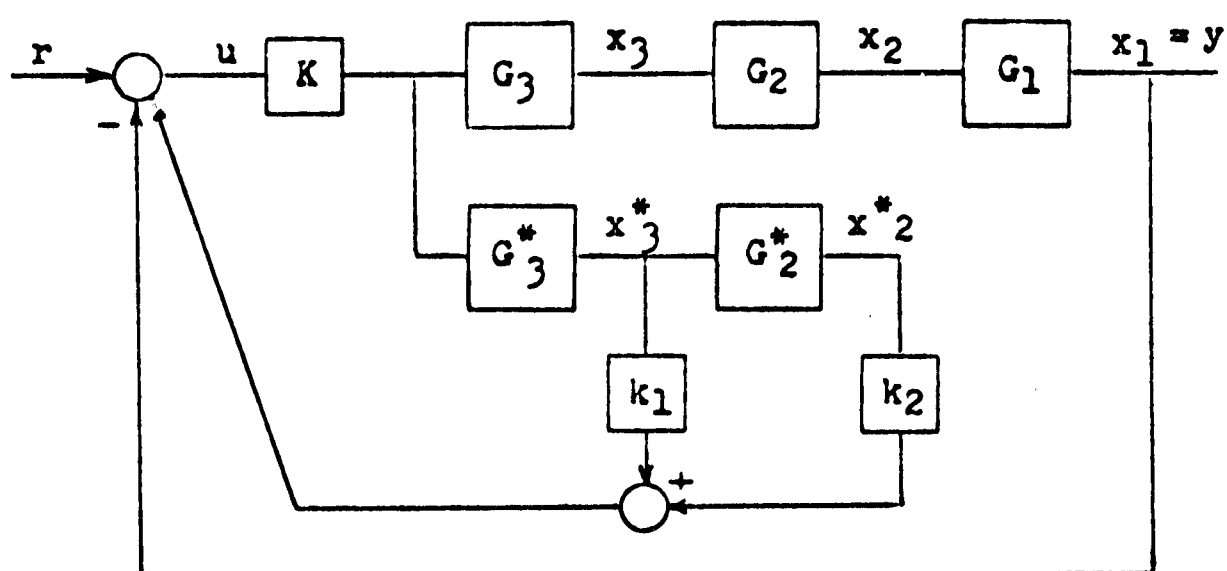


Figure 3.7 Third-Order System

CHAPTER IV

OBSERVER SYSTEM

This chapter discusses another method of generating unavailable state variables. An observer, as developed by Luenberger (1963), is used to generate the unavailable states. The observer is a second linear system that is driven by the available outputs and the input to the plant. The states of the new system are related to the unavailable states of the plant by a linear transformation.

The generated states, along with the available states of the plant, are fed back to realize a desired closed-loop response. New feedback coefficients are defined, but, as the poles of the observer are moved out to improve the sensitivities of the plant parameters, the new feedback coefficients become very large.

4.1 Observer Theory

The theory is developed in matrix notation. Most modern control theory texts, such as Schultz and Melsa (1967), describe the representation of control systems using matrices.

The time-invariant linear plant of n th order is described by the matrix differential equation (2.1), repeated here as

$$\dot{\underline{x}} = \underline{A}\underline{x} + \underline{b}u \quad (4.1)$$

where

\underline{x} is an $(n \times 1)$ state vector

\underline{A} is an $(n \times n)$ system matrix

\underline{b} is an $(n \times 1)$ input vector

u is the scalar control input

The state vector, \underline{x} , completely describes the present state of the system, and the future behavior is governed by the first-order matrix differential equation (4.1).

If it is only desired to generate the unavailable states of the plant, then the observer is of m th order, where m is the number of unavailable states. The observer is also described by a first-order matrix differential equation of the form

$$\dot{\underline{z}} = \underline{D}\underline{z} + \underline{E}\underline{x} + \underline{g}u \quad (4.2)$$

where

\underline{z} is an $(m \times 1)$ state vector

\underline{D} is an $(m \times m)$ system matrix

\underline{E} is an $(m \times n)$ input matrix

g is an $(m \times 1)$ input vector

\underline{x} and u are as defined in equation (4.1)

It is assumed that the states of the observer and the plant are related by a linear transformation

$$\underline{z} = \underline{T} \underline{x} \quad (4.3)$$

Equation (4.3) is substituted into equation (4.2) for \underline{z} and $\dot{\underline{z}}$ to find the relations that the observer matrices must satisfy. If this is done, then

$$\underline{T} \dot{\underline{x}} = (\underline{D} \underline{T} + \underline{F}) \underline{x} + \underline{g} u \quad (4.4)$$

Equation (4.1) is pre-multiplied by \underline{T} to give

$$\underline{T} \dot{\underline{x}} = \underline{T} \underline{A} \underline{x} + \underline{T} \underline{b} u \quad (4.5)$$

Comparing equations (4.4) and (4.5) shows

$$\underline{D} \underline{T} + \underline{F} = \underline{T} \underline{A}$$

or

$$\underline{T} \underline{A} - \underline{D} \underline{T} = \underline{F} \quad (4.6)$$

and

$$\underline{g} = \underline{T} \underline{b} \quad (4.7)$$

The matrices \underline{A} and \underline{b} are known. If the observer is chosen, equation (4.6) may be solved for \underline{T} . If \underline{A} and \underline{D} have no common eigenvalues.

It is originally assumed that \underline{z} and \underline{x} were related by a linear transformation. That this is a valid assumption may be shown in the following way. Equation (4.5) is subtracted from equation (4.2), giving

$$\dot{\underline{z}} - \underline{T}\dot{\underline{x}} = \underline{D}\underline{z} - \underline{T}\underline{A}\underline{x} + \underline{E}\underline{x} + (\underline{g} - \underline{T}\underline{b})\underline{u} \quad (4.6)$$

Using equation (4.6) to substitute for $\underline{T}\underline{A}$ in the above equation gives

$$\dot{\underline{z}} - \underline{T}\dot{\underline{x}} = \underline{D}(\underline{z} - \underline{T}\underline{x}) \quad (4.9)$$

By choosing $\underline{g} = \underline{T}\underline{b}$, the above differential equation can be integrated giving

$$\underline{z} = \underline{T}\underline{x} + e^{\underline{D}t} [\underline{z}(0) - \underline{T}\underline{x}(0)] \quad (4.10)$$

If the initial conditions are also related by the linear transformation, the second term drops out, and

$$\underline{z} = \underline{T}\underline{x}$$

It is probable that the initial conditions do not match; therefore, the eigenvalues of \underline{D} should be chosen sufficiently far out in order for the initial condition term in equation (4.10) to be small after a short time.

This initial condition term represents the error between \underline{z} and $T\underline{x}$, and the sooner it disappears, the better.

4.2 An Example

As an example of how the equations are solved, consider again the example of Chapter III. The plant is shown again in Figure 4.1. It is assumed that x_2 and x_3 are unavailable. The system matrix for the plant is

$$\underline{A} = \begin{bmatrix} 0 & 1 & 0 \\ 0 & -1 & 5 \\ 0 & 0 & -5 \end{bmatrix}$$

and for $K = 8$, the input vector, \underline{b} , is

$$\underline{b} = \begin{bmatrix} 0 \\ 0 \\ 16 \end{bmatrix}$$

The observer, with its poles chosen at $s = -6$ and $s = -7$, is shown in Figure 4.2. The system matrix for the observer is

$$\underline{D} = \begin{bmatrix} -7 & 1 \\ 0 & -6 \end{bmatrix}$$

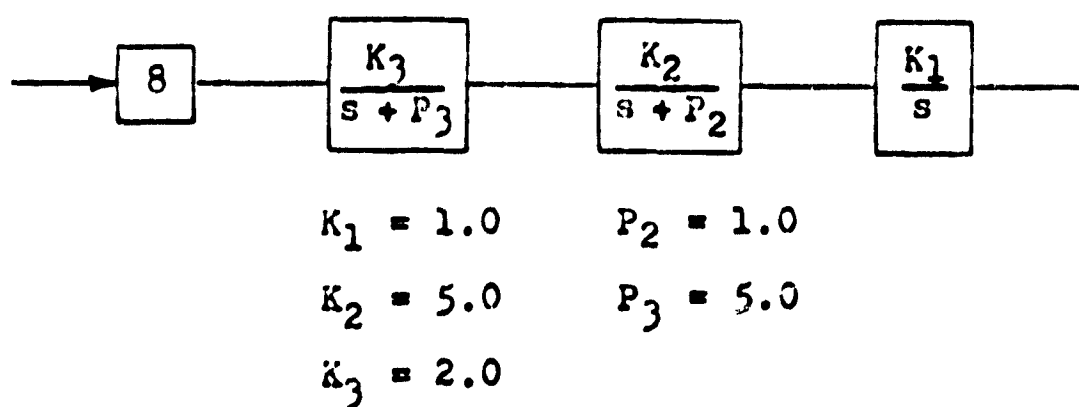


Figure 4.1 Open-Loop Plant

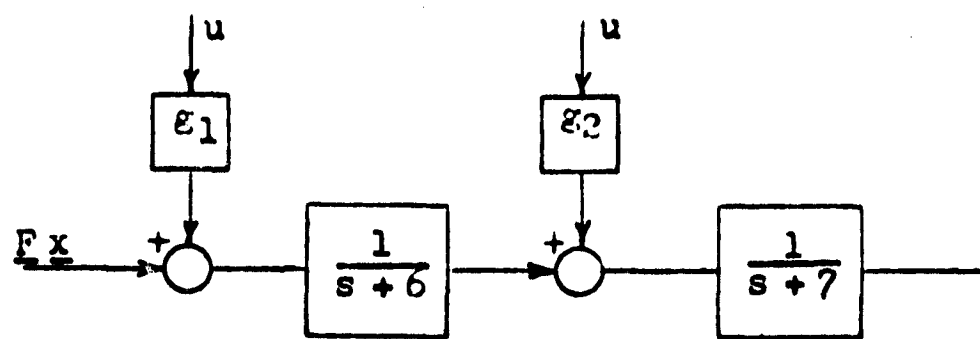


Figure 4.2 Observer

The (2×3) transformation matrix, \underline{T} , is found using equation (4.6), and it is repeated here as

$$\underline{T} \underline{A} - \underline{D} \underline{T} = \underline{F}$$

where

$$\underline{T} = \begin{bmatrix} t_{11} & t_{12} & t_{13} \\ t_{21} & t_{22} & t_{23} \end{bmatrix}$$

and the input matrix for the observer is

$$\underline{F} = \begin{bmatrix} 0 & 0 & 0 \\ 1 & 0 & 0 \end{bmatrix}$$

After substituting the appropriate matrices into equation (4.6), the result is

$$\begin{bmatrix} t_{11} & t_{12} & t_{13} \\ t_{21} & t_{22} & t_{23} \end{bmatrix} \begin{bmatrix} 0 & 1 & 0 \\ 0 & -1 & 5 \\ 0 & 0 & -5 \end{bmatrix} - \begin{bmatrix} -7 & 1 \\ 0 & -6 \end{bmatrix} \begin{bmatrix} t_{11} & t_{12} & t_{13} \\ t_{21} & t_{22} & t_{23} \end{bmatrix} = \begin{bmatrix} 0 & 0 & 0 \\ 1 & 0 & 0 \end{bmatrix}$$

Performing the above matrix multiplications and equating

corresponding elements results in the following set of equations for the elements of \underline{T} :

$$7t_{11} - t_{21} = 0$$

$$t_{11} + 6t_{12} + t_{22} = 0$$

$$5t_{12} + 2t_{13} - t_{23} = 0$$

$$6t_{21} = 1$$

$$t_{21} + 5t_{22} = 0$$

$$5t_{22} + t_{23} = 0$$

The preceding equations may be solved to give

$$\underline{T} = \begin{bmatrix} \frac{1}{42} & -\frac{1}{105} & \frac{3}{28} \\ \frac{1}{6} & -\frac{1}{30} & \frac{1}{6} \end{bmatrix}$$

Now the control input vector for the observer is found from

$$\underline{g} = \underline{T} \underline{b}$$

as

$$\underline{g} = \begin{bmatrix} \frac{12}{7} \\ \frac{8}{3} \end{bmatrix}$$

The unavailable states of the plant are now found in terms of the available states of the plant and the states of the observer using equation (4.3) as

$$\begin{bmatrix} z_1 \\ z_2 \end{bmatrix} = \begin{bmatrix} \frac{1}{42} & -\frac{1}{105} & \frac{3}{28} \\ \frac{1}{6} & -\frac{1}{30} & \frac{1}{6} \end{bmatrix} \begin{bmatrix} x_1 \\ x_2 \\ x_3 \end{bmatrix}$$

Solving for x_2 and x_3 gives

$$x_2^* = 7x_1 + 84z_1 - 54z_2$$

$$x_3^* = \frac{2}{5}x_1 + \frac{84}{5}z_1 - \frac{24}{5}z_2$$

where the stars have been introduced to indicate that x_2^* and x_3^* are only estimates of the actual states of the plant.

Figure 4.3 shows the plant and observer with the generated states. The feedback coefficients, that were found in Chapter II for this problem, could now be fed back from x_1 , x_2^* , and x_3^* to give the desired closed-loop response. Rather than actually finding x_2^* and x_3^* , it is simpler to find new feedback coefficients that are fed back directly from z_1 , z_2 , and x_1 . The next section defines new feedback coefficients in terms of the transformation matrix and the original feedback coefficients.

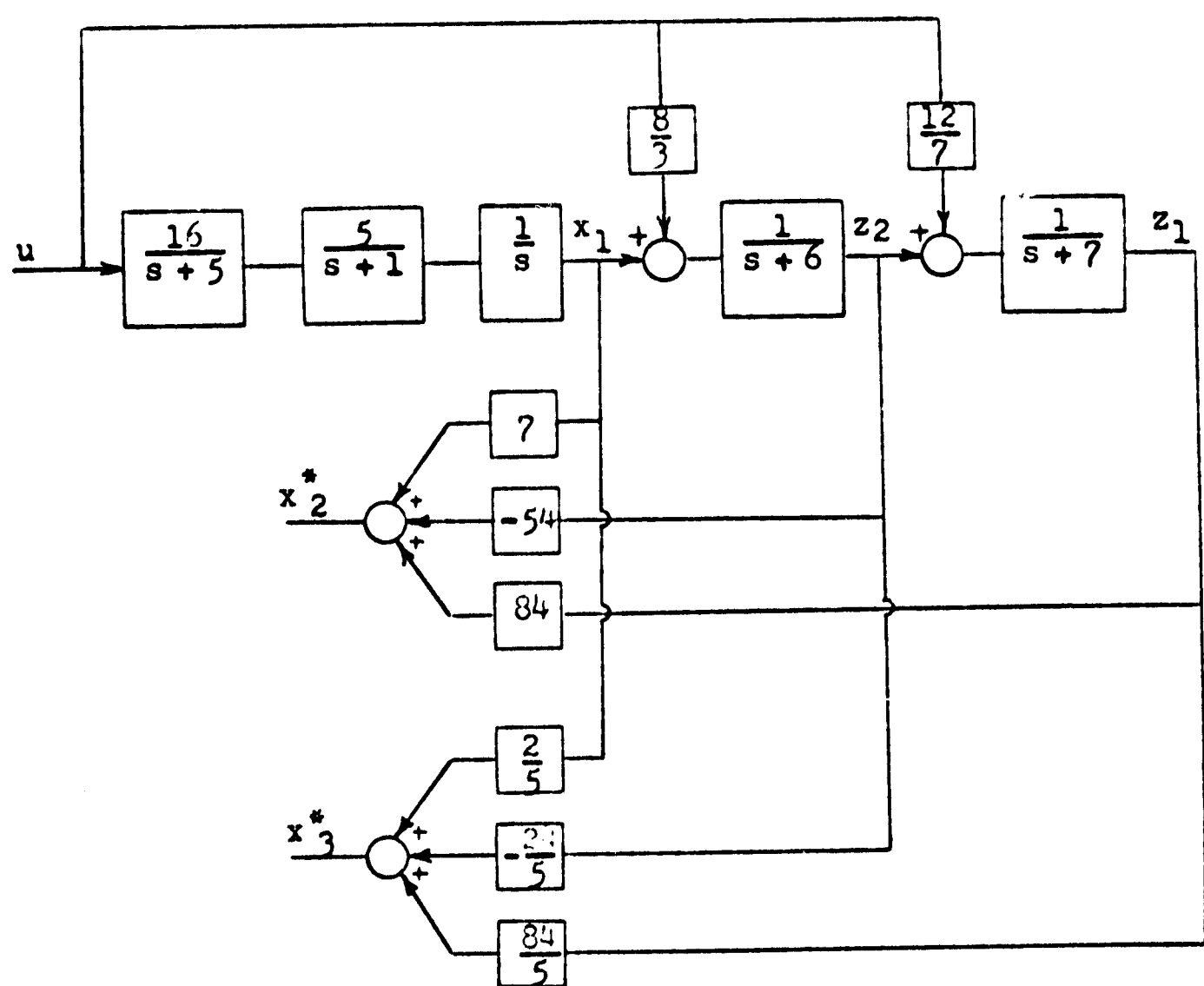


Figure 4.3 Plant and Observer with Generated States

4.3 Closed-Loop System

This section discusses the closed-loop system and defines new feedback coefficients. The state-variable feedback coefficients can be found as if all the states are available, and the available states of the plant and the generated states can be used for control. It is simpler to find new feedback coefficients that may be fed back directly from the available states and the states of the observer.

It should be pointed out that the overall response using an observer is of $n + m$ order. However, the poles of the observer show up as poles and zeroes of the overall response and cancel to give the desired n th-order response. If any of the parameters of the system are perturbed, the cancellation is inexact and the response is of $m + m$ order.

The new feedback coefficients, \underline{k}^* , are found as follows. The \underline{k} and \underline{x} vectors and the \underline{T} matrix are partitioned as

$$\underline{x} = \begin{bmatrix} \underline{x}^1 \\ \underline{x} \\ \cdots \\ \underline{x}^2 \end{bmatrix}$$

$$\underline{k}^T = \begin{bmatrix} \underline{k}^{1T} & | & \underline{k}^{2T} \end{bmatrix}$$

$$\underline{T} = \begin{bmatrix} \underline{T}^1 & | & \underline{T}^2 \end{bmatrix}$$

where

\underline{x}^1 is the available states $((n - m) \times 1)$

\underline{x}^{*2} is the generated unavailable states $(m \times 1)$

\underline{k}^1 corresponds to the available states $((n - m) \times 1)$

\underline{k}^2 corresponds to the unavailable states $(m \times 1)$

\underline{T}^1 is an $((n - m) \times m)$ matrix

\underline{T}^2 is an $(m \times m)$ matrix

In terms of the partitioned matrices, equation (4.3) is solved for the unavailable states, as

$$\underline{z} = \begin{bmatrix} \underline{T}^1 & \underline{T}^2 \end{bmatrix} \begin{bmatrix} \underline{x}^1 \\ \underline{x}^{*2} \end{bmatrix}$$

or

$$\underline{x}^{*2} = (\underline{T}^2)^{-1} (\underline{z} - \underline{T}^1 \underline{x}^1)$$

The feedback is

$$\underline{k}^{1T} \underline{x}^1 + \underline{k}^{2T} \underline{x}^{*2}$$

Substituting for \underline{x}^{*2} gives

$$\underline{k}^{2T} (\underline{T}^2)^{-1} \underline{z} + \underline{k}^{1T} - \underline{k}^{2T} (\underline{T}^2)^{-1} \underline{T}^1 \underline{x}^1$$

The new feedback vector is

$$\underline{k}^{*T} = \begin{bmatrix} \underline{k}^{2T}(\underline{T}^2)^{-1} & | & (\underline{k}^{1T} - \underline{k}^{2T}(\underline{T}^2)^{-1} \underline{T}^1) \end{bmatrix} \quad (4.11)$$

The closed-loop system configuration, in terms of the new feedback coefficients, is as shown in Figure 4.4 for the case where only the output is available. The steps involved in solving a closed-loop problem are listed in Figure 4.5.

4.4 Closed-Loop Example

A second-order plant with one unavailable state is chosen. The single pole of the observer is left arbitrary to show the effect of different pole locations. The example is almost trivial, but it suffices to demonstrate how the new feedback coefficients become large as the poles of the observer are moved out.

The plant to be controlled and the chosen observer are shown in Figure 4.6. The desired closed-loop response is

$$\frac{y(s)}{r(s)} = \frac{6}{s^2 + 3s + 6}$$

Letting k_1 equal unity for zero steady-state position

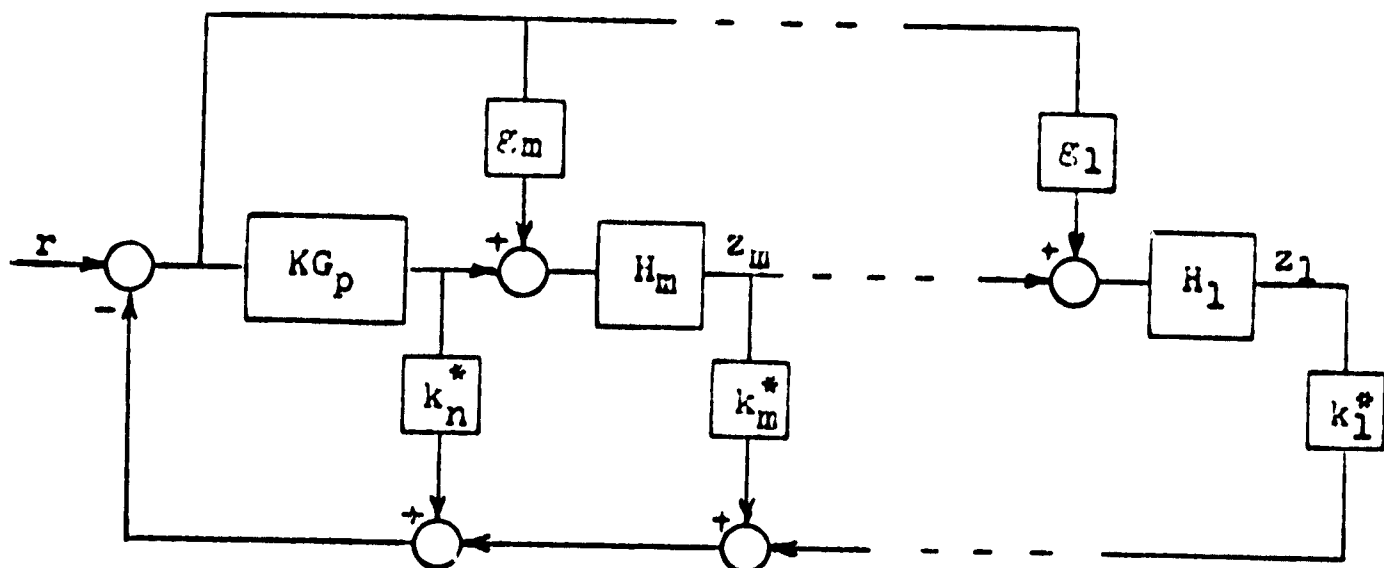


Figure 4.4 Closed-Loop System

Step	Description
1	Find \underline{k} and K as if all states were available
2	Choose an observer of m th order
3	Solve $\underline{T}\underline{A} - \underline{D}\underline{T} = \underline{E}$ for \underline{T}
4	Find \underline{g} using $\underline{g} = \underline{T}\underline{b}$
5	Find new feedback coefficients using $\underline{k}^{*T} = \begin{bmatrix} \underline{k}^2 \underline{T} (\underline{T}^2)^{-1} & & (\underline{k}^1 \underline{T} - \underline{k}^2 \underline{T} (\underline{T}^2)^{-1} \underline{T}^1) \end{bmatrix}$

Figure 4.5 Steps in Solving Closed-Loop Problem

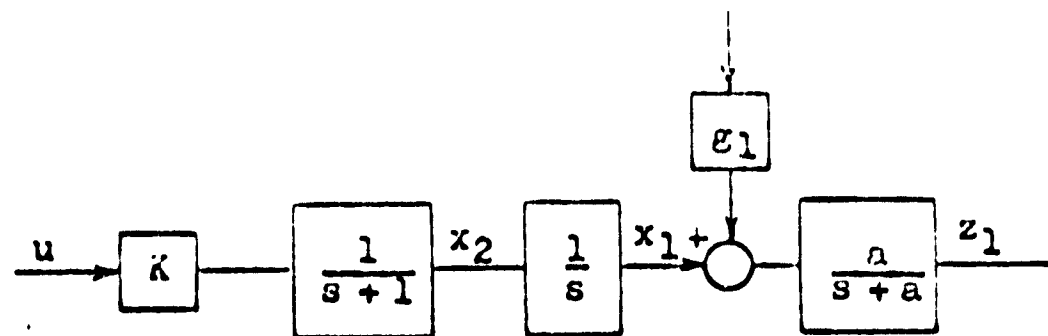


Figure 4.6 Plant and Observer

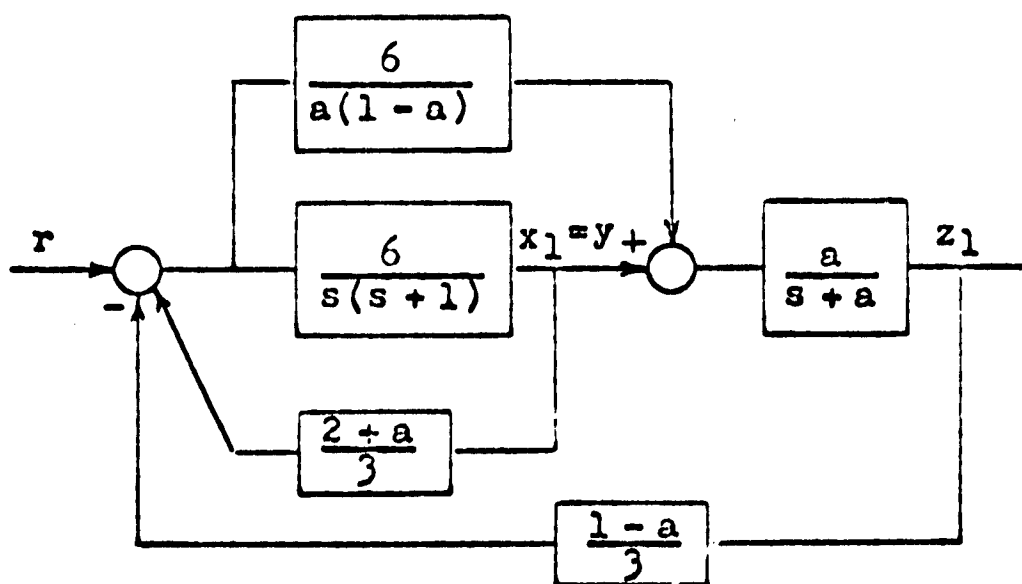


Figure 4.7 Closed-Loop System

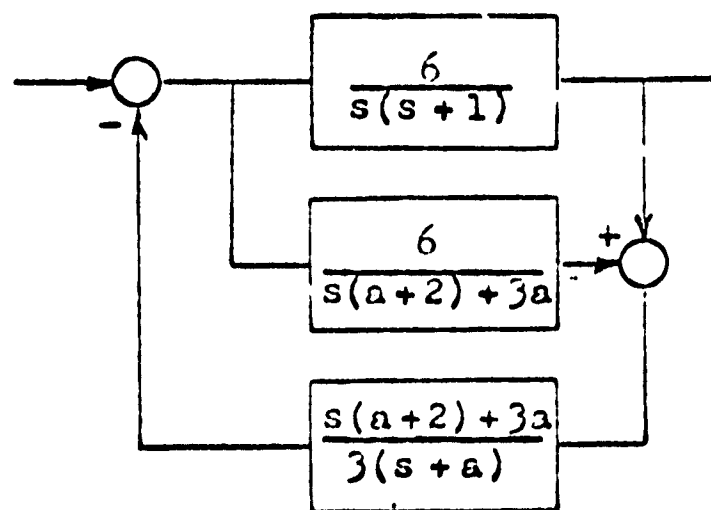


Figure 4.8 Modified Closed-Loop System

error, the \underline{k} vector and K are

$$\underline{k}^T = \begin{bmatrix} 1.0 & 1/3 \end{bmatrix}$$

$$K = 6.0$$

The \underline{A} and \underline{b} matrices are

$$\underline{A} = \begin{bmatrix} 0 & 1 \\ 0 & -1 \end{bmatrix} \quad \underline{b} = \begin{bmatrix} 0 \\ 6 \end{bmatrix}$$

The \underline{D} matrix reduces to a scalar, $-a$, for this problem.

Solving $\underline{T}\underline{A} - \underline{D}\underline{T} = \underline{E}$ for \underline{T} , gives

$$\underline{T} = \begin{bmatrix} 1 & \frac{1}{1-a} \end{bmatrix}$$

The input vector for the observer is

$$g = \frac{b}{a(1-a)}$$

The new feedback coefficients are

$$\underline{k}^{*T} = \begin{bmatrix} \frac{1}{3}(1-a) & \frac{1}{3}(2+a) \end{bmatrix}$$

The closed-loop system is shown in Figure 4.7.

As "a" is increased in Figure 4.7, the new feedback coefficients become large. One feedback coefficient goes towards plus infinity and the other towards negative infinity, while the weighting on u becomes small. It is suspected that letting "a" go to infinity would result in $H_{\text{equivalent}}(s)$, since $H_{\text{eq}}(s)$ has its poles at infinity (if the plant contains no zeroes) and has zero weighting on u . As "a" becomes infinite in Figure 4.8, the network that is driven by u goes to zero while the feedback network becomes $H_{\text{eq}}(s)$; that is,

$$\lim_{a \rightarrow \infty} \frac{6}{s(a + 2) + 3a} = 0$$

and

$$\lim_{a \rightarrow \infty} \frac{3(a + 2) + 3a}{3(s + a)} = \frac{1}{3}s + 1$$

The configuration of Figure 4.7 still gives zero steady-state error, since the original k_1 was unity, even though k_2^* is not unity. For a step input, in the steady-state, there is still a signal being applied to the observer. The feedback from the observer and the plant add up to one in the steady-state to give zero position error. Unfortunately, the new feedback coefficients become large as the observer pole is moved out. The next section shows, by example, the effect of observer pole location on plant sensitivities.

4.5 Sensitivity Example

This section considers again the third-order example of Chapter II and III. The problem was started in section 4.1 with the poles of the observer at $s = -6$ and $s = -7$, but the new feedback coefficients have yet to be found. The plant sensitivities and final system for the same problem with the observer poles at $s = -10$ and $s = -12$ are also given.

The feedback coefficients to realize the closed-loop response

$$\frac{y(s)}{r(s)} = \frac{80}{(s + 10)(s^2 + 4s + 8)}$$

for the plant of Figure 4.1 were found in Chapter II to be

$$\underline{k}^T = \begin{bmatrix} 1.0 & \frac{7}{16} & \frac{1}{2} \end{bmatrix}$$

The new feedback coefficients are found using equation (4.11), repeated below

$$\underline{k}^{*T} = \begin{bmatrix} \underline{k}^{2T}(\underline{T}^2)^{-1} & | & (\underline{k}^{1T} - \underline{k}^{2T}(\underline{T}^2)^{-1}\underline{T}^1) \end{bmatrix}$$

where

$$\underline{T}^1 = \begin{bmatrix} \frac{1}{42} \\ \frac{1}{6} \end{bmatrix} \quad (\underline{T}^2)^{-1} = \begin{bmatrix} 84 & -54 \\ \frac{84}{5} & -\frac{24}{5} \end{bmatrix}$$

and

$$\underline{k}^1 = 1 \quad \underline{k}^2 = \begin{bmatrix} \frac{2}{16} \\ \frac{1}{2} \end{bmatrix}$$

The new feedback vector becomes

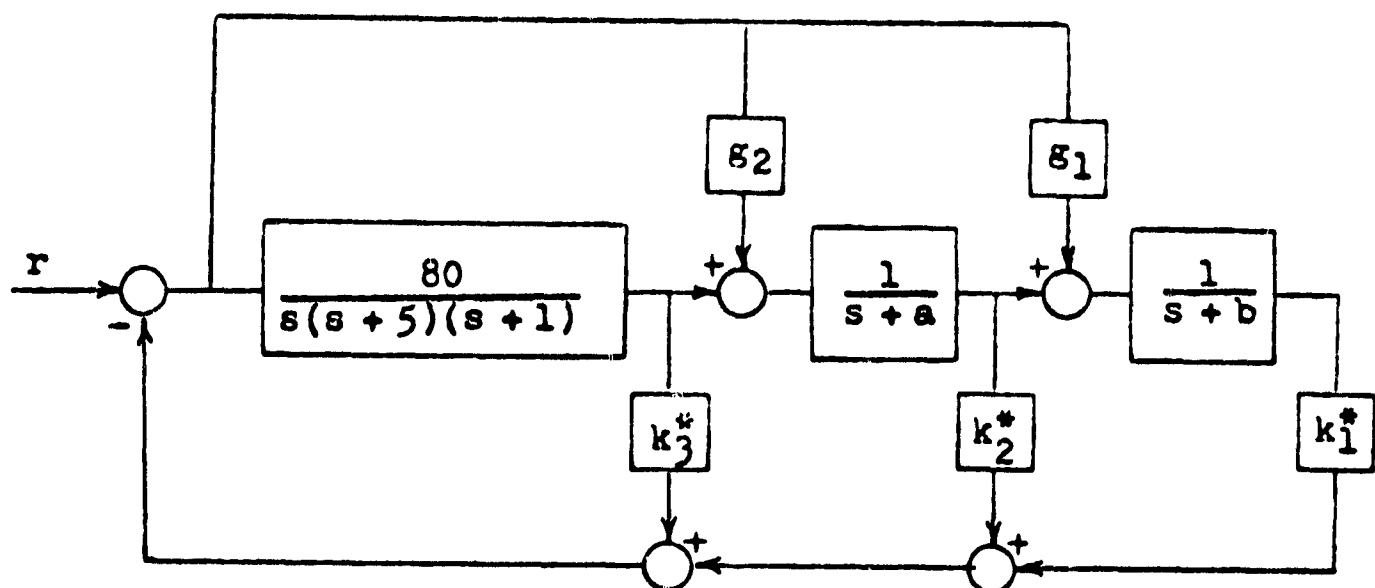
$$\underline{k}^{*T} = \begin{bmatrix} \frac{903}{20} & -\frac{1041}{40} & \frac{341}{80} \end{bmatrix}$$

or

$$\underline{k}^{*T} = \begin{bmatrix} 45.15 & -26.02 & 4.26 \end{bmatrix}$$

The final closed-loop system is shown in Figure 4.9. The parameter values that result if the observer poles are picked at 10 and 12 are also given. Moving the observer poles about twice as far out has increased the feedback coefficients tremendously.

Table 4.1 lists the peak and integral sensitivities of the plant parameters for both observer systems. The sensitivities for the state-variable feedback configuration, the $H_{eq}(s)$ configuration, and the series-compensated system are also shown again for comparison. The data for the $H_{eq}(s)$ system is included because it is the least sensitive system, but it is not physically realizable.



Parameter	Poles of Observer at	
	6 & 7	10 & 12
$a & b$		
g_1	1.86	.0156
g_2	2.77	.178
k_1^*	45.2	866.2
k_2^*	-26.1	-177.2
k_3^*	4.26	11.5

Figure 4.9 Closed-Loop System

Table 4.1 Sensitivities for Observer System

Param- eter	System				
	1	2	3	4	5
K_1	.593	.140	.593	.401	.317
K_2	.321	.140	.593	.401	.317
K_3	.140	.140	.593	.401	.317
P_2	.148	.061	.329	.190	.144
P_3	.120	.120	.548	.358	.279

Peak Sensitivities

Param- eter	System				
	1	2	3	4	5
K_1	.286	.012	.286	.106	.063
K_2	.067	.012	.286	.106	.063
K_3	.012	.012	.286	.106	.063
P_1	.019	.0031	.133	.032	.017
P_2	.0096	.0096	.260	.092	.053

Integral Sensitivities

System	Description
1	State-Variable Feedback
2	$H_{eq}(s)$ Configuration
3	Series Compensation or Parallel Simulation
4	Observer System with Poles at $s = -6$ and $s = -7$
5	Observer System with Poles at $s = -10$ and $s = -12$

It appears that the observer approach may be of value if the large feedback coefficients can be avoided. The next chapter looks at a modification of the observer system that attempts to eliminate the large feedback coefficients.

CHAPTER V

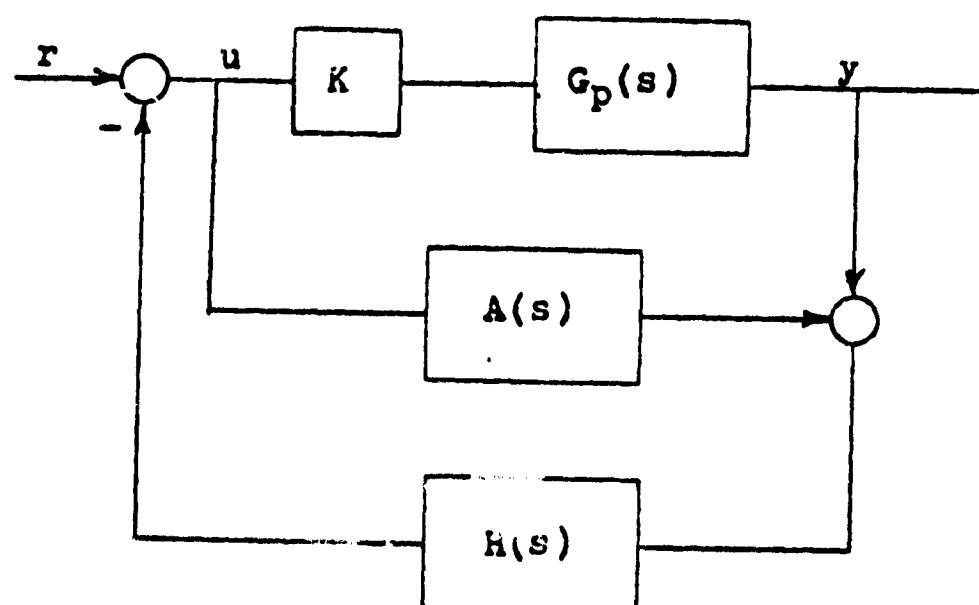
MODIFIED OBSERVER SYSTEM

This chapter discusses a modification of the closed-loop observer system. This new configuration has been developed in an attempt to avoid the large feedback coefficients that result when the observer poles are chosen far out. The modified observer system is developed for the "worst" case where only the output state is available. It is also shown how the technique may be applied when additional states are available.

5.1 System Configuration

The new system configuration was discovered by manipulating second and third order observer systems. A second order example is shown in Figure 4.8. The general system configuration is shown in Figure 5.1. The feedback is a function of both the input, u , and the output of the plant as in the observer system. In Figure 5.1, $KG_p(s)$ is the plant and associated gain. If n is the order of the plant, $A(s)$ is defined as

$$A(s) = \frac{a_{n-2}s^{n-2} + \dots + a_1s + a_0}{h_{n-1}s^{n-1} + \dots + h_1s + h_0} \quad (5.1)$$



$$G_p(s) = G_1(s) \cdot G_2(s) \dots G_n(s)$$

Figure 5.1 General System Configuration

and $H(s)$ is defined as

$$H(s) = \frac{h_{n-1}s^{n-1} + \dots + h_1s + h_0}{b_{n-1}s^{n-1} + \dots + b_1s + b_0}$$

The denominator of $A(s)$ is the same as the numerator of $H(s)$. The $n-1$ roots of the denominator of $H(s)$ are chosen in the same manner as the poles of the observer. These roots may be distinct or all the same.

The example of section 5.2 shows that the sensitivities of the plant parameters improve as these poles are moved further out. As the poles of $H(s)$ are moved out, the weighting on u decreases and $H(s)$ looks like an approximate realization of $H_{eq}(s)$. White (1967) showed that for the $H_{eq}(s)$ configuration the sensitivities of the plant parameters were, in general, better than the sensitivities for a state-variable feedback system. If the plant has no zeroes, $H_{eq}(s)$ has its poles at infinity, and the weighting on u is zero.

It is simpler to solve directly for the transfer functions $A(s)$ and $H(s)$ rather than manipulating an observer system. To solve a problem using this new configuration, $y(s)/r(s)$ is found from Figure 5.1 in terms of the transfer functions.

$$\frac{y(s)}{r(s)} = \frac{KG_p(s)}{1 + H(s) [KG_p(s) + A(s)]} \quad (5.2)$$

If $G_p(s)$, $H(s)$, and $A(s)$ are written in terms of numerator and denominator polynomials as,

$$G_p(s) = \frac{GN}{GD}$$

$$H(s) = \frac{HN}{HD}$$

$$A(s) = \frac{AN}{AD} \quad (5.3)$$

then $y(s)/r(s)$ can be written in terms of these polynomials by substituting the equations (4.3) into (5.2) as

$$\frac{y(s)}{r(s)} = \frac{K \cdot GN \cdot HD \cdot AD}{HD \cdot GD \cdot AD + K \cdot GN \cdot HN \cdot AD + AN \cdot GD \cdot HN}$$

Since AD was chosen equal to HN , the AD 's can be cancelled in the above expression to give

$$\frac{y(s)}{r(s)} = \frac{K \cdot GN \cdot HD}{HD \cdot GD + K \cdot GN \cdot HN + AN \cdot GD} \quad (5.4)$$

where GN and GD are known, HD is chosen, K is the same as for a state-variable feedback system, and HN and AN are unknown. Assuming the desired closed-loop response is known, its numerator and denominator can be multiplied by HD to give the actual response that is realized. Now the coefficients of the actual response and equation (5.4) can be equated and the unknown coefficients of $A(s)$ and $H(s)$ found.

In general, the denominator of the closed-loop response, equation (5.4), is of $(2n - 1)$ order. To see this, consider a fourth-order plant as an example. The denominator of the closed-loop response is

$$HD \cdot GD + K \cdot GN \cdot HN + AN \cdot GD \quad (5.5)$$

where, from equation 5.1

$$AN = a_2s^2 + a_1s + a_0$$

and

$$HN = h_3s^3 + h_2s^2 + h_1s + h_0$$

The denominator of the plant transfer function is represented by

$$GD = s^4 + g_3s^3 + g_2s^2 + g_1s + g_0$$

and the numerator is a constant, that is

$$GN = K$$

Since the first term in equation (5.5) is known, let it be represented as

$$HD \cdot GD = s^7 + c_6s^6 + \dots + c_1s + c_0$$

These polynomials are substituted into equation (5.5), multiplications are performed, and like powers combined.

to give

$$\begin{aligned}
 & s^7 + (c_6 + g_4a_2)s^6 + (c_5 + g_3a_2 + g_4a_1)s^5 \\
 & + (c_4 + g_2a_2 + g_3a_1 + a_0)s^4 + (c_3 + g_1a_2 \\
 & + g_2a_1 + g_3a_0 + kh_3)s^3 + (c_2 + g_0a_2 + g_1a_1 \\
 & + g_2a_0 + kh_2)s^2 + (c_1 + g_0a_1 + g_1a_0 + kh_1)s \\
 & + (c_0 + g_0a_0 + kh_0)
 \end{aligned}$$

In the above expression, the a's and h's are the unknowns. Starting with the highest power of s, each successive term contains a new unknown, so that any 7th order polynomial could be realized by the proper selection of the a's and h's. Section 5.2 shows the equations for a third-order example. In the general case, the characteristic equation is of the form

$$\begin{aligned}
 & s^{2n-1} + (c_{2n-2} + g_n a_{n-2})s^{2n-2} + (c_{2n-3} + g_n a_{n-3}) \\
 & + g_{n-1} a_{n-2})s^{2n-3} + \dots + (c_1 + g_0 a_1 + g_1 a_0 \\
 & + kh_1)s + (c_0 + g_0 a_0 + kh_0)
 \end{aligned}$$

where a new "a" term appears in each successive term, such that the s^n term contains a_0 through a_{n-2} . The first "h" term, h_{n-1} , appears in the s^{n-1} term, with a new "h" appearing in each successive term.

If the plant possesses zeroes, the h 's will appear in higher order terms. If an n th-order plant contains one zero, there is an h_{n-1} term in the s^n term. Therefore, the s^n term will contain two new unknowns over the s^{n+1} term. Although $(2n-1)$ equations and $(2n-1)$ unknowns still result if the plant does contain zeroes, it is not possible to say that the equations are always independent. The next section presents a third-order example with no zeroes.

5.2 Example One

As an example, consider again the problem of Chapter II, III, and IV. The plant is shown in Figure 3.4. The desired closed-loop transfer function is

$$\frac{y(s)}{r(s)} = \frac{80}{s^3 + 14s^2 + 48s + 80}$$

The poles of $H(s)$ are chosen at $s = -10$, giving

$$HD = (s + 10)^2$$

The $y(s)/r(s)$ that must actually be realized is

$$\frac{y(s)}{r(s)} = \frac{80(s + 10)^2}{(s^3 + 14s^2 + 48s + 80)(s + 10)^2} \quad (5.6)$$

or

$$\frac{y(s)}{r(s)} = \frac{80(s + 10)^2}{s^5 + 34s^4 + 428s^3 + 2440s^2 + 6400s + 8000}$$

The polynomials of equation (5.3) are

$$GN = 10$$

$$GD = s(s + 1)(s + 5)$$

$$AN = a_1s + a_0$$

$$HN = h_2s^2 + h_1s + h_0$$

$$RD = (s + 10)^2 \quad (5.7)$$

The polynomials, equations (5.7), are substituted into equation (5.4) to give

$$\begin{aligned} \frac{y(s)}{r(s)} = & \frac{10K(s^2 + 20s + 100)}{s^5 + (26 + a_1)s^4 + (225 + a_0 + 6a_1)s^3} \\ & + (700 + 5a_1 + 6a_0 + 10Kh_2)s^2 \\ & + (500 + 5a_0 + 10Kh_1)s + 10Kh_0 \end{aligned} \quad (5.8)$$

Equating the coefficients of equations (5.6) and (5.8) gives the following set of equations:

$$10K = 80$$

$$26 + a_1 = 34$$

$$225 + a_0 + 6a_1 = 428$$

$$720 + 5a_1 + 6a_0 + 10Kh_2 = 2440$$

$$500 + 5a_0 + 10Kh_1 = 61.00$$

$$10Kh_0 = 8000$$

which may be solved to give

$$K = 8.0$$

$$a_1 = 8.0$$

$$a_0 = 155.0$$

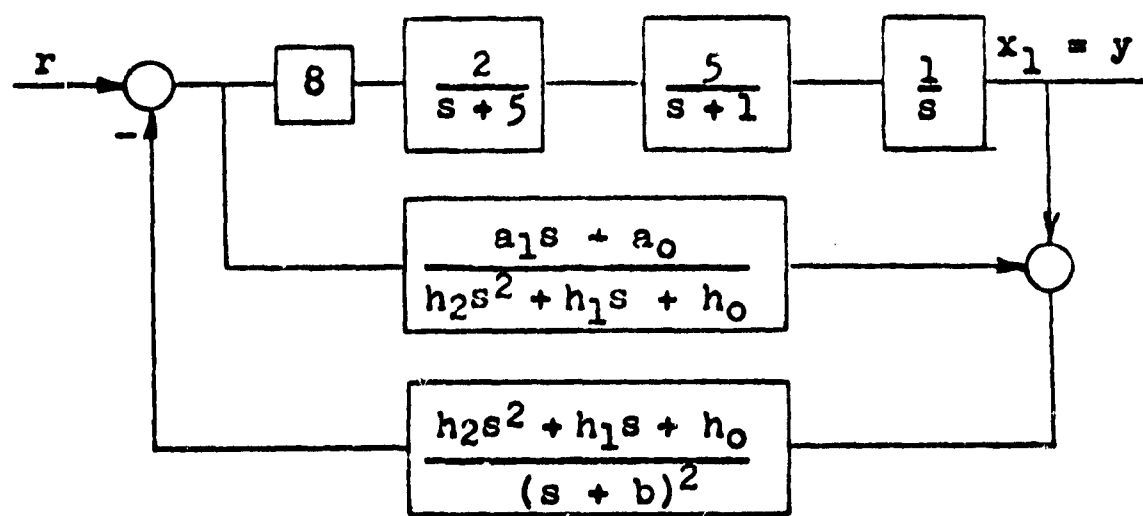
$$h_2 = 9.625$$

$$h_1 = 64.0625$$

$$h_0 = 100.0$$

The closed-loop system is shown in Figure 5.2 along with the resulting system if the poles of $H(s)$ are chosen at $s = -50$. The high frequency gain of $H(s)$, h_2 , becomes prohibitively large for the system with poles of $H(s)$ at $s = -50$. The system with poles of $H(s)$ at $s = -10$ has a reasonable value for h_2 .

Table 5.1 lists the sensitivities of the plant parameters for both systems. The results are also included for the systems considered in the previous chapters for comparison. The modified observer system with poles of $H(s)$ at $s = -10$ results in sensitivities of the same order of magnitude as for the observer system with poles of $s = -10$ and $s = -12$.



Parameter	Poles of $H(s)$	
b	10	50
a_0	155.0	795.0
a_1	8.0	8.0
h_0	100.0	2500.0
h_1	64.0625	1394.0
h_2	9.624	244.625
K	8.0	8.0

Figure 5.2 Modified Observer System for Example One

Table 4.1 Sensitivities for Modified Observer System

Param- eter	System						
	1	2	3	4	5	6	7
K_1	.593	.140	.593	.401	.317	.332	.189
K_2	.321	.140	.593	.401	.317	.332	.189
K_3	.140	.140	.593	.401	.317	.332	.189
P_1	.148	.061	.329	.190	.144	.152	.086
P_2	.120	.120	.548	.358	.279	.293	.166

Peak Sensitivities

Param- eter	System						
	1	2	3	4	5	6	7
K_1	.286	.012	.286	.106	.063	.070	.022
K_2	.067	.012	.286	.106	.063	.070	.022
K_3	.012	.012	.286	.106	.063	.070	.022
P_1	.019	.0031	.133	.032	.017	.019	.0062
P_2	.0096	.0096	.260	.092	.053	.059	.018

Integral Sensitivities

System	Description
1	State-Variable Feedback
2	$H_{eq}(s)$ Configuration
3	Series Compensation or Parallel Simulation
4	Observer System with Poles at $s = -6$ and $s = -7$
5	Observer System with Poles at $s = -10$ and $s = -12$
6	Modified Observer System, Poles at $s = -10$
7	Modified Observer System, Poles at $s = -50$

It was stated in Chapter IV that the weighting on the available outputs of the plant increased, while the weighting on the input decreased, as the poles of the observer were moved out. The poles of $H(s)$ have the same effect. To see this, consider the frequency responses (Bode) of $A(s)$ and $H(s)$ in Figures 5.3 and 5.4 respectively for the example of this section.

$H(s)$ is about the same as an approximate realization of the corresponding $H_{eq}(s)$. From Chapter II, $H_{eq}(s)$ was found to be

$$H_{eq}(s) = \frac{1}{10}s^2 + \frac{43}{80}s + 1$$

If $H_{eq}(s)$ were approximately realized by adding two poles at $s = -10$, the result is

$$H'_{eq}(s) = \frac{10s^2 + 53.7s + 100}{(s + 10)^2}$$

The corresponding $H(s)$ for the same pole location is

$$H(s) = \frac{9.524s^2 + 64.1s + 100}{(s + 10)^2}$$

Therefore, the modified observer system is like an approximate $H_{eq}(s)$ system, but the modified observer system realizes the desired response exactly.

The configuration of Figure 5.2 gives zero steady-state position error, but only if the "100" terms in the

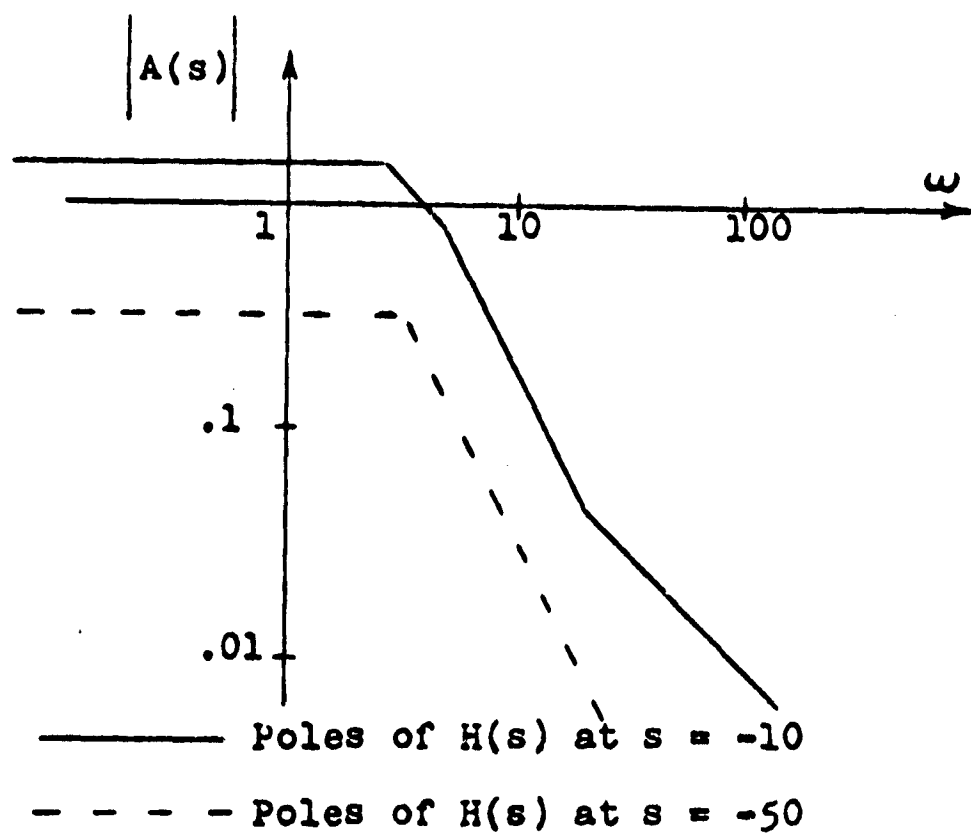


Figure 5.3 Approximate Frequency Response of $A(s)$

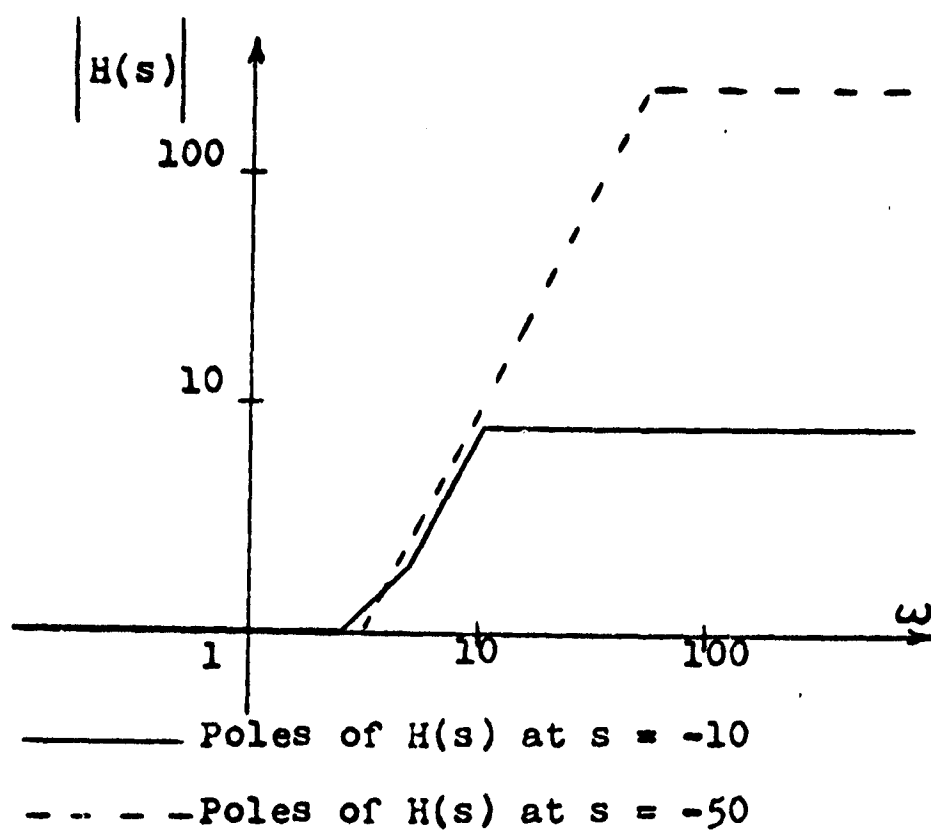


Figure 5.4 Approximate Frequency Response of $H(s)$

numerator and denominator of $H(s)$ are equal. As an alternate realization of $H(s)$, consider the configuration of Figure 5.5. Here $H(s)$ has been divided out to give

$$H(s) = 1 + \frac{s(8.625s + 41)}{s^2 + 20s + 100}$$

Now zero steady-state position error is assured by the unity feedback and the integrator at the output of the plant.

5.3 Example Two

It was stated at the beginning of the chapter that the technique could also be applied when additional states are available. This section demonstrates the procedure using the running third-order example of this study. The problem is first solved with x_1 and x_2 available and then with x_1 and x_3 available.

It is necessary to assume that the state-variable feedback coefficients and forward gain, that were found in Chapter II, are known. Figure 5.6 shows the state-variable feedback system. The technique is exactly the same as when only the output was available, but the transfer function from r to x_2 is the desired response. From Figure 5.6, this transfer function is

$$\frac{x_2(s)}{r_2(s)} = \frac{80}{s^2 + 14s + 48} \quad (5.9)$$

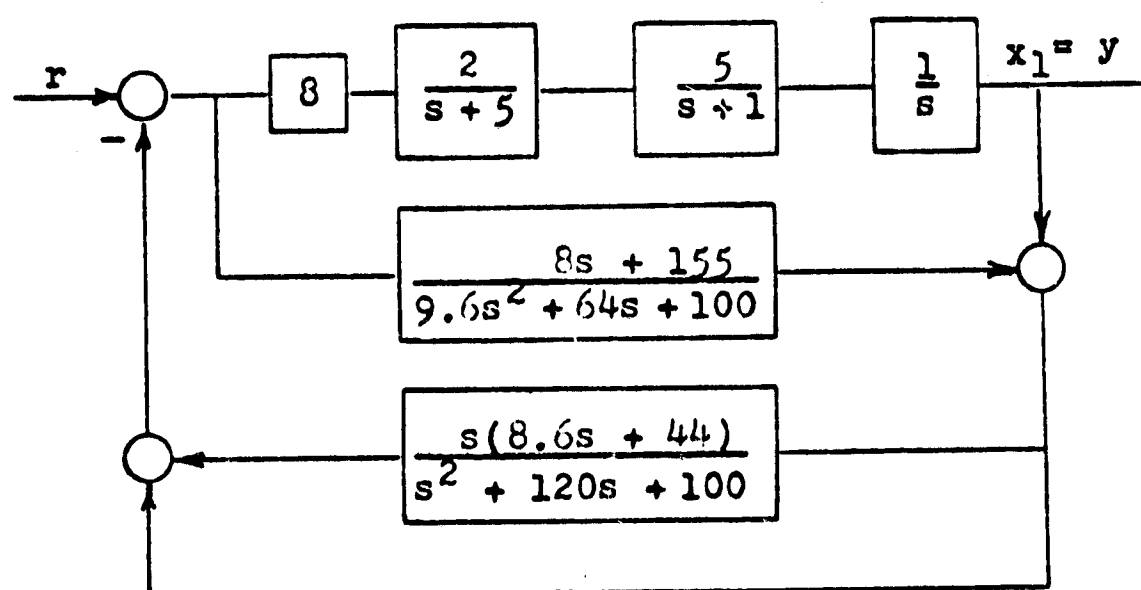


Figure 5.5 Alternate Closed-Loop System

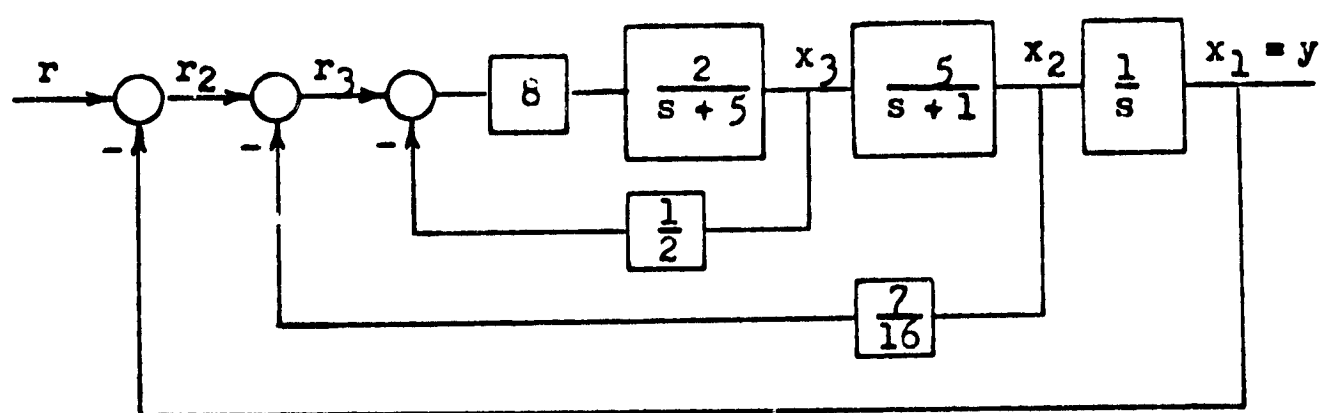


Figure 5.6 State-Variable Feedback System

and the corresponding plant transfer function is

$$\frac{x_2(s)}{u(s)} = \frac{80}{(s + 1)(s + 5)}$$

Choosing the pole of $H(s)$ at $s = -10$, the polynomials of equation (5.4) are

$$GN = 80$$

$$GD = (s + 1)(s + 5)$$

$$HN = h_1 s + h_0$$

$$HD = s + 10$$

$$AN = c_0$$

Substituting these equations into equation (5.4) and combining like terms gives

$$\frac{x_2(s)}{r_2(s)} = \frac{80(s + 10)}{s^3 + (16 + a_0)s^2 + (65 + a_0 + 80h_1)s + (60 + 5a_0 + 80h_0)}$$

The actual response that is realized is found by multiplying numerator and denominator of equation (5.9) by $(s + 10)$ to give

$$\frac{x_2(s)}{r_2(s)} = \frac{80(s + 10)}{s^3 + 24s^2 + 188s + 480}$$

Equating coefficients of like powers of s in the two expressions for $x_2(s)/r_2(s)$ gives the following set of equations:

$$a_0 + 16 = 24$$

$$65 + 6a_0 + 80h_1 = 188$$

$$60 + 5a_0 + 80h_0 = 480$$

which may be solved to give

$$a_0 = 8.0$$

$$h_1 = .938$$

$$h_0 = 4.75$$

Since there is only one additional state, which is available, the problem is solved. The resulting closed-loop system is shown in Figure 5.7.

The second case considers x_1 and x_3 as available. From Figure 5.6, the transfer function from r_3 to x_3 is

$$\frac{x_3(s)}{r_3(s)} = \frac{16}{s + 13}$$

In this case, $H(s)$ reduces to a constant, h_0 , and $A(s)$ is zero. Of course, the constant, h_0 , is just the state-variable feedback coefficient k_3 .

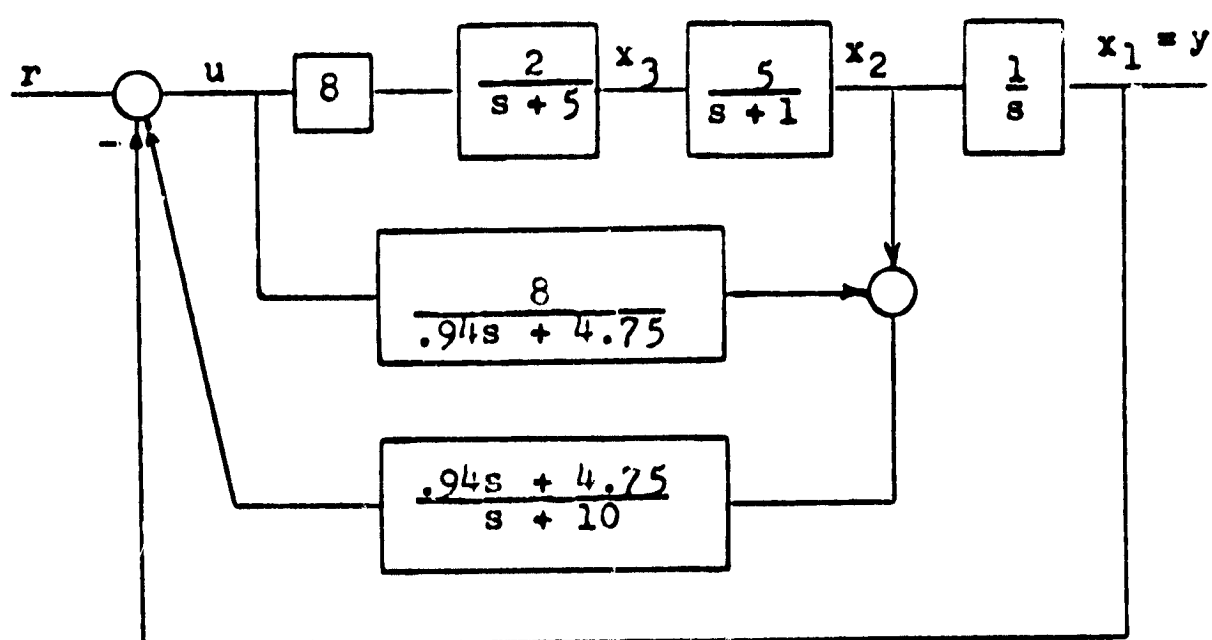


Figure 5.7 Modified Observer System with x_1 and x_2 available

Now the technique is applied at the x_1 node with a new plant transfer function, which is

$$\frac{x_1(s)}{u(s)} = \frac{80}{s(s+1)(s+13)}$$

With the poles of $H(s)$ again at $s = -10$, the polynomials of equation (5.4) are

$$GN = 80$$

$$GD = s(s+1)(s+13)$$

$$AN = a_1s + a_0$$

$$HN = h_2s^2 + h_1s + h_0$$

$$HD = (s+10)^2$$

These polynomials are substituted into equation (5.4) to give

$$\frac{y(s)}{r(s)} = \frac{80(s+10)^2}{s^5 + (34 + a_1)s^4 + (393 + 14a_1 + a_0)s^3}$$

$$+ (1660 + 13a_1 + 14a_0 + 80h_2)s^2$$

$$+ (1300 + 13a_0 + 80h_1)s + 80h_0$$

The actual response that is realized is

$$\frac{y(s)}{r(s)} = \frac{80(s + 10)^2}{s^5 + 34s^4 + 428s^3 + 2440s^2 + 6400s + 8000}$$

Equating coefficients in the two expressions for $y(s)/r(s)$ and solving for the unknowns gives

$$a_1 = 0$$

$$a_0 = 35$$

$$h_2 = 3.625$$

$$h_1 = 58.0625$$

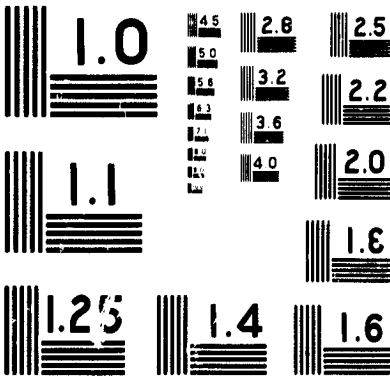
$$h_0 = 100$$

The overall system configuration is shown in Figure 5.8. Figure 5.9 shows the alternate configuration that results if $H(s)$ is divided out to give

$$H(s) = 1 + \frac{2.6s(s + 14.5)}{s^2 + 20s + 100}$$

The configuration of Figure 5.9 assures zero steady-state position error.

Peak and integral sensitivities were found for both configurations of this section. Table 5.2 lists the sensitivities for these systems along with the state-variable feedback system and the modified observer system with only x_1 available for comparison. The plant parameters are as defined in Figure 3.4. For most parameters, the



MICROCOPY RESOLUTION TEST CHART
NATIONAL BUREAU OF STANDARDS - 1963

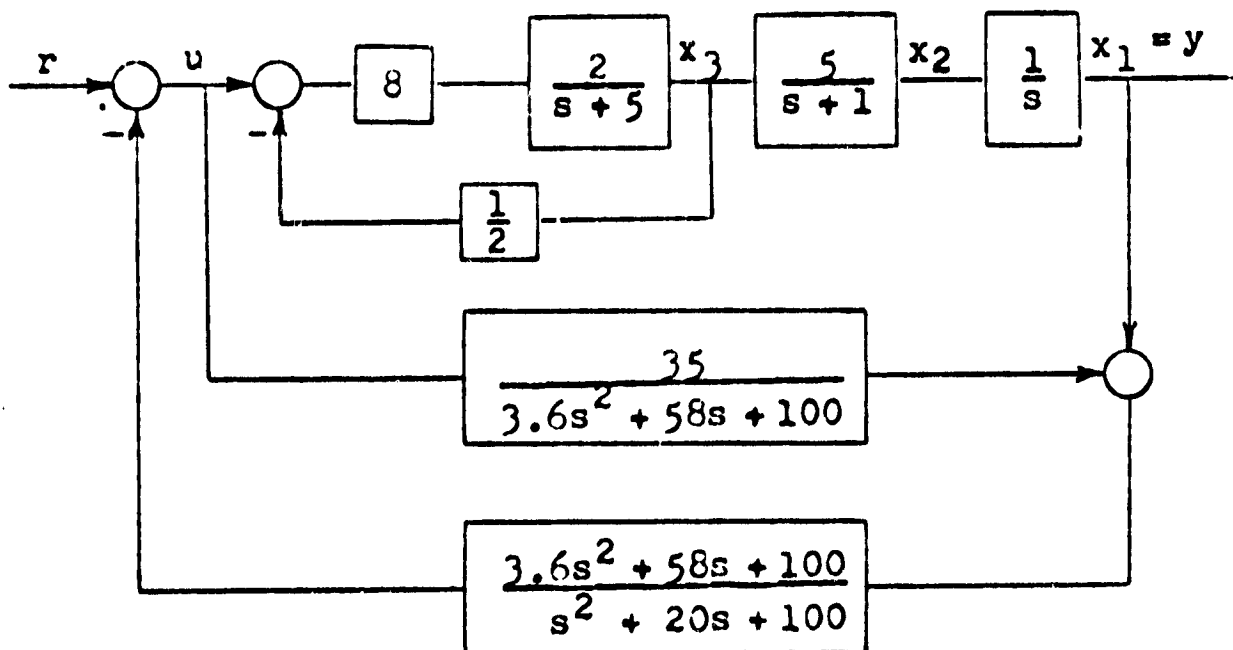


Figure 5.8 Modified Observer System with x_1 and x_3 Available

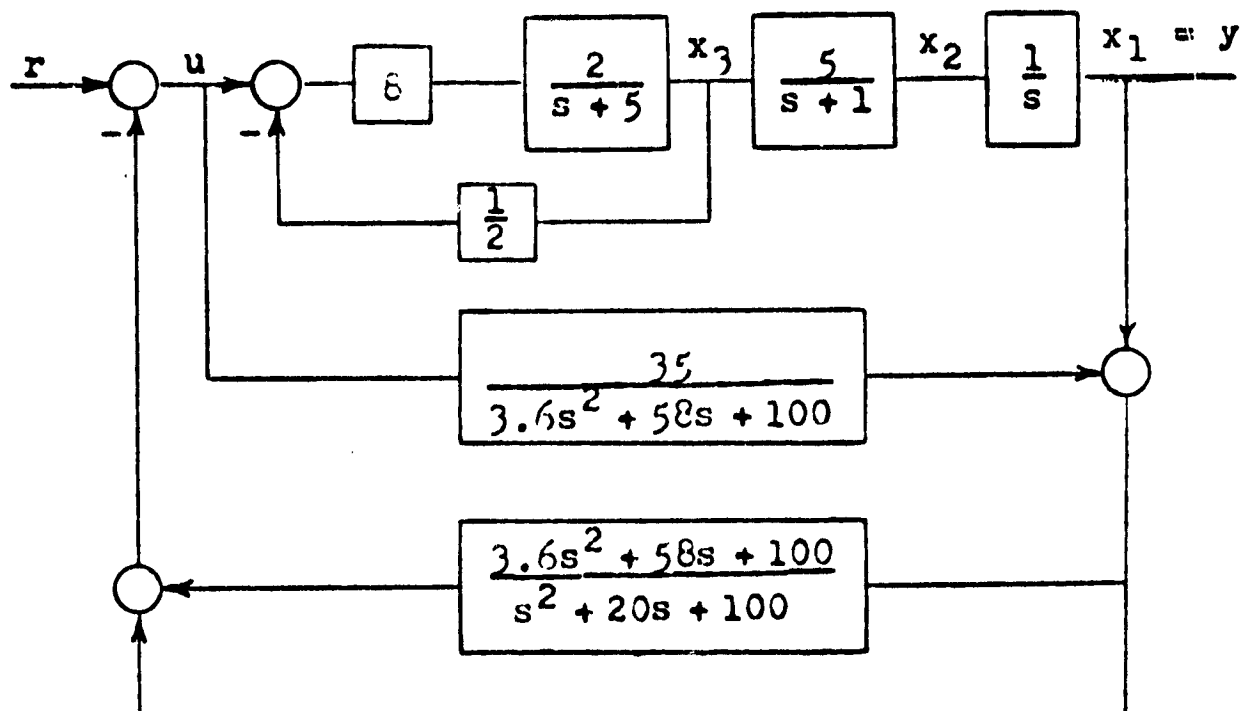


Figure 5.9 Alternate Configuration with x_1 and x_3 Available

Table 5.2 Sensitivities for Example Two

Param- eter	System			
	1	2	3	4
K_1	.593	.332	.498	.412
K_2	.321	.332	.246	.412
P_2	.148	.152	.111	.197
P_3	.120	.293	.217	.156

Peak Sensitivities

Param- eter	System			
	1	2	3	4
K_1	.286	.070	.287	.113
K_2	.067	.070	.038	.113
P_2	.019	.019	.010	.034
P_3	.0096	.059	.032	.016

Integral Sensitivities

System	Description
1	State-Variable Feedback
2	x_1 available, Poles of $H(s)$ at $s = -10$
3	x_1 and x_2 available, Poles of $H(s)$ at $s = -10$
4	x_1 and x_3 available, Poles of $H(s)$ at $s = -10$

Sensitivities are slightly better for the system with x_1 and x_2 available. The system with x_1 and x_2 available is also the most appealing with the unity feedback from x_1 .

5.4 Physical Realizability

Since the poles of $H(s)$ are chosen, it should always be realizable. If $H(s)$ has zeros in the right-half plane, then $A(s)$ will have poles in the right half plane and will not be physically realizable.

However, this problem can be avoided if the block diagram shown in Figure 5-1 is redrawn in a slightly different form. The new form of the system is shown in Figure 5-10.

Since the zeros of $H(s)$ are equal to the poles of $A(s)$ they cancel, leaving only the realizable parts of $H(s)$ and $A(s)$. It is possible that $1/(1-AH)$ which represents the equivalent series compensation has poles in the right half plane. Special effort in the selection of the poles of $H(0)$ must be made to avoid this situation.

The form of the block diagram obtained in Figure 5-10, combined with the knowledge that the zeros of $H(s)$ are close to the zeros of $H_{eq}(s)$, suggest the following intuitive interpretation of the modified observer system, although this new approach is somewhat different except in the case where the poles of $H(s)$ are very far from the origin.

The desired system is of the $H_{eq}(s)$ form; however, $H_{eq}(s)$ is not realizable. In order to get around this problem

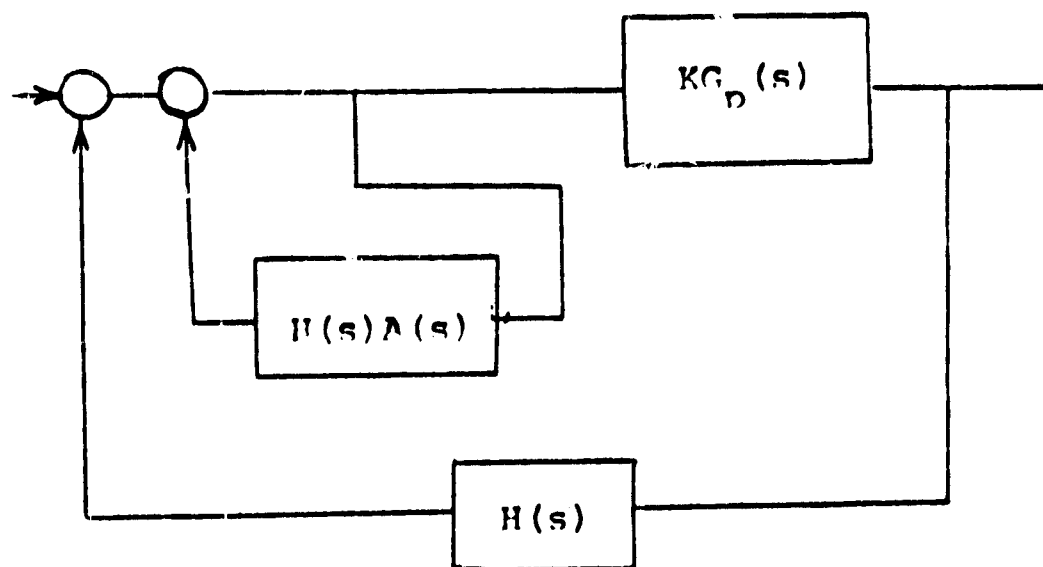
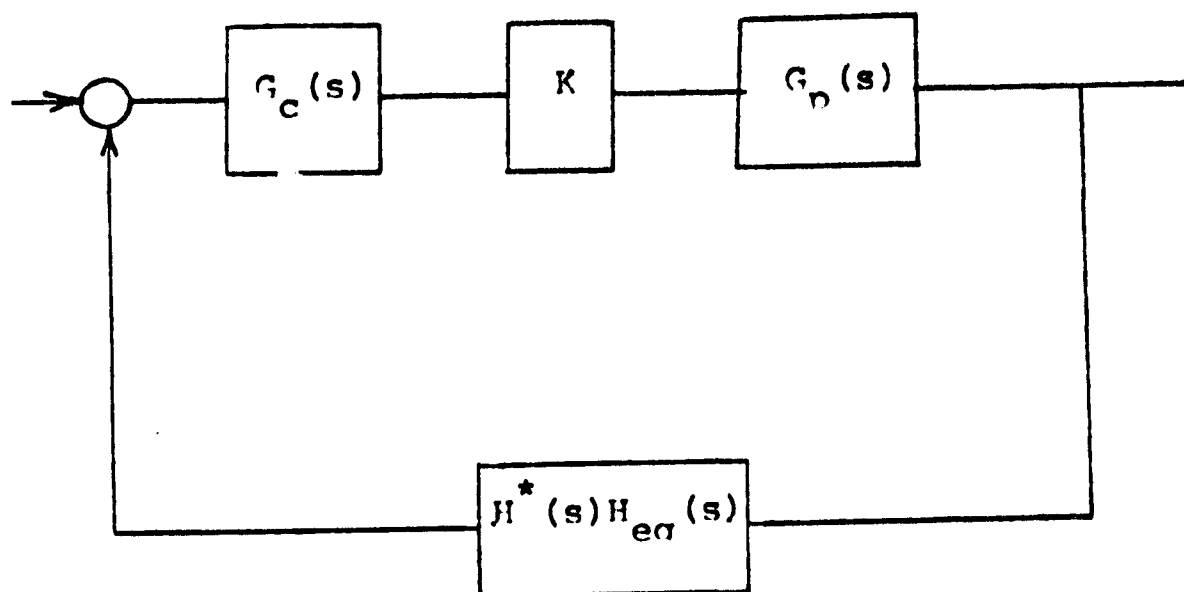


Figure 5-10 Realizable Form of Modified Observer



Figures 5-11 Alternate Method of Obtaining
Realizable $H_{eq}(s)$ Type System

poles are introduced into $H_{eq}(s)$. Call the new feedback transfer function $H_{eq}(s) H^*(s)$. $H_{eq}(s) H^*(s)$ is physically realizable; however, $y(s)/r(s)$ no longer has the desired form. To solve this problem a series compensator, G_c , is placed in the forward loop. The block diagram now has the form shown in Figure 5-11.

The required form for $G_c(s)$ can now be obtained by equating the transfer function obtained from 5-11, to the transfer function from a system in $H_{eq}(s)$ form and solving for $G_c(s)$.

$$\frac{KG_p(s)}{1 + KG_p(s) H_{eq}(s)} = \frac{KG_c(s) G_p(s)}{1 + KG_c(s) G_p(s) H_{eq}(s) H^*(s)} \quad (5.10)$$

$$G_c(s) = \frac{1}{1 + KG_c(s) H_{eq}(s) (1 - H^*(s))} \quad (5.11)$$

If this method is compared to the modified observer method it is obvious that the form of the resulting system is similar; however, the modified observer provides a simpler expression for $G_c(s)$ than does solving for $G_c(s)$ using Equation 5.11. Thus, the modified observer system can be considered to be a method of finding a realizable form for $H_{eq}(s)$ in order to realize the sensitivity advantages of that form while retaining the desired $y(s)/r(s)$. $H^*(s)$ should be selected so that $G_c(s)$ is realizable.

5.5 Summary

The modified observer system avoids the large feed-

back coefficients, but has the sensitivity advantages of an observer system. The feedback network, $H(s)$, is comparable to an approximate $H_{eq}(s)$ that was realized by adding poles, and the modified observer system has the added advantage of giving the desired response.

CHAPTER VI CONCLUSIONS

Three configurations have been presented that may be used when not all the states are available for feedback. A parallel simulation, an observer system, and the modified observer system were described. All three gave the desired response exactly if the parameters of the system did not vary.

The parallel system configuration was shown to be the same as a series compensated system. The system was only driven by the input to the plant and not by the available output. In practical problems there may be a tendency for the two systems to drift apart, since they would only be exact around some linearized operating point of the plant.

The second configuration discussed was the observer system. The poles for the observer system could be selected far out so as to improve the sensitivities of the plant parameters. Unfortunately, the new feedback coefficients become large in magnitude as the poles are moved out. Moving the poles out increases the dependence of the observer on the available outputs of the plant while decreasing the weighting on the input of the plant. The observer poles show up as poles and zeroes of the overall response so that the desired response is achieved through cancellation. The poles of the observer should be chosen far enough out so that the

response is not appreciably affected if exact cancellation does not occur. Sensitivities of plant parameters can be made nearly as small as those achieved using state-variable feedback by placing the observer poles far enough out. The resulting large values for the new feedback coefficients makes this impractical.

The modified observer system was developed in order to avoid the large feedback coefficients of the observer system. Although individual coefficients of the observer system go to infinity, their sum is finite. Sensitivities of plant parameters in the outer blocks can be improved over a state-variable feedback system by picking the poles of $H(s)$ far enough out, while the high frequency gain of $H(s)$ is still reasonable.

It is shown that the modified observer system can be considered to be a method of obtaining a system which is physically realizable from the non-realizable $H_{eq}(s)$ form, in order to retain some of the sensitivity advantages of the $H_{eq}(s)$ type system. A method was given whereby the modified observer system could be synthesized directly by algebraic manipulation of polynomials in the frequency domain. The technique could be applied when only the output was available, or when additional states were also available. Unity feedback of the output could be employed with the new configuration to insure zero steady-state position error.

As an overall conclusion from this work, it was concluded that any system used to generate unavailable states should be weighted as heavily as possible on the available outputs and as little as possible on the inputs of the plant to be controlled. If block diagram manipulations are used when only one state is unavailable, it is best to move the origin of the feedback towards the output.

REFERENCES

J. H. Dial, "The Specification and Synthesis of High-Order Control Systems," M.S. Thesis, The University of Arizona, June 1967.

D. G. Luenberger, "Observing the State of A Linear System," IEEE Transactions on Military Electronics, April 1964.

D. G. Schultz and J. L. Melsa, State Functions and Linear Control Systems, McGraw-Hill, 1967.

J. G. Truxal, Automatic Feedback Control System Synthesis, McGraw-Hill, 1955.

R. C. White, "Sensitivity and State-Variable Feedback," M.S. Thesis, The University of Arizona, August 1967.